University of California

Santa Barbara

Integrable Dynamics in Gauge Theories

A dissertation submitted in partial satisfaction

of the requirements for the degree

Doctor of Philosophy

in

Physics

by

Hiroki Kawai

Committee in charge:

Professor David Berenstein, Chair

Professor Nathaniel Craig

Professor Xiao Luo

June 2026

The dissertation of Hiroki Kawai is approved.

Professor Nathaniel Craig

Professor Xiao Luo

Professor David Berenstein, Chair

June 2026

Integrable Dynamics in Gauge Theories

Hiroki Kawai

Dedicated to my parents Hideki and Yuki Kawai, and to my wife Lara.

Acknowledgements

The work carried for this dissertation was supported in part by the Department of Energy under Award No. DE-SC0019139.

First, I would like to express my deepest gratitude to my advisor Professor David Berenstein. His tremendous support and mentorship throughout my graduate study have taught me a wide range knowledge and insights in physics and trained me to become a theoretical physicist. I also personally thank him for taking me on hikes at Lizard's Mouth and to dinners.

I would like to thank my committee members Professor Nathaniel Craig and Professor Xiao Luo for agreeing to be part of the committee and giving me guidance and feedback on this project. I also thank other faculty members of the Physics Department for discussions and providing me with many insights to deepen my understanding of physics. I would like to thank Professor Tengiz Bibilashvili for having me as a teaching assistant for many of his classes and mentoring me on how to teach physics.

I would like to thank my undergraduate advisor Professor Richard Brower, who introduced me to research in theoretical physics and encouraged me to change my academic career from engineering to physics. I would also like to thank all other physicists who have supported me and have had discussions with me, including my past and current collaborators, especially Dr. Adolfo Holguin, and Professor Esuko Ito and Professor Masazumi Honda for arranging my stay at the Yukawa Institute for Theoretical Physics as a short-term visitor. I thank other fellow students and researchers at the Physics Department for having fun conversations about both physics and other topics of daily life. I am particularly grateful to Jiuci Xu and Dan Sehayek for many discussions about our research and for being my climbing and hiking buddies. I would also like to thank current and former students in the Berenstein group, including Dr. George Hulsey, Dr.

Shannon Wang, Dr. David Grabovsky, Dr. Robinson Mancilla, Dr. Peter Thomas Lloyd, and Ziyi Frazier Li, for many discussions during and outside of the group meetings and daily conversations. I appreciate all my friends for hanging out with me and giving me time to distract myself from work and the stressful life as a graduate student.

I would also like to thank Lara's mother Sinem, aunt Sibel, and uncle Dodo for their support and love. There are not enough words to thank my parents Hideki and Yuki Kawai for their unconditional love and support. If they had not let me study abroad, I would not be writing this thesis now or earning Ph.D. in theoretical physics. Not only the education but also all the life experiences and happiness they provided me have shaped who I am today. Lastly, I am deeply grateful to my wife Lara for always supporting and cheering me on and sharing both our daily lives and our travels with me. Thanks to her, I could survive the graduate school, and my life has been full of love, happiness, and joy. I cannot wait to start a new chapter of our lives together in Dublin.

Vita of Hiroki Kawai

Education

Doctor of Philosophy in Physics, University of California, Santa Barbara, June 2026 (Expected)

Master of Arts in Physics, University of California, Santa Barbara, June 2024

Bachelor of Arts in Physics and Bachelor of Science in Computer Engineering, Boston University, May 2021

Experience

Graduate Student Researcher, University of California, Santa Barbara, 2021-Present

Teaching Assistant, University of California, Santa Barbara, 2021-Present

Visiting Researcher, Yukawa Institute for Theoretical Physics, 2021 Summer, 2024 Summer

Undergraduate Research Assistant, Boston University, 2018-2021

Research Internship, Qunasys Inc., 2019 Summer

Talks

Governor's Office of Business and Economic Development Quantum Convening Strategy Meeting

March 13th, 2026, Santa Barbara, California, USA, Talk

Title: "Spin chains from large-N QCD at strong coupling"

KITP High Energy and Gravity Seminars

October 23rd, 2025, Santa Barbara, California, USA, Talk

Title: "Integrability and conformal blocks for Gukov-Witten surface defects in $\mathcal{N} = 4$ SYM"

Strings and Fields 2024

August 5-9, 2024, Kyoto, Japan, Poster (in Japanese)

Title: "Surface defect in N=4 SYM and integrability"

RIKEN iTHEMS Theoretical Physics Seminar

July 17, 2024, Saitama, Japan, Talk

Title: "Surface defect in N=4 SYM and integrability"

YITP Seminar

July 5, 2024, Kyoto, Japan, Talk

Title: "Surface defect in N=4 SYM and integrability"

The International Symposium on Lattice Field Theory

July 31-August 4, 2023, Batavia, Illinois, USA, Talk

Title: "Confining strings as integrable spin chains in large N lattice Yang-Mills theory"

The Sixth International Conference for Young Quantum Information Scientists (YQIS 6)

April 12-16, 2021, Online, Poster

Title: "U(1) link dynamics from gauged fermions towards quantum computing"

Quantum Computing on Quantum Field Theories

January 5-8, 2021, Online, Invited talk

Title: "Quantum links for $U(1)$ gauge theory on qubits and its simulation with digital

quantum circuit"

Quantum Techniques in Machine Learning 2020 (QTML 2020)

November 9-12, 2020, Online, Poster

Title: "Predicting excited states from ground state wavefunction by supervised quantum machine learning"

Asia-Pacific Symposium for Lattice Field Theory (APLAT 2020)

August 4-7, 2020, Online, Talk

Title: "Quantum links for $U(1)$ gauge theory on qubits and reduction to $\mathbb{Z}_2$ gauge theory and toric code"

QuLat Collaboration Annual Meeting

July 7-8, 2020, Online, Talk

Title: "Quantum links for $U(1)$ gauge theory on qubits and reduction to $\mathbb{Z}_2$ gauge theory and toric code"

Machine Learning for Signal Processing (MLSP 2019)

October 13-16, 2019, Pittsburgh, Pennsylvania, USA, Poster

Title: "VAE/WGAN-based image representation learning for pose-preserving seamless identity replacement in facial images"

Honors, Awards, and Fellowships

Outstanding Teaching Assistant Award, UCSB, 2024-2025

Graduate Division Dissertation Fellowship, UCSB, 2025

College Prize for Excellence in Physics, Boston University, 2021

Publications

David Berenstein and Hiroki Kawai. "Spin Chains from large-N QCD at strong coupling". In: (Mar. 2026). arXiv: 2603.04506 [hep-th].

Adolfo Holguin and Hiroki Kawai. "Integrability and conformal blocks for surface defects in $\mathcal{N} = 4$ SYM". In: *JHEP* 11 (2025), p. 043. DOI: 10.1007/JHEP11(2025)043. arXiv: 2503.09944 [hep-th].

David Berenstein, Hiroki Kawai, and Richard Brower. "U(1) fields from qubits: An approach via D-theory algebra". In: *Phys. Rev. D* 110.1 (2024), p. 014506. DOI: 10.1103/PhysRevD.110.014506. arXiv: 2201.02412 [hep-th].

David Berenstein and Hiroki Kawai. "Integrable Spin Chains from large-N QCD at strong coupling". In: (Aug. 2023). arXiv: 2308.11716 [hep-th].

Richard C. Brower, David Berenstein, and Hiroki Kawai. "Lattice Gauge Theory for a Quantum Computer". In: *PoS* LATTICE2019 (2020), p. 112. DOI: 10.22323/1.363.0112. arXiv: 2002.10028 [hep-lat].

Hiroki Kawai and Yuya O. Nakagawa. "Predicting excited states from ground state wavefunction by supervised quantum machine learning". In: *Machine Learning: Science and Technology* (2020). URL: http://iopscience.iop.org/10.1088/2632-2153/aba183.

H. Kawai et al. "VAE/WGAN-Based Image Representation Learning For Pose-Preserving Seamless Identity Replacement In Facial Images". In: (2019), pp. 1–6.

Abstract

Integrable Dynamics in Gauge Theories

by

Hiroki Kawai

This dissertation discusses various quantum integrable structures underlying gauge theories. We demonstrate that such structures naturally emerge when we connect the gauge theories to string theory by taking the large N limit of the color degrees of freedom. Such integrable structures are not only tools for exact computations for various physical quantities in gauge theory, but also give guidance to further elucidate the correspondence between gauge theory and string theory.

We first discuss the integrable spin chains appearing in the weak 't Hooft coupling expansion of the $\mathcal{N} = 4$ super Yang-Mills theory, which has been well known to be dual to type IIB string theory on the $\mathrm{AdS}_5 \times S^5$ geometry. We specifically focus on the boundary conditions induced by the Gukov-Witten-type superconformal surface defects, which happen to be integrable at some special points in the defect moduli space but not for generic configurations. Additionally, aspects of the surface defects are further studied by taking advantage of the superconformal symmetry for future investigation of their (non-)integrability.

The second part of the dissertation discusses the spin chain structures emerging in the confining string sectors of large N lattice Yang-Mills theory. The nontriviality of the confining string theory, distinct from the ordinary Nambu-Goto theory, is due to the unitarity constraint, or the so-called zigzag constraint, that is naturally required for gauge theory due to the gauge holonomy being a unitary group. We indeed find that the spin chains for certain closed subsectors are integrable when the unitarity constraint is trivial,

but the integrability is violated generally due to the constraint. We also demonstrate that the integrability can be utilized to study the physics of the gauge theory. In particular, it successfully estimates the roughening transition point from the energy spectra exactly computed using the Bethe ansatz method.

Contents

List of Figures

List of Tables

Chapter I: Background

I.1 Introduction

The development of quantum field theory (QFT) is one of the greatest successes for theoretical physics. In particular, the Standard Model (SM) has explained many experimental phenomena stemming from three of the four fundamental interactions: electromagnetic, weak, and strong interactions. All the particles predicted by the SM have now been observed in experiments; it was completed when the Higgs boson was discovered by the Large Hadron Collider (LHC) [2, 46]. It is a non-Abelian gauge theory with a gauge group of $U(1)_Y \times SU(2) \times SU(3)$. The $U(1)_Y \times SU(2)$ group corresponds to the electroweak interaction [151, 72, 157] while the $SU(3)$ part corresponds to the strong interaction [67, 167], which is particularly called quantum chromodynamics (QCD). Ordinary weak-coupling perturbation theory for QFTs, which expands the correlators around the free-theory limit, works well for the electroweak theory as a result of the small fine structure constant in the typical infrared (IR) scale and the weak boson masses. On the other hand, to study the IR physics of QCD, perturbation theory cannot give accurate estimates due to asymptotic freedom [81, 142]. In general, the one-loop beta function for gauge theory with gauge coupling g, gauge group G, n_{R_f} flavors of Weyl fermion matter fields in the representation R_f of G, and n_s flavors of real scalars in the representation of R_s of G is

$$\beta(g) = -\left[\frac{11}{3}T(\text{adj.}) - \frac{2}{3}\sum_{R_f} n_{R_f} T(R_f) - \frac{1}{6}\sum_{R_s} n_{R_s} T(R_s)\right] \frac{g^3}{16\pi^2} + O(g^5), \qquad \text{(I.1.1)}$$

where $T(r)$ is the index of R. The 1-loop value of $\beta(g)$ for QCD with three generations of quarks is $-7\frac{g^3}{16\pi^2}$, which is negative and means that the theory is strongly coupled in the IR. This makes the IR phenomena of QCD quite interesting, particularly quark confinement. However, the first-principles understanding of hadron dynamics from QCD requires nonperturbative analysis because of this asymptotic freedom and hence is extremely challenging.

A question to ask is: is there any other expansion than weak-coupling perturbation to study the strong-coupling regime of QCD? One obvious candidate is the strong-coupling expansion about $1/g$. This was achieved by Wilson [158] by considering QCD in discrete spacetime (lattice QCD). Lattice QCD also enabled numerical computations of various observables, as it reduces the mathematically ill-defined infinite-dimensional path integral of field theory into a finite-dimensional integral. We will review lattice QCD in more detail in section I.2.1.

Another expansion was proposed by 't Hooft [1]; it takes the large color degrees of freedom N limit, while keeping the 't Hooft coupling $\lambda \equiv g^2 N$ fixed. This limit corresponds to the semi-classical limit of the theory, and correlators generally factorize. One can also make an analogy of the expansion about $1/N$ to the genus expansion in string theory, which later lead to the discovery of the anti-de Sitter/conformal field theory (AdS/CFT) correspondence [127], the most precise realization of the correspondence between gauge theory and string theory. 't Hooft's large N limit will be reviewed in detail in section I.2.2.

The goal of this dissertation is to explore the exactly solvable structures of gauge theory. In particular, we focus on the quantum integrable systems emerging with the above expansions. It is remarkable that quantum integrable systems, which have mainly

been developed to study two-dimensional systems, can be applied to exactly compute the spectra of higher-dimensional theories. Indeed, we will see that the origin of integrability can be understood as the integrability of string theory, a theory on a two-dimensional world-sheet.

I.2 Gauge theory and string theory

String theory was originally proposed independently by Nambu, Nielsen, and Susskind [136, 137, 154] to provide a microscopic explanation for the Veneziano amplitude [155] [1], which was constructed as a phenomenological expression of the four-point meson scattering amplitudes in terms of the Euler beta functions and the Mandelstam variables s, t, u:

$$T = g^2 \left[B(-\alpha(s), -\alpha(t)) + B(-\alpha(s), -\alpha(u)) + B(-\alpha(t), -\alpha(u)) \right], \quad B(x,y) \equiv \frac{\Gamma(x)\Gamma(y)}{\Gamma(x+y)}. \tag{I.2.1}$$

Note that it obviously admits crossing symmetry. $\alpha(s)$ is the linear Regge trajectory

$$\alpha(s) = \alpha(0) + \alpha' s, \tag{I.2.2}$$

where the values of $\alpha(0)$ and α' vary for each meson family (or quantum numbers) and describe the (approximately) linear relation between the mass squared and the angular momenta of the particles in the family. A meson can be interpreted as a spinning string.

Let us start with the Nambu-Goto action formalism of string theory in D-dimensional Minkowski spacetime M. The action of a string world-sheet Σ parameterized with $\sigma^a = (\tau, \sigma)$ is proportional to the area of Σ:

$$S_{\mathrm{NG}} = -\frac{1}{2\pi\alpha'} \int_\Sigma d\tau d\sigma \, \sqrt{-\det h_{ab}}, \tag{I.2.3}$$

[1] Refer also to [153] for the detailed history.

where X^μ are scalar fields that describe the embedding of the world-sheet Σ to $\mathcal{M}$, $X^M : \Sigma \to \mathcal{M}$ $(M = 0, 1, ..., D-1)$, and $h_{ab} \equiv \partial_a X^M \partial_b X_M$ is the induced metric on the world-sheet. It is convenient to present another formulation with the Polyakov action

$$S_{\rm P} = -\frac{1}{4\pi\alpha'} \int_\Sigma d\tau d\sigma \, \sqrt{-\det \gamma_{ab}} \gamma^{ab} \partial_a X^M \partial_b X_M, \tag{I.2.4}$$

where γ_{ab} is a world-sheet metric. The equation of motion for this action constrains γ_{ab} to be proportional to the induced metric h_{ab}: $\sqrt{-\det \gamma_{ab}}\gamma_{ab} = \sqrt{-\det h_{ab}} h_{ab}$, and therefore the Polyakov action is indeed on-shell equivalent to the Nambu-Goto action. The action is invariant under the two-dimensional general coordinate transformation, or diffeomorphism, on the world-sheet, as well as the Weyl transformation. These are gauge invariance of the theory, and hence, when quantizing the theory via a path integral, the integral has to be quotient by these transformations. Since the gauge transformations have three independent parameters, one can choose to fully fix the three independent components of γ_{ab} with them. The simplest choice is to fix it to be a flat metric $\gamma_{ab} = \eta_{ab}$, or slightly relax it to be a conformally flat space $\gamma_{ab} = e^{2\omega(\sigma)}\eta_{ab}$. For the latter case, the Polyakov action becomes a theory of free scalars

$$S_X = -\frac{1}{4\pi\alpha'} \int_\Sigma d\tau d\sigma \, \partial^a X^M \partial_a X_M \tag{I.2.5}$$

plus the action of Faddeev-Popov free ghost fields. One can exactly solve such free theories since the path integrals are Gaussian, indicating the integrability structure that the bosonic string theory possesses. The four-point amplitude of this theory matches correctly with the Veneziano amplitude at the tree level.

We can add another term preserving the symmetries (Weyl, diffeomorphism, and D-dimensional Lorentz symmetry):

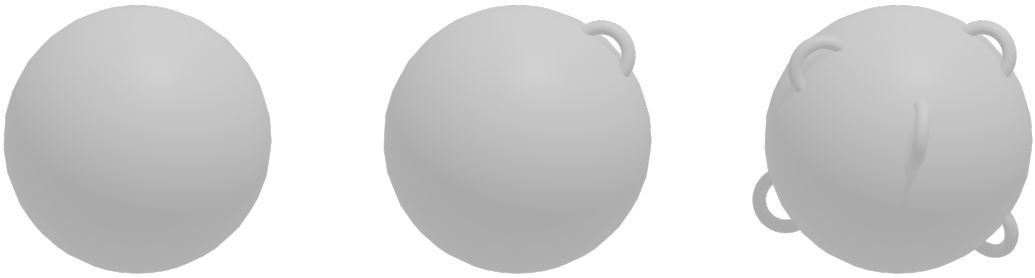

(a) (b) (c)

Figure I.1: Examples of world-sheet topologies. (a) The leading-order contribution in the genus expansion comes from a world-sheet topologically a two-sphere ($g = 0$). (b) A sub-leading contribution with genus $g = 1$ with a handle. It is topologically a two-torus. (c) World-sheets with more handles or higher genus contribute at higher orders in g_s.

$$-\Phi_0 \chi = -\Phi_0 \int_\Sigma d\tau d\sigma \sqrt{-\det \gamma_{ab}} R. \tag{I.2.6}$$

R is the Ricci scalar with respect to γ_{ab}. Notice that the overall action is now the Einstein-Hilbert action in two dimensions with vanishing cosmological constant. The Einstein equation $R_{ab} - \frac{1}{2} R \gamma_{ab} = 0$ is identically satisfied, and so eq. (I.2.6) is fully topological. Indeed, χ can be identified as the Euler number of Σ. Φ_0 is the value of the background dilaton field, and $g_s \equiv e^{\Phi_0}$ determines the strength of the coupling between strings and hence is called string coupling. Contributions to string amplitudes (or any observables) can therefore be expanded in terms of $g_s^{-\chi} = g_s^{2g-2}$, where g is the genus of a world-sheet. In the weak coupling region, it gives a genus expansion, where string scatterings described by a world-sheet homeomorphic to a two-sphere ($g = 0$) give the leading contributions, and world-sheets with higher genus (i.e. with more "handles") give corrections to them (fig. I.1).

Despite its successful description of the Veneziano amplitude, the above bosonic string theory suffers several flaws as a description of hadron dynamics in four-dimensional space-time. The Weyl symmetry, which is proportional to cR where c is the central charge of

the theory and R is the Ricci scalar of the world-sheet, is in general anomalous, unless $c = 0$. The central charge of the ghost theory is $c_{\rm g} = -26$, and since each scalar has a unit central charge, the Weyl anomaly is canceled only when $D = 26$, which is called the critical dimension. Moreover, the lowest energy state has negative mass squared (tachyon), and the first excited state is massless. Their existence contradicts the experimental observations that hadrons are all massive. QCD has been considered as a more accurate description of the strong interaction since its asymptotic freedom was shown [78, 142, 81, 79], and string theory later came to be regarded primarily as a potential formulation of quantum gravity, provided that the closed string spectrum contains spin-2 excitations.

Still, it is an interesting question to ask whether QCD has a string theoretic structure and whether such *QCD string* theory can be formulated as a modification of the above bosonic string theory. Such a modification is expected to make the string theory non-integrable [62]. It is natural to expect that the dynamics of a gluon excitation between confined quarks, or a color flux tube, can be effectively described as the dynamics of an open string with quarks at its endpoints.

I.2.1 Lattice gauge theory

Wilson [158] proposed the lattice version of the QCD action by discretizing the spacetime to a lattice with some finite spacing a

$$S_{\rm Wilson} = \frac{2N}{g^2} \sum_P \left[1 - \frac{1}{N} \,{\rm tr}\Big(U_P + U_P^\dagger \Big) \right] + \text{fermions}, \tag{I.2.7}$$

where P is a single loop or a *plaquette* of the lattice spacetime. The bare coupling g here is dimensionless, and coincides with the gauge coupling of the continuum theory when the spacetime is four-dimensional. When $D \neq 4$, the continuum gauge coupling (denoting it $g_{\rm YM}$) becomes dimensionful and therefore is related to g as $g = g_{\rm YM} a^{4-D}$. U_P is the product of the link variable $U(x, x+\hat{\mu}) = e^{iagA_\mu(x)}$ defined on the directed link

from x to $x+\hat{\mu}$ ($\hat{\mu}$ is a unit vector in the μ direction in terms of a) for the gauge field A_μ. The finite lattice spacing acts as an ultraviolet cutoff. Namely, for P extending in the μ, ν direction in the hypercubic lattice at position x, U_P is

$$U_P = U(x, x+\hat{\mu})U(x+\hat{\mu}, x+\hat{\mu}+\hat{\nu})U^\dagger(x+\hat{\nu}, x+\hat{\mu}+\hat{\nu})U^\dagger(x, x+\hat{\nu}). \tag{I.2.8}$$

One can easily see that this action classically converges to the continuum QCD action in the zero lattice spacing limit $a \to 0$. Quantum machanically, the bare coupling g is under the effect of renormalization and depends on a. Just as calculated in continuum QCD, g admits asymptotic freedom, so g flows towards weak coupling in the continuum limit $a \to 0$. Wilson discussed that the strong-coupling expansion of the Wilson loop expectation value can be performed naturally in lattice QCD, and leads to the area law. Namely, the expectation value of the Wilson loop in the fundamental representation on a closed loop C is

$$\langle W_C \rangle \propto \exp(-\sigma A), \tag{I.2.9}$$

where A is the area of the minimal two-dimensional region enclosed by C and σ is some coefficient. One can see that this apparently indicates the stringy behavior of confinement in strong coupling as follows. Considering a rectangular C that extends to the Euclidean time direction and one of the spatial directions, the Wilson loop can be interpreted as the parallel world-lines of a quark and an antiquark separated by distance L, which are pair-created, travel for a certain amount of time T, and annihilate with each other. Then, the Wilson loop expectation value corresponds to the transition amplitude between the quark-antiquark pair state evolved for time T and the same quark-antiquark state:

$$\langle W_C \rangle = \langle q\bar{q}|e^{-HT}|q\bar{q}\rangle = e^{-V_{q\bar{q}}(r)T}, \tag{I.2.10}$$

where $V_{q\bar{q}}(r)$ is the potential energy between the quark-anti-quark pair. Therefore, the potential energy is $V_{q\bar{q}}(r) = \sigma R$, and the parameter σ can be interpreted as a string tension, while the gluon excitation between quarks can be viewed as a one-dimensional string.

Although this stringy behavior of the quark-anti-quark bound state in the strong-coupling limit makes us tempted to expect that the color flux tubes in QCD can effectively be described as some string theory even in the continuum, it is actually expected to experience a phase transition as taking the continuum $a \to 0$ limit, and hence the behavior of the string drastically changes there [91, 84, 125, 135, 124]. This transition is called the roughening transition, at which the effective string tension becomes small, and hence the string delocalizes in the transverse directions. This roughening behavior can be seen by considering the breaking of the translation symmetries in the transverse directions. Their spontaneous breaking induces $D-2$ Nambu-Goldstone bosons as an effective two-dimensional theory on the flux tube, which can be interpreted as branons in the transverse directions. This is not the case for the lattice theory, since the translation symmetries are already broken to a discrete subgroup. The massless scalars in two dimensions have correlators that logarithmically diverge; $\langle X(x)X(y)\rangle \sim \log|x-y|^2$. Interpreting these scalars as the transverse positions of the string, this explains the roughening behavior.

I.2.2 't Hooft limit

The $SU(N)$ gauge field kinetic term of the QCD action, or the Yang-Mills action [162] can be written in terms of N and the 't Hooft coupling $\lambda \equiv g_{\rm YM}^2 N$ as [1] [2]

$$S_{\rm YM} = -\frac{N}{4\lambda}\int d^4x\, F_{\mu\nu}F^{\mu\nu}. \tag{I.2.11}$$

[2]Here, the definition of the gauge field is different from the convention used in section I.2.1 by the gauge coupling, related as $A_\mu(\text{here}) = g_{\rm YM}A_\mu(\text{there})$. This gives the prefactor $-1/4g_{\rm YM}^2$ instead of $-1/4$ in the Yang-Mills action and the $1/g_{\rm YM}^2$ contributions from the vertices.

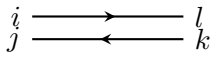

Figure I.2: A ribbon diagram representing the gauge field propagator in large N.

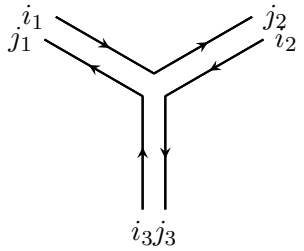

Figure I.3: A ribbon diagram representing the three-point vertex in large N.

The 't Hooft limit takes $N \to \infty$ while λ fixed, which exactly corresponds to the classical limit of $e^{-S/\hbar}$ with $\hbar \to 0$. The gauge field propagator is

$$\langle (A_\mu(x))_{ij} (A_\nu(y))_{kl} \rangle = \Delta_{\mu\nu}(x-y) \left(\delta_{il}\delta_{jk} - \frac{1}{N}\delta_{ij}\delta_{kl} \right), \tag{I.2.12}$$

where $\Delta_{\mu\nu}(x-y)$ is the propagator for the Abelian gauge field, whose exact expression is irrelevant for the present discussion. The second term becomes negligible in the $N \to \infty$ limit. Therefore, the gauge field propagator can be represented with the "ribbon" diagram with directed edges, as in fig. I.2. Each propagator gives the contribution of $g_{\mathrm{YM}}^2 = \lambda/N$. Since the theory is non-Abelian, the action contains three-point and four-point interactions, which can be represented as ribbon diagrams as fig. I.3. Each of them contributes by $1/g_{\mathrm{YM}}^2 = N/\lambda$. Moreover, every closed loop contributes by N due to the trace. The overall contribution of a certain Feynman diagram to some observable of the theory is therefore proportional to N^{F+V-E}, where E is the number of edges, F is the number of closed loops, and V is the number of vertices. Notice that the exponent $F+V-E$ is exactly the Euler number χ of the two-dimensional surface that is tessellated to the Feynman diagram under consideration. χ is related to the genus g of the two-dimensional surface as $\chi = 2-2g$, so the expansion in $1/N$ is exactly the genus expansion of the diagrams contributing to the observable. The leading contribution in the $1/N$ expansion

comes from the diagrams corresponding to a two-sphere ($g = 0$), which are called planar diagrams since it has no ribbon crossing and can be projected to a two-dimensional plane. Thus, taking the large N limit elucidates the string theoretic behavior of gauge theory; the $1/N$ expansion corresponds to the weak-coupling expansion of string theory. This similarity eventually leads to the discovery of the *AdS/CFT correspondence* [127], which we will discuss in more detail in the next section.

I.2.3 D-branes and AdS/CFT correspondence

The most precise realization of the correspondence between gauge theory and string theory is the duality between the $\mathcal{N} = 4$ super Yang-Mills (SYM) theory and type IIB string theory on the $\mathrm{AdS}_5 \times S^5$ background in large N [127]. Here, we review how these two theories are related by the dynamics of D3-branes.

Consider an open string world-sheet that is parameterized by $\tau \in (-\infty, \infty)$ and $\sigma \in [0, \ell]$. The variation of the Polyakov action consists of the bulk variation plus the boundary term

$$\delta S_{\mathrm{P}} = \frac{1}{2\pi\alpha'} \int d\tau \int_0^\ell d\sigma \, \sqrt{-\det \gamma_{ab}} \delta X^M \nabla^2 X_M - \frac{1}{2\pi\alpha'} \int d\tau \, \sqrt{-\det \gamma_{ab}} \delta X^M \partial^\sigma X_M \Big|_{\sigma=0}^{\sigma=\ell}. \tag{I.2.13}$$

In order for the boundary term to vanish, we can impose either of the two boundary conditions for each X^μ at each boundary:

- **Neumann boundary conditions:** $\partial^\sigma X_M = 0$.
- **Dirichlet boundary conditions:** $X\mu = c_M$ (constant).

Let us impose Neumann conditions on $X^0, ..., X^p$, and the other $X^{p+1}, ..., X^{D-1}$ to have the Dirichlet conditions. One can interpret it as the string ending on a $p+1$-dimensional hypersurface called a *Dp-brane* [140]. The Chan-Paton factor [138], which was originally

introduced as internal degrees of freedom at the ends of the strings to add the isospin factors to the Veneziano amplitude, can be naturally interpreted as the choice of coincident D-branes on which the string ends. For example, N coincident D-branes introduce the degrees of freedom in the fundamental representation of $U(N)$. This can be understood as the gauge symmetry of the effective field theory on the D-branes.

From now on, we consider type II superstrings in critical dimensions ($D = 10$). The Gliozzi–Scherk–Olive (GSO) projection [73] removes the tachyonic states from the spectrum, so the lowest-energy states are massless. The low-energy effective action, which is equivalent to taking the $\alpha' \to 0$ limit, is a theory of massless modes. It contains the spin-2 states from the closed string spectrum, and therefore the effective action is a ten-dimensional supergravity theory. Specifically, it is type IIA or IIB supergravity, depending on the chirality of the world-sheet spinors. The field contents of these theories are as follows

- Type IIA: $g_{\mu\nu}, B_{\mu\nu}, \Phi, C_1, C_3$
- Type IIB: $g_{\mu\nu}, B_{\mu\nu}, \Phi, C_0, C_2, C_4,$

where $g_{\mu\nu}$ is the ten-dimensional spacetime metric, $B_{\mu\nu}$ is the NS-NS field, Φ is the dilaton, and C_{p+1} is the $p+1$-form R-R field which couples to Dp-branes.

Let us now focus on D3-branes in type IIB theory. A stack of N D3-branes corresponds to the supergravity solution

$$ds^2 = f(r)^{-1/2}\eta_{\mu\nu}dx^\mu dx^\nu + f(r)^{1/2}(dr^2 + r^2 d\Omega_5^2), \quad f(r) = 1 + \frac{R^4}{r^4}, \quad R^4 = 4\pi g_s N \alpha'^2, \tag{I.2.14}$$

$$e^\Phi = g_s, \quad C_4 = g_s^{-1}(f(r)^{-1} - 1)dx^0 \wedge \cdots \wedge dx^3, \tag{I.2.15}$$

where $\eta_{\mu\nu}$ is the Minkowski metric in the four dimensions parallel to the D3-branes. We now take the decoupling limit

$$\alpha' \to 0, \quad U \equiv \frac{r}{\alpha'} = \text{fixed}, \tag{I.2.16}$$

then the second term of $f(r)$ dominates, and the resulting metric is the $\mathrm{AdS}_5 \times S^5$ geometry with the Poincaré patch

$$ds^2 = \alpha' \left[\frac{U^2}{R^2} \eta_{\mu\nu} dx^\mu dx^\nu + \frac{R^2}{U^2} dU^2 + R^2 d\Omega_5^2 \right], \tag{I.2.17}$$

where both the sphere and the AdS have the same radius R.

The D3-branes break half of the supersymmetry of type IIB theory; in other words, only 16 out of 32 supercharges are conserved. This implies that the theory on the D3-branes must preserve $\mathcal{N} = 4$ superconformal symmetry. Indeed, the theory must have the $U(N)$ gauge field A_μ and six real scalar fields ϕ^I, $I = 1, 2, ..., 6$ which correspond to the transverse positions of the D3-branes. The bosonic fields have eight on-shell real degrees of freedom in total, so the supersymmetry implies that the theory must have four Weyl fermions. These field contents form $\mathcal{N} = 4$ supermultiplet in four dimensions, and therefore we can conclude that the effective theory must be $\mathcal{N} = 4$ SYM in the low-energy $\alpha' \to 0$ limit [3]. Furthermore, the isometry group of the $\mathrm{AdS}_5 \times S^5$ geometry is $SO(2,4) \times SO(6)$, which exactly coincides with the bosonic part of the $\mathcal{N} = 4$ superconformal symmetry.

From these observations, we can conjecture that there is a duality between type IIB string theory on the $\mathrm{AdS}_5 \times S^5$ and the $\mathcal{N} = 4$ SYM theory. The string coupling g_s and the Yang-Mills coupling g_{YM} are related as

$$4\pi g_s = g_{\mathrm{YM}}^2, \tag{I.2.18}$$

which can be seen from the fact that the three-point vertex of the gauge field A^3 con-

[3] The full theory must contain higher-derivative terms, similarly to the single brane case where the full action is the Abelian DBI action.

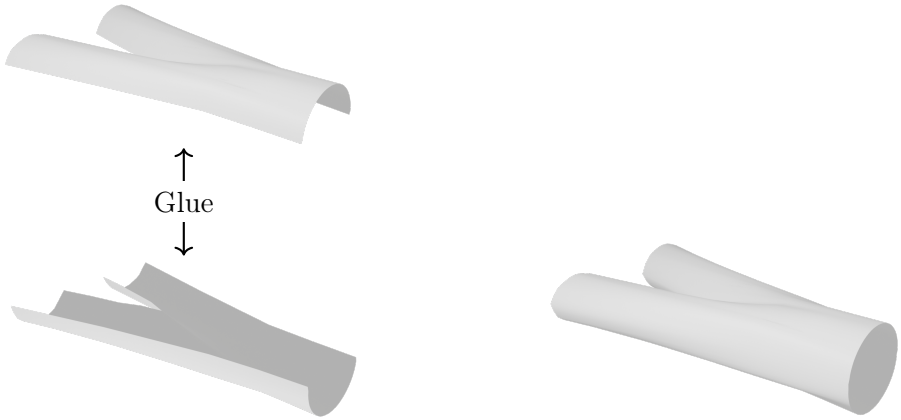

(a) (b)

Figure I.4: The three-point interaction of open strings (each world-sheet in (a)) corresponds to the three-point interaction of gauge fields in the Yang-Mills theory. When two of them are glued together at the boundaries that are the world-lines of the string endpoints, the resulting world-sheet is the three-point interaction of closed strings (b). This explains the relation between the Yang-Mills coupling and the string coupling eq. (I.2.18).

tributes by g_{YM} and corresponds to the three-point vertex of open strings, while the three-point vertex of closed strings can be obtained by gluing the two open string three-point vertices and contributes by g_s (fig. I.4).

The correspondence is well-defined in the limit where the supergravity description on the string theory side is valid, namely when the AdS/sphere radius R is larger than the string length l_s, which requires $4\pi g_s \gg 1$, and the genus correction is suppressed $g_s \ll 1$. This is equivalent to taking the 't Hooft large-N limit with strong coupling $\lambda = g_{\mathrm{YM}}^2 N \gg 1$. However, the strong version of the AdS/CFT correspondence conjectures the duality beyond this limit, where nonperturbative string theory effects or quantum gravity effects may become nontrivial and therefore not well-defined to our knowledge.

Correspondence of the spectra

A part of the conjecture is that the Hilbert spaces on both sides of the duality are isomorphic. Many efforts have been made to identify microscopic states in string theory or supergravity with the CFT states. One of the most remarkable discoveries was the correspondence between gauge theory operators called the Berenstein-Maldacena-Nastase

String		$\mathcal{N}=4$ SYM
String states		BMN operators
$\vert 0; L\rangle$	$\Longleftrightarrow$	$\mathrm{Tr}\left[Z^L\right]$
$a^{I\dagger}0\,\vert 0; L\rangle$	$\Longleftrightarrow$	$\mathrm{Tr}\left[\phi^I Z^L\right]$
$a_n^{I\dagger}a_{-n}^{J\dagger}\,\vert 0; L\rangle$	$\Longleftrightarrow$	$\sum \ell e^{i2\pi\ell n/L}\,\mathrm{Tr}\left[\phi^I Z^\ell \phi^J Z^{L-\ell}\right]$
	$\vdots$	

Table I.1: The correspondence between some of the low-energy states in the world-sheet spectrum and the BMN operators. The string excitations correspond to the insertions of the Higgs scalar ϕ^I to Z's. L is the angular momentum of the state in one of the angular directions in S^5 on the string side, while it is the R-charge on the gauge theory side.

(BMN) operators [32] and the energy eigenstates of the world-sheet Hamiltonian with light-cone quantization on the pp-wave background. See table I.1 for some examples of the correspondence for low-energy states in the spectrum. The operators are single-trace operators consisting of many complex fields $Z = \phi^1 + i\phi^2$ with insertions of real scalars ϕ^I. The lowest energy state of the string rotating with a certain angular momentum L in S^5 corresponds to the half-BPS operator consisting of a chain only of Z with length L. This means that the excitations on the string side correspond to the impurities inserted in the single-trace operator on the gauge theory side. The scaling dimensions are the analogues of masses in $\mathcal{N}=4$ SYM, which lacks the idea of masses due to its conformal symmetry, and indeed they correspond to the string mass on the string side. The BMN operators above the ground state are not BPS, and their dimensions are generally not protected under changes of the gauge coupling but receive some corrections which we call *anomalous dimensions*. The operators mix with each other in a certain closed sector once the higher-loop contributions are considered. One must diagonalize such operator mixing in order to compute the anomalous dimensions. It was found that the one-loop anomalous dimensions of the BMN operators consisting only of Higgs scalars can be computed as the eigenvalues of the Hamiltonian of an $SO(6)$ spin chain [131]. This spin chain is integrable, so the anomalous dimensions and various other physical aspects in the weak-coupling regime can be studied using techniques for integrable spin chains. We

will review the emergence of the one-loop $SO(6)$ spin chain in section I.4. Multi-trace operators consisting of a product of multiple traces can be interpreted as a bound state of multiple strings.

I.3 Integrable systems

Integrability is a precise notion for a system to be exactly solvable. It implies certain geometric and algebraic structures with enough symmetries that constrain the dynamics, and hence the differential equations associated with them can be integrated. Integrability can be defined for both classical and quantum systems. In either case, the system or the scattering processes can be factorized into the solvable one-body or two-body problems.

I.3.1 Classical integrability

The precise notion of integrability for a classical mechanical system was first introduced by Liouville, and the modern version of the theorem was formulated and proven by Arnold [10].

Arnold-Liouville Theorem *Consider a $2n$-dimensional symplectic manifold M with a symplectic structure ω. A set of n functions $\{f_i\}_{i=1,...,n}$ on M is an integrable system if the functions are*

- *independent of each other, in other words $df_1 \wedge df_2 \wedge \cdots \wedge df_n \neq 0$.*
- *pairwise in involution, namely $\{f_i, f_j\} = 0 \; \forall i, j = 1, ..., n$ where $\{\cdot, \cdot\}$ is the Poisson bracket with respect to ω.*

For a level set $M_c \equiv \{x \in M | f_i(x) = c_i\} \subset M$, an integrable system $\{f_i\}$ satisfies the following:

1. *M_c is invariant under the Hamiltonian flow generated by $H = f_1$ (and equivalently under flows by other functions f_i).*

2. *If M_c is compact and connected, it is diffeomorphic to an n-torus.*

3. *There exists a local coordinate system $\{\omega_i, \varphi_i\}_{i=1,\ldots,n}$ on M_c called action-angle coordinates, which satisfy*

$$\dot{\omega}_i \equiv \{\omega_i, H\} = 0, \quad \dot{\varphi}_i \equiv \{\varphi_i, H\} = \omega_i, \tag{I.3.1}$$

and hence can be integrated by quadratures.

Physically, the n independent conserved charges constrain the dynamics in the phase space and prohibit chaotic behavior. The system can be decomposed into n independent one-body systems associated to each pair of the action-angle coordinates.

I.3.2 Quantum integrability

Integrability of general quantum systems

This notion of integrability can be uplifted to quantum mechanical systems. Functions acting on a phase space are now replaced by Hermitian operators acting on a Hilbert space, and the Poisson brackets become the commutators of the operators. A quantum integrable system consists of infinitely many Hermitian operators Q_n (with Q_1 being the Hamiltonian H of the quantum system) that commute with each other, and so the dynamics is constrained by infinitely many charges.

From now on, we focus on a 1+1-dimensional quantum system. This makes the spatial ordering of particles well-defined independent of the frames. Consider the scattering process involving multiple particles with the initial state $|P_i(\theta_i)\rangle$ for incoming particles P_i, $i \in$ *incoming particles* with particle momenta p_i^μ and the final state $|P_f(\theta_f)\rangle$ for outgoing particles P_f, $f \in$ *outgoing particles* with momenta p_f^μ. θ is the rapidity of a particle specifying its momentum as

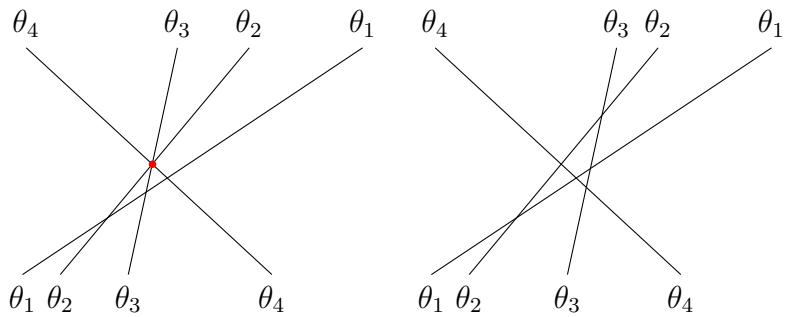

Figure I.5: (a) An example of a scattering process in an integrable system. The particle momenta are preserved during the process, so the world-lines can be represented as straight lines with the corresponding rapidities as their slopes. It has two-body interactions (line intersections) and one three-body interaction (a red dot). (b) The scattering process is invariant under parallel translations of world-lines. This allows the many-body interactions to be factorized into two-body interactions. For example, here the world-line for θ_3 is moved to the right so that the three-body interaction is resolved.

$$p^0 = m\cosh\theta, \quad p^1 = m\sinh\theta, \tag{I.3.2}$$

The infinitely many charges $\{Q_n\}$ constrain the sets of momenta for incoming and outgoing particles to be equivalent, $\{p_i^\mu\} = \{p_f^\mu\}$. There is no particle creation or annihilation, and the scattering processes can be represented with straight world-lines corresponding to the momenta in the set $\{p_i^\mu\} = \{p_f^\mu\}$ (e.g. fig. I.5a). A general scattering process can be described using an S-matrix

$$|P_{i_1}(\theta_{i_1})\cdots P_{i_n}(\theta_{i_n})\rangle = \sum_{j_1,\ldots,j_n} S_{i_1\cdots i_n}^{j_1\cdots j_n}\, |P_{j_1}(\theta_{j_1})\cdots P_{j_n}(\theta_{j_n})\rangle\,. \tag{I.3.3}$$

The S-matrices depend only on the difference between rapidities due to their Lorentz invariance. This means that different scattering processes with different orders of particle interactions but with the same particle orderings for the initial and final states should be equivalent. This invariance allows the particle world-lines to be moved around so that the scattering involves only two-body interactions (fig. I.5b). Therefore, any scattering

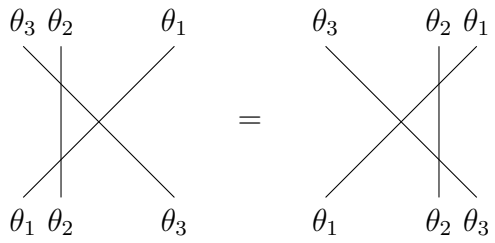

Figure I.6: The schematic representation of the Yang-Baxter equation eq. (I.3.4).

process in an integrable system can be factorized into a product of two-body interactions. The simplest case is the invariance of three-body scattering under the parallel translation of the world-line with the medium rapidity (fig. I.6). In terms of the two-body S-matrices,

$$\begin{aligned}&\sum_{k_1,k_2,k_3} S^{k_1k_2}_{i_1i_2}(\theta_1-\theta_2)S^{k_3j_3}_{k_2i_3}(\theta_1-\theta_3)S^{j_1j_2}_{k_1k_3}(\theta_2-\theta_3)\\&=\sum_{k_1,k_2,k_3} S^{j_1j_2}_{k_1k_3}(\theta_2-\theta_3)S^{k_3j_3}_{k_2i_3}(\theta_1-\theta_3)S^{k_1k_2}_{i_1i_2}(\theta_1-\theta_2),\end{aligned} \tag{I.3.4}$$

which is called the *Yang-Baxter (YB) equation*. Actually, the YB equation is a necessary and sufficient condition for the quantum system to be integrable. We will see the sufficiency in the next section.

Integrability of spin chains

Here, we review quantum integrability in more concrete settings: $1+1$-dimensional spin chains, which will be relevant for our later discussions. The spin chain is defined on a spatial lattice consisting of L sites, and each site has a finite-dimensional Hilbert space $\mathbb{C}^n$. The Hilbert space for the entire system is the tensor product $(\mathbb{C}^n)^{\otimes L}$. As an analogy to the S-matrix in the last section, we define an intertwiner known as the *R-matrix*, $R_{i,j}(u) : (\mathbb{C}^n)^{\otimes 2} \to (\mathbb{C}^n)^{\otimes 2}$. It is a function of the so-called spectral parameter u, which corresponds to the rapidity for the S-matrix case. The subscripts i and j denote the lattice site on which the R-matrix acts, and u is the rapidity parameter, just as in the S-matrix case. The R-matrix describes the interaction between two lattice sites, and can

be diagrammaticly represented as an intersection of two world-lines, where each line can also be interpreted as a single-site Hilbert space $\mathbb{C}^n$. The Yang-Baxter equation for a spin chain can be written using the R-matrices as

$$R_{i,i+1}(u)R_{i,i+2}(u+v)R_{i+1,i+2}(v) = R_{i+1,i+2}(v)R_{i,i+2}(u+v)R_{i,i+1}(u). \tag{I.3.5}$$

The R-matrix determines the dynamics of the system. To see that, we define a monodromy matrix $T(u)$ whose support is the tensor product of the physical Hilbert space $(\mathbb{C}^n)^{\otimes L}$ and an auxiliary space, which we choose to be identical to a single-site Hilbert space $\mathbb{C}^n$ for convenience:

$$T_a(u) = L_{a,L}(u)L_{a,L-1}(u)\cdots L_{a,1}(u), \tag{I.3.6}$$

where we defined the Lax operators $L_{i,j}(u) \equiv R_{i,j}(u - \frac{i}{2})$ for convenience, and a denotes the auxiliary space. The partial trace of $T_a(u)$ over the auxiliary space,

$$t(u) = \mathrm{tr}_a\, T_a(u) \tag{I.3.7}$$

is the transfer matrix. For later use, let us write the expansion of the transfer matrix in terms of the rapidity

$$t(u) = \sum_{n=0}^{L} Q_{n+1}u^n. \tag{I.3.8}$$

These matrices can be expressed diagrammaticly as in fig. I.7.

The monodromy matrix and the R-matrix satisfy the following equation:

$$T_a(u)T_b(v)R_{a,b}(u-v) = R_{a,b}(u-v)T_b(v)T_a(u), \tag{I.3.9}$$

which can be easily proven by applying the YB equations repetitively for each site

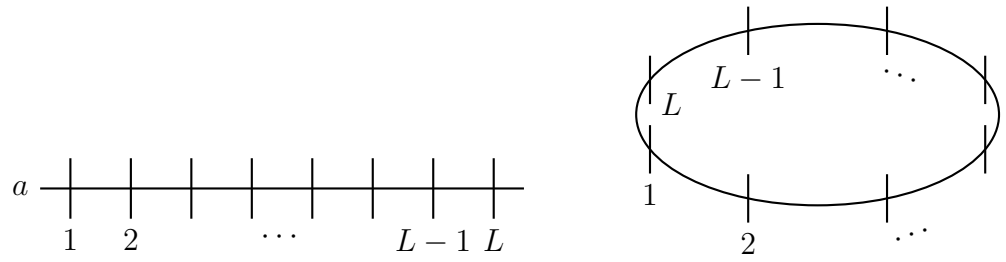

Figure I.7: (a) A pictorial representation of the monodromy matrix $T_a(u)$. Each vertical line represents the Hilbert space for each physical site, while the horizontal line corresponds to the auxiliary Hilbert space. Each vertex at the intersection of world-lines corresponds to the Lax operator acting on the two corresponding Hilbert spaces. (b) The transfer matrix $t(u)$ can be obtained by contracting both ends of the horizontal line of the monodromy matrix. This procedure corresponds to the partial trace over the auxiliary space.

(fig. I.8). Here, a and b are two distinct auxiliary spaces. Multiplying both sides of eq. (I.3.9) with $(R_{a,b}(u-v))^{-1}$ and taking the partial traces for the a and b spaces and using the cyclicity of the traces, one can conclude that the transfer matrices commute with each other:

$$[t(u), t(v)] = 0. \tag{I.3.10}$$

This is true if and only if all of the coefficients of the expansion eq. (I.3.8) commute with each other

$$[Q_n, Q_m] = 0. \tag{I.3.11}$$

Thus, if the quantum spin chain satisfies the YB equation, it must contain enough conserved charges (or infinitely many of them in the thermodynamic limit $L \to \infty$) $\{Q_n\}$ to constrain the dynamics of the system, and therefore it is integrable. In general, Q_2 is identified as the Hamiltonian H for spin chains with nearest-neighbor interactions.

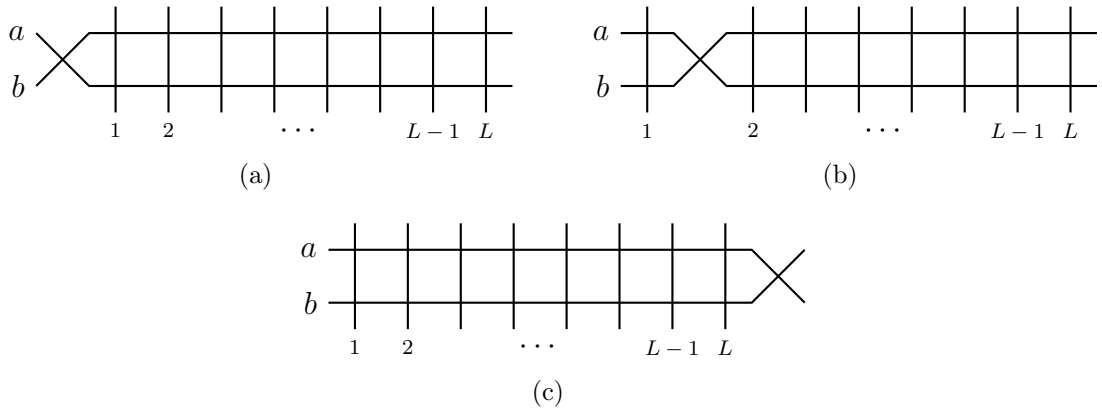

Figure I.8: (a) The diagram representing the left-hand side of eq. (I.3.9). The two rows represent the monodromy matrices $T_a(u)$ and $T_b(v)$, while the intersection of the horizontal lines on right is the R-matrix $R_{ab}(u-v)$. (b) Using the Yang-Baxter equation (one can easily find the equivalent equation involving one R-matrix and two Lax operators from eq. (I.3.5)), the R-matrix R_{ab} can be moved to the right. (c) By repeating it, the R-matrix ends on the left-most side, which corresponds to the right-hand side of eq. (I.3.9).

Algebraic Bethe ansatz

There are various approaches to compute the spectrum of the integrable spin chain Hamiltonian. Here, we focus on the use of the algebraic Bethe ansatz (also called the quantum inverse scattering method) for the Heisenberg spin chain Hamiltonian

$$H_{\mathrm{XXX}} = -4 \sum_{l=1}^{L} \left(\vec{S}_l \cdot \vec{S}_{l+1} - \frac{1}{4} \right) \tag{I.3.12}$$

with periodic boundary conditions as the simplest example for demonstration. $\vec{S}_l$ are the spin-1/2 operators acting on the l-th site. It can be constructed from the R-matrix

$$R_{i,j}(u) = u + iP_{i,j}, \tag{I.3.13}$$

where $P_{i,j}$ is the permutation matrix acting on the i-th and j-th sites. Let us write the components of the monodromy matrix constructed from this R-matrix in the auxiliary space as

$$T_a(u) = \begin{pmatrix} A(u) & B(u) \\ C(u) & D(u) \end{pmatrix}. \tag{I.3.14}$$

The matrices A, B, C, D act only on the physical Hilbert space, and the transfer matrix is $t(u) = A(u) + D(u)$. The state only with upspins $|\Omega\rangle \equiv |\uparrow\uparrow ... \uparrow\rangle$ is an eigenstate of the transfer matrix and therefore of the Hamiltonian since the matrices A, D act on it as

$$A(u)\,|\Omega\rangle = \left(u + \frac{i}{2}\right)^L |\Omega\rangle\,, \quad D(u)\,|\Omega\rangle = \left(u - \frac{i}{2}\right)^L |\Omega\rangle\,. \tag{I.3.15}$$

Also, it is annihilated by the C matrix. We call $|\Omega\rangle$ a Bethe reference state.

By writing the equation eq. (I.3.9) component by component, one obtains the commutation relations of the matrices

$$B(u)B(v) = B(v)B(u), \tag{I.3.16}$$

$$A(u)B(v) = \frac{u - v - i}{u - v} B(v)A(u) + \frac{i}{u - v} B(u)A(v) \tag{I.3.17}$$

$$D(u)B(v) = \frac{u - v + i}{u - v} B(v)D(u) - \frac{i}{u - v} B(u)D(v). \tag{I.3.18}$$

Some of the states orthogonal to $|\Omega\rangle$ can be generated by acting the B matrices with distinct spectral parameters on it:

$$|\vec{u}\rangle = B(u_1) \cdots B(u_K)\,|\Omega\rangle\,. \tag{I.3.19}$$

We want to find a choice of the spectral parameters $\vec{u}$ that makes $|\vec{u}\rangle$ an eigenstate. Acting $A(u)$ on $|\vec{u}\rangle$ from the left and moving it to the right using the commutation relation eq. (I.3.17), the contribution due to the first term of eq. (I.3.17) is parallel to $|\vec{u}\rangle$:

$$\left(u+\frac{i}{2}\right)^{L}\prod_{K=1}^{k}\frac{u-u_k-i}{u-u_k}\,|\vec{u}\rangle\,. \tag{I.3.20}$$

The contributions from the second term of eq. (I.3.17) are not parallel in general. The conditions for each spectral parameter so that the non-parallel terms to vanish are called the Bethe ansatz equations, namely

$$\left(\frac{u_j+i/2}{u_j-i/2}\right)^{L}=\prod_{k\neq j}^{K}\frac{u_j-u_k+i}{u_j-u_k-i}. \tag{I.3.21}$$

Thus, the problem of finding the energy spectrum is reduced to the algebraic problem of solving the system of L equations. The solutions of the Bethe ansatz equations are called the Bethe roots. One can make a similar argument to see how $D(u)$ acts on $|\vec{u}\rangle$, and indeed the state is also an eigenstate of $D(u)$ if $\vec{u}$ are the Bethe roots. Therefore, $|\vec{u}\rangle$ with the Bethe roots is an eigenstate of the transfer matrix, and so is it of the Hamiltonian.

I.3.3 Boundary integrability and integrable states

The discussion so far has considered the integrability of the system without any boundary effect, or the *bulk integrability*. One can extend the notion of integrability to the case involving a boundary. The requirement for boundary conditions to preserve the bulk integrability is that the set of the particle momenta does not change during the scattering process up to a spatial reflection. If the initial state is in the infinite past and the final state is in the infinite future, all incoming particles bounce at the boundary and change their parity while keeping the set of the masses and momenta, or namely the set of the rapidities satisfy

$$\{u_i\}=\{-u_f\}. \tag{I.3.22}$$

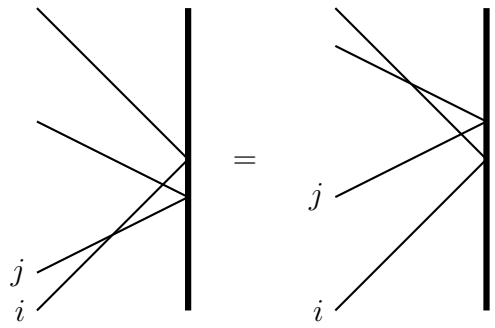

Figure I.9: The schematic representation of the boundary Yang-Baxter equation. The equation requires the invariance of the scattering under the parallel shift of one of the world-lines.

In other words, the boundary scattering must be elastic. The necessary and sufficient condition for such integrable boundaries is called the boundary Yang-Baxter (bYB) equation:

$$K_i(u)S_{ij}(u+v)K_j(v)S_{ij}(v-u) = S_{ij}(v-u)K_j(v)S_{ij}(u+v)K_i(u), \tag{I.3.23}$$

where $K_i(u)$ is the reflection matrix at the boundary for the particle i with rapidity u. This equation means that the boundary conditions do not violate the bulk integrability only if the scattering is still invariant under the parallel shift of world-lines even when they involve some reflections at the boundary (fig. I.9).

Integrable boundary states in the closed channel

One can also consider the channel rotation of the open system to treat it as a closed (periodic) system with a certain fixed initial state, or we call it a *boundary state*. Its integrability condition for spin systems was considered in [139]. To demonstrate the derivation of the condition, here we discuss the XXZ spin chain

$$H = \sum_{l=1}^{L} \left[S_l^x S_{l+1}^x + S_l^y S_{l+1}^y + \Delta(S_l^z S_{l+1}^z - 1) \right], \tag{I.3.24}$$

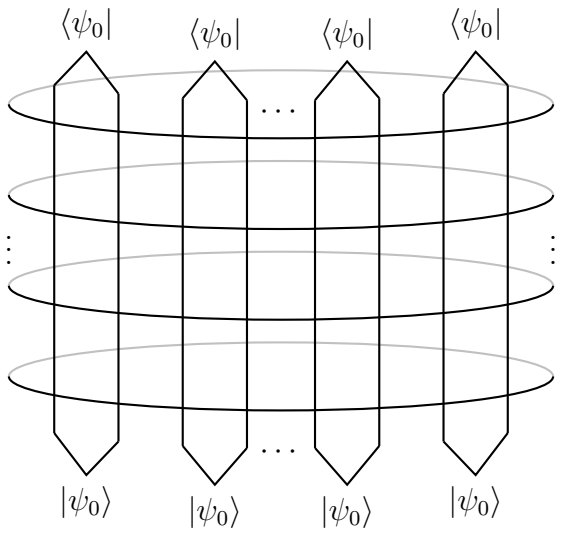

Figure I.10: The graphical representation of the discretized partition function eq. (I.3.26). The periodic direction is spatial, and the state evolves vertically with the Trotter-decomposed imaginary time evolution $e^{-\beta H}$.

where $S^{x,y,z}l$ are the spin-1/2 generators acting on the l-th site and Δ is the anisotropy. We assume that the length of the spin chain L is even from now on. We also choose the boundary state in the simplest possible structure for the discussion

$$|\Psi_0\rangle = |\psi_0\rangle^{\otimes L/2}\,, \tag{I.3.25}$$

where $|\psi_0\rangle \in \mathbb{C}^2 \otimes \mathbb{C}^2$ is a two-site state. We expect to be able to extend the resulting condition for general systems and initial states. Consider the partition function with this state as initial and final states, then the Euclidean time evolution can be discretized with infinitesimal imaginary time steps with the Trotter decomposition as

$$\langle\Psi_0|e^{-\beta H}|\Psi_0\rangle = \lim_{M\to\infty} \langle\Psi_0|\left(1-\frac{\beta}{M}H\right)^M|\Psi_0\rangle\,. \tag{I.3.26}$$

See fig. I.10 for its pictorial representation. This limit corresponds to the thermodynamic limit in the open channel. Each Trotter step can be written in terms of the transfer matrix [103, 104]

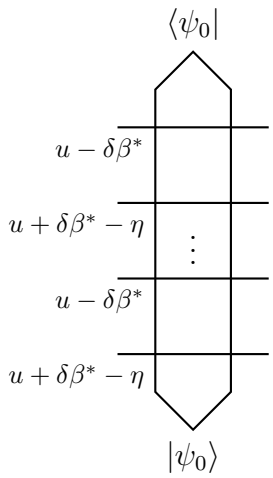

Figure I.11: $\mathcal{T}(u)$ in the factorization of the partition function eq. (I.3.28). The columns represent the quantum transfer matrix acting on the $2j+1$-th and $2j+2$-th sites, and each intersection corresponds to the R-matrix with the specified spectral parameter. Contracting the external horizontal legs with others gives the partition function fig. I.10.

$$1-\frac{\beta}{M}H \propto t(\delta\beta^*)t(\eta-\delta\beta^*) \tag{I.3.27}$$

up to some normalization, where $\delta\beta^* \equiv \beta\sinh\eta/4M$ with $\eta \equiv \operatorname{arccosh}\Delta$. Given the definition of the transfer matrix eq. I.3.7 and our assumption of the tensor product structure of $|\Psi_0\rangle$ (eq. (I.3.25)), the partition function can be factorized as

$$\langle\Psi_0|e^{-\beta H}|\Psi_0\rangle = \lim_{M\to\infty}\operatorname{tr}\bigl(\mathcal{T}(u)^{L/2}\bigr), \quad \mathcal{T}(u) \equiv \langle\psi_0|T^{\mathrm{QTM}}_{2j+1}(0)\otimes T^{\mathrm{QTM}}_{2j+2}(0)|\psi_0\rangle\,. \tag{I.3.28}$$

The *quantum transfer matrix* $T^{\mathrm{QTM}}_l(u)$ is defined as

$$T^{\mathrm{QTM}}_l(u) = R_{2M,l}(u-\delta\beta^*)R_{2M-1,l}(u+\delta\beta^*-\eta)\cdots R_{2,l}(u-\delta\beta^*)R_{1,l}(u+\delta\beta^*-\eta) \tag{I.3.29}$$

with the R-matrices whose one of the supports $(1,2,...,2M)$ is in the temporal direction and the other (l) in the spatial direction, which corresponds to fig. I.11. The exponent $L/2$ means matrix products or contractions of the indices in the temporal direction.

Now, let us consider the partition function in the open channel instead, which can

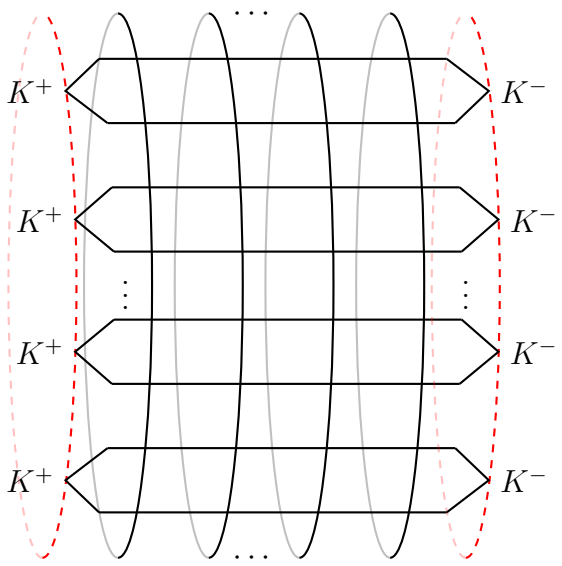

Figure I.12: The graphical representation of the partition function in the open channel.

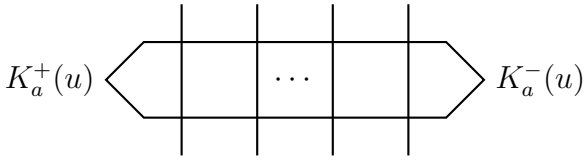

Figure I.13: The two-row transfer matrix eq. (I.3.30). Equating this with $\mathcal{T}(u)$ (fig. I.11), The local two-site state $|\psi_0\rangle$ can be related to the reflection matrices $K^{\pm}(u)$.

be formally written as $\mathrm{tr}\left(e^{-\tilde{\beta}H_{\mathrm{open}}}\right)$, where H_{open} is the XXZ spin chain Hamiltonian with boundary terms with the reflection matrices $K^{\pm}$ respectively taking account for the left and right boundary conditions (fig. I.12). The corresponding object to $\mathcal{T}(u)$ is the two-row transfer matrix (fig. I.13)

$$t_{K^{\pm}}(u) = \mathrm{tr}_a(K_a^+(u)T_a(u)K_a^-(u)\tilde{T}_a(u-\eta)), \tag{I.3.30}$$

where $K_a^{\pm}(u)$ are the left and right reflection matrices acting on the auxiliary space a.

The exact form of $K^{\pm}(u)$ can be determined by solving the bYB equations but is irrelevant to our discussion. $\tilde{T}_a(u)$ is the parity reflection of the monodromy matrix,

$$\tilde{T}_a(u) = R_{a,1}(u)R_{a,2}(u)\cdots R_{a,L}. \tag{I.3.31}$$

The partition function in the open channel can be calculated as the product of $t_{K^\pm}(u)$. In order for the partition functions in the open and closed channels to be equivalent, $\mathcal{T}(u)$ and $t_{K^\pm}(u)$ must be equivalent up to some normalization. This reduces to the relation between the state $|\psi_0\rangle$ and the reflection matrices by explicitly solving it for the components of the matrices and the states in the auxiliary space. Namely, $|\psi_0\rangle$ has to be

$$|\psi_0\rangle = -k^-_{12}(0)\,|\uparrow\uparrow\rangle + k^-_{11}(0)\,|\uparrow\downarrow\rangle - k^-_{22}(0)\,|\downarrow\uparrow\rangle + k^-_{21}(0)\,|\downarrow\downarrow\rangle\,, \tag{I.3.32}$$

where $k^-_{ij}(u)$ is the i,j-th element of $K^-(u)$, and a similar relationship can be found between $\langle\psi_0|$ and the elements of $K^+(u)$. To translate the bYB equation eq. (I.3.23) (with the R-matrices instead of the S-matrices) into the closed channel description, we generalize the initial state to be rapidity dependent

$$|\psi_0(u)\rangle = -k^-_{12}(u)\,|\uparrow\uparrow\rangle + k^-_{11}(u)\,|\uparrow\downarrow\rangle - k^-_{22}(u)\,|\downarrow\uparrow\rangle + k^-_{21}(u)\,|\downarrow\downarrow\rangle\,, \tag{I.3.33}$$

then the equation is equivalent to

$$\check{R}_{3,4}(v-u)\check{R}_{2,3}(-u-v)\,|\psi_0(u)\rangle\otimes|\psi_0(v)\rangle = \check{R}_{1,2}(v-u)\check{R}_{2,3}(-u-v)\,|\psi_0(v)\rangle\otimes|\psi_0(u)\rangle\,, \tag{I.3.34}$$

where $\check{R}_{i,j}(u) = P_{i,j}R_{i,j}(u)$ are the permuted R-matrices with the permutation matrix P_{ij} which exchanges the spins at the i-th and j-th sites. This equation schematically looks exactly like the channel rotation of the bYB equation (fig. I.14).

Now, we consider a chain on the tensor product of the physical Hilbert space with length L and two auxiliary sites a and b in the closed channel. Iteratively applying eq. (I.3.34) with $v=0$, we obtain an equation on the entire chain (fig. I.15)

$$\begin{aligned}&\check{R}_{b,L}(-u)\check{R}_{L,L-1}(-u)\cdots\check{R}_{2,1}(-u)\,|\psi_0(u)\rangle_{a,1}\otimes|\psi_0\rangle_{2,3}\otimes\cdots\otimes|\psi_0\rangle_{L,b}\\ &= \check{R}_{a,1}(-u)\check{R}_{1,2}(-u)\cdots\check{R}_{L-1,L}(-u)\,|\psi_0\rangle_{a,1}\otimes\cdots\otimes|\psi_0\rangle_{L-2,L-1}\otimes|\psi_0(u)\rangle_{L,b}\,.\end{aligned} \tag{I.3.35}$$

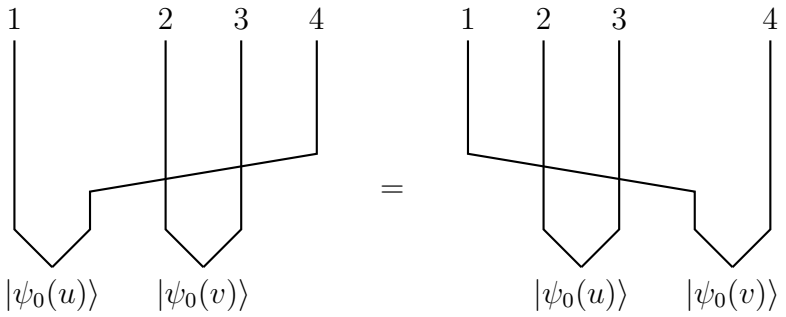

Figure I.14: A diagrammatic representation of eq. (I.3.34). It is easy to see that the diagram looks exactly like the channel rotation of the boundary Yang-Baxter equation fig. I.9.

By moving the permutation matrices in the permuted R-matrices to the right and acting them on the initial state, the equation reads

$$\begin{aligned} &R_{b,L}(-u)R_{b,L-1}(-u)\cdots R_{b,1}(-u)P_{a,b}\,|\psi_0(u)\rangle_{a,b}\otimes|\Psi_0\rangle \\ &= R_{a,1}(-u)R_{a,2}(-u)\cdots R_{a,L}(-u)P_{a,b}\,|\psi_0(u)\rangle_{a,b}\otimes|\Psi_0\rangle\,, \end{aligned} \tag{I.3.36}$$

where $|\Psi_0\rangle$ is the original initial state under consideration eq. (I.3.25) in the physical Hilbert space. By solving the equation component by component in the auxiliary spaces and taking the trace over them, we obtain

$$t(u)\,|\Psi_0\rangle = \Pi t(u)\Pi\,|\Psi_0\rangle\,, \tag{I.3.37}$$

where $\Pi t(u)\Pi = \mathrm{tr}_a(\tilde{T}_a(u)) = \mathrm{tr}_a[R_{a,1}(u)R_{a,2}(u)\cdots R_{a,L}]$. Diagrammatically, the derivation corresponds to connecting the external legs for the auxiliary spaces of fig. I.15a and fig. I.15c. The time ordering of the R-matrices acting on $|\Psi_0\rangle$ for each diagram determines the parity, and so the equivalence of the two diagrams leads to the parity invariance of $|\Psi_0\rangle$.

This is the general integrability condition for initial states, which is expected to hold even for more general cases than eq. I.3.25, such as matrix product states as shown also in [139]. Considering the expansion of the transfer matrix eq. (I.3.8), we obtain a slightly

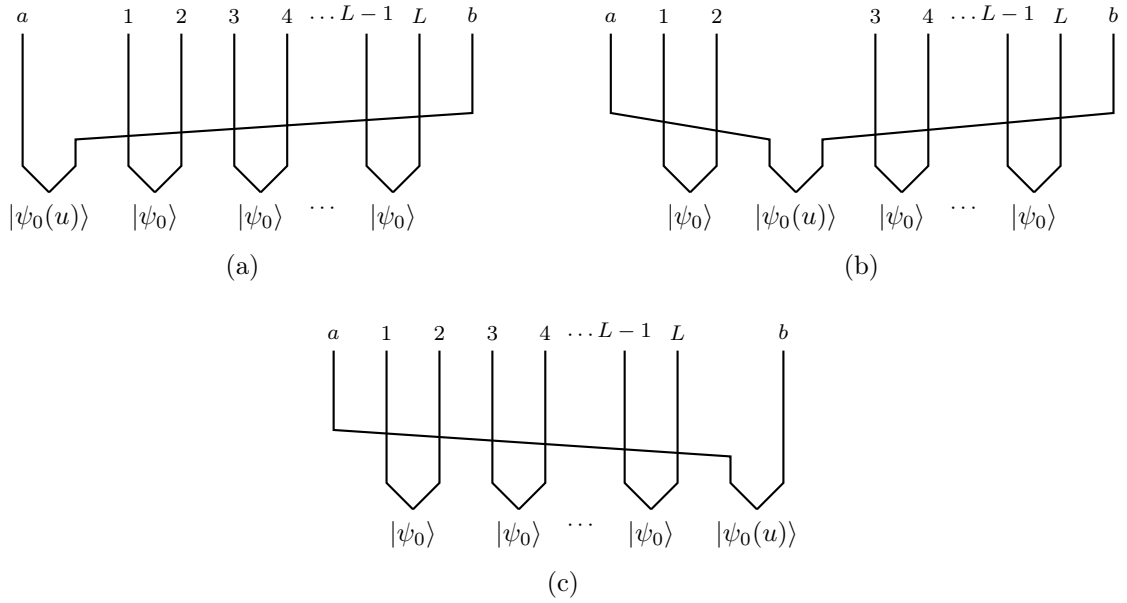

Figure I.15: A diagrammatic derivation of eq. (I.3.35). One side of the equation, which is depicted as (a), can be deformed into (b) using the channel rotation of the bYB equation eq. (I.3.34). By repeating this step globally, one obtains the other side of eq. (I.3.35) depicted as (c).

weaker version of the integrability condition

$$Q_{2n+1} |\Psi_0\rangle = 0, \quad \forall n = 1, ..., L/2 - 1 \tag{I.3.38}$$

namely, an integrable state must be annihilated by all of the odd charges, which transform under the parity reflection as $\Pi Q_{2n+1} \Pi = -Q_{2n+1}$. This weaker condition often gives enough constraints to study the states exactly, so some literature considers it a sufficient condition for integrability. It can also be justified given that the integrability condition for boundary states in QFTs derived in [68] can be interpreted as the annihilation of the state with infinitely many odd charges.

I.4 Integrable structures in the $\mathbf{AdS}_5 \times S^5/\mathcal{N} = 4$ SYM correspondence

Here, we review the integrable spin chain structure emerging in the one-loop calculations of anomalous dimensions in $\mathcal{N} = SYM$. We focus specifically on the $SO(6)$ sector, which is the most general sector of the single-trace operators consisting only of Higgs scalars. Integrable spin chain structures were also later found for the full $PSU(2,2|4)$ sector [21] and for higher-loop corrections [22]. The integrable behaviors of $\mathcal{N} = 4$ SYM reflect the integrability of the Green-Schwarz sigma model on the $\mathrm{AdS}_5 \times S^5$ spacetime [130] on the classical level [23] (and perhaps on the quantum level also). This sigma model takes the target space to be the coset

$$G/H = PSU(2,2|4)/(SO(1,4) \times SO(5)), \tag{I.4.1}$$

whose bosonic part is exactly $\mathrm{AdS}_5 \times S^5$. We consider the $SU(N)$ gauge group for the discussion in this section. Integrable structures of $\mathcal{N} = 4$ SYM with other types of Lie gauge groups, such as the orthogonal and symplectic groups, are considered in [43], for example.

I.4.1 Superconformal algebra $PSU(2,2|4)$

The components of the massless supermultiplet for $\mathcal{N} = 4$ supersymmetric theories are two vector fields, four Weyl fermions (i.e. eight fermionic d.o.f.), and six real Higgs scalars, which are all in the adjoint representation of $SU(N)$. The index of the adjoint representation is $T(\text{adj.}) = N$, so the 1-loop beta function eq. (I.1.1) vanishes. Even beyond 1-loop, it has been discussed that the beta function vanishes for all orders in the literature, such as [35] and [128]. Since the supermultiplet contains fields from spin-0 to spin-1, a non-gravitational $\mathcal{N} = 4$ theory has to be always a gauge theory. We have a

unique choice for such a gauge theory, which is $\mathcal{N} = 4$ SYM.

The global symmetry of $\mathcal{N} = 4$ SYM is $\mathcal{N} = 4$ superconformal symmetry $PSU(2, 2|4)$. Its bosonic part is the direct product of the four-dimensional conformal symmetry $SU(2, 2) \simeq SO(2, 4)$ and the R-symmetry $SU(4)_R \simeq SO(6)_R$. The conformal symmetry has fifteen generators: (i) one dilatation generator D, (ii) four translation generators $P\mu$, (iii) six Lorentz generators $M_{\mu\nu}$, and (iv) four special conformal transformation generators K_μ. Considering a local operator $\mathcal{O}(x)$ with scaling dimension Δ, i.e. it transforms as $\mathcal{O} \to \lambda^{-\Delta}\mathcal{O}$ under the scaling $x \to \lambda x$, then the action of the dilatation operator on this operator is

$$[D, \mathcal{O}(x)] = -i(\Delta - x^\mu \partial_\mu)\mathcal{O}(x). \tag{I.4.2}$$

The translation generator P_μ raises the dimension by 1 as

$$[D, [P_\mu, \mathcal{O}(0)]] = -i(\Delta + 1)[P_\mu, \mathcal{O}(0)], \tag{I.4.3}$$

while K_μ lowers the dimension by 1 as

$$[D, [K_\mu, \mathcal{O}(0)]] = -i(\Delta - 1)[K_\mu, \mathcal{O}(0)]. \tag{I.4.4}$$

The local operators in unitary conformal field theories must have a positive dimension unless it is an identity operator, which has zero dimension. An operator $\tilde{\mathcal{O}}$ with the lowest weight annihilated by K_μ as $[K_\mu, \tilde{\mathcal{O}}(0)] = 0$ is called a primary operator. Its descendants generated by acting P_μ on a primary with the primary itself span a Verma module.

The R-symmetry $SU(4)_R$ is a rank 3 Lie group, so its Cartan subalgebra has three commuting generators. Let us call the $SO(6)$ generators R^a with $a = 1, ..., 15$, and the generators of the Cartan subalgebra R^1, R^2, and R^3. Each operator is characterized by

the corresponding R-symmetry charges (J_1, J_2, J_3) under this symmetry.

The fermionic part of the superconformal symmetry is generated by sixteen supercharges $Q_{\alpha i}$ and $\tilde{Q}_b^j$ with the spinor indices $\alpha, \dot{\alpha} = 1, 2$ and $i, j = 1, ..., \mathcal{N} = 4$ and the sixteen superconformal charges S_α^i and $\tilde{S}_{\dot{\alpha}j}$. The supercharges have dimension $+1/2$, and the superconformal charges have dimension $-1/2$. The anticommutation relations between the supercharges and the superconformal charges are

$$\{Q_{\alpha i}, S_\beta^j\} = -i\epsilon_{\alpha\beta}(B^a)i^j R^a + \sigma_{\alpha\beta}^{\mu\nu}\delta_i^j M_{\mu\nu} - \frac{1}{2}\epsilon_{\alpha\beta}\delta_i^j D \tag{I.4.5}$$

$$\{\tilde{Q}_{\dot{\alpha}}^i, \tilde{S}_{\dot{\beta}j}\} = +i\epsilon_{\dot{\alpha}\dot{\beta}}(B^a)^i{}_j R^a + \sigma_{\dot{\alpha}\dot{\beta}}^{\mu\nu}\delta_j^i M_{\mu\nu} - \frac{1}{2}\epsilon_{\dot{\alpha}\dot{\beta}}\delta_j^i D \tag{I.4.6}$$

$$\{Q_{\alpha i}, \tilde{S}_{\dot{\beta}j}\} = \{\tilde{Q}_{\dot{\alpha}}^i, S_\beta^j\} = 0. \tag{I.4.7}$$

The matrices B^a are in the fundamental of $SU(4)$. Those corresponding to the Cartan generators are

$$B^1 = \begin{pmatrix} 1 & 0 & 0 & 0 \\ 0 & 1 & 0 & 0 \\ 0 & 0 & -1 & 0 \\ 0 & 0 & 0 & -1 \end{pmatrix}, \quad B^2 = \begin{pmatrix} 1 & 0 & 0 & 0 \\ 0 & -1 & 0 & 0 \\ 0 & 0 & 1 & 0 \\ 0 & 0 & 0 & -1 \end{pmatrix}, \quad B^3 = \begin{pmatrix} 1 & 0 & 0 & 0 \\ 0 & -1 & 0 & 0 \\ 0 & 0 & -1 & 0 \\ 0 & 0 & 0 & 1 \end{pmatrix}. \tag{I.4.8}$$

This gives the action on the scalar primary field to be

$$[\{Q_{\alpha i}, S_\beta^j\}, \tilde{\mathcal{O}}(0)] = \left[-i\epsilon_{\alpha\beta}(B^a)_i{}^j R^a - \frac{1}{2}\epsilon_{\alpha\beta}\delta_i^j D, \tilde{\mathcal{O}}(0)\right]. \tag{I.4.9}$$

The superconformal operators lower the dimension of an operator by $1/2$, so there exist primary operators that are annihilated by all the superconformal operators. For this kind of primary operators, the left-hand side of eq. (I.4.9) vanishes due to the Jacobi identity:

$$[\{Q_{\alpha i}, S_\beta^j\}, \tilde{\mathcal{O}}(0)] = \{[Q_{\alpha i}, \tilde{\mathcal{O}}(0)], S_\beta^j\} = 0. \tag{I.4.10}$$

χ	Δ	S_1	S_2	J_1	J_2	J_3
Z	1	0	0	1	0	0
W	1	0	0	0	1	0
X	1	0	0	0	0	1
ψ	$\frac{3}{2}$	$\pm\frac{1}{2}$	0	$\pm\frac{1}{2}$	$\pm\frac{1}{2}$	$\pm\frac{1}{2}$
$\overline{\psi}$	$\frac{3}{2}$	0	$\pm\frac{1}{2}$	$\pm\frac{1}{2}$	$\pm\frac{1}{2}$	$\pm\frac{1}{2}$
F_+	2	m	0	0	0	0
F_-	2	0	m	0	0	0

Table I.2: Field contents of $\mathcal{N}=4$ SYM and their charges under the bosonic subgroup $SO(2,4)\times SO(6)_R$. m takes a value of $m=0,\pm 1$.

This indicates that if the primary operator $\tilde{\mathcal{O}}(0)$ with dimension Δ has the R-charge $(J_1,J_2,J_3)=(\Delta,0,0)$, it is annihilated by $Q_{\alpha 1}$ and $Q_{\alpha 2}$. One can also show with a similar argument that they are annihilated by $\tilde{Q}^3_{\dot{\alpha}}$ and $\tilde{Q}^4_{\dot{\alpha}}$. These primary operators commuting with half of the supercharges are called *chiral primary operators* or half-BPS operators. Similarly, primary operators with R-charge $(J_1,J_2,J_3)=(0,\Delta,0)$ are also chiral primaries annihilated by $Q_{\alpha 1}$, $Q_{\alpha 3}$, $\tilde{Q}^2_{\dot{\alpha}}$ and $\tilde{Q}^4_{\dot{\alpha}}$, so are those with R-charge $(J_1,J_2,J_3)=(0,0,\Delta)$ annihilated by $Q_{\alpha 1}$, $Q_{\alpha 4}$, $\tilde{Q}^2_{\dot{\alpha}}$ and $\tilde{Q}^3_{\dot{\alpha}}$. In general, the local operators must satisfy the BPS bound $\Delta\geq J$, which is saturated only for the chiral primaries.

The operators in the theory are characterized by their representation under the bosonic subgroup $SO(2,4)\times SO(6)_R$: $(\Delta;S_1,S_2;J_1,J_2,J_3)$, where Δ is the dimension, S_1 and S_2 are the spins of the Lorentz group $SO(1,3)\sim SU(2)1\times SU(2)2$, and (J_1,J_2,J_3) are the R-charges. For the later use, let us introduce the complex scalar fields $Z=\frac{1}{\sqrt{2}}(\phi^1+i\phi^2)$, $Y=\frac{1}{\sqrt{2}}(\phi^3+i\phi^4)$ and $X=\frac{1}{\sqrt{2}}(\phi^5+i\phi^6)$, each of which has a unit R-charge $J_{1,2,3}=1$ respectively. We can split the field strength into the odd self-dual and even self-dual parts $F_\pm$ as $F^{\mu\nu}\pm=\pm\frac{1}{2}\epsilon^{\mu\nu\sigma\rho}F_{\pm\mu\nu}$. See table I.2 for the representations of the field contents. A single-trace operator is an example of a local gauge invariant operator constructed as a trace of the product of the covariant fields

$$\mathcal{O}(x)=\mathrm{Tr}[\chi_1(x)\chi_2(x)\cdots\chi_L(x)]. \tag{I.4.11}$$

One can also include covariant derivatives acting on the fields inside of the trace. The spectrum of the theory contains local operators as a product of multiple traces, called multi-trace operators. General local operators of $\mathcal{N} = 4$ SYM are linear combinations of these single- and multi-trace operators.

A single-trace operator consisting only of the Z field

$$\Psi_L := \mathrm{Tr}\big[Z^L\big] \tag{I.4.12}$$

with $L \geq 2$ is half-BPS, since its charge is $(L; 0, 0; L, 0, 0)$ satisfying the BPS condition $\Delta = J$. As we mentioned earlier, according to the BMN dictionary, this operator corresponds to the ground state of a rotating string with angular momentum L in a certain direction of S^5. A more general half-BPS operator can be constructed as the Schur polynomial $\chi_R(Z)$, where R is the gauge group representation of the operator. Its charge is also $(L; 0, 0; L, 0, 0)$, where L is the number of boxes in the Young tableau corresponding to R.

The dimension of an operator depends on the Yang-Mills coupling g_{YM} in general. $\Delta = \Delta_0$ at $g_{\mathrm{YM}} = 0$, i.e. in the free limit, is called the bare dimension of the operator. The correction γ to it after the coupling is turned on is called the anomalous dimension. The dimensions of half-BPS operators are protected due to the preserved supersymmetries, and so their anomalous dimensions are zero.

I.4.2 1-loop anomalous dimensions and spin chains

To find the anomalous dimension of an operator $\mathcal{O}$, it is convenient to consider the two-point correlator with itself $\big\langle \mathcal{O}(x)\overline{\mathcal{O}}(y)\big\rangle$. Let $\Delta = \Delta_0 + \gamma(g_{\mathrm{YM}})$ be the scaling dimension of $\mathcal{O}$ with the bare dimension Δ_0 and the correction γ from the nonzero coupling g_{YM}. At least in the weak-coupling region $g_{\mathrm{YM}} \ll 1$, the correction is small relative to the bare dimension $\gamma \ll \Delta_0$. In this region the correlator can be approximated as

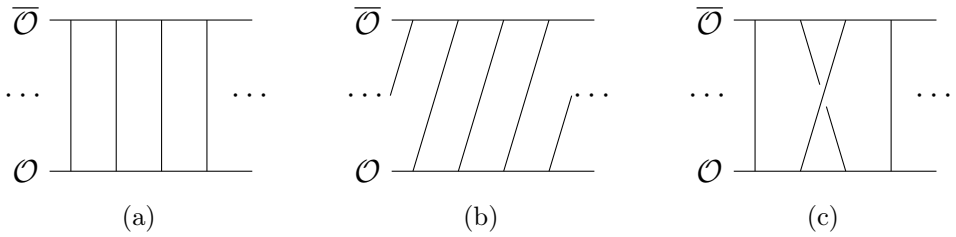

Figure I.16: (a) One of the tree-level planar diagrams for $\langle \mathcal{O}\overline{\mathcal{O}} \rangle$. (b) Another planar diagram. The indices are still in order. (c) Non-planar diagram, which is sub-leading in the large N limit.

$$\langle \mathcal{O}(x)\overline{\mathcal{O}}(y) \rangle \sim \frac{1}{|x-y|^{2\Delta}} \approx \frac{1}{|x-y|^{2\Delta_0}} \left[1 - \gamma \ln\left(\Lambda^2 |x-y|^2\right)\right]. \tag{I.4.13}$$

For our interest, we would like to compute the correlator $\left\langle \mathcal{O}_{I_1,\ldots,I_L}(x)\overline{\mathcal{O}}^{J_1,\ldots,J_L}(y) \right\rangle$ of a single-trace operator $\mathcal{O}_{I_1,\ldots,I_L}(x) = A_{I_1,\ldots,I_L} \operatorname{Tr}[\phi_{I_1}\phi_{I_2}\cdots\phi_{I_L}]$ consisting only of the Higgs scalars. These operators form the $SO(6)$ sector, which is closed under operator mixing up to one-loop corrections. The normalization factor $A_{I_1,\ldots,I_L}$ is chosen so that the two-point function of $\mathcal{O}$ with its conjugate is properly normalized. The propagator of the Higgs scalar fields is

$$\left\langle (\phi_I(x))^A_B (\phi_J(y))^{A'}B' \right\rangle = \frac{1}{8\pi^2}\delta_{IJ}\left(\delta^A_{B'}\delta^{A'}B - \frac{1}{N}\delta^A_B\delta^{A'}B'\right)\frac{1}{|x-y|^2}, \tag{I.4.14}$$

where A and B are the fundamental indices of the gauge group. We consider the large $N \to \infty$ limit from now on. Then, all the contributions due to the second term of the propagator proportional to $\delta^A_B\delta^{A'}_{B'}$ vanish. Also, as discussed in section I.2.2, only planar diagrams remain to contribute. At tree-level, each $\phi_{I_i}(x)$ is contracted with one of $\phi_{J_i}(y)$. For the diagram with such contractions to be planar, I's and J's have to be contracted in order as fig. I.16a and I.16b, but with no crossings like fig. I.16c. Hence, the tree-level correlator is

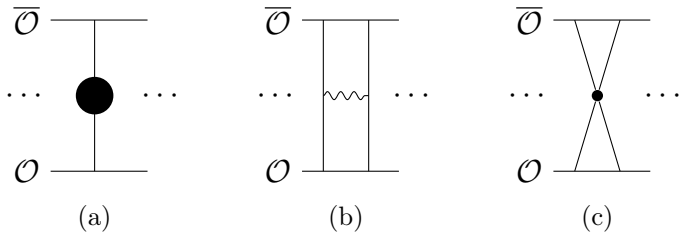

Figure I.17: (a) The 1-loop self-energy correction to the scalar correlator. (b) The 1-loop correction coming from the scalar-scalar-gauge interaction. (c) The correction coming from the quartic scalar interaction.

$$\left\langle \mathcal{O}_{I_1,\ldots,I_L}(x)\overline{\mathcal{O}}^{J_1,\ldots,J_L}(y)\right\rangle_{\text{tree}} = \frac{1}{C_{I_1,\ldots,I_L}}\sum_{c\in\mathbb{Z}_L}(\delta^{c(J_1)}I_1\delta^{c(J_2)}I_2\cdots\delta^{c(J_L)}I_L)\frac{1}{|x-y|^{2L}}, \tag{I.4.15}$$

where $\mathbb{Z}_L$ is a cyclic group of order L, and $C_{I_1,\ldots,I_L}$ is a symmetry factor which can be nontrivial when $I_1,\ldots,I_L$ is invariant under some cyclic shift, e.g. if they are invariant under a shift by some $n < L$ then $C_{I_1,\ldots,I_L} = L/n$, so that the two-point function is properly normalized.

The 1-loop diagrams replaces one of the propagators with the self-energy corrected one (fig. I.17a) or two of the neighborhood propagators with three- or four-point interactions (fig. I.17b and I.17c). Replacing non-neighboring correlators leads to a non-planar diagram. Overall, the one-loop correlator at the planar level is

$$\begin{aligned}&\left\langle \mathcal{O}_{I_1,\ldots,I_L}(x)\overline{\mathcal{O}}^{J_1,\ldots,J_L}(y)\right\rangle_{\text{1-loop}}\\ &= \frac{1}{|x-y|^{2L}}\left[1-\frac{\lambda}{16\pi^2}\ln\big(\Lambda^2|x-y|^2\big)\sum_{\ell=1}^{L}(2P_{\ell,\ell+1}-K_{\ell,\ell+1}-1+C)\right]\\ &\quad\times\sum_{c\in\mathbb{Z}_L}(\delta^{c(J_1)}_{I_1}\delta^{c(J_2)}_{I_2}\cdots\delta^{c(J_L)}_{I_L}),\end{aligned} \tag{I.4.16}$$

where $\lambda = g^2_{\text{YM}}N$ is the 't Hooft coupling, $P_{\ell,\ell+1} = \delta^{J_{\ell+1}}_{I_\ell}\delta^{J_\ell}_{I_{\ell+1}}$ is the exchange operator, and $K_{\ell,\ell+1} = \delta_{I_\ell I_{\ell+1}}\delta^{J_{\ell+1}J_\ell}$ is the trace operator. Comparing this to the approximation eq. (I.4.13), the anomalous dimension γ should be found as the eigenvalue of the operator

$$\Gamma = \frac{\lambda}{16\pi^2}\sum_{\ell=1}^{L}(2P_{\ell,\ell+1} - K_{\ell,\ell+1} - 1 + C), \tag{I.4.17}$$

while one can find the operator mixing as its eigenstate. This operator can be regarded as a spin-chain Hamiltonian. It has the $SO(6)$ symmetry and is indeed integrable [146], given that Γ is the charge Q_2 of eq. (I.3.8) where the transfer matrix is constructed from the R-matrix

$$R_{ij} = \frac{1}{n-2}[u(2u+2-n)I_{ij} - (2u+2-n)P_{ij} + 2uK_{ij}], \tag{I.4.18}$$

which satisfies the YB equation eq. (I.3.5). Since the chiral primaries like eq. (I.4.12) receive neither 1-loop corrections nor operator mixing, it is already an eigenstate of Γ with zero eigenvalue. Therefore, they can be considered as the reference state once Γ is solved with the Bethe ansatz.

I.4.3 Integrability of defects

A defect in a QFT introduces singular classical profiles to some of its field contents. For $\mathcal{N} = 4$ SYM, it generally corresponds to another set of D-branes that intersect nontrivially with the D3-branes on which the gauge theory lives. It is a natural question to ask whether the defect background, or equivalently the bound state of the D-branes, retains the integrability of the original $\mathcal{N} = 4$ SYM or the strings in $\mathrm{AdS}_5 \times S^5$. On the string theory side, the problem becomes the classification of integrable boundaries of the Green-Schwarz sigma model and their identification with the D-brane configurations. Some configurations are classified in [56].

Here, we review how to discuss this problem using the integrable spin chain that we derived in the last section. We focus on the D3-D5 bound state, which was the first and most understood example considered in the literature [116, 40, 54, 107]. It corresponds to

the codimension-one superconformal domain wall in $\mathcal{N} = 4$ SYM, where the gauge group is partially broken from $SU(N)$ on one side of the domain wall to $SU(N-k)$ on the other side. Defect integrability has been considered for other types of superconformal defects, including codimension-three defects, such as the 't Hooft loop [109], and codimension-two defects [87, 44]. We will discuss the codimension-two case in detail in chapter II.

The superconformal domain wall introduces nontrivial classical profiles to three of the six real Higgs scalars. The BPS equations corresponding to this defect are the Nahm equations

$$\frac{d\phi^I}{dz} = \frac{i}{2}\epsilon^{IJK}[\phi^J, \phi^K], \tag{I.4.19}$$

where z is the transverse distance from the domain wall, and ϵ^{IJK} with $I, J, K = 1, 2, 3$ is the Levi-Civita symbol. The other scalars $\phi^{4,5,6}$ remain zero. The solutions take values in the k-dimensional representation of the generators of the $\mathfrak{su}(2)$ algebra as

$$\phi^I = \frac{1}{z}\begin{pmatrix} t_k^I & 0 \\ 0 & 0 \end{pmatrix} \tag{I.4.20}$$

where t_k^I is the k-dimensional representation of one of the three generators of the $\mathfrak{su}(2)$ algebra, and the distance dependence $1/z$ makes the field singular on the domain wall. The fields take trivial classical values on one side of the domain wall maintaining the full $SU(N)$ gauge group, while they have these singular profiles on the other side, breaking the gauge symmetry to $SU(N-k)$.

The domain wall also partially breaks the $PSU(2,2|4)$ superconformal symmetry, so local operators may obtain nonzero vacuum expectation values. We will see that such local operators "probe" the integrability of the domain wall. Consider a linear combination of single-trace operators with the same bare dimension in the $SO(6)$ sector

$$\mathcal{O}(x) = \Psi_{I_1,\ldots,I_L} \operatorname{tr}\big[\phi^{I_1}(x)\cdots\phi^{I_L}(x)\big]. \tag{I.4.21}$$

The coefficients $\Psi_{I_1,\ldots,I_L}$ can be considered as a vector on which the dilatation operator Γ acts. Let us assume that we have diagonalized the 1-loop Γ with the Bethe ansatz method, and $\Psi_{I_1,\ldots,I_L}$ is a Bethe eigenstate corresponding to some Bethe roots $\vec{u}$. The one-point function at tree-level can simply be calculated by plugging the classical profiles of the Higgs scalars,

$$\langle\mathcal{O}(x)\rangle_{\text{tree}} = \Psi_{I_1,\ldots,I_L} \operatorname{tr}\big[\langle\phi^{I_1}(x)\rangle\cdots\langle\phi^{I_L}(x)\rangle\big] = \frac{1}{z^L}\Psi_{I_1,\ldots,I_L} \operatorname{tr}\big[t_k^{I_1}\cdots t_k^{I_L}\big]. \tag{I.4.22}$$

The contractions of the $I_1,\ldots,I_L$ indices can be expanded with Kronecker deltas $\delta_{I_l,J_l} = \langle I_l|J_l\rangle$ where $|I_l\rangle$ is a single-site $SO(6)$ spin state in the orthonormal basis. Then, the one-point function up to normalization is

$$\langle\mathcal{O}(x)\rangle_{\text{tree}} = \frac{1}{z^L}\langle\Psi|\text{MPS}\rangle, \tag{I.4.23}$$

where $|\Psi\rangle = \Psi_{I_1,\ldots,I_L}|I_1,\ldots,I_L\rangle$, and $|\text{MPS}\rangle = \operatorname{tr}\big[t_k^{I_1}\cdots t_k^{I_L}\big]|I_1,\ldots,I_L\rangle$. The matrix product state $|\text{MPS}\rangle$ can be interpreted as the state corresponding to the domain wall. Therefore, the integrability of the domain wall can be discussed by determining whether $|\text{MPS}\rangle$ satisfies the state integrability criterion discussed in section I.3.3 with Γ as the bulk Hamiltonian. Indeed, [54] showed that it satisfies condition eq. (I.3.37) for the $SO(6)$ sector.

In general, if the boundary state satisfies the integrability condition, it gives many constraints and selection rules to analytically determine the overlap $\langle\Psi|\text{MPS}\rangle$. For example, for the D3-D5 case, the overlap can be written in terms of the Baxter polynomials and the Gaudin determinants [116, 40, 54].

Chapter II: Integrability and Conformal Blocks for Surface Defects in $\mathcal{N} = 4$ SYM

II.1 Introduction

Integrability and holography are powerful tools for understanding the dynamics of strongly coupled large N gauge theories, leading to the solution of the spectral problem of planar maximally supersymmetric Yang-Mills theory [19]. At weak coupling, the mixing problem of single trace operators is equivalent to computing the spectrum of an integrable spin chain [131], mirroring the integrability of the classical sigma model on $AdS_5 \times S^5$ [23]. Similar ideas have been adopted for studying the planar limit of the ABJM theory [132, 13], which is dual to eleven-dimensional supergravity theory $AdS_4 \times \mathbb{CP}^3$ [4]. A more ambitious goal has been to use tools from integrability to compute CFT data beyond the spectrum, such as OPE data. This idea has had fruitful implementations in the context of a certain type of three-point correlators involving determinant operators [93, 163], and in defect CFTs (dCFTs) arising from extended operators [116, 71, 108, 109] (also refer to [111] for a review). In such set-ups the simplicity of the OPE data is closely associated with the integrability of the spin chain (or string) with open boundaries. These boundaries are often associated with D-branes wrapping maximal cycles at strong coupling,

and the OPE data encodes absorption/emission amplitudes of closed string states. The integrability of said boundary conditions was first exploited in the context of open string operators [31], but its role as an integrable boundary state was noticed in the computation of one-point functions in defect CFT. An important tool for this has been the notion of an integrable boundary, or quench, for spin chains [139]. Although the connection between integrable boundaries and integrable boundary states is not fully fledged for spin systems, a compelling picture exists connecting integrable matrix product states (MPS) to solutions of the boundary Yang-Baxter equation leading to new interesting integrable quenches. This technique has been useful for computing one-point functions of single trace operators with nontrivial boundary conditions both in $\mathcal{N} = 4$ SYM and in ABJM, such as various conformal domain wall setups [116, 40, 115, 54, 107], the dCFT associated to a supersymmetric Wilson/'t Hooft loop [109, 94], and cross-cap states [42], and also for computing correlation functions involving maximal giant gravitons [93, 163] or in the Coulomb branch [92]. The hope is that this data can be used to set-up a bootstrap program for higher point correlators [117, 11].

An interesting question is to classify all possible integrable boundaries that appear in $\mathcal{N} = 4$ SYM. Most of the work in this direction stems from strong coupling considerations [129, 56, 123, 122]. At weak coupling, determining whether a boundary condition is integrable involves constructing a solution to the corresponding boundary Yang-Baxter equation [57, 47, 31, 86, 52, 53] which in principle requires information about non-planar contributions to the dilatation operator. A more tractable approach is to instead check the selection rules satisfied by the corresponding boundary state and to use said state to construct a solution to the boundary Yang-Baxter equation. The precise integrability conditions of the boundary or quench state proposed in [139] are obtained by channel rotation of the boundary Yang-Baxter equation. In [114] a weaker condition was used to identify integrable matrix product states associated to defects in $\mathcal{N} = 4$ SYM, reproducing many of the integrable quenches for the $SO(m)$ Heisenberg chain. This was

done in an attempt to identify the integrable boundaries enumerated in [56]. While the integrable and BPS codimension one and three defects can be identified with the D3-D5 Nahm pole and with Wilson/'t Hooft loops operators, the codimension two cases remain to be studied in detail. The $AdS_3 \times S^5$ was argued to correspond to a fuzzy S^5 solution to the equations of motion [114], which leaves the case of $AdS_3 \times S^1$. Expectedly the dual of said integrable D-brane configuration must belong to the class of surface defects introduced in [82, 83], but it is a priori not clear which ones exactly. Part of the goal of this chapter is to address this issue.

The singular solutions describing a half-BPS defect on a two-dimensional surface in $\mathcal{N} = 4$ SYM were first found by Gukov and Witten [82] in order to introduce ramification to the gauge theory description of the geometric Langlands program. It is realized by probing D3 branes wrapping $AdS_3 \times S^1$ as long as the number of the probe branes is enough smaller than the gauge symmetry rank N [82, 61]. The supergravity description dual to the case where the backreaction is non-negligible was found shortly after that [77]. The one-point functions of half-BPS local operators on the gauge theory side were computed in [61], where it was confirmed that the leading-order term in weak-coupling perturbation matches with the highest-order term in the gravity result, i.e. in the strong-coupling regime. The finiteness of the expansion was further confirmed recently by [48]. The Gukov-Witten defects are somewhat peculiar in comparison to the other half-BPS supersymmetric defects. One important difference is the explicit dependence of the field profiles on the angular direction transverse to the defect due to the twisting of the spacetime and R-symmetries. This somewhat unusual feature results in correlation functions that have explicit dependence on the transverse angular direction for scalar operators of generic R-symmetry polarizations. This also has important consequences for the superconformal block decomposition of two-point correlation functions [119]. We elaborate on this point by solving the superconformal Ward identities for one-point and two-point functions involving chiral primaries. This is a first step towards

setting a bootstrap program for surface defects in $\mathcal{N} = 4$ SYM. To our knowledge this has not been elaborated on in the literature. Another feature is the appearance of continuous moduli; while most of the integrable defects known depend on discrete data such as the rank of the MPS, the GW defect admits a continuous moduli space parametrized by a set of central charges $(\mathfrak{Z}, \alpha, \eta)$. Most of the known integrable boundary states do not depend on continuous parameters[1] and indeed we find evidence for the breaking of integrability for generic points in the moduli space. We identify the integrable defect with a special point of the moduli space $\alpha = \mathfrak{Z} = 0$ at which the fields develop logarithmic behaviour signaling spontaneous breaking of scaling symmetry [83]. The defects at this singular point are rigid and the corresponding boundary state describes a fuzzy circle much like the other defects described by fuzzy spheres. Note that by rigid we simply mean that they do not depend on continuous parameters, rather than the rigidity condition required by [83]. Their condition is more strict in the sense that their conjugacy classes cannot be continuously deformed to nearby conjugacy classes. For $G = SU(N)$, the rigid surface defect we consider here obtained by setting $\alpha = \beta = \gamma = 0$ has the conjugacy class as the limit of that of the generic case, i.e. its hyperkähler moduli of the 2d Higgs branch in the corresponding 4d-2d description is nontrivial and hence the defect is non-rigid in their definition[2]. They are also singled out by the appearance of an additional dilatation mode associated to the spontaneously broken scaling symmetry.

This chapter is based on the results reported in [87] and is organized as follows. In section II.2, we review the disorder defect description of the Gukov-Witten defects, and comment on their holographic description. In section II.3, we derive the superconformal Ward identities relevant for the two-point functions of bulk chiral primaries. We use these in section II.4 to determine the form of the superconformal block expansion of

[1] A notable exception are the single site states relevant for Coulomb branch operators [92].

[2] [83] found the operators with rigid conjugacy classes for the $SO(N)$ and $Sp(N)$ gauge theories. There is a difference between $SO(2n)$ groups and $SO(2n+1)$ groups since the former is self-dual under S-duality while the latter is dual to $Sp(n)$. The difference comes from the existence of "discrete torsion" in the holographic description [160].

bulk two-point functions, and we also constraint the form of one-point function and bulk-to-defect two-point functions. In section II.5, we study one-point functions of non-protected operators at leading order in perturbation theory. We find that although scalar operators can be associated to an integrable boundary state, this integrability does not persist to sectors with spin due to the broken rotational symmetry transverse to the defect. This symmetry is restored in the rigid case and the resulting integrable states are analogous to those relevant for the D3-D5 interface and the maximal giant graviton. In section II.6, we review the quantization of the theory around a generic (non-rigid) defect by mapping it to a theory on $AdS_3 \times S^1$. In section II.7, we compute the leading-order contribution to the two point function of chiral primaries show that it organizes according to our superconformal block expansion by identifying the exchanged modes. Finally, we conclude and comment on future directions.

II.2 BPS Surface Defects

Before discussing the details of the Gukov-Witten defects, let us comment some generalities about defect conformal field theories. A defect CFT in $D+1$ dimensions is characterized by coupling a bulk CFT to a lower dimensional conformal theory living on a $p+1$-dimensional defect in a way that preserves the conformal invariance of the defect. In Euclidean signature, one usually places the defect along a hyperplane $\mathbb{R}^{p+1} \subset \mathbb{R}^{D+1}$ and the resulting space is conformally equivalent to $AdS_{p+2} \times S^{D-p-1}$:

$$ds^2 = \delta_{\mu\nu} dx^\mu dx^\nu + dr^2 + r^2 d\Omega^2 = r^2 \left(\frac{\delta_{\mu\nu} dx^\mu dx^\nu + dr^2}{r^2} + d\Omega^2 \right) \tag{II.2.1}$$

In the new conformal frame, the defect is placed at the boundary of AdS, while the original CFT lives in the bulk of the spacetime. The same coordinate transformation can be done in a Poincaré patch of the Lorentzian cylinder $\mathbb{R} \times S^D$, and the coordinates can be extended to global AdS coordinates. This formulation is useful since it makes

the residual conformal symmetry manifest as the spacetime isometry, and it gives a natural language for describing correlation functions in terms of Witten diagrams. Because the full conformal symmetry is partially broken, the operators of the bulk theory can have non-vanishing one-point functions. These nonzero one-point functions translate to nonzero asymptotic values of the field operators near the boundary of AdS. This implies that certain bulk operators can be associated with boundary operators by expanding the operator near the boundary:

$$\mathcal{O}_{\text{bulk}}(r,\vec{x},\Omega)=\frac{1}{r^{\Delta}}\sum_{\hat{\mathcal{O}}}\mathsf{b}_{\mathcal{O}\hat{\mathcal{O}}}r^{\hat{\Delta}}\hat{D}(r,\Omega,\partial_{\mu})\hat{\mathcal{O}}_{\text{bdy}}(\vec{x},\Omega)+\ldots, \tag{II.2.2}$$

where $\hat{D}$ are differential operations determined by the boundary conformal symmetry. This is the usual defect operator product expansion. For general codimensions, one can also expand the dependence of the operator on the normal coordinates to the defect by performing a mode expansion on S^{D-p-1}:

$$\hat{\mathcal{O}}_{\text{bdy}}(\vec{x},\Omega)=\sum_{J}\frac{x_{\perp}^{i_1}\ldots x_{\perp}^{i_J}}{r^J}\,\hat{\mathcal{O}}_{\text{bdy}}^{i_1\ldots i_J}(\vec{x}). \tag{II.2.3}$$

The resulting operators in the expansion are primary operators of the boundary (defect) theory. The leading term in the expansion $\mathsf{b}_{\mathcal{O}\hat{\mathbb{I}}}=\mathsf{a}_{\mathcal{O}}$ encodes the one-point functions of bulk operators, or equivalently the coupling to the identity operator of the defect theory. These new couplings are additional data necessary to specify the defect operators, and their values are generically not determined by conformal symmetry alone. However, their values are not completely independent of the conformal data of the bulk and defect due to constraints arising from the crossing equations. These constraints are a consequence of the fact that the two-point function of bulk primaries has two different expansions depending on whether the operators are first fused with the bulk OPE or first decomposed with the boundary-defect operator expansion. In either case, the kinematic dependence of the correlator is not fully fixed by conformal invariance, but the result can be expanded into bulk and defect conformal partial waves which give an infinite set of equations

relating bulk OPE coefficients to bulk-to-defect couplings.

The class of surface defects we will focus on are those introduced in [82, 83], although there are other maximally supersymmetric surface operators for the $\mathcal{N} = 4$ SYM theory. For a comprehensive review of maximally supersymmetric defects of general codimension, see [156]. This class of surface defects differs from the supersymmetric defects of codimension one and three in that they are generically parametrized by a continuous moduli. The coordinates of this moduli space are a set of central charges $(\mathfrak{Z}_I, \alpha_I, \eta_I)$. The parameters α_I and η_I are circled valued, and they encode information about the monodromy of line operators in the presence of the surface operator. These cannot be measured by the insertion of local operators, so they will not play a prominent role in our discussion. The remaining complex coordinate $\mathfrak{Z}_I$ parametrizes the expectation value of certain scalar operators. One well-studied observable is the one-point function of chiral primary operators in the presence of a surface defect [61, 48]. Such correlators are protected by supersymmetry and can be computed using techniques from supersymmetric localization; they have also been studied at strong coupling using holographic methods. Some results on correlators of the stress tensor $T^{\mu\nu}$ and the displacement operators $\mathbf{D}_{z,\bar{z}}$ in more general $\mathcal{N} = 2$ theories have been obtained [33] from their associated chiral algebras. Two-point functions of chiral primaries with surface defects have not been studied in detail, unlike the codimension-one case where a bootstrap program has been proposed [119], mainly due to the fact that the residual conformal symmetry of the Gukov-Witten is somewhat unconventional in that the transverse rotational symmetry is broken, which allows for a richer structure for correlation functions. More precisely, the residual symmetry of the system is $(PSU(1,1|2) \times PSU(1,1|2)) \ltimes SO(2)_t$, where the $SO(2)_t$ symmetry is a diagonal subgroup of the product $SO(2) \times SO(2)_R \subset SO(2,4) \times SO(6)$. In non-supersymmetric set-ups, the residual $SO(2)$ symmetry plays an important role in fixing the dependence of correlation functions of bulk operators on the angle transverse to the defect [34]. For instance, the one-point functions of operators carrying transverse spin

vanish in those cases, which is not the case for this Gukov-Witten dCFT. This also makes the defect conformal block expansion of bulk two-point functions more intricate.

II.2.1 Gukov-Witten Defect: Generic Case

The Gukov-Witten defect [82, 83] is an extended operator of the $\mathcal{N} = 4$ SYM theory defined on a codimension two surface. We will work with the theory in flat space $\mathbb{R}^4$ placing the defect along a two dimensional plane $\mathbb{R}^2 \subset \mathbb{R}^4$. Often we will use the complex coordinate z to denote the holomorphic coordinate normal to the defect. The defect can be described by a singular boundary condition on the fields of the theory, we will concentrate on the case in which the defect preserves one-half of the supersymmetries which corresponds to the breaking of the full $PSU(2,2|4)$ symmetry to $(PSU(1,1|2) \times PSU(1,1|2)) \ltimes SO(2)_t$[3]. The details of the embedding of the residual symmetry to the bulk symmetry are discussed in the next section. The bosonic part of this residual symmetry is $SO(2,2) \times SO(4)_R \times SO(2)_t$. The two copies of $PSU(1,1|2)$ respectively contain the holomorphic and antiholomorphic parts of the two-dimensional conformal symmetry $SO(1,3)$, as well as they contain each of the left and right $SU(2)$ components of $SO(4)_R$. The $SO(2)_t$ symmetry is the diagonal part of the direct product of the spacetime and R-symmetry rotations in the transverse directions. Vanishing of the flux of the supercurrent through the defect imposes the BPS equations:

$$\begin{aligned} F_{z\bar{z}} + [Z, \bar{Z}] &= 0 \\ D_{\bar{z}} Z &= 0, \end{aligned} \tag{II.2.4}$$

where $Z = \phi_1 + i\phi_2$[4]. They are exactly Hitchin's equations obtained by dimensional reduction of the parallel directions to the defect. Solutions consistent with classical scale invariance are of the form

[3]Another way of describing this surface defect is by coupling the two-dimensional $\mathcal{N} = (4,4)$ superconformal sigma model or quiver gauge theory to the four-dimensional theory. The target space of this sigma model is the moduli space of the solutions of Hitchin's equations. This 4d-2d description is studied in detail in [82, 65, 66].

[4]We take the convention where all the adjoint fields take Hermitian values.

$$Z = \frac{\phi_1 + i\phi_2}{\sqrt{2}} = \frac{\beta + i\gamma}{z} \qquad \text{(II.2.5)}$$
$$A_\psi = \alpha d\psi,$$

where z is the coordinate normal to the defect and $z = re^{i\psi}$. We choose a specific gauge where the part of the gauge field A proportional to dr vanishes. The parameters α, β, γ are commuting matrices in the Lie algebra $\mathfrak{su}(N)$. Specifically, they take values in either the Cartan subalgebra $\mathfrak{t}$ of $\mathfrak{su}(N)$ or the maximal torus $\mathbb{T}$:

$$(\alpha, \beta, \gamma) \in (\mathbb{T},\, \mathfrak{t},\, \mathfrak{t})/W_{\mathbb{L}} \qquad \text{(II.2.6)}$$

$\mathbb{L} = S(\prod_{l=1}^{M} U(N_l))$ $(\sum_{l=1}^{M} N_l = N)$ is the Levi subgroup of $SU(N)$, and the gauge symmetry breaking pattern is specified by the values of the diagonal elements of α, β, γ to be $SU(N) \to \mathbb{L}$. We take the quotient by the Weyl group $W_{\mathbb{L}}$ to account for the equivalence under the exchanges of the Cartan elements having the same values in α, β, γ. This is a consequence of the BPS equations, and the description is semiclassical. In other words, the insertion of the surface operator leads to a new saddle of the path integral; these are classical solutions to the equations of motion with the correct charges. The quantum description of the surface operator is as a boundary condition for the field operators at the location of the defect in the path integral. There is also an additional parameter η, taking a value in the maximal torus of the Langlands dual of the gauge group, associated with theta terms on the defect but they will not be important for our discussion.

Holographic dual of the generic case

The Gukov-Witten defect is holographically dual to M stacks of D3 branes wrapping an $AdS^3 \times S^1$ inside of $AdS_5 \times S^5$. There are two ways of describing these D3 branes, either as probes or as a solution to type IIB supergravity. To describe the probe, which is valid as long as the number of the intersecting D3-branes is much smaller than N, one chooses

a slicing of $AdS_5 \times S^5$:

$$ds^2 = \frac{\cosh^2 u}{r^2}\left(-dt^2 + dx_1^2 + dr^2\right) + du^2 + \sinh^2 u d\psi^2 + d\Omega_5^2. \tag{II.2.7}$$

The branes sit at a constant non-zero value of u_0 and at an equator of the S^5 with coordinate $\phi = \phi_0 - \psi$. The induced metric on the brane is that of an $AdS_3 \times S^1$ of size $\cosh u_0$, and the moduli of the defect are identified with the position of the probes as

$$\beta + i\gamma = \frac{\sqrt{\lambda}}{4\pi} \sinh u_0 \, e^{i\phi_0}. \tag{II.2.8}$$

When the number of branes is comparable to N, the more appropriate description is in terms of a backreacted background. The dual supergravity solutions were found in [77] by analytic continuation of the LLM solutions [121]:

$$\begin{aligned} ds^2 &= \mathcal{H}^{-2}\left[\left(\zeta + \frac{1}{2}\right) ds^2_{AdS_3} + \left(\zeta - \frac{1}{2}\right) d\Omega_3^2 + (d\psi + V)^2\right] + \mathcal{H}^2(dy^2 + d\xi_i^2) \\ \mathcal{H} &= \frac{\sqrt{\zeta^2 - \frac{1}{4}}}{y}. \end{aligned} \tag{II.2.9}$$

The metric is fully fixed in terms of a single function $\zeta(\xi_i, y)$ whose domain is $\mathbb{R}^2 \times \mathbb{R}_+$, satisfying an $SO(4)$ symmetric Poisson's equation in six-dimensions. The boundary conditions considered in [77] are specified in terms of a set of M point charges in this three-dimensional base space. The coordinate ψ smoothly degenerates at these points, and the local geometry is that of a Taub-NUT space around the sources. Note that this is qualitatively different from the boundary conditions for LLM geometries which are specified by a boundary condition at $y = 0$ where different S^3 cycles degenerate smoothly. The resulting space is smooth and is a result of fibering $AdS_3 \times S^3 \times S^1$ on a three-dimensional base space $\mathbb{R}^2 \times \mathbb{R}_+$. The isometry of the fiber is exactly the bosonic part of the residual symmetry $SO(2,2) \times SO(4) \times SO(2)$. The gauge symmetry breaking of $\mathcal{N} = 4$ SYM theory is characterized by the point charge sources in $\mathbb{R}^2 \times \mathbb{R}_+$, where the S^1 direction becomes degenerate. More specifically, the dimension of each of the diagonal

blocks of the Levi subgroup corresponds to the position of the particle in $\mathbb{R}_+$. The Higgs scalar VEVs are exactly the positions in $\mathbb{R}^2$. α and η correspond to the holonomies of two-form NS-NS and R-R gauge fields around the disks starting from each of the particles and ending on the asymptotic boundary.

II.2.2 Residual Symmetry

Now we review aspects of the residual symmetry $PSU(1,1|2)^2 \ltimes SO(2)_t$. The four fermionic generators for each of the $PSU(1,1|2)$ groups are explicitly written down for example in [156]. They can be found by solving the Killing spinor equations $\Gamma^{1245}\epsilon_\pm = \epsilon_\pm$ regarding the supersymmetry equations for this half-BPS configuration. We follow the notations in [156] for the bulk $PSU(2,2|4)$ generators to express the residual symmetry generators, except the R-symmetry charges are indexed with the $SO(6)$ vector indices $I = 1, 2, ..., 6$, instead of the 10d notations[5]. The fermionic generators of the two copies of $\mathfrak{psu}(1,1|2)$ in terms of the full bulk algebra $\mathfrak{psu}(2,2|4)$ are

$$\begin{aligned}
\hat{Q}_{1a} &= \frac{1}{\sqrt{2}}(Q_{1a\dot{a}} - i(\sigma^1)^{\dot{b}}{}_{\dot{a}} Q_{1a\dot{b}}), \quad \hat{\bar{Q}}_{1a} = \frac{1}{\sqrt{2}}(\bar{Q}_{1a\dot{a}} - i(\sigma^1)^{\dot{b}}{}_{\dot{a}} \bar{Q}_{1a\dot{b}}), \\
\hat{S}_{1a} &= \frac{1}{\sqrt{2}}(S_{2a\dot{a}} - i(\sigma^1)^{\dot{b}}{}_{\dot{a}} S_{2a\dot{b}}), \quad \hat{\bar{S}}_{1a} = \frac{1}{\sqrt{2}}(\bar{S}_{2a\dot{a}} - i(\sigma^1)^{\dot{b}}{}_{\dot{a}} \bar{S}_{2a\dot{b}})
\end{aligned} \tag{II.2.10}$$

and

$$\begin{aligned}
\hat{Q}_{2a} &= \frac{1}{\sqrt{2}}(Q_{2a\dot{a}} + i(\sigma^1)^{\dot{b}}{}_{\dot{a}} Q_{2a\dot{b}}), \quad \hat{\bar{Q}}_{2a} = \frac{1}{\sqrt{2}}(\bar{Q}_{2a\dot{a}} + i(\sigma^1)^{\dot{b}}{}_{\dot{a}} \bar{Q}_{2a\dot{b}}), \\
\hat{S}_{2a} &= \frac{1}{\sqrt{2}}(S_{1a\dot{a}} + i(\sigma^1)^{\dot{b}}{}_{\dot{a}} S_{1a\dot{b}}), \quad \hat{\bar{S}}_{2a} = \frac{1}{\sqrt{2}}(\bar{S}_{1a\dot{a}} + i(\sigma^1)^{\dot{b}}{}_{\dot{a}} \bar{S}_{1a\dot{b}})
\end{aligned} \tag{II.2.11}$$

We choose the basis with $a = \dot{a}$ on the right-hand side. We further package these odd generators together with the bosonic generators on a new basis as

[5]Here we define $Q(\tilde{Q})$ and $S(\tilde{S})$ as the (anti)chiral generators in terms of the 4d chiral operator γ^5, and the Q operators and S operators are distinguished in terms of the 10d chiral operator Γ^{11}.

$$\left(\begin{array}{c|c} (\mathfrak{L}_i)^{\alpha}{}_{\dot\alpha} & (\mathfrak{Q}_i)^{\alpha}{}_{a} \\ \hline (\mathfrak{S}_i)^{\dot a}{}_{\dot\alpha} & (\mathfrak{R}_i)^{\dot a}{}_{a} \end{array}\right), \quad (\mathfrak{Q}_i)^{\alpha}{}_{a} = \begin{pmatrix} \hat{Q}_{i1} & \hat{Q}_{i2} \\ \hat{\tilde{S}}_{i1} & \hat{\tilde{S}}_{i2} \end{pmatrix}, \quad (\mathfrak{S}_i)^{\dot a}{}_{\dot\alpha} = \begin{pmatrix} \hat{S}_{i2} & -\hat{\tilde{Q}}_{i2} \\ \hat{S}_{i1} & -\hat{\tilde{Q}}_{i1} \end{pmatrix} \tag{II.2.12}$$

The bosonic generators of $\mathfrak{g}_0 = \mathfrak{su}(1,1) \oplus \mathfrak{su}(2) \subset \mathfrak{psu}(1,1|2)$ are, in terms of the full $\mathfrak{psu}(2,2|4)$ algebra generators,

$$\begin{aligned} (\mathfrak{L}_i)^{\alpha}{}_{\dot\alpha} &= \frac{1}{2}\begin{pmatrix} \pm D + iM_{34} & -2P_{1\dot 1} \\ 2K_{2\dot 2} & -(\pm D + iM_{34}) \end{pmatrix}, \\ (\mathfrak{R}_i)^{\dot a}{}_{a} &= \frac{1}{2}\begin{pmatrix} i(\pm R_{62} - R_{14}) & -(R_{43} \pm R_{56} + i(R_{53} \mp R_{46})) \\ (R_{43} \pm R_{56} + i(R_{53} \mp R_{46})) & -i(\pm R_{62} - R_{14}) \end{pmatrix} \end{aligned} \tag{II.2.13}$$

The signs on top are for the first copy $i = 1$ and the ones on bottom are for the second copy $i = 2$. One can verify the $\mathfrak{psu}(1,1|2)$ algebra in this basis as

$$\begin{aligned} &\{(\mathfrak{Q}_i)^{\alpha}{}_{a}, (\mathfrak{Q}_i)^{\beta}{}_{b}\} = 0, \quad \{(\mathfrak{S}_i)^{\dot a}{}_{\dot\alpha}, (\mathfrak{S}_i)^{\dot b}{}_{\dot\beta}\} = 0 \\ &\{(\mathfrak{Q}_i)^{\alpha}{}_{a}, (\mathfrak{S}_i)^{\dot b}{}_{\dot\beta}\} = \delta^{\dot b}_{a}(\mathfrak{L}_i)^{\alpha}{}_{\dot\beta} + \delta^{\dot\beta}_{\alpha}(\mathfrak{R}_i)^{\dot b}{}_{a} + \delta^{\dot b}_{a}\delta^{\dot\beta}_{\alpha}\mathfrak{C} \end{aligned} \tag{II.2.14}$$

This choice of the basis we made is for being consistent with the notations for $\mathfrak{psu}(2|2)$ in [20]. $\mathfrak{C}$ is the generator of the central extension $SO(2)_t$ common to both algebras, which is identified to be $i(M_{12} + R_{12})$. Representations of this algebra can be constructed using two copies of representations of $\mathfrak{sl}(2|2)$ by setting their central charges to be equal to each other. More details on the representations of the residual algebra are given in appendix II.C. One important feature of the algebra $\mathfrak{psl}(2|2)$ is that we can turn on two other central extensions besides $\mathfrak{C}$:

$$\begin{aligned} \{(\mathfrak{Q}_i)^{\alpha}{}_{a}, (\mathfrak{Q}_i)^{\beta}{}_{b}\} &= \epsilon^{\alpha\beta}\epsilon_{ab}\mathfrak{P}, \\ \{(\mathfrak{S}_i)^{\dot a}{}_{\dot\alpha}, (\mathfrak{S}_i)^{\dot b}{}_{\dot\beta}\} &= \epsilon_{\dot\alpha\dot\beta}\epsilon^{\dot a\dot b}\mathfrak{K}. \end{aligned} \tag{II.2.15}$$

The two additional extensions play a key role in determining the asymptotic spectrum of closed string states and of open strings attached to giant gravitons [20, 24]. The centrally extended algebra has an additional $\mathfrak{sl}(2,\mathbb{C})$ outer automorphism that can be used to relate

the representations of the algebra without central extensions to the centrally-extended case. For the defect algebra this outer automorphism acts as $SU(2)_a$ transformation that leaves the norm of the vector $(\mathfrak{C}, \mathfrak{P}, \mathfrak{K})$ invariant. For the surface operator, the defect moduli $(\mathfrak{Z}, \mathfrak{Z}^\dagger)$ plays the role of these central extensions. The BPS representations of the centrally extended algebra satisfy shortening conditions involving $\mathfrak{C}^2 + |\mathfrak{P}|^2$ whose eigenvalues we can associate to $\ell^2 + |\mathfrak{Z}_{ij}|^2$, where ℓ is the spin of the operator along the transverse directions to the defect. This leads to composite defect operators with dimensions

$$\hat{\Delta} + S = \sum_{i,j} \sqrt{\ell^2 + |\mathfrak{Z}_{ij}|^2}. \tag{II.2.16}$$

We will see that these are precisely the off-diagonal fluctuations of the $\mathcal{N} = 4$ SYM fields. The physical operators do not carry the central charge $\mathfrak{P}$ due to gauge invariance.

II.2.3 Singular Limit $\alpha, \beta, \gamma \to 0$: Fuzzy Circle Solutions

The insertion of the surface operator is supposed to introduce singularities for some of the fields, but naively taking the limit $\alpha, \beta, \gamma \to 0$ leaves no divergent fields. This naive assumption is false given that the moduli space has an additional branch corresponding to another family of less divergent solutions for the BPS equations [82, 83]. We can rewrite the BPS equations by introducing a one-form $\phi = Zdz + \bar{Z}d\bar{z}$ and the field strength $F = F_{z\bar{z}}dz \wedge d\bar{z}$, and the covariant derivative $d_A = d - iA$ as

$$\begin{aligned} F - i\phi \wedge \phi &= 0 \\ d_A\phi &= 0 \\ d_A \star \phi &= 0. \end{aligned} \tag{II.2.17}$$

One can assume the general form of the solutions with rotational invariance in the transverse directions to the defect as

$$\begin{aligned} \phi &= a_1(r)\frac{dr}{r} + a_2(r)d\psi \\ A &= a_3(r)d\psi \end{aligned} \tag{II.2.18}$$

We again choose a gauge so that the dr part of the gauge field A vanishes. Changing variables to $\rho = -\log(r/\Lambda)$, the BPS equations reduce to a set of Nahm equations

$$\frac{da_a}{d\rho} = -i\epsilon^{abc}[a_b, a_c]. \tag{II.2.19}$$

The field profile is related to the one-point function of the relevant operator in the defect background, so we usually assume that a_i are constants to be consistent with conformal symmetry. This assumption is exactly what we made for the generic case we considered in Sec. II.2.1. However, solutions with ρ dependence are still consistent with conformal symmetry, provided the scale Λ is treated as a zero mode. These solutions are of the form

$$a_i = \frac{t_i}{\rho}, \tag{II.2.20}$$

where t_i satisfy an $SU(2)$ algebra. Now, field profiles contain an additional logarithmic behavior near $r = 0$. This multiplicative factor can be interpreted as an additional dilatation mode of the defect. Naively this field profile breaks conformal invariance due to the appearance of a cut-off scale Λ, but the value of Λ is unphysical since it can be set to any value by using scaling transformations. A more precise statement is that the field profile of the scalar field depends on the zero value of a dilaton mode $\chi_0(r) = 1/\log(r/\Lambda)$

$$Z^{cl} = \frac{e^{-i\psi}}{2r}(t_1 - it_2)\,\chi_0(r) \tag{II.2.21}$$

This mode appears as a Goldstone boson for the spontaneously broken scaling symmetry. As explained in [83], the correct treatment in this case is to quantize the theory in the presence of this dilaton mode. In other words, including the fluctuations of this field restores the scaling symmetry. In practice, this means that we should couple the theory to a dynamical dilaton field which replaces the derivatives with respect to r with a Weyl connection [134]. The logarithmic divergence alleviates the leading singularity in the $r \to 0$ limit, so these solutions appear near the defect only when the leading divergent terms

disappear. The logarithmic behavior of the correlators should be interpreted as operator mixing due with the dilaton. Now the surface defect is labeled by a representation of $SU(2)$ and a map $\pi:\ SU(2)\to U(N)$. We will refer to this class of defects as *rigid* since they do not depend on continuous moduli.

One important distinction of these solutions to the generic defect is that the $SO(2)_R$ symmetry is no longer broken. The scalar field profiles near the defect are given by

$$\begin{aligned}
\phi_1^{cl} &= \frac{1}{r\log r/\Lambda}\left[t_1\cos\psi - t_2\sin\psi\right] = \chi_0(r)\frac{\mathcal{U}_\psi^\dagger t_1 \mathcal{U}_\psi}{r} = \chi_0(r)\tilde{\phi}_1^{cl} \\
\phi_2^{cl} &= \frac{1}{r\log r/\Lambda}\left[t_1\sin\psi + t_2\cos\psi\right] = \chi_0(r)\frac{\mathcal{U}_\psi^\dagger t_2 \mathcal{U}_\psi}{r} = \chi_0(r)\tilde{\phi}_2^{cl} \\
A_\psi^{cl} &= \chi_0(r)t_3 = \chi_0(r)\tilde{A}_\psi^{cl}, \quad \mathcal{U}_\psi = e^{-it_3\psi}.
\end{aligned} \tag{II.2.22}$$

Note that the "bare" scalars $\tilde{\phi}_{1,2}^{cl}$ are covariantly constant with respect to $\partial_\psi - i\tilde{A}_\psi^{cl}$, which means that we restore the rotational symmetry in ψ by turning on a background gauge. Additionally, since the scalar VEVs satisfy the algebra of $SO(3)$ along with A_ψ, we can think of them as coordinates on a fuzzy circle. Strictly speaking, we have a collection of fuzzy circles whose radii depend on the eigenvalue of t_3. Clearly, there is a symmetry $SO(2)$ generated by t_3 that rotates $\phi_{1,2}$ leaving their relations fixed. For the generic defect this symmetry is an outer automorphism that maps inequivalent defects to each other, but at the origin of the moduli space this outer automorphism becomes a symmetry, untwisting the transverse symmetry.

Holographic dual of the singular case

The dual description of these kinds of defect should be qualitatively different from the generic case. Intuitively, one expects that the singular limit corresponds to taking $u_0\to 0$. In that case, the ψ direction disappears, and the brane wraps a maximal AdS_3 cycle inside of AdS_5. On the S^5 coordinates, we are free to wrap the remaining direction along the equator giving an induced metric on the brane of $AdS_3\times S^1$. This $S^1\subset S^5$ should be interpreted as a fuzzy circle. Since the solution sits at a special point where the

ψ coordinate disappears, the rotational symmetry along the ψ coordinate is restored. Moreover, the rotational symmetry along the equator of the sphere is restored since the brane wraps the whole equator. The spacetime circle disappears, so we cannot thread NS-NS or R-R 1-form flux, and the defect lacks any continuous theta angles. This solution appeared before in [56] and is known to correspond to an integrable boundary for the type IIB superstring on $AdS_5 \times S^5$.

II.3 Superconformal Ward Identities

In this section, we find the superconformal Ward identities (SCWIs) for the two-point functions of half-BPS scalar operators in the generic background. Finding these symmetry constraints is required for fully determining the superconformal blocks composing the two-point function. We utilize the harmonic superspace formalism, which is set up for this Gukov-Witten defect by [119], for a simple comprehensive expression of the superconformal transformations of the bosonic and fermionic coordinates. This superspace formalism approach for finding SCWIs is first considered in [59] for the four-point function of the $\mathcal{N} = 4$ theory, and also considered for the codimension-one defect case in [119]. The harmonic superspace formalism and the action of the residual $PSU(1,1|2)^2 \ltimes SO(2)_t$ symmetry on it is reviewed in appendix II.A. The spacetime coordinates x^μ and the R-symmetry space polarization Y^I can be packaged as a $(2|2)$ matrix together with the Grassmann odd coordinates as

$$X^{A\dot{A}} = \begin{pmatrix} x^{\alpha\dot{\alpha}} & \theta^{\alpha\dot{a}} \\ \bar{\theta}^{a\dot{\alpha}} & y^{a\dot{a}} \end{pmatrix}, \quad A, \dot{A} = 1, ..., 4, \ a, \dot{a}, \alpha, \dot{\alpha} = 1, 2. \tag{II.3.1}$$

Let us call the harmonic superspace coordinates of the two operator-insertion points X_1 and X_2. X's can be split to the parallel components and to the transverse components with respect to the surface defect as $X_i = X_{iS} + X_{i\perp}$. The number of the residual supertranslation and superspecial conformal transformation generators is 16 in total, so

we can fix the 16 components of X_{1S} and X_{2S} to be zero.

We need to find the quantity containing the cross-ratios between the two insertion points regarding the residual superconformal symmetry. Note that the eigenvalues of the quantity $X_{12\perp} \equiv X_{1\perp}X_{2\perp}^{-1} = \begin{pmatrix} \chi_{1\perp}\chi_{2\perp}^{-1} & 0 \\ 0 & \bar{\chi}_{1\perp}\bar{\chi}_{2\perp}^{-1} \end{pmatrix}$ are $PSU(1,1|2)^2 \ltimes SO(2)_t$ invariant. Each of the superspace positions X_1 and X_2 has the eight independent fermionic coordinates $\theta^{\alpha\dot{a}}$ and $\bar{\theta}^{a\dot{\alpha}}$. Each group element of the residual symmetry has 16 independent fermionic parameters corresponding to the Q and S generators, which allow us to fix the fermionic coordinates of both X_1 and X_2 to be all zero (notice this is obviously compatible with the choice $\chi_S = \bar{\chi}_S = 0$ that we already made). This means that the two-point function is fully determined by considering the top components in the supermultiples. Hence, the matrices $\chi_{1\perp}$, $\chi_{2\perp}$, and their barred counterparts are diagonal with only bosonic elements. The eigenvalues of $X_{12\perp}$ are

$$X_{12\perp} \sim \mathrm{diag}\left(\frac{(\chi_{1\perp})_{11}}{(\chi_{2\perp})_{11}}, \frac{(\bar{\chi}_{1\perp})_{11}}{(\bar{\chi}_{2\perp})_{11}}, \frac{(\chi_{1\perp})_{22}}{(\chi_{2\perp})_{22}}, \frac{(\bar{\chi}_{1\perp})_{22}}{(\bar{\chi}_{2\perp})_{22}}\right) \equiv \mathrm{diag}(u, \bar{u}, v, \bar{v}). \tag{II.3.2}$$

The set of these eigenvalues has a one-to-one correspondence[6] with the four cross-ratios χ, χ_R, ϕ, and ϕ_R which we define in section II.4.3. $(\chi_\perp)_{11}$ coincides with the $z = x^1 + ix^2 = re^{i\psi}$ coordinate of the transverse directions, and $(\bar{\chi}_\perp)_{11}$ coincides with $\bar{z}$ for the top components with zero odd coordinates. Because the Gukov-Witten defect preserves only the diagonal $SO(2)_t$ part of the $SO(2) \times SO(2)_R$ rotations in the perpendicular directions of the spacetime and the R-symmetry space, the two-point functions of the operators charged under the broken part of these transverse rotations have the dependence on the two additional angular variables η_1 and η_2:

[6]Namely, the cross-ratios can be expressed in terms of these eigenvalues as

$$\chi = \frac{u\bar{u}+1}{\sqrt{u\bar{u}}}, \quad \chi_R = \frac{v\bar{v}+1}{\sqrt{v\bar{v}}}, \quad \cos\phi = \frac{u+\bar{u}}{2\sqrt{u\bar{u}}}, \quad \cos\phi_R = \frac{v+\bar{v}}{2\sqrt{v\bar{v}}} \tag{II.3.3}$$

when the fermionic coordinates are all zero.

$$\cos\eta_1 \equiv \frac{1}{2}\left(\left(\frac{\mathrm{sdet}(\chi_{1\perp})}{\mathrm{sdet}(\bar{\chi}_{1\perp})}\right)^{1/2} + \left(\frac{\mathrm{sdet}(\bar{\chi}_{1\perp})}{\mathrm{sdet}(\chi_{1\perp})}\right)^{1/2}\right), \tag{II.3.4}$$

$$\cos\eta_2 \equiv \frac{1}{2}\left(\left(\frac{\mathrm{sdet}(\chi_{2\perp})}{\mathrm{sdet}(\bar{\chi}_{2\perp})}\right)^{1/2} + \left(\frac{\mathrm{sdet}(\bar{\chi}_{2\perp})}{\mathrm{sdet}(\chi_{2\perp})}\right)^{1/2}\right). \tag{II.3.5}$$

They are invariant under the mixed $SO(2)_t$ rotations but not under each of the individual $SO(2)$ rotations in the spacetime and the R-symmetry space. Actually, there is a combination of the eigenvalues of $X_{12\perp}$ linearly dependent with the combination $\eta = \eta_1 - \eta_2$, so we can say the two-point function depends on only one of the η angles besides the eigenvalues.

We write the general expression of the two-point function as

$$\langle \mathcal{O}_1(X_1)\mathcal{O}_2(X_2)\rangle = \frac{\mathcal{F}_{\mathcal{O}_1\mathcal{O}_2}(u,\bar{u},v,\bar{v},\eta_i)}{\mathrm{sdet}(\chi_{1\perp})^{\Delta_1/2}\,\mathrm{sdet}(\bar{\chi}_{1\perp})^{\Delta_1/2}\,\mathrm{sdet}(\chi_{2\perp})^{\Delta_2/2}\,\mathrm{sdet}(\bar{\chi}_{2\perp})^{\Delta_2/2}}. \tag{II.3.6}$$

To find the SCWIs, we think of the expansion of this function $\mathcal{F}_{\mathcal{O}_1\mathcal{O}_2}$ about the fermionic coordinates around $\theta = \bar{\theta} = 0$. We consider the subset of the supersymmetry transformations considered in [59] restricting them to be in the residual symmetry $PSU(1,1|2)^2 \ltimes SO(2)_t$. This means that the parameters of the infinitesimal supersymmetry transformations $\epsilon^{\alpha\dot{a}}$ and $\bar{\epsilon}^{a\dot{\alpha}}$ have only diagonal elements. The infinitesimal transformations of the odd coordinates under this subset of the residual symmetry are

$$\delta\theta^{\alpha\dot{a}} = \begin{pmatrix} (v-u)\epsilon^{11} & 0 \\ 0 & (\bar{v}-\bar{u})\epsilon^{22} \end{pmatrix}, \quad \delta\bar{\theta}^{a\dot{\alpha}} = \begin{pmatrix} (v-u)\bar{\epsilon}^{11} & 0 \\ 0 & (\bar{v}-\bar{u})\bar{\epsilon}^{22} \end{pmatrix}, \tag{II.3.7}$$

and the transformations of the bare eigenvalues $u, \bar{u}, v, \bar{v}$ are

$$\begin{aligned} \delta u &= \epsilon^{11}\bar{\theta}^{11} + \theta^{11}\bar{\epsilon}^{11}, \quad \delta\bar{u} = \epsilon^{22}\bar{\theta}^{22} + \theta^{22}\bar{\epsilon}^{22}, \\ \delta v &= -\bar{\epsilon}^{11}\theta^{11} - \bar{\theta}^{11}\epsilon^{11}, \quad \delta\bar{v} = -\bar{\epsilon}^{22}\theta^{22} - \bar{\theta}^{22}\epsilon^{22}. \end{aligned} \tag{II.3.8}$$

The linear part of the eigenvalues of $X_{12\perp}$ after the transformation can be seen from these

transformation laws as

$$\tilde{u} = u - \frac{\theta^{11}\bar{\theta}^{11}}{u-v}, \quad \tilde{\bar{u}} = \bar{u} - \frac{\theta^{22}\bar{\theta}^{22}}{\bar{u}-\bar{v}}, \quad \tilde{v} = v - \frac{\theta^{11}\bar{\theta}^{11}}{u-v}, \quad \tilde{\bar{v}} = \bar{v} - \frac{\theta^{22}\bar{\theta}^{22}}{\bar{u}-\bar{v}}. \tag{II.3.9}$$

The transformation law (II.3.9) suggests that as we expand $\mathcal{F}_{\mathcal{O}_1\mathcal{O}_2}$ regarded as a function of $(u, \bar{u}, v, \bar{v})$ (plus the η variables) around $\theta = \bar{\theta} = 0$, it encounters a spurious singularity in the R-symmetry space at $v \to u$ or $\bar{v} \to \bar{u}$. This spurious singularity must be suppressed due to the harmonic analyticity of $\mathcal{F}_{\mathcal{O}_1\mathcal{O}_2}$. These two limits $v \to u$ and $\bar{v} \to \bar{u}$ are actually equivalent when we consider the top components, i.e. the case when all of the odd coordinates are zero, since the unbarred and barred variables are complex conjugates of each other. The independence of the (u, v) part and the $(\bar{u}, \bar{v})$ part allows us to take care of these singularities separately by considering the SUSY transformation with either $\epsilon^{11} = \bar{\epsilon}^{11} = 0$ or $\epsilon^{22} = \bar{\epsilon}^{22} = 0$. For these transformations, the change of $\mathcal{F}_{\mathcal{O}_1\mathcal{O}_2}$ due to the changes of η_1 and η_2 is zero since their changes in the linear order are proportional to $\epsilon^{11}\bar{\epsilon}^{22}$ and $\epsilon^{22}\bar{\epsilon}^{11}$, and the change in the quadratic order is proportional to $\epsilon^{11}\bar{\epsilon}^{11}\epsilon^{22}\bar{\epsilon}^{22}$. This makes sense since the η dependence is due to the broken part of the twisted symmetry, and the SCWIs are not expected to determine it. Let us first consider the case of $\epsilon^{22} = \bar{\epsilon}^{22} = 0$. In this case, only θ^{11} and $\bar{\theta}^{11}$ can be the nonzero odd coordinates of $X_{12\perp}$. Due to the nilpotency of the odd coordinates, the u, v part of the expansion of $\mathcal{F}_{\mathcal{O}_1\mathcal{O}_2}$ becomes exact with the linear part only:

$$\mathcal{F}_{\mathcal{O}_1\mathcal{O}_2}\left(u + \delta u, \bar{u}, v + \delta v, \bar{v}, \eta_i\right) = \mathcal{F}_{\mathcal{O}_1\mathcal{O}_2}(u, \bar{u}, v, \bar{v}, \eta_i) - \frac{\theta^{11}\bar{\theta}^{11}}{u-v}(\partial_u + \partial_v)\mathcal{F}_{\mathcal{O}_1\mathcal{O}_2}(u, \bar{u}, v, \bar{v}, \eta_i). \tag{II.3.10}$$

Hence, the harmonic analyticity of $\mathcal{F}_{\mathcal{O}_1\mathcal{O}_2}$ at $v \to u$ requires the numerator of the linear correction to be zero:

$$(\partial_u + \partial_v)\mathcal{F}_{\mathcal{O}_1\mathcal{O}_2}(u, \bar{u}, v, \bar{v}, \eta_i)\Big|_{v\to u} = 0. \tag{II.3.11}$$

Similarly, for the other case $\epsilon^{11} = \bar{\epsilon}^{11} = 0$, the harmonic analyticity requires

$$(\partial_{\bar{u}} + \partial_{\bar{v}})\mathcal{F}_{\mathcal{O}_1\mathcal{O}_2}(u, \bar{u}, v, \bar{v}, \eta_i)\Big|_{\bar{v}\to\bar{u}} = 0. \tag{II.3.12}$$

These are the superconformal Ward identities for the two-point function.

II.4 Half-BPS Correlation functions

Here, we determine the general forms of the one-point functions and the two-point functions from the superconformal symmetry. We are going to work in the embedding formalism, where the four-dimensional spacetime is embedded in the six-dimensional space by mapping the points in $\mathbb{R}^{1,3}$ to a light cone $\subset \mathbb{R}^{2,4}$. With this formalism, the conformal symmetry $SO(2,4)$ acts linearly on the coordinates in $\mathbb{R}^{2,4}$. Specifically, the spacetime coordinates x^μ is mapped to a six-dimensional null vector as

$$x^\mu \mapsto P^M = (P^\mu, P^+, P^-) = (x^\mu, 1, x^2). \tag{II.4.1}$$

The insertion of the flat conformal surface defect Σ splits this space to

$$P^M = (P^I, P^A), \qquad I = 1, 2, \quad A = 3, 4, +, -. \tag{II.4.2}$$

The residual two-dimensional conformal symmetry $SO(2,2)$ now linearly acts as a Lorentz symmetry on P^A. We follow the convention in [34], where the dot products are denoted with $\cdot$ for the whole six-dimensional vectors, $\circ$ for the transverse directions to the defect, and $\bullet$ for the parallel directions. The R-symmetry space coordinates Y^I are split in the same manner as $Y^M = (Y^I, Y^A)$, where the first two "transverse" $I = 1, 2$ directions

correspond to the real scalars ϕ^1, ϕ^2 with nonzero VEVs. The twisting of the transverse spacetime and R-symmetry $SO(2)$ rotations in the residual symmetry defines the dot product between P^I and Y^I. We denote this also as $P \circ Y$.

II.4.1 One-point Functions

Let us first consider the simplest class of one-point functions. The lowest spin of a half-BPS multiplet is a scalar operator transforming in the symmetric traceless tensor representation of $SU(4)_R$. Like with spinning primaries, we can deal with the $SU(4)_R$ indices by contracting them with an auxiliary null six vector Y

$$\mathcal{O}_\Delta(Y, P) = Y_{I_1} \dots Y_{I_\Delta} \mathcal{O}_\Delta^{I_1 \dots I_\Delta}(P). \tag{II.4.3}$$

One can use the residual conformal symmetry to set the parallel components of the insertion point to zero, and so the one-point function can only depend on the normal coordinates to the defect $z, \bar{z}$. The residual $SO(4)_R$ symmetry allows us to set the components of a generic Y^A to be proportional to $(1, 0, 0, 0)$ which leaves a little group $SO(3)$ symmetry. Using a conformal transformation, we can further set an additional component of P^A to zero as long as $|z| \neq 0$. In Euclidean signature this would be the Lorentz transformation that brings P^A to a center of mass frame:

$$P^M \to (z, \bar{z}, 0, 0, 0, |z|) \tag{II.4.4}$$
$$Y^M \to (Y_1, Y_2, Y_3, 0, 0, 0). \tag{II.4.5}$$

The residual symmetry left after fixing this frame is $SO(1,2) \times SO(3)$, where both factors are the diagonally embedded Lorentz groups of $SO(2,2) \times SO(4)_R$. The full supersymmetry algebra preserved can be shown to be a diagonal $\mathfrak{psu}(1,1|2)$ of $\mathfrak{psu}(1,1|2)^2$ [119]. The one-point function of half-BPS operators is invariant under this subgroup, so only defect multiplets that contain a singlet under this would appear. The $SO(4)_R$ symmetry acting on Y can be traded for a transformation acting on the defect which leaves it

invariant, so only $SO(4)_R$ singlets are allowed. The branching of the half-BPS multiplet in the $SU(4)_R$ representation $[0, \Delta, 0]$ is

$$[0, \Delta, 0] \to \bigoplus_{n=0}^{\Delta} \bigoplus_{j=-(\Delta/2-n)}^{\Delta/2-n} [\tfrac{n}{2}, \tfrac{n}{2}]_{2j} \tag{II.4.6}$$

where $[\frac{n}{2}, \frac{n}{2}]_m$ labels the representation of $SO(4)_R \times SO(2)_R$. The $SO(4)_R$ invariance requires that the only allowed quantum numbers are $n = 0$. The spacetime symmetry implies that only defect scalars appear, but there is no constraint for operators carrying transverse spin. The $SO(2)_R$ spin has no constraint either. There is however a constraint coming from the Ward identity for the mixed $SO(2)_t$. The only operators with non-zero one-point functions have vanishing central charge under this. Putting these constraints all together, the general form of a one-point function of half BPS operators is

$$\begin{aligned} \langle O_\Delta(Y, P)\rangle &= \frac{(Y \circ Y)^{\Delta/2}}{(P \circ P)^{\Delta/2}} \left[\mathsf{a}_{\Delta,0} + \sum_{q=1}^{\Delta/2} \left(\frac{(\bar{w}z)^q \, \mathsf{a}^+_{\Delta,q} + (w\bar{z})^q \, \mathsf{a}^-_{\Delta,q}}{(Y \circ Y)^{q/2} \, (P \circ P)^{q/2}} \right) \right] \\ &= \frac{(Y \circ Y)^{\Delta/2}}{(P \circ P)^{\Delta/2}} \times \mathcal{A}_O(\eta), \end{aligned} \tag{II.4.7}$$

where we introduced $w = Y_1 + iY_2$ to parametrize the R-symmetry polarization. Note that this includes contributions from boundary operators carrying spin in the directions orthogonal to the defect, since the field $\boldsymbol{\phi}$ should not be treated as a scalar with this twisted symmetry $SO(2)_t$. We can interpret the one-point function as being fixed not in terms of a single number, but a function $\mathcal{A}_I(\eta)$ of the invariant $e^{i2\eta} = \bar{w}z/w\bar{z}$, which specifies the angle between the transverse position vector P^I and the polarization Y^I in this twisted space.

II.4.2 Bulk-Defect Two-point Functions

Bulk operators can have nonzero two-point functions with the defect operators due to their nontrivial OPE decompositions in terms of the defect operators. A defect primary is labeled by its quantum numbers under $PSU(1,1|2)^2 \ltimes SO(2)_t$. Since we will exclusively deal with bulk chiral primaries, the bulk-defect OPE is restricted to have only defect primaries without parallel spin. In that case, the quantum numbers under the bosonic symmetries are $\left(\hat{\Delta}, [\frac{n}{2}, \frac{m}{2}], \ell\right)$ where $[\frac{n}{2}, \frac{m}{2}]$ are $SO(4)_R$ spins. In the decomposition of chiral primaries, only $n = m$ representations appear as in (II.4.6). The symmetry fixing the defect origin and the bulk insertion point is the one fixing the conformal frame, namely $PSU(1,1|2)$. So, the only allowed quantum numbers of the defect operators in the OPE correspond to the representations containing a singlet under this stability subgroup. We can do this by taking the top component of the multiplet of the $\mathfrak{psu}(1,1|2)^2$ to have $\left([\frac{\hat{\Delta}}{2}, \frac{\hat{\Delta}}{2}], [\frac{n}{2}, \frac{n}{2}]\right)$ quantum numbers under the maximal bosonic subalgebra. The shortening conditions for $\mathfrak{su}(1,1|2)$ (see appendix II.C) imply the shortening conditions of the residual superconformal symmetry for these defect operators appearing OPE to be $\ell = \pm(\hat{\Delta} + n)$ or $\ell = \pm(-\hat{\Delta} + n + 2)$. The most general defect OPE will involve a sum over the defect supermultiplets.

$$O_\Delta(P,Y) = \sum_{\hat{O}^{\hat{\rho}}} \frac{\mathcal{C}(P^A, Y^A, \partial_{\hat{P}}, \partial_{\hat{W}})}{(P \circ P)^{\frac{1}{2}(\Delta - \hat{\Delta})}} \mathcal{F}(z/\bar{z}, w/\bar{w})\, e^{i\ell\psi}\, \hat{O}^{\hat{\rho}}_{(\hat{\Delta},n,\ell)}(\hat{P}, \hat{W}), \quad \hat{W} \bullet \hat{W} = 0. \tag{II.4.8}$$

where $\hat{O}^{\hat{\rho}}$ is the top component of a supermultiplet $\hat{\rho}$ and $\mathcal{C}$ is a differential operator that takes into account the contribution from superconformal descendants and the hatted vectors are the projections into the defect coordinates. In our case, $\hat{\rho}$ are the defect $\mathfrak{psu}(1,1|2)^2 \ltimes SO(2)$ representations. The details of the representations of this Lie superalgebra and their branching to the bosonic components are in appendix II.C. We also need to introduce an auxiliary complex null vector to take into account the $SO(4)_R$ in-

dices. The dependence in ψ can be understood as follows. In the untwisted case, we would have the spacetime $SO(2)$ symmetry in the transverse directions, so the defect operators should be multiplied by additional factors of $(z/\bar{z})^{\ell/2} = e^{i\ell\psi}$ in the OPE, where ℓ is the spin in the transverse direction. In our case, this symmetry is twisted with the residual R-symmetry, so the correct eigenfunctions on the circle transform as sections of a non-trivial bundle. We should think of this as having a constant R-symmetry gauge field on the circle. The most general form this can take is $e^{i\ell\psi}$ times a polynomial in the invariant coordinate $e^{i2\eta} = \frac{z\bar{w}}{\bar{z}w}$. Since the only $SO(4)_R$ covariant structure is $Y \bullet \hat{W}$, the bulk-defect two-point function has the general form

$$\left\langle O_\Delta(P,Y)\, \hat{O}^{\hat{\rho}}_{(\hat{\Delta},n,\ell)}(\hat{P},\hat{W})\right\rangle = \frac{(Y\circ Y)^{\frac{1}{2}(\Delta-n)}}{(P\circ P)^{\frac{1}{2}(\Delta-\hat{\Delta})}}\frac{(Y\bullet\hat{W})^n}{(P\bullet\hat{P})^{\hat{\Delta}}}\mathcal{B}_{O,\hat{O}}(\eta). \tag{II.4.9}$$

To fix the form of $\mathcal{B}_{O,\hat{O}}$ it is best to expand $O_\Delta(P,Y)$ in a basis that is covariant under $SO(2,2)\times SO(2)\times SO(4)_R\times SO(2)_R$ and then perform the defect OPE. The basis functions are specified by the quantum numbers (Δ, j, m, k) corresponding to each subgroup of $SO(2,2)\times SO(2)\times SO(4)_R\times SO(2)_R$. The most general form of this expansion is

$$O_\Delta(P,Y) = \sum_j \sum_{m=0}^{\Delta} \sum_{|k|\leq\frac{\Delta-m}{2}} C_{\Delta,m,k}(Y\circ Y)^{\frac{(\Delta-m)}{2}}\left(\frac{w}{\bar{w}}\right)^k \mathcal{D}(Y^A,\partial_{\hat{W}})e^{ij\psi}O^{(j)}_{(\Delta,m,2k)}(P,\hat{W}), \tag{II.4.10}$$

Where $\mathcal{D}$ is an operator accounts for the change of basis between $SO(6)$ and $SO(4)$, and its role is to take into account the contribution of R-symmetry descendants. The same operator must appear in the defect OPE so we do not need its explicit form. Clearly it is the operators $\tilde{O}^{(j)}_{(\Delta,m,2k)}(x_\parallel, r, \hat{W})$ with $\ell + j + 2k = 0$ that contribute to the two point function. Using this we can deduce that the form of the function is

$$\mathcal{B}_{O,\hat{O}}(\eta) = \sum_{|k|\leq\frac{\Delta-n}{2}} \mathsf{b}_{O^{(2k-\ell)}_{(\Delta,n,2k)},\hat{O}_{(\hat{\Delta},n,\ell)}}\, C_{\Delta,n,k}\, e^{i2k\eta}, \tag{II.4.11}$$

and the coefficients $C_{\Delta,n,k}$ do not depend on defect CFT data and can be determined

from bulk branching rules; these can be reabsorbed into the definition of $\mathsf{b}_{O,\hat{O}}$. Just like the one-point function, we can interpret the bulk-defect two-point function as being encoded in a function.

II.4.3 Bulk-Bulk Two-point Function

For the two-point function of bulk operators, superconformal symmetry is not powerful enough to fix the whole correlator. In general there are two ways of expanding the bulk-bulk two-point function, one where we perform the bulk OPE to fuse the two operators and then sum the contributions of each one-point function, and another where each operator is re-written as a sum over boundary operators. Both expressions give different conformal block expansions for the two-point function. We will concentrate on the second expansion, the defect conformal block expansion, for the two-point function of bulk half-BPS operators. We start from defining the cross-ratios invariant under the residual symmetry:

$$\chi = -\frac{2P_1 \bullet P_2}{(P_1 \circ P_1)^{1/2}(P_2 \circ P_2)^{1/2}}, \quad \chi_R = -\frac{2Y_1 \bullet Y_2}{(Y_1 \circ Y_1)^{1/2}(Y_2 \circ Y_2)^{1/2}}$$
$$\cos\phi = \frac{P_1 \circ P_2}{(P_1 \circ P_1)^{1/2}(P_2 \circ P_2)^{1/2}}, \quad \cos\phi_R = \frac{Y_1 \circ Y_2}{(Y_1 \circ Y_1)^{1/2}(Y_2 \circ Y_2)^{1/2}}. \tag{II.4.12}$$

ϕ and ϕ_R measures the angles between the position vectors and the polarizations of the two insertion points in the transverse directions, respectively. We can fix the frame with the mixed $SO(2)$ rotation so that $\psi_2 = 0$ and $\psi = \psi_1 = \phi$. We can start by expanding the $SO(6)_R$ quantum numbers into a mutual $SO(4)_R$ basis. By symmetry, the only contributions come from the components of the operator that have the same $SO(4)_R$ quantum numbers, but the $SO(2)_R$ of the bulk theory is no longer conserved. This can be interpreted as having a constant $SO(2)_R$ background gauge field along the S^1 normal to the defect just as we mentioned for the bulk-defect two-point function case. As a simple example, let us consider the case of two uncharged chiral primaries under

$SO(2)_R$, $O_{\Delta_{1,2},n_{1,2},m_{1,2}=0}$. These modes are unaffected by the background gauge field so their two point functions behave as they would if the rotational symmetry normal to the defect was unbroken:

$$\begin{aligned}\left\langle O_{(\Delta_1,n,0)}(P_1,\hat{W}_1)O_{(\Delta_2,n,0)}(P_2,\hat{W}_2)\right\rangle &= \frac{(\hat{W}_1\bullet\hat{W}_2)^n}{(P_1\circ P_1)^{\Delta_1/2}(P_2\circ P_2)^{\Delta_2/2}}\,\mathcal{G}(\chi,\psi,\chi_R)\\ \mathcal{G}(\chi,\psi,\chi_R) &= \sum_{\{\hat{O}\}}\mathsf{b}_{1,\hat{\mathsf{O}}}\mathsf{b}_{1,\hat{\mathsf{O}}}\,\mathfrak{f}_{\hat{\Delta}}(\chi)\,\mathfrak{f}^R_{[\frac{n}{2},\frac{n}{2}]}(\chi_R)\,\mathfrak{h}_\ell(\psi).\end{aligned} \tag{II.4.13}$$

where $\mathfrak{f}_{\hat{\Delta}}(\chi)$, $\mathfrak{f}^R_{[\frac{n}{2},\frac{n}{2}]}(\chi_R)$, $\mathfrak{h}_\ell(\psi)$ are the conformal blocks corresponding to each of the representations of the bosonic subgroups, $SO(2,2), SO(4)_R$, and $SO(2)$, respectively. Their forms are determined by solving the quadratic Casimir equations for this residual bosonic symmetry as

$$\mathfrak{f}_{\hat{\Delta}}(\chi) = \chi^{-\hat{\Delta}}{}_2F_1\left(\frac{\hat{\Delta}+1}{2},\frac{\hat{\Delta}}{2};\hat{\Delta};\frac{4}{\chi^2}\right) \tag{II.4.14}$$

$$\mathfrak{f}^R_{[\frac{n}{2},\frac{n}{2}]}(\chi_R) = \chi_R^n\,{}_2F_1\left(\frac{-n+1}{2},-\frac{n}{2};n;\frac{4}{\chi_R^2}\right) \tag{II.4.15}$$

$$\mathfrak{h}_j(\psi) = e^{ij\psi}. \tag{II.4.16}$$

Refer to appendix II.B for their full derivations. For charged operators, the expansion is more complicated. This is mainly because there are more invariant quantities than in the case with unbroken transverse rotational symmetry. These extra invariants are exactly the η angles for each of the insertion points. Extending the intuition from the previous correlators, we expect that the most natural way of packaging the defect conformal block expansion is by promoting the couplings to functions $\mathsf{b}\to\mathcal{B}(\eta)$:

$$\left\langle O_{\Delta_1}O_{\Delta_2}\right\rangle = (\texttt{kinematic})\left[\mathcal{A}_1(\eta_1)\mathcal{A}_2(\eta_2)+\sum_{\hat{\rho}}\mathcal{B}_{1,\hat{\rho}}(\eta_1)\mathcal{B}_{2,\hat{\rho}}(\eta_2)\hat{\mathfrak{F}}_{\hat{\rho}}(\chi,\chi_R,\psi,\eta)\right] \tag{II.4.17}$$

where $\eta=\eta_1-\eta_2=\psi-\phi_R$ and the sum is over defect superconformal primaries $\hat{\rho}$ appearing in the bulk-defect OPE. To compute these, it is more convenient to further

decompose the superconformal blocks with regard to the residual bosonic symmetry, with the blocks computed again as a product of (II.4.14), (II.4.15), and (II.4.16)

$$\hat{\mathfrak{F}}_{\hat{\rho}} = \sum_{\hat{\Delta},n} C^{\hat{\rho}}_{\hat{\Delta},n}(\eta)\, \mathfrak{f}_{\hat{\Delta}}(\chi)\, \mathfrak{f}^{R}_{[\frac{n}{2},\frac{n}{2}]}(\chi_R)\, \mathfrak{h}_{\ell}(\psi). \tag{II.4.18}$$

The decomposition is specified by the branching of $\hat{\rho}$ to the bosonic symmetry representations. Once we figure out the decomposition, we can fix the correct linear combination using the superconformal Ward identities. Note that the components of the supermultiplet all have the same charge under $SO(2)_t$.

One of the simplest nontrivial examples is the symmetric representation with zero central charge $\hat{\mathcal{S}}_0 = \langle \mathcal{V}(1), 0\rangle_{\mathrm{II}\pm} \otimes \langle \mathcal{V}(1), 0\rangle_{\mathrm{II}\pm}$. The spinless bosonic components with nonzero contribution to the bulk-defect OPE of a chiral primary operator are

$$\hat{\mathcal{S}}_0 \supset \left\{ [\mathcal{V}(1), 0] \otimes [\mathcal{V}(1), 0], \left[\mathcal{V}\left(\tfrac{1}{2}\right), \tfrac{1}{2}\right] \otimes \left[\mathcal{V}\left(\tfrac{1}{2}\right), \tfrac{1}{2}\right] \right\} \tag{II.4.19}$$

where $\mathcal{V}(\ell)$ are infinite-dimensional representations with either highest weight or lowest weight ℓ, depending on the sign of ℓ. The scaling dimensions of the bosonic states are $\hat{\Delta} = 1$ and 2, and the $SO(4)_R$ representations are correspondingly $[\frac{1}{2}, \frac{1}{2}]$ and $[0, 0]$. The functions $C^{\hat{\rho}}_{\hat{\Delta},n}(\eta)$ take into account the broken $SO(2)_R$ symmetry of each state in the multiplet. So, the most general ansatz for the superconformal block of $\hat{\mathcal{S}}_0$ is

$$\hat{\mathfrak{F}}_{\hat{\mathcal{S}}_0} = \sum_{k=0,1} c_k\, e^{\pm ik\eta}\, \mathfrak{f}_{k+1}(\chi)\, \mathfrak{f}^{R}_{[\frac{1-k}{2},\frac{1-k}{2}]}(\chi_R). \tag{II.4.20}$$

The coefficients c_k are determined up to the overall scale by requiring this superconformal block to satisfy the superconformal Ward identities (II.3.11) and (II.3.12). Remember that the dependence on the cross-ratios can be translated to that on the eigenvalues of the invariant quantity (II.3.2). The η dependence is automatically ignored in the $v \to u$ and $\bar{v} \to u$ limits, which are translated to be $\eta \to 0$. Regarding these, the SCWIs fix the coefficients to be $c_0 = -c_1/2$.

We can also consider a slightly less simple example with the symmetric representations with some nonzero central charge ℓ: $\hat{\mathcal{S}}_\ell = \big\langle \mathcal{V}(\frac{\ell}{2}), 0\big\rangle_{\text{I}-} \otimes \big\langle \mathcal{V}(\frac{\ell}{2}), 0\big\rangle_{\text{I}-}$. The only states in these multiplets that can contribute to the defect OPE are the following spinless bosonic components

$$\hat{\mathcal{S}}_\ell \supset \{[\mathcal{V}(\tfrac{\ell}{2}), 0] \otimes [\mathcal{V}(\tfrac{\ell}{2}), 0], [\mathcal{V}(\tfrac{\ell\pm1}{2}), 1] \otimes [\mathcal{V}(\tfrac{\ell\pm1}{2}), 1], [\mathcal{V}(\tfrac{\ell\pm2}{2}), 0] \otimes [\mathcal{V}(\tfrac{\ell\pm2}{2}), 0]\}, \quad \text{(II.4.21)}$$

The plus signs are for $\ell \in \mathbb{Z}_+$ of lowest weight representations, and the minus signs are for $\ell \in \mathbb{Z}_-$ of highest weight representations. The scaling dimensions are $\hat{\Delta} = |\ell + 1| + 1, |\ell| + 1, |\ell - 1| + 1$, and the corresponding $SO(4)_R$ representations are $[0, 0], [\frac{1}{2}, \frac{1}{2}], [0, 0]$. The most general ansatz for the superconformal block of $\hat{\mathcal{S}}_\ell$ is

$$\hat{\mathfrak{F}}_{\hat{\mathcal{S}}_\ell} = \sum_{k=-1,0,1} c_k \, e^{i\ell\psi} e^{ik\eta} \, \mathfrak{f}_{|\ell+k|+1}(\chi) \, \mathfrak{f}^R_{[\frac{1-|k|}{2}, \frac{1-|k|}{2}]}(\chi_R). \quad \text{(II.4.22)}$$

The SCWIs (II.3.11) and (II.3.12) fix the coefficients as $c_{-1} = c_1$ and $c_0 = -c_\pm$.

II.5 One-Point Functions: Non-protected operators

Our previous discussions focused on the correlation functions of the protected operators with a surface defect. We can more generally consider correlation functions involving non-protected single trace operators. Superconformal symmetry fixes the structure of the one-point function up to a function of the η, which we can assume to be a trigonometric polynomial from symmetry considerations:

$$\langle \mathcal{O}_\Delta(P) \rangle = \frac{\mathcal{C}(\eta)}{(P \circ P)^{\Delta/2}}. \quad \text{(II.5.1)}$$

At one-loop, scalar operators in the $SO(6)$ sector only mix among themselves and the mixing problem can be mapped to the diagonalization of the integrable $SO(6)$ Heisenberg chain. The R-matrix of the model is

$$R(u) = u(u+2)\mathbb{I} + (u+2)\mathbb{P} - u\mathbb{K}. \tag{II.5.2}$$

where the R-matrix and the operators are intertwiners of two **6** representations corresponding to two neighboring spin sites. Specifically, $\mathbb{I} = \delta_I^{I'}\delta_J^{J'}$, $\mathbb{P} = \delta_I^{J'}\delta_J^{I'}$, and $\mathbb{K} = \delta_{IJ}\delta^{I'J'}$ in the matrix representation. The eigenstates of the Hamiltonian are labelled by three sets of Bethe roots $\{u_i, v_j, w_k\}$ satisfying a set of Bethe equations. We denote the eigenstates as $|\boldsymbol{u}\rangle$. The leading-order result for the one-point function of the operator associated to the eigenstate $|\boldsymbol{u}\rangle$ is given by evaluating the operator on the classical values of the fields, which is equivalent to taking the overlap of $|\boldsymbol{u}\rangle$ with a matrix product state

$$\begin{aligned} \mathcal{C}(\eta) &= \langle \mathsf{MPS}(\eta)|\boldsymbol{u}\rangle \\ |\mathsf{MPS}(\eta)\rangle &= \sum_i \mathrm{tr}[\omega_{I_1}\dots\omega_{I_L}]\,|I_1\dots I_L\rangle\,, \quad \omega_{I_n} = \langle\phi_{I_n}\rangle\,. \end{aligned} \tag{II.5.3}$$

In order to avoid confusion with the spectral parameter dependence, we choose to omit the dependence on η for the moment. For the case of a generic Gukov-Witten defect, the matrices ω_I are reducible in the sense that they are block diagonal whose structure depends on the breaking of the gauge group to the Levi subgroup $\mathbb{L}$, and each block behaves like a one-site product state. We will comment on the singular cases later. In general, a state $|\mathsf{B}\rangle$ is said to be integrable if it is annihilated by infinitely many charges of the system. More precisely, the state should satisfy [139]

$$t(u)\,|\mathsf{B}\rangle = \Pi t(u)\Pi\,|\mathsf{B}\rangle\,, \tag{II.5.4}$$

where Π is the parity operator on the spin chain. This condition can be interpreted as the channel rotation of the boundary Yang-Baxter equation. It is known that for the case of a matrix product state, the integrability condition is satisfied if there exists a solution to the so-called *square root relation* [144]:

$$\check{R}_{12}(u)\,(\psi(u)\otimes\omega) = \check{R}_{12}(u)\,(\omega\otimes\psi(u))\,, \tag{II.5.5}$$

where we group the matrices in the MPS into a $\mathrm{End}(\mathbb{C}^N)$-valued vector $\omega \in \mathbb{C}^6 \otimes \mathrm{End}(\mathbb{C}^N)$, the hatted R-matrices are given by $\check{R}(u) = \mathbb{P}R(u)$, and we introduce an additional collection of matrices $\psi_{ab}(u) \in \mathbb{C}^6 \otimes \mathbb{C}^6 \otimes \mathrm{End}(\mathbb{C}^N)$. The product $\otimes$ in $\omega \otimes \psi(u)$ takes the tensor product of the $\mathbb{C}^6$ indices with the matrix products between their $\mathrm{End}(\mathbb{C}^N)$ values. A solution of the square-root relation can then be used to construct solutions to the *twisted* boundary Yang-Baxter equation. The solutions to these equations with various kinds of symmetries were studied in [144]. The relevant symmetry pair for the Gukov-Witten defect is $(\mathfrak{so}(6), \mathfrak{so}(2) \oplus \mathfrak{so}(4))$. For one-site product states, the solution is:

$$\psi_{ab}(u) = (2u+2)\,\omega_a\omega_b - u\,\omega_c\omega_d\,\delta^{cd}\,\delta_{ab}. \tag{II.5.6}$$

Overlaps for this class of states were studied in [55] and were used to compute one-point functions in the presence of BPS 't-Hooft loop operators [109, 110] and in the Coulomb branch [92]; for a general formalism see [74].

II.5.1 $SL(2)$ Sector

As a concrete example, we will take a particular R-symmetry polarization and study the leading-order one-point functions in that case. The simplest primary operators we can consider belong to the $SU(2)$ and $SL(2)$ closed sectors. The tree-level one-point functions for excited states in the $SU(2)$ sectors must vanish due to the $SO(4)_R$ symmetry of the defect regardless of how we orient the vacuum state inside of $SO(6)$. One can understand it from the spin chain viewpoint as because the excited states belong to $SU(2)$ representations with one or more antisymmetric indices, and the classical field configurations commute. For the $SL(2)$ states, we can choose the operator to be

$$
\begin{aligned}
O_{\Delta,S}(P) &= \sum_{n_1+\cdots+n_L=S} \Psi_{n_1,\ldots n_L}\, \mathrm{tr}\Big[D^{n_1}\tilde{Z}\ldots D^{n_L}\tilde{Z}\Big] \\
D &= \partial_t - D_{x_1} \\
\tilde{Z} &= \frac{1}{2}\left(Z+\bar{Z}+i(Y-\bar{Y})\right) \\
z &= x_1+ix_2
\end{aligned}
\tag{II.5.7}
$$

In this case, the boundary state is similar to the one studied in [109] for 't Hooft loops [75]; it is given by

$$
\begin{aligned}
|\mathsf{Bst}\rangle &= \mathrm{tr}\Big[|\mathsf{B}\rangle^{\otimes L}\Big] \\
\langle \mathsf{B}| &= \sum_{n=0}^{\infty} \langle 0|\, \frac{(-K)^n}{n!}\big[\beta\cos((n+1)\psi)+\gamma\sin((n+1)\psi)\big] \\
&= \sum_{n=0}^{\infty}(-1)^n(\beta^2+\gamma^2)T_{n+1}\left[\cos(\psi-\delta)\right]\langle n|\,.
\end{aligned}
\tag{II.5.8}
$$

The only difference between this boundary state and the 't Hooft loop boundary state is that the Legendre polynomials are replaced by Chebyshev polynomials. The overlap with a two magnon state can be found to be (up to an unimportant phase factor)

$$
\frac{\langle \mathsf{Bst}|\{u,-u\}\rangle}{\langle\{u,-u\}|\{u,-u\}\rangle} = 2L\,\mathrm{tr}\big[\,(\beta^2+\gamma^2)(\beta\cos\psi+\gamma\sin\psi)^{L-2}\,\big]\sin^2\psi\,\frac{u}{\sqrt{L(L+1)(u^2+\frac{1}{4})}},
\tag{II.5.9}
$$

which is the same as the two magnon overlap for the case of 't Hooft loop, up to a momentum independent polynomial in β,γ. We verified that for odd spin S the overlap with the boundary state vanishes, but for even S it does not satisfy the selection rules $\{\boldsymbol{u}\} = \{-\boldsymbol{u}\}$ which we take as evidence against integrability for the generic Gukov-Witten defect. This is somewhat similar to what occurs for three-point functions of non-protected operators with half-BPS sub-determinant operators. In that case, only a BPS special operator, the maximal giant graviton, leads to an integrable boundary state even though there is a large class of operators that preserve the same symmetry. Despite this, there are integrable subsectors corresponding to operators that do not carry the

non-conserved charge in perturbation theory [26]. We expect something similar to occur for the surface defect case, meaning that at generic point of the moduli space, the defect breaks the integrability of the system for a generic sector due to the broken rotational symmetry. For the scalar $SO(6)$ sector, we expect that integrability is preserved at one-loop since we can construct a solution to the boundary Yang-Baxter equation, but mixing with operators outside this subsector should spoil this at higher loops.

II.5.2 Rigid Limit: $SU(2)$ Sector

Now we consider the singular case $\alpha = \beta = \gamma = 0$. In that case, the field profiles are given by block diagonal matrices where each of the blocks satisfies the algebra of $SU(2)$. Without loss of generality, we can restrict to a single $k \times k$ block

$$\begin{aligned} Z^{cl} &= \frac{t_1 - i t_2}{z \log r} \\ A^{cl}_{\psi} &= \frac{t_3}{r \log r}. \end{aligned} \tag{II.5.10}$$

If we focus on operators belonging to the $SU(2)$ sector, the tree-level one-point functions are related to those of the D3-D5 defect set-up [116], and the residual symmetry is related to the one relevant for studying three-point functions of half-BPS operators [15, 93]. For example, we can restrict our attention to operators made out of two complex scalars

$$\begin{aligned} \tilde{Z} &= \frac{1}{2}\left(Z + \bar{Z} - i(Y - \bar{Y})\right) \\ \tilde{Y} &= \frac{1}{2}\left(Y + \bar{Y} - i(Z - \bar{Z})\right), \end{aligned} \tag{II.5.11}$$

which correspond to the down and up spin states of the spin chain. The MPS in this case can be written as

$$\begin{aligned} |\mathsf{MPS}_k\rangle &= \sum_{i_n} \mathrm{tr}_k[M_{i_1}(\psi) \dots M_{i_L}(\psi)]\, |i_1 \dots i_L\rangle \\ M_{\downarrow}(\psi) &= t_1 \cos\psi - t_2 \sin\psi \\ M_{\uparrow}(\psi) &= t_1 \sin\psi + t_2 \cos\psi. \end{aligned} \tag{II.5.12}$$

The matrices $M_i(\psi)$ are a $U(1)$ rotation of the standard basis for the $SU(2)$ algebra so they can be replaced by t_1 and t_2 inside the trace. The result of the overlaps are the same as those found in [116, 40], see also [93]. They are given by

$$\frac{\langle \mathsf{MPS}_k|\boldsymbol{u}\rangle}{\langle \boldsymbol{u}|\boldsymbol{u}\rangle} = 2^{L-1} C_2\left(\{u_j\}\right) \sum_{j=\frac{1-k}{2}}^{\frac{k-1}{2}} j^L \prod_{i=1}^{\frac{M}{2}} \frac{u_i^2\left(u_i^2+\frac{k^2}{4}\right)}{\left[u_i^2+(j-\frac{1}{2})^2\right]\left[u_i^2+(j+\frac{1}{2})^2\right]} \tag{II.5.13}$$

$$C_2\left(\{u_j\}\right) = 2\left[\left(\frac{2\pi^2}{\lambda}\right)^L \frac{1}{L}\prod_j \frac{u_j^2+\frac{1}{4}}{u_j^2}\,\frac{\det G_+^{SU(2)}}{\det G_-^{SU(2)}}\right]^{\frac{1}{2}} \tag{II.5.14}$$

$$\tag{II.5.15}$$

where the Gaudin matrices $G_\pm^{SU(2)}$ are $M/2\times M/2$ given by

$$\begin{aligned}\left(G_\pm^{SU(2)}\right)_{ij} &= \left[L\partial_u p(u_i) + \sum_{k=1}^{\frac{M}{2}} \mathcal{K}_+(u_i,u_k)\right]\delta_{ij} - \mathcal{K}_\pm(u_i,u_j)\\ \mathcal{K}_\pm(u,v) &= \frac{1}{i}\left[\partial_u \log S^{SU(2)}(u,v) \pm \partial_u \log S^{SU(2)}(u,-v)\right].\end{aligned} \tag{II.5.16}$$

We expect that because the symmetry algebra for the rigid defects is an analytic continuation of that of the maximal giant graviton, the results of [93] can be applied to this case as well. We expect that the rigid defects remain integrable at finite 't Hooft coupling. This is somewhat clear in scalar sectors where the dilaton doesn't play a role. In sectors involving derivatives, one needs to be careful about using operators that are scale invariant when computing one-point functions as substituting the classical solutions at tree level leads to violations in the selection rules for the magnon momenta. These violations come from derivatives acting on the classical dilaton profile and they should be reabsorbed by using a Weyl invariant connection. This requires a more careful understanding of the quantization in the presence of the dilaton. We leave this for future work.

II.6 Quantizing the Defect

In this section, we perform the semiclassical quantization of $\mathcal{N} = 4$ SYM in this surface defect background. This is a starting point for performing perturbative calculations. We expand the fields around their classical background values, and calculate the propagators of their quantum fluctuations. Similar calculations have been carried out in the domain wall and 't Hooft line backgrounds [39, 69, 70, 109]. The scalar propagators in the surface defect setting appeared before in [48] and here we generalize by including fermionic fields. We also clarify the relation between field fluctuations and the defect primaries they couple to.

First we are going to review some of the conventions for the $\mathcal{N} = 4$ supersymmetry algebra in four dimensions. Usually it is easier to begin with $\mathcal{N} = 1$ SUSY in ten-dimensions and to reduce it to 4d. The supercharges transform in one of the 16 dimensional spinor representation of $SO(1, 9)$. The gamma matrices Γ^M, $M = 0, 1, \ldots 9$ satisfy a Clifford algebra

$$\{\Gamma^M, \Gamma^N\} = 2g^{MN}, \tag{II.6.1}$$

and they can be thought of as either maps between the two spinor representations $\Gamma^I : \mathcal{S}^\pm \to \mathcal{S}^\mp$, or as a bilinear pairing $\Gamma^I : \mathcal{S}^\pm \times \mathcal{S}^\pm \to \mathbb{R}$ (in Lorentzian signature). The spinor representations are real and dual to each other in Lorentz signature, and they are distinguished by their eigenvalue under the chirality operator

$$\bar{\Gamma} = \Gamma^0\Gamma^1 \ldots \Gamma^9, \tag{II.6.2}$$

which acts as ± 1 on the $\mathcal{S}^\pm$. Another common notation are the gamma matrices with multiple indices $\Gamma^{I_1 I_2 \ldots I_k}$ which is defined as the product $\Gamma^{I_1}\Gamma^{I_2} \ldots \Gamma^{I_k}$ for pairwise distinct indices, and zero otherwise. This is equivalently the fully antisymmetrized product. The lagrangian for 10d SYM takes the form

$$S_{10d} = -\frac{1}{g^2}\int d^{10}x \,\mathrm{tr}\left(\frac{1}{2}F^{MN}F_{MN} + i\bar{\lambda}\Gamma^I D_I\lambda\right). \tag{II.6.3}$$

The supersymmetry generator in this case are constant spinors $\nabla_I\epsilon = 0$ (i.e. Killing spinor) satisfying the chirality projection

$$\bar{\Gamma}\epsilon = \epsilon. \tag{II.6.4}$$

The supersymmetry transformations are

$$\begin{aligned}\delta A_I &= i\bar{\epsilon}\,\Gamma_I\lambda \\ \delta\lambda &= \Gamma^{IJ}F_{IJ}\epsilon.\end{aligned} \tag{II.6.5}$$

To obtain $\mathcal{N} = 4$ SYM we reduce on six of the ten flat dimensions which reduces the 10d Lorentz symmetry to the 4d Lorentz symmetry and the R-symmetry as

$$SO(1,9) \to SO(1,3) \times SO(6)_R. \tag{II.6.6}$$

The spinors ϵ can then be decomposed as follows. The 10d chirality matrix factorizes into a Lorentz and R-symmetry components

$$\bar{\Gamma} = \hat{\Gamma}\Gamma' \tag{II.6.7}$$

The eigenvalues of these chirality matrices are $\pm i$, so the eigenvalues of $\hat{\Gamma}$ and Γ' have to be opposites. The spin representations of $SO(1,3) \sim SU(2) \times SU(2)$ are $(1,2)$ and $(2,1)$, and the spin representations of $SO(6)_R \sim SU(4)_R$ are the fundamental $\mathbf{4}$ and its complex conjugate $\bar{\mathbf{4}}$. So the 4d supersymmetries transform as a spinor in

$$\mathcal{S}^+ = (\mathbf{2},\mathbf{1},\bar{\mathbf{4}}) \oplus (\mathbf{1},\mathbf{2},\mathbf{4}) \tag{II.6.8}$$

We now introduce the generic surface defect in the $M = 0,3$ directions in the four-dimensional space. Among the Higgs scalars emerging from $A^{5,6,\ldots,10}$ after the dimensional reduction, let us choose A^5 and A^6 to be the ones acquiring singular configurations. To carry out the perturbative calculations in the nontrivial background due to the surface

defect, it is convenient to expand the fields around their classical singular configurations as

$$A^M = \mathsf{A}^M + a^M \tag{II.6.9}$$

Let us write the flat 10d metric taking polar coordinates for the transverse spatial direction to the defect:

$$ds^2 = -dt^2 + dx^2 + dr^2 + r^2 d\psi^2 + \sum_{i=1}^{6} dy_i dy_i, \tag{II.6.10}$$

In this coordinate basis, the background fields are

$$\begin{aligned} \mathsf{A}_\psi &= \alpha \\ \mathsf{A}_5 &= \frac{\beta\cos\psi + \gamma\sin\psi}{r} \\ \mathsf{A}_6 &= \frac{\gamma\cos\psi - \beta\sin\psi}{r}. \end{aligned} \tag{II.6.11}$$

Alternatively we could use complex coordinates

$$ds^2 = -dt^2 + dx^2 + 2dzd\bar{z} + \sum_{a=1}^{4} dy_a dy_a + 2dwd\bar{w} \tag{II.6.12}$$

and the background fields are

$$\begin{aligned} \mathsf{A}_z &= \frac{1}{2i}\frac{\alpha}{z} \\ \mathsf{A}_w &= \frac{\beta + i\gamma}{\sqrt{2}z} \end{aligned} \tag{II.6.13}$$

The classical configuration of the 10d field strength is

$$\begin{aligned} \mathsf{F}_{z\bar{z}} &= \alpha\,\delta(z,\bar{z}) \\ \mathsf{F}_{Mi} &= \mathsf{D}_M \mathsf{A}_i \\ \mathsf{F}_{ij} &= [\mathsf{A}_i, \mathsf{A}_j] = 0 \end{aligned} \tag{II.6.14}$$

where D_M is the gauge covariant derivative with respect to the classical configuration of the gauge field, $\mathsf{D}_M = \partial_M - i[\mathsf{A}_M, \cdot]$. These are the source of the defect CFT operators.

II.6.1 Gauge Fixing

We choose the gauge

$$\mathsf{D}_M A^M = 0, \tag{II.6.15}$$

which can be implemented with the gauge fixing term

$$\mathcal{L}_{gf} = -\frac{2}{g^2}\,\mathrm{tr}\left(\mathsf{D}_M \bar{c}\, D^M c\right) \tag{II.6.16}$$

After expanding the fields into the background and fluctuation parts, the action in this gauge is given by

$$\begin{aligned} S_{gf+\Phi} = -\frac{1}{g^2}\int d^4x\,\mathrm{tr}\Big[& a_M\left(-\eta^{MN}\mathsf{D}^2 + 2i\mathsf{F}^{MN}\right)a_N + i\bar{\lambda}\Gamma^M \mathsf{D}_M\lambda + 2\bar{c}(-\mathsf{D}^2)c \\ & - 2i\mathsf{D}_M a_N[a^M, a^N] + \bar{\lambda}\Gamma^M[a_M,\lambda] + 2i\mathsf{D}_M\bar{c}\,[a^M, c] - \frac{1}{2}[a_M, a_N]^2\Big]. \end{aligned} \tag{II.6.17}$$

We can classify the fields into easy and hard fields depending on whether they mix or not due to their nonzero background values. The nontrivial mixing between the scalars and vector fields comes from F_{Mi} for $i = 5, 6$. The second covariant derivative term is (in polar coordinates)

$$\begin{aligned} \mathrm{tr}\left[a\,\mathsf{D}^2 a\right] &= \mathrm{tr}\left[a\partial^2 a + 2ia\,[\mathsf{A}^M, \partial_M a] - a\,[\mathsf{A}^M, [\mathsf{A}_M, a]]\right] \\ &= \mathrm{tr}\left[a\left(\eta^{\alpha\beta}\partial_\alpha\partial_\beta + \partial_r^2 + \frac{1}{r}\partial_r\right)a + a\mathsf{D}^\psi \mathsf{D}_\psi a - a[\mathsf{A}^5,[\mathsf{A}_5,a]] - a[\mathsf{A}^6,[\mathsf{A}_6,a]]\right] \end{aligned} \tag{II.6.18}$$

The indices $\alpha, \beta = 0, 3$ run for the parallel directions to the defect.

II.6.2 Propagators

Now we can consider the quadratic action for an arbitrary Gukov-Witten defect. The first step is to get rid of the non-trivial derivatives in ψ. These terms only appear for

$\alpha \neq 0$ and they make the fields transform as a non-trivial line bundle on S^1. We can eliminate the α dependence by introducing the modified fields

$$a = \mathcal{U}_\alpha^\dagger \, \tilde{a} \, \mathcal{U}_\alpha = e^{-i\psi\alpha} \tilde{a} \, e^{i\psi\alpha}. \tag{II.6.19}$$

The action of the background covariant derivatives D_z on a results in regular derivatives acting on $\tilde{a}$. Substituting these fields into the action reduces it to the case with $\alpha = 0$, so no local operator can detect non-zero α as expected. From now on we drop the tildes, after which the 10d Kinetic term common to all bosons except $a_{r,\psi}$ reduces to

$$\mathrm{tr}\left[a \, \mathsf{D}^2 a\right] = \mathrm{tr}\left[a \left(\eta^{\alpha\beta}\partial_\alpha\partial_\beta + \partial_r^2 + \frac{1}{r}\partial_r + \frac{1}{r^2}\partial_\psi^2\right) a - \frac{1}{r^2} a[\beta,[\beta,a]] - \frac{1}{r^2} a[\gamma,[\gamma,a]]\right] \tag{II.6.20}$$

To simplify the derivative terms we do a field redefinition $a = a'/r$, and passing the derivatives through we get

$$\begin{aligned} \mathrm{tr}\left[a \, \mathsf{D}^2 a\right] &= r^{-4} \, \mathrm{tr}\left[a' \left(r^2\eta^{\alpha\beta}\partial_\alpha\partial_\beta + r\partial_r^2 - r\partial_r + 1 + \partial_\psi^2\right) a' - a'[\beta,[\beta,a']] - a'[\gamma,[\gamma,a']]\right] \\ &= r^{-1}\sqrt{g_{AdS_3\times S^1}} \, \mathrm{tr}\left[a' \left(\Delta_{AdS_3\times S^1} + 1\right) a' - a'[\beta,[\beta,a']] - a'[\gamma,[\gamma,a']]\right] \end{aligned} \tag{II.6.21}$$

The additional factor of $1/r$ cancels precisely with the volume factor of the flat space metric with polar coordinates along two of the directions. For $M = 5, \ldots, 10$ this is a Weyl transformation and the additional mass term arises from the conformal coupling to the background. For $a_{r,\psi}$ the kinetic terms take the form

$$\begin{aligned} \mathrm{tr}\left[a_r \, \mathsf{D}^2 a_r\right] &= \mathrm{tr}\left[a_r \left(\eta^{\alpha\beta}\partial_\alpha\partial_\beta + \partial_r^2 + \frac{1}{r}\partial_r + \frac{1}{r^2}\partial_\psi^2 - \frac{1}{r^2}\right) a_r - \frac{2}{r^2} a_r \partial_\psi a_\psi \right. \\ &\qquad \left. - \frac{1}{r^2} a_r[\beta,[\beta,a_r]] - \frac{1}{r^2} a_r[\gamma,[\gamma,a_r]]\right] \\ \mathrm{tr}\left[a_\psi \, \mathsf{D}^2 a_\psi\right] &= \mathrm{tr}\left[a_\psi \left(\eta^{\alpha\beta}\partial_\alpha\partial_\beta + \partial_r^2 + \frac{1}{r}\partial_r + \frac{1}{r^2}\partial_\psi^2 - \frac{1}{r^2}\right) a_\psi + \frac{2}{r^2} a_\psi \partial_\psi a_r \right. \\ &\qquad \left. - \frac{1}{r^2} a_\psi[\beta,[\beta,a_\psi]] - \frac{1}{r^2} a_\psi[\gamma,[\gamma,a_\psi]]\right]. \end{aligned} \tag{II.6.22}$$

After rescaling by $1/r$ the only modification is an additional -1 in the mass term and the cross term with the single ψ derivative. Next we should deal with the coupling to the background field strength F^{MN}. If we regularize the singularity by imposing a cut-off at $r = \epsilon$, we can ignore the coupling to $F^{z\bar{z}}$. First we work in complex coordinates where the terms take the form

$$\begin{aligned}\mathrm{tr}\big[a_M \mathsf{F}^{MN} \circ a_N\big] = \frac{1}{\sqrt{2}r^2}\Bigg(\mathrm{tr}\Bigg[&- a_r[(\beta - i\gamma)e^{i\psi}, a_w] + a_w[(\beta - i\gamma)e^{i\psi}, a_r] \\ &+ ia_\psi[(\beta - i\gamma)e^{i\psi}, a_w] - ia_w[(\beta - i\gamma)e^{i\psi}, a_\psi]\Bigg] + c.c.\end{aligned} \tag{II.6.23}$$

Then we should eliminate the factors of $e^{i\psi}$; we can do this by turning on a background $U(1)_R$ gauge field

$$\begin{aligned} a_w &= e^{-iq_R\psi}\varphi_w = e^{-i\psi}\varphi_w \\ \partial_\psi a_w &= (\partial_\psi - iq_R)\varphi_w. \end{aligned} \tag{II.6.24}$$

This is consistent with the supersymmetry of the theory on $AdS_3 \times S^1$; after this we perform the rescaling $a = a'/r$ which gives

$$\begin{aligned}\mathrm{tr}\big[a_M \mathsf{F}^{MN} \circ a_N\big] = \frac{1}{\sqrt{2}r^4}\Bigg(\mathrm{tr}\Bigg[&- a'_r[(\beta - i\gamma), \varphi'_w] + \varphi'_w[(\beta - i\gamma), a'_r] \\ &+ ia'_\psi[(\beta - i\gamma), \varphi'_w] - i\varphi'_w[(\beta - i\gamma), a'_\psi]\Bigg] + c.c.\end{aligned} \tag{II.6.25}$$

and all the bosons are now written covariantly in $AdS_3 \times S^1$. The bosons naturally split into easy/transverse and hard/longitudinal modes. The transverse modes are $a_{0,3}$, $\phi_{a\dot{a}} = a_{7,8,9,10}$, and the ghosts c. The fields ϕ_I transform as bi-spinors of the residual $SO(4)_R = SU(2) \times SU(2)$ symmetry. The hard modes are the normal components of the gauge field to the boundary $a_{r,\psi}$ and the complex scalar φ_w. Both of these modes are vectors due to the one-form nature of $\phi = \varphi_w dz + \varphi_{\bar{w}} d\bar{z}$. As explained in [3], vector fields in AdS can be described in terms of conformally coupled scalars, which is precisely what we have with our choice of gauge. The mass terms are only nontrivial for off-diagonal

components of the fields. The common mass term for all the fields is

$$|\mathfrak{Z}_{ij}|^2 = (\beta_i - \beta_j)^2 + (\gamma_i - \gamma_j)^2, \tag{II.6.26}$$

where i, j denote the $U(N)$ matrix indices of the fields.

II.6.3 Easy Bosons

The propagator for the easy scalar is the solution to

$$\left[-\Delta_{AdS_3} - \partial_\psi^2 + (|\mathfrak{Z}_{ij}|^2 - 1)\right] G(x, x', \psi, \psi') = 0. \tag{II.6.27}$$

We can solve this equation by performing a KK-reduction on S^1

$$a(\psi, x) = \sum_{\ell=-\infty}^{\infty} e^{i\ell\psi} a^{(\ell)}(x), \tag{II.6.28}$$

where the reality condition on the fields implies

$$(a^*)^{(\ell)} = a^{(-\ell)}, \tag{II.6.29}$$

so we are left with a tower of conformally coupled scalars in AdS_3 with masses $\left(m_{ij}^{\boldsymbol{s}}\right)^2 = \ell^2 + |\mathfrak{Z}_{ij}|^2 - 1$. These fields couple to scalar operators on the defect with conformal dimensions

$$\hat{\Delta}^{\boldsymbol{s}} = 1 + \sqrt{\ell^2 + |\mathfrak{Z}_{ij}|^2}. \tag{II.6.30}$$

The bulk-to-bulk propagator for each of the KK modes is given by

$$G_{\hat{\Delta}}(x_1, x_2) = \frac{\tilde{\chi}^{\hat{\Delta}}}{2^{\hat{\Delta}+1}} \, {}_2F_1\left(\frac{\hat{\Delta}}{2}, \frac{\hat{\Delta}}{2} + \frac{1}{2}; \hat{\Delta}; \tilde{\chi}^2\right), \tag{II.6.31}$$

where $\tilde{\chi}$ is the geodesic distance between the operator insertions which is given by

$$\tilde{\chi} = \frac{2r_1 r_2}{r_1^2 + r_2^2 + (\vec{x}_1 - \vec{x}_2)^2} \tag{II.6.32}$$

For diagonal modes $i = j$, the fields couple to operators belonging to family of short representations of the defect superconformal algebra $\hat{\Delta} = 1 + |\ell|$, the symmetric representations. Off-diagonal modes belong to short multiplets of a central extension of the defect superconformal algebra with $\mathfrak{P}$ and $\mathfrak{K}$, so we expect their dimensions to be protected from quantum corrections. These representations are related to the defect BPS by an outer automorphism [20].

II.6.4 Hard Bosons

The kinetic terms for the φ_w modes are of the form

$$2\pi \sum_{\ell} \int d^3x \sqrt{g_{AdS_3}} \Big((\varphi_{\bar{w}})^{(-\ell)}_{ij} \left(\Delta_{AdS_3} - (|\mathfrak{Z}_{ij}|^2 + (\ell-1)^2 - 1) \right) (\varphi_w)^{(\ell)}_{ji} \\ + (\varphi_w)^{(-\ell)}_{ij} \left(\Delta_{AdS_3} - (|\mathfrak{Z}_{ij}|^2 + (\ell+1)^2 - 1) \right) (\varphi_{\bar{w}})^{(\ell)}_{ji} \Big). \tag{II.6.33}$$

The reality condition on the fields implies

$$\left(\varphi^{(\ell)}_w\right)^* = \varphi^{(-\ell)}_{\bar{w}}. \tag{II.6.34}$$

For the hard bosons we first perform the KK reduction on S^1. Because of the background $U(1)_R$ gauge field the diagonal terms of the mass matrix for φ_w are shifted relative to those of $a_{r,\psi}$. This gives a mass matrix of the following form for the fields in AdS_3:

$$\begin{pmatrix} a^{(\ell)}_r \\ a^{(\ell)}_\psi \\ \varphi^{(\ell)}_w \\ \varphi^{(\ell)}_{\bar{w}} \end{pmatrix}^*_{ij} \begin{pmatrix} (|\mathfrak{Z}_{ij}|^2 + \ell^2) & 2i\ell & -i\sqrt{2}\,\mathfrak{Z}^\dagger_{ij} & -i\sqrt{2}\,\mathfrak{Z}_{ij} \\ -2i\ell & (|\mathfrak{Z}_{ij}|^2 + \ell^2) & -\sqrt{2}\,\mathfrak{Z}^\dagger_{ij} & \sqrt{2}\,\mathfrak{Z}_{ij} \\ i\sqrt{2}\,\mathfrak{Z}_{ij} & -\sqrt{2}\,\mathfrak{Z}_{ij} & (|\mathfrak{Z}_{ij}|^2 + (\ell-1)^2 - 1) & 0 \\ i\sqrt{2}\,\mathfrak{Z}^\dagger_{ij} & \sqrt{2}\,\mathfrak{Z}^\dagger_{ij} & 0 & (|\mathfrak{Z}_{ij}|^2 + (\ell+1)^2 - 1) \end{pmatrix} \begin{pmatrix} a^{(\ell)}_r \\ a^{(\ell)}_\psi \\ \varphi^{(\ell)}_w \\ \varphi^{(\ell)}_{\bar{w}} \end{pmatrix}_{ji}. \tag{II.6.35}$$

This is slightly different from the conventions used in [48] for their background field computation. The eigenvalues of the AdS_3 mass matrix are

$$(m^{ij}_\pm)^2 = \left(\sqrt{|\mathfrak{Z}_{ij}|^2 + \ell^2} \pm 1 \right)^2 - 1; \tag{II.6.36}$$

note the -1 corresponding to the conformal coupling to the curvature. These correspond to 1-form operators on the boundary with conformal dimensions

$$\hat{\Delta}^{\boldsymbol{v}}_{\pm} = \sqrt{|\mathfrak{Z}_{ij}|^2 + \ell^2} \pm 1. \tag{II.6.37}$$

II.6.5 Fermions

For the fermion fields we need to reduce the spinors from 10d to 3d in two steps; by first reducing to $\mathbb{R}^{1,3}$ and then doing a further S^1 reduction; we also have to decompose the $SO(6)_R$ labels. Our conventions for the gamma matrices are such that Γ^0 in the Lorentz signature is related to Γ^4 in Euclidean signature by multiplication by i, and so the indices run from $\mu = 0, 1, 2, 3$ and $I = 5, 6, 7, 8, 9, 10$. The gamma matrices decompose as follows

$$\begin{aligned} \Gamma^{\mu} &= \gamma^{\mu} \otimes \mathbf{1}_2 \otimes \mathbf{1}_4 \quad \mu = 0, 1, 2, 3 \\ \Gamma^{5,6} &= \gamma_5 \otimes \sigma^{1,2} \otimes \mathbf{1}_4 \\ \Gamma^{A} &= \gamma_5 \otimes \sigma^3 \otimes \tilde{\gamma}^{A-6}, \quad A = 7, 8, 9, 10 \end{aligned} \tag{II.6.38}$$

where γ^{μ} and $\tilde{\gamma}^A$ are $SO(1,3)$ and $SO(4)_R$ gamma matrices. The $SO(1,9)$ quantum numbers split into $SO(1,3) \times SO(2)_R \times SO(4)_R$ labels. It will be convenient to split the 10d chiral spinor into eigenstates of the chirality matrices for each factor;

$$\begin{aligned} \gamma_5 &= i\gamma^0\gamma^1\gamma^2\gamma^3 \\ \tilde{\gamma}^5 &= -\tilde{\gamma}^1\tilde{\gamma}^2\tilde{\gamma}^3\tilde{\gamma}^4 \\ \Gamma^{11} &= (-i\gamma^5) \otimes (i\sigma^3) \otimes \tilde{\gamma}^5 \end{aligned} \tag{II.6.39}$$

The $SO(2)_R$ charge generator will also be important

$$\frac{i}{4}[\Gamma^5, \Gamma^6] = \mathbf{1}_4 \otimes \left(-\frac{1}{2}\sigma^3\right) \otimes \mathbf{1}_4. \tag{II.6.40}$$

In this convention, the $SO(2)_R$ charge carries the opposite sign relative to the 2d chirality. Then a chiral spinor in 10d decomposes into

$$\begin{aligned} \mathbf{16}_+ \to &[(1/2, 0) \otimes (-1/2) \otimes (1/2, 0)] \oplus [(0, 1/2) \otimes (+1/2) \otimes (1/2, 0)] \\ &\oplus [(1/2, 0) \otimes (+1/2) \otimes (0, 1/2)] \oplus [(0, 1/2) \otimes (-1/2) \otimes (0, 1/2)], \end{aligned} \tag{II.6.41}$$

and so we can think of a 10d chiral spinor as a pair of 4d Dirac fermions tranforming in the $(1/2, 0)$ and $(0, 1/2)$ representation of the residual $SO(4)_R$ symmetry. Next we need to impose the 10d Majorana condition. The reality condition on the gamma matrices in Lorentz signature is

$$\Gamma^* = \mathcal{C}\Gamma^0\Gamma\left(\mathcal{C}\Gamma^0\right)^{-1} \tag{II.6.42}$$

The charge conjugation matrix $\mathcal{C} = \Gamma^1\Gamma^3\Gamma^6\Gamma^7\Gamma^9$decomposes as

$$\mathcal{C} = \gamma^1\gamma^3\gamma^5 \otimes \sigma^2 \otimes \tilde{\gamma}^1\tilde{\gamma}^3, \tag{II.6.43}$$

where the first factor can be taken to be the 4d charge conjugation matrix, the second factor is also the charge conjugation in 2d while the last factor is the time reversal matrix in 4d. The Majorana condition for a 10d spinor λ is then

$$\lambda^* = \mathcal{C}\Gamma^0\lambda = (\mathcal{C}_4\gamma^0 \otimes \mathcal{C}_2 \otimes \tilde{\mathcal{T}}_4)\lambda, \tag{II.6.44}$$

and since we want to reduce to 4d it will be useful to relate this condition to the Majorana condition in 4d. To understand this, we can decompose the 10d spinor into its components under (II.6.41);

$$\begin{aligned}\lambda = \chi_a \otimes \epsilon^- \otimes \hat{c}^a + \eta_a^\dagger \otimes \epsilon^+ \otimes \hat{c}^a \\ + \xi_{\dot{a}} \otimes \epsilon^+ \otimes \hat{c}^{\dot{a}} + \zeta_{\dot{a}}^\dagger \otimes \epsilon^- \otimes \hat{c}^{\dot{a}}\end{aligned} \tag{II.6.45}$$

where we suppressed the Lorentz spinor indices. Clearly the Majorana condition does not mix the dotted and undotted $SO(4)_R$ indices which suggest that we should pair χ and $\eta^\dagger$ into a Dirac spinor and similarly for the remaining spinors. For a moment, let us ignore the $SO(4)$ indices; we can always multiply $\mathcal{C}$ with a phase such that $\mathcal{C}_2$ acts as follows on $\epsilon^\pm$

$$\mathcal{C}_2\epsilon^\pm = \epsilon_\mp \tag{II.6.46}$$

which we should understand as maps between the two different $SO(2)$ chiralities. Com-

plex conjugation raises and lowers the indices of $\epsilon^{\pm}$ but does not mix chiralities, and $\mathcal{C}_2$ maps the chiralities into each other while raising/lowering the indices. So we can define component-wise

$$\epsilon^{+} = -\epsilon_{-} \tag{II.6.47}$$

and so on. Similarly $\mathcal{C}_4\gamma^0$ changes the Lorentz chirality without lowering/raising the spinor indices:

$$\left(\mathcal{C}_4\gamma^0 \otimes \mathcal{C}_2\right) \begin{pmatrix} \chi_\alpha \otimes \epsilon^{-} \\ \eta^{\dagger\dot{\alpha}} \otimes \epsilon^{+} \end{pmatrix} = \begin{pmatrix} \eta^{\dagger\dot{\beta}} \otimes \epsilon_{-} \\ \chi_\beta \otimes \epsilon_{+} \end{pmatrix}. \tag{II.6.48}$$

For the last factor we can use $\tilde{\mathcal{T}}_4$ to raise and lower the remaining indices. Complex conjugation raises and lowers the indices as well without exchanging the chiralities. Putting everything together, this implies that

$$\begin{aligned} \chi &= \eta \\ \xi &= \zeta, \end{aligned} \tag{II.6.49}$$

which means that we have four Majorana fermions in 4d after dimensional reduction. The kinetic term is

$$\mathrm{tr}\left[\bar{\lambda}(\gamma^\mu\partial_\mu \otimes \mathbf{1}_2 \otimes \mathbf{1}_4)\lambda + \frac{1}{\bar{z}}\bar{\lambda}(\gamma^5 \otimes \sigma^{+} \otimes \mathbf{1}_4)[\mathfrak{Z}^\dagger, \lambda] + \frac{1}{z}\bar{\lambda}(\gamma^5 \otimes \sigma^{-} \otimes \mathbf{1}_4)[\mathfrak{Z}, \lambda]\right]. \tag{II.6.50}$$

Since this expression is $SO(4)_R = SU(2) \times SU(2)$ symmetric we can ignore the $SO(4)_R$ indices for the time being. To simplify the dependence on the coordinates we should turn on a background $SO(2)$ field

$$\lambda = e^{\frac{i}{2}(\mathbf{1}_4 \otimes \sigma^3 \otimes \mathbf{1}_4)\psi}\,\lambda_0; \tag{II.6.51}$$

the reason we do this is so that the ψ dependence on the mass term cancels

$$\frac{1}{\bar{z}}\bar{\lambda}(\gamma^5 \otimes \sigma^{+} \otimes \mathbf{1}_4)[\mathfrak{Z}^\dagger, \lambda] = \frac{1}{r}\bar{\lambda}_0(\gamma^5 \otimes \sigma^{+} \otimes \mathbf{1}_4)[\mathfrak{Z}^\dagger, \lambda_0] \tag{II.6.52}$$

From now on we will drop the lower label and use λ to represent the spinor after including the background gauge field. Defining the 4d Majorana spinors

$$\lambda^+ = \begin{pmatrix} \chi \\ \chi^\dagger \end{pmatrix}, \quad \lambda^- = \begin{pmatrix} \xi \\ \xi^\dagger \end{pmatrix}, \tag{II.6.53}$$

the mass terms can be rewritten in the form

$$\frac{1}{r}\,\mathrm{tr}\left[\xi_{\dot{a}}[\mathfrak{Z}, \xi^{\dot{a}}] + \xi^\dagger_{\dot{a}}[\mathfrak{Z}^\dagger, \xi^{\dagger\dot{a}}] + \chi_a[\mathfrak{Z}^\dagger, \chi^a] + \chi^\dagger_a[\mathfrak{Z}, \chi^{\dagger a}]\right] \tag{II.6.54}$$

Mapping to AdS_3

Now we can perform the boundary expansion of the fields by performing a field redefinition

$$\lambda \to \frac{\lambda'}{r^{3/2}} \tag{II.6.55}$$

after which the fermion kinetic terms become

$$-\frac{1}{g^2}\int \sqrt{g_{AdS_3\times S^1}}d^4x\ \mathrm{tr}\left[i\bar{\lambda}'\left(e^\mu_{\hat{\alpha}}\,\Gamma^{\hat{\alpha}}\partial_\mu - \Gamma^r + \frac{i}{2}\Gamma^\psi\left(\mathbf{1}_4\otimes\sigma^3\otimes\mathbf{1}_4\right)\right)\lambda'\right] \tag{II.6.56}$$

This is the action of a fermion on $AdS_3 \times S^1$ with a background gauge field along the circle direction. The action of $\mathbf{1}_4 \otimes \sigma^3 \otimes \mathbf{1}_4$ can be replaced with $\pm\gamma_5$ on $\lambda^\pm$, with the upper indices denoting the $SO(4)_R$ chirality, due to the 10d chirality of the spinor which allows us to rewrite everything in 4d language:

$$\begin{aligned}
&-\frac{1}{g^2}\int \sqrt{g_{AdS_3\times S^1}}d^4x\ \mathrm{tr}\left[i\bar{\lambda}^{+\,a}\left(e^\mu_{\hat{\alpha}}\,\gamma^{\hat{\alpha}}\nabla_\mu + \frac{i}{2}\gamma^\psi\gamma^5\right)\lambda^+_a + i\bar{\lambda}^{-\,\dot{a}}\left(e^\mu_{\hat{\alpha}}\,\gamma^{\hat{\alpha}}\nabla_\mu - \frac{i}{2}\gamma^\psi\gamma^5\right)\lambda^-_{\dot{a}}\right] \\
&= -\frac{1}{g^2}\int \sqrt{g_{AdS_3\times S^1}}d^4x\ \mathrm{tr}\left[i\bar{\lambda}^{+\,a}\left(e^\mu_{\hat{\alpha}}\,\gamma^{\hat{\alpha}}\nabla_\mu + \frac{1}{2}\gamma^\star\right)\lambda^+_a + i\bar{\lambda}^{-\,\dot{a}}\left(e^\mu_{\hat{\alpha}}\,\gamma^{\hat{\alpha}}\nabla_\mu - \frac{1}{2}\gamma^*\right)\lambda^-_{\dot{a}}\right],
\end{aligned} \tag{II.6.57}$$

where $\gamma^* = \gamma^0\gamma^1\gamma^2$ is the product over the gamma matrices in the AdS directions. To reduce from 4d to 3d we should pick a basis of gamma matrices that remains real after

the dimensional reduction such that the 3d spinors are Majorana. In such a basis the 4d chirality matrix is not diagonal, so the mass term is not as simple. For example we can take the 4d gamma matrices in a basis

$$\begin{aligned}\gamma^{0,1,2} &= \begin{pmatrix} 0 & \hat{\gamma}^{0,1,2} \\ \hat{\gamma}^{0,1,2} & 0 \end{pmatrix}, \quad \gamma^3 = \begin{pmatrix} \mathbf{1}_2 & 0 \\ 0 & -\mathbf{1}_2 \end{pmatrix} \\ \gamma^5 &= \begin{pmatrix} 0 & -i\mathbf{1}_2 \\ i\mathbf{1}_2 & 0 \end{pmatrix}.\end{aligned} \tag{II.6.58}$$

where $\hat{\gamma}^k$ are the 3d gamma matrices. In this basis $\gamma^0\mathcal{C}_4$ is equal to the identity. Since $\tilde{\mathcal{T}}_4$ commutes with the $SO(4)$ chirality matrix, we can formally diagonalize $\mathcal{C}_2 \otimes \tilde{\mathcal{T}}_4$[7] and restrict to the subspace with eigenvalue equal to one. The eigenvalues of $\mathcal{C}_2$ and $\tilde{\mathcal{T}}_4$ are $\pm i$ if we work with a convention such that $\mathcal{C}^T = \mathcal{C}^{-1}$. In this basis the 10d Majorana condition is just

$$\lambda^* = \lambda, \tag{II.6.59}$$

and the 10d spinor splits into four Majorana spinors

$$\Psi^-_+, \quad \Psi^+_-, \quad \tilde{\Psi}^-_+, \quad \tilde{\Psi}^+_-, \tag{II.6.60}$$

where now the upper indices denote the sign of the eigenvalue of $\mathcal{C}_2$, and the lower index labels the $SU(2) \times SU(2)$ basis where $\mathcal{T}_4$ is diagonal. Because the signs are always opposite the upper indices are redundant and we will omit them. To reduce from 4d to 3d we simply split the four components into pairs of two-dimensional real spinors which are eigenvectors of $\gamma^\psi = \gamma^3$;

$$\Psi_\pm = \begin{pmatrix} \chi_\pm \\ \eta_\pm \end{pmatrix}, \tag{II.6.61}$$

and similarly for the fields with negative $SO(4)_R$ chirality. The 10d chirality condition allows us to replace the background $SO(2)$ gauge field by a chirality transformation

$$\Gamma^{11}\lambda = \lambda \Rightarrow \left(\mathbf{1}_4 \otimes \sigma^3 \otimes \mathbf{1}_4\right)\lambda = \left(\gamma^5 \otimes \mathbf{1}_2 \otimes \tilde{\gamma}^5\right)\lambda. \tag{II.6.62}$$

[7] We say formally because this matrix is a map between complex conjugate representations.

so we just need to split kinetic terms for the fermions according to their $SO(4)_R$ chirality. The kinetic terms (for one of the $SO(4)_R$ chiralities) are then

$$\begin{aligned}
&= \mathrm{tr}\left[i\bar{\Psi}^{\,a}\left(e^{\mu}_{\hat{\alpha}}\,\gamma^{\hat{\alpha}}\nabla_{\mu}+\frac{1}{2}\gamma^{\star}\right)\Psi_{a}\right]\\
&= \mathrm{tr}\left[i\bar{\chi}^{\,a}\left(e^{\mu}_{\hat{\alpha}}\,\hat{\gamma}^{\hat{\alpha}}\nabla_{\mu}+\frac{1}{2}\right)\chi_{a}+i\bar{\eta}^{\,a}\left(e^{\mu}_{\hat{\alpha}}\,\hat{\gamma}^{\hat{\alpha}}\nabla_{\mu}+\frac{1}{2}\right)\eta_{a}+i\bar{\eta}^{a}\partial_{\psi}\chi_{a}-i\bar{\chi}^{a}\partial_{\psi}\eta_{a}\right].
\end{aligned} \tag{II.6.63}$$

An important comment is that the barred spinors in the second line are defined in 3d, $\bar{\chi}=\chi^{\dagger}\hat{\gamma}^{0}$, whereas the barred spinors in the first line are 4d spinors. Now can easily perform the S^1 reduction

$$\chi(\psi)=\sum_{\ell}e^{i\ell\psi}\chi^{(\ell)} \tag{II.6.64}$$

and similarly for all the other modes. To simplify the mass terms we need to compute the matrix elements of $\gamma^{5}\otimes\sigma^{\pm}\otimes\mathbf{1}$ in the Majorana basis. In the basis where σ^3 is diagonal, the eigenvectors of $\mathcal{C}_2\otimes\mathcal{T}_4$ are given by

$$\frac{1}{\sqrt{2}}\Psi_{\mp}\otimes\begin{pmatrix}1\\ \pm i\end{pmatrix}=\Psi_{\mp}\otimes v_{\pm}. \tag{II.6.65}$$

Here we should be careful when taking the complex conjugate, since the basis vectors themselves are complex but the coefficients of the spinors are real. After assembling the vectors $v_{\pm}$ into a matrix V, the relevant matrix elements are

$$\begin{aligned}
M^{a}_{b}&=V^{\dagger}\sigma^{+}V=\frac{1}{2}\begin{pmatrix}1 & -i\\ -i & -1\end{pmatrix}\\
M^{\dagger\,a}_{b}&=V^{\dagger}\sigma^{-}V=\frac{1}{2}\begin{pmatrix}1 & i\\ i & -1\end{pmatrix}
\end{aligned} \tag{II.6.66}$$

All the terms are $SO(2,2)$ invariant so the mass terms are diagonal in the AdS_3 spinor space; the resulting mass matrix for the positive $SO(4)_R$ chirality modes is

$$\begin{pmatrix}\bar{\chi}^{a}\\ \bar{\eta}^{a}\end{pmatrix}\begin{pmatrix}\mathfrak{Z}M^{\dagger\,b}_{a}+\mathfrak{Z}^{\dagger}M^{b}_{a}+\frac{1}{2}\delta^{b}_{a} & i\ell\delta^{b}_{a}\\ -i\ell\delta^{b}_{a} & -\mathfrak{Z}M^{\dagger}{}^{b}_{a}-\mathfrak{Z}^{\dagger}M^{b}_{a}+\frac{1}{2}\delta^{b}_{a}\end{pmatrix}\begin{pmatrix}\chi_{b}\\ \eta_{b}\end{pmatrix}. \tag{II.6.67}$$

The eigenvalues are doubly degenerate and given by:

$$\left(m^{+}_{f,\pm}\right)_{ij} \in \left\{\frac{1}{2}+\sqrt{\ell^2+|\mathfrak{Z}_{ij}|^2}, -\left(-\frac{1}{2}+\sqrt{\ell^2+|\mathfrak{Z}_{ij}|^2}\right)\right\}. \tag{II.6.68}$$

From this we can infer the eigenvalues for the remaining modes (negative $SO(4)_R$ chirality)

$$\left(m^{-}_{f,\pm}\right)_{ij} \in \left\{-\left(\frac{1}{2}+\sqrt{\ell^2+|\mathfrak{Z}_{ij}|^2}\right), -\frac{1}{2}+\sqrt{\ell^2+|\mathfrak{Z}_{ij}|^2}\right\}. \tag{II.6.69}$$

These fields correspond to defect operators with dimensions

$$\hat{\Delta}^{\boldsymbol{f}}_{\pm} = 1+|m^{+}_{f,\pm}|. \tag{II.6.70}$$

The boundary conditions for fermions are more subtle than those of the vector or scalar fields since the Dirac equation is first order; for a detailed discussion see [3, 89, 9]. A Dirac spinor in AdS_3 restricts to a pair of chiral fermions on the boundary, with the chirality matrix being the gamma matrix for the radial direction. These two chiral fermions are canonically conjugate to each other, so one of the modes must have Dirichlet boundary conditions, depending on the sign of the mass. The normalizable mode is the one with a positive mass. To be more concrete let us take one of the fermion modes and call it ξ. Near $r=0$ the solutions to the Dirac equation have the following asymptotic form

$$\xi_{\pm} \sim A_{\pm}(x) r^{1\mp m} + B_{\pm} r^{2\pm m} + \ldots, \tag{II.6.71}$$

so the boundary conditions on the fields depend on the sign of m. If $m>0$, the first term is dominant for ξ_+ and we should fix A_+ at the boundary. The Dirac equation implies that $A_\pm$ is related to $B_\mp$ so that fixing A_+ also fixes B_-. If $m<0$ we should fix A_-.

The fermion bulk-to-bulk propagator can be expressed in terms of scalar propagators [102]

$$S(x,x') = \sqrt{\frac{r'}{r}}\left[e^{\mu}_{\hat{\alpha}}\hat{\gamma}^{\hat{\alpha}}\nabla_{\mu}+\frac{1}{2}\hat{\gamma}^{r}+m\right]\left[G_{\hat{\Delta}-\frac{1}{2}}(x,x')\mathcal{P}_{-}+G_{\hat{\Delta}+\frac{1}{2}}(x,x')\mathcal{P}_{+}\right], \tag{II.6.72}$$

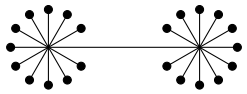

Figure II.1: An example of the leading-order diagrams for the two-point functions of the single trace operators. Two vertices at the centers represent each of the single trace operators, connected by a single edge corresponding to the scalar propagator. The black dots represent the one-point functions $\langle\phi\rangle$ for each Higgs scalar in the surface defect background.

where $\mathcal{P}_\pm = \frac{1}{2}(1 \pm \hat{\gamma}^r)$.

II.7 Perturbative Two-point Function

Here, we perturbatively compute the two-point function of single trace operators to compare it with the conformal block expansion in the generic surface defect background. This will allow us to compute bulk-to-defect couplings of BPS operators at leading order in the coupling. As the simplest case, let us consider the two-point function of the half-BPS scalar single trace operators:

$$\langle \mathcal{O}_{\Delta_1}(x_1)\mathcal{O}_{\Delta_2}(x_2)\rangle = \left\langle Y^1_{I_1}\cdots Y^1_{I_{\Delta_1}}\,\mathrm{Tr}\big[\phi^{I_1}\cdots\phi^{I_{\Delta_1}}\big]Y^2_{J_1}\cdots Y^2_{J_{\Delta_2}}\,\mathrm{Tr}\big[\phi^{J_1}\cdots\phi^{J_{\Delta_2}}\big]\right\rangle \quad \text{(II.7.1)}$$

We are interested in the leading-order connected contribution, since self-contractions only contribute to the one-point functions. A similar contribution is considered in for example [117, 11] for the domain wall in $\mathcal{N} = 4$ SYM. The Feynman diagram for the leading connected contribution is obtained by contracting one of the scalars from each operator as in fig. II.1 with the uncontracted ones giving the contributions of its one-point function in the defect background. This leads to the leading-order contribution of

$$
\begin{aligned}
&\langle \mathcal{O}_{\Delta_1}(X_1)\mathcal{O}_{\Delta_2}(X_2)\rangle \\
&= \frac{1}{\Delta_1\Delta_2}\sum_{m,n} Y^1_{I_1}\cdots Y^1_{I_{\Delta_1}} Y^2_{J_1}\cdots Y^2_{J_{\Delta_2}} \\
&\times \left\langle \phi^{I_1}\right\rangle_{i_{\Delta_1} i_1} \left\langle \phi^{I_2}\right\rangle_{i_i i_2} \cdots \left\langle \phi^{I_{m-1}}\right\rangle_{i_{m-2} i_{m-1}} \left\langle \phi^{I_{m+1}}\right\rangle_{i_m i_{m+1}} \cdots \left\langle \phi^{I_{\Delta_1}}\right\rangle_{i_{\Delta_1-1} i_{\Delta_1}} \\
&\times \left\langle \phi^{J_1}\right\rangle_{j_{\Delta_2} j_1} \left\langle \phi^{J_2}\right\rangle_{j_i j_2} \cdots \left\langle \phi^{J_{n-1}}\right\rangle_{j_{n-2} j_{n-1}} \left\langle \phi^{J_{n+1}}\right\rangle_{j_n j_{n+1}} \cdots \left\langle \phi^{J_{\Delta_2}}\right\rangle_{j_{\Delta_2-1} j_{\Delta_2}} \\
&\times \left\langle \phi^{I_m}_{i_{m-1} i_m}(x_1)\phi^{J_n}_{j_{n-1} j_n}(x_2)\right\rangle
\end{aligned}
\tag{II.7.2}
$$

where $\frac{1}{\Delta_1\Delta_2}$ is the symmetry factor, and the i and j indices are in the fundamental of the gauge group. For the nonsingular case, the VEVs $\left\langle \phi^I \right\rangle$ take nonzero values in diagonal matrices as (II.2.5) when $I = 1, 2$. Let us write the i-th diagonal element as M^I_i. The propagator $\left\langle \phi^I \phi^J \right\rangle$ is the Higgs scalar propagator in the defect background derived in section II.6.

The important note for this leading-order contribution is that only the diagonal part $i_{m-1} = i_m$ and $j_{n-1} = j_n$ contributes in the propagator, due to the fact that the one-point functions are diagonal, making $i_1 = i_2 = \cdots = i_{\Delta_1}$ and $j_1 = j_2 = \cdots = j_{\Delta_1}$ for the nonzero terms. Furthermore, the propagator $\left\langle \phi^I_{ij}\phi^J_{kl}\right\rangle$ contains the factor $\delta_{il}\delta_{jk}$, which restricts the nonzero terms to have all i's to be the same as j's. Thus, the two-point function can be written as

$$
\langle \mathcal{O}_{\Delta_1}(X_1)\mathcal{O}_{\Delta_2}(X_2)\rangle_1 = \sum_i (Y^1 \circ M^1_i)^{\Delta_1-1}(Y^2 \circ M^2_i)^{\Delta_2-1} \sum_{m,n} Y^1_{I_m} Y^2_{J_n} \left\langle \phi^{I_m}_{ii}(x_1)\phi^{J_n}_{ii}(x_2)\right\rangle
\tag{II.7.3}
$$

$\circ$ denotes the dot product in the $I = 1, 2$ directions only. The scalar propagators of the diagonal elements of ϕ's are quite simple since the contributions to the effective masses from $\mathfrak{Z}_{ii}$ all vanish. The only remaining mass contributions are due to the KK momenta in the ψ direction. Especially, the diagonal parts of the scalars ϕ^1_{ii} and ϕ^2_{jj} fully decouple with each other and also from the gauge field fluctuations, and are no longer different from the other scalars. The propagator can be thus written as

$$\left\langle \phi_{ii}^{I_m}(x_1)\phi_{ii}^{J_n}(x_2)\right\rangle = \frac{g_{\rm YM}^2}{4\pi}\frac{1}{r_1 r_2}\delta^{I_m J_n}\sum_{\ell} e^{i\ell\psi}G_{\hat{\Delta}}(x_1,x_2) \tag{II.7.4}$$

where $G_{\hat{\Delta}}(x_1,x_2)$ is the AdS_3 propagator (II.6.31) with $\hat{\Delta} = 1+|\ell|$. The sign of the conformal weight $\hat{\Delta}$ is chosen so that it is positive to satisfy the unitarity for all ℓ. The geodesic distance $\tilde{\chi}$ is related to the cross-ratio χ as $2/\chi = \tilde{\chi}$. This matches exactly with the defect conformal symmetry part of the superconformal block by identifying $\hat{\Delta}$ as the scaling dimension of the internal defect operators in the bulk-defect OPE.

The product between the polarization vector together with the factor $\delta^{I_m J_n}$ from the propagator gives the inner product between the polarizations of the two operators

$$Y^1_{I_m}Y^2_{J_n}\delta^{I_m J_n} = (Y^1\circ Y^1)^{1/2}(Y^2\circ Y^2)^{1/2}\left(-\frac{\chi_R}{2}+\cos\phi_R\right). \tag{II.7.5}$$

Lastly, the factor $(Y\circ M_i)^{\Delta-1}$ can be expanded in terms of the cross-ratios and the VEVs of the scalar fields as

$$\begin{aligned}(Y\circ M_i)^{\Delta-1} &= \frac{1}{2^{\Delta-1}}\frac{(Y\circ Y)^{(\Delta-1)/2}}{(P\circ P)^{(\Delta-1)/2}}\left((\beta_i+i\gamma_i)e^{i\eta}+(\beta_i-i\gamma_i)e^{-i\eta}\right)^{\Delta-1}\\ &= \frac{1}{2^{\Delta-1}}\frac{(Y\circ Y)^{(\Delta-1)/2}}{(P\circ P)^{(\Delta-1)/2}}\sum_{k=0}^{\Delta-1}\binom{\Delta-1}{k}(\beta_i+i\gamma_i)^{\Delta-k-1}(\beta_i-i\gamma_i)^k e^{i(\Delta-2k-1)\eta}\end{aligned} \tag{II.7.6}$$

Overall, the two-point function in the leading order in terms of the cross ratios looks like

$$\langle \mathcal{O}_{\Delta_1}(X_1)\mathcal{O}_{\Delta_2}(X_2)\rangle = \frac{g_{\rm YM}^2}{4\pi}\frac{1}{2^{\Delta_1+\Delta_2}}\frac{(Y^1\circ Y^1)^{\Delta_1/2}(Y^2\circ Y^2)^{\Delta_2/2}}{(P^1\circ P^1)^{\Delta_1/2}(P^2\circ P^2)^{\Delta_2/2}}$$
$$\times\sum_{k_1=0}^{\Delta_1-1}\sum_{k_2=0}^{\Delta_2-1}C(k_1,k_2)e^{ik_1'\eta_1}e^{ik_2'\eta_2}\left(-\frac{\chi_R}{2}+\cos\phi_R\right)$$
$$\times\sum_{\ell}e^{i\ell\psi}\chi^{-(1+|\ell|)}{}_2F_1\left(\frac{|\ell|+1}{2},\frac{|\ell|}{2}+1;|\ell|+1;\frac{4}{\chi^2}\right) \qquad \text{(II.7.7)}$$

where $C(k_1,k_2)$ is a coefficient

$$C(k_1,k_2)=\binom{\Delta_1-1}{k_1}\binom{\Delta_2-1}{k_2}\sum_i(\beta_i+i\gamma_i)^{\Delta_1+\Delta_2-k_1-k_2-2}(\beta_i-i\gamma_i)^{k_1+k_2} \qquad \text{(II.7.8)}$$

and $k_i'=\Delta_i-2k_i-1$. You can further rewrite it by using $\cos\phi_R e^{i\ell\psi}=\frac{1}{2}\left(e^{i(\ell+1)\psi-i\eta}+e^{i(\ell-1)\psi+i\eta}\right)$ with $\eta=\psi-\phi_R=\eta_1-\eta_2$ and shifting ℓ so that the terms have the same central $SO(2)_t$ charge as

$$\langle \mathcal{O}_{\Delta_1}(X_1)\mathcal{O}_{\Delta_2}(X_2)\rangle_1$$
$$=\frac{g_{\rm YM}^2}{4\pi}\frac{1}{2^{\Delta_1+\Delta_2+1}}\frac{(Y^1\circ Y^1)^{\Delta_1/2}(Y^2\circ Y^2)^{\Delta_2/2}}{(P^1\circ P^1)^{\Delta_1/2}(P^2\circ P^2)^{\Delta_2/2}}$$
$$\times\sum_{k_1=0}^{\Delta_1-1}\sum_{k_2=0}^{\Delta_2-1}\sum_{\ell}C(k_1,k_2)e^{ik_1'\eta_1+ik_2'\eta_2}e^{i\ell\psi}$$
$$\times\left(-\hat{\mathfrak{f}}^R_{[\frac{1}{2},\frac{1}{2}]}(\chi_R)\hat{\mathfrak{f}}_{|\ell|+1}(\chi)+e^{-i\eta}\hat{\mathfrak{f}}^R_{[0,0]}(\chi_R)\hat{\mathfrak{f}}_{|\ell-1|+1}(\chi)+e^{i\eta}\hat{\mathfrak{f}}^R_{[0,0]}(\chi_R)\hat{\mathfrak{f}}_{|\ell+1|+1}(\chi)\right) \qquad \text{(II.7.9)}$$
$$=\frac{(Y^1\circ Y^1)^{\Delta_1/2}(Y^2\circ Y^2)^{\Delta_2/2}}{(P^1\circ P^1)^{\Delta_1/2}(P^2\circ P^2)^{\Delta_2/2}}\times\sum_{\hat{\mathcal{O}}}\sum_{\ell}\mathcal{B}_{\mathcal{O}_1,\hat{\mathcal{O}}_\ell}(\eta_1)\mathcal{B}_{\mathcal{O}_2,\hat{\mathcal{O}}_\ell}(\eta_2)\hat{\mathfrak{F}}_{\hat{\mathcal{S}}_\ell} \qquad \text{(II.7.10)}$$

Now, it is obvious how the terms can be packaged as superconformal blocks. For a finite ℓ, the terms coincide with those appearing in the superconformal blocks corresponding to the representation (II.4.22). The $\ell=0$ terms match with two copies of the superconformal block in the representation (II.4.20). One can see that the relations between the prefactors satisfy the SCWI constraints. The states that appear in the OPE expansion have degeneracy according to the breaking of the gauge symmetry.

These states describe point-like open string starting and ending on each of the probe D3-branes.

II.8 Discussion and future directions

In this chapter we studied correlation functions in the presence of supersymmetric surface operators in $\mathcal{N} = 4$ SYM. We used superconformal symmetry to constraint one- and two-point correlation functions of chiral primaries, elaborating on the superconformal block expansion of correlators and the superconformal Ward identities [119]. Unlike supersymmetric defects of other codimensions, the residual superconformal algebra for a generic surface defect is not enough to fully specify one- and two-point functions and these necessarily become functions of the transverse angular direction and R-symmetry polarizations. As a check, we quantized the theory around a generic defect by mapping to a supersymmetric vacuum of $\mathcal{N} = 4$ SYM on $AdS_3 \times S^1$. This language should be useful for perturbative calculations since the symmetries of the system are manifest and many techniques for AdS/CFT are applicable. We perturbatively computed the leading-order two-point function of chiral primaries at weak coupling and found that it matches our expansion in terms of superconformal blocks.

We also investigated the integrability of half-BPS surface defect operators finding evidence against it for generic defects. This is somewhat expected, since all integrable boundaries known correspond to branes wrapping maximal cycles at strong coupling. The integrable surface defect found in [56] is identified with a class of rigid defects sitting at the origin of the moduli space. This set-up is particularly interesting since its quantization necessitates the introduction of additional modes in order to restore the scaling symmetry of the theory. The integrability of the rigid defect system should open the possibility of computing one-point functions of single trace operators at finite coupling.

We conclude with some future directions:

- Two-point functions of chiral primaries and Lorentzian inversion formula: one interesting direction independent of integrability is to apply analytic bootstrap techniques to the GW defect. For instance, bulk three-point functions of chiral primaries are protected as well as their defect one-point functions [48]. Can one use Lorentzian inversion [118] to determine bulk-to-defect couplings using this data, and if so, what are the exchanged states in the defect channel? What is the dominant exchange at large transverse spin, or at large charge?

- Analytic bootstrap and cohomological sections: Our results are supplementary to the analysis of [119]. Although we did not give a general solution to the superconformal Ward identities for generic multiplets, we believe that there are no clear obstructions. This would be essential for adapting bootstrap techniques to the Gukov-Witten dCFT. For instance, it should be expected that the crossing equations become algebraic equations in cohomological subsectors of the theory [18, 33]. This would allow to exploit results from supersymmetric localization to compute more general protected correlators [48]. Another interesting direction would be to study the coupling dependence for bulk-to-defect two-point functions of BPS operators along the lines of [12]. The GW defect two-point function shares many parallels with the bulk four-point function of chiral primaries since their symmetry algebras are analytic continuations of one another. This suggests the possibility that the bulk-to-defect two-point functions of BPS operators are analogous to bulk three-point functions of half-BPS operators.

- Localization and big operators: Recently, it was shown that the one-point functions of chiral primaries in the Gukov-Witten dCFT can be computed using supersymmetric localization [48]. This was used to prove that holographic one-point functions of single-trace operators are finite polynomials in the coupling, with all the contributions coming from tree diagrams at weak coupling. An interesting av-

enue to explore would be to study correlation functions of determinant, or more Schur polynomial, operators [51]. These correlators describe intersections of giant graviton branes ending on the probe D3-branes. For these correlators non-planar corrections are important and they encode nonperturbative information in N.

- Quantization of rigid defects and integrability: the quantization around the rigid defect solutions remains an important problem. We expect that this can be carried out by mapping to a $AdS_3 \times S^1$ with a dilaton field. In that case we expect that the conformal coupling of the fields to the background metric should be modified accordingly to realize the underlying superconformal symmetry [64]. It would also be important to perform checks at strong coupling in the rigid case, especially along the lines of [93]. This work does not fully cover the rigid surface defects discovered in [83]. Although the rigid operators we considered here in the $SU(N)$ gauge theory have the monodoromy whose conjugacy class is a limit of that of the generic cases, the conjugacy classes of the rigid operators in the $SO(N)$ and $Sp(N)$ gauge theories are strictly isolated from the generic ones and hence rigid. They also found some examples of operators with the rigid conjugacy class with diagonal classical profiles for the $SO(N)$ and $Sp(N)$ theories. The relation between the integrability condition and the rigidity of the conjugacy class should be investigated. The extension of our arguments about the integrability to the other semisimple Lie groups is straightforward given the planar limit of these models is essentially the same to that of the $SU(N)$ theory but with additional projections [43]. One step towards this would be to understand the parity projection beyond the $SU(2)$ sector and compare with the selection rules coming from the boundary state. It should also be an interesting question whether this integrability can be discussed from the 4d-2d viewpoint. This is because the $SU(N)$ theory can also have a rigid operator with a rigid conjugacy class, which for the $SU(2)$ case for example, can be constructed by taking a double cover of the target space of the 2d hypermultiplet

corresponding to the rigid defect obtained by the $\alpha, \beta, \gamma \to 0$ limit [83]. In general, such a cover can be taken when the partition of the embedding of $\mathfrak{su}(2)$ to $\mathfrak{su}(N)$ has the greatest common divisor greater than one, and hence the fundamental group of the nilpotent conjugacy class is nontrivial. This construction is unclear from the solely bulk perspective with singular boundary conditions, so taking a cover or not seems not to affect its integrability from our approach. This has to be validated from the more obvious 4d-2d view point.

II.A Harmonic Superspace Formalism

The harmonic superspace formalism is utilized for studying various types of the superconformal field theories, for example in [59, 60, 120, 119]. The setup for the surface defect configuration under our consideration is already provided in [119]. The spacetime coordinates and the $SO(6)_R$ polarization can be packaged as a (2|2) matrix together with the Grassmann odd coordinates as

$$X^{A\dot{A}} = \begin{pmatrix} x^{\alpha\dot{\alpha}} & \theta^{\alpha\dot{a}} \\ \bar{\theta}^{a\dot{\alpha}} & y^{a\dot{a}} \end{pmatrix}. \tag{II.A.1}$$

The uppercase indices run from $1, ..., 4$, and the lowercase indices run from $1, 2$. $x^{\alpha\dot{\alpha}}$ is the ordinary four-dimensional coordinates in the spinor representation. $y^{a\dot{a}}$ specifies the polarization. The null vector Y^I $(I = 1, 2, ..., 6)$ characterizing the 1/2-BPS operators is related to $y^{a\dot{a}}$ as

$$Y^I = \left(y^\mu, \frac{1}{2}(1 - y^2), \frac{i}{2}(1 + y^2) \right), \quad y^{a\dot{a}} = y^\mu (\sigma_\mu)^{a\dot{a}}, \tag{II.A.2}$$

where σ_μ are the Pauli matrices. θ and $\bar{\theta}$ are the odd coordinates. The $PSU(2, 2|4)$ group elements act on the vector space of $X = \begin{pmatrix} A & B \\ C & D \end{pmatrix}$ as

$$g \circ X = (AX + B)(CX + D)^{-1}. \tag{II.A.3}$$

X can be split into the directions parallel to the surface and perpendicular to the surface as $X = X_S + X_\perp$, where

$$X_S = \chi_S \otimes \begin{pmatrix} 1 & 0 \\ 0 & 0 \end{pmatrix} + \bar{\chi}_S \otimes \begin{pmatrix} 0 & 0 \\ 0 & 1 \end{pmatrix}, \quad X_\perp = \chi_\perp \otimes \begin{pmatrix} 0 & 1 \\ 0 & 0 \end{pmatrix} + \bar{\chi}_\perp \otimes \begin{pmatrix} 0 & 0 \\ 1 & 0 \end{pmatrix}. \tag{II.A.4}$$

The elements of the residual subgroup $PSU(1,1|2)^2 \ltimes SO(2)_t$ acts just as eq. (II.A.3) with the elements

$$g = \begin{pmatrix} A & B \\ C & D \end{pmatrix} = \begin{pmatrix} a & b \\ c & d \end{pmatrix} \otimes \begin{pmatrix} 1 & 0 \\ 0 & 0 \end{pmatrix} + \begin{pmatrix} \bar{a} & \bar{b} \\ \bar{c} & \bar{d} \end{pmatrix} \otimes \begin{pmatrix} 0 & 0 \\ 0 & 1 \end{pmatrix}. \tag{II.A.5}$$

The lowercase variables (χ's and the roman alphabets) are all $(1|1)$ matrices, and the superdeterminants of $\begin{pmatrix} a & b \\ c & d \end{pmatrix}$ and $\begin{pmatrix} \bar{a} & \bar{b} \\ \bar{c} & \bar{d} \end{pmatrix}$ are both unity. It is worth noting the specific transformations of the superspace under this subgroup:

- Supertranslations ($A = D = 1_{(2|2)}$, $B = \mathrm{diag}(b, \bar{b})$, $C = 0$)

$$(\chi_S, \bar{\chi}_S, \chi_\perp, \bar{\chi}_\perp) \mapsto (\chi_S + b, \bar{\chi}_S + \bar{b}, \chi_\perp, \bar{\chi}_\perp) \tag{II.A.6}$$

- Superrotations ($A = \mathrm{diag}(a, \bar{a})$, $D = \mathrm{diag}(d, \bar{d})$, $B = C = 0$)

$$(\chi_S, \bar{\chi}_S, \chi_\perp, \bar{\chi}_\perp) \mapsto (a\chi_S d^{-1}, \bar{a}\bar{\chi}_S \bar{d}^{-1}, a\chi_\perp \bar{d}^{-1}, \bar{a}\bar{\chi}_\perp d^{-1}) \tag{II.A.7}$$

- Superspecial conformal transformations
  - with $\bar{c} = 0$ ($A = D = 1_{(2|2)}$, $C = \mathrm{diag}(c, 0)$, $B = 0$)

$$(\chi_S, \bar{\chi}_S, \chi_\perp, \bar{\chi}_\perp)$$
$$\mapsto (\chi_S(1+c\chi_S)^{-1}, \bar{\chi}_S - \bar{\chi}_\perp(1+c\chi_S)^{-1}c\chi_\perp, (1+\chi_S c)^{-1}\chi_\perp, \bar{\chi}_\perp(1+c\chi_S)^{-1}) \tag{II.A.8}$$

– with $c = 0$ ($A = D = 1_{(2|2)}$, $C = \mathrm{diag}(0, \bar{c})$, $B = 0$)

$$(\chi_S, \bar{\chi}_S, \chi_\perp, \bar{\chi}_\perp)$$
$$\mapsto (\chi_S - \chi_\perp(1+\bar{c}\bar{\chi}_S)^{-1}\bar{c}\bar{\chi}_\perp, \bar{\chi}_S(1+\bar{c}\bar{\chi}_S)^{-1}, \chi_\perp(1+\bar{c}\bar{\chi}_S)^{-1}, (1+\bar{\chi}_S\bar{c})^{-1}\bar{\chi}_\perp) \tag{II.A.9}$$

Notice that on the surface $\chi_\perp = \bar{\chi}_\perp = 0$, the superspecial conformal transformations do not mix χ_S and $\bar{\chi}_S$.

II.B Calculation of conformal blocks

The bulk-defect OPEs decompose the bulk operators to the sum of the defect operators. This can be seen from the radial quantization around some point on the defect and the defect vacuum $\left|\hat{\Omega}\right\rangle$ is defined as a state on a sphere around the point [34]. The action of some bulk operator in this case is deforming the sphere so that the operator goes from its exterior to interior, or vice versa. The two-point function can be related to the bulk-defect OPEs by inserting the resolution of the identity as

$$\langle \mathcal{O}_1 \mathcal{O}_2 \rangle = \left\langle \hat{\Omega} \middle| \mathcal{O}_1 \mathcal{O}_2 \middle| \hat{\Omega} \right\rangle = \sum_{\hat{\alpha}} \left\langle \hat{\Omega} \middle| \mathcal{O}_1 \middle| \hat{\alpha} \right\rangle \left\langle \hat{\alpha} \middle| \mathcal{O}_2 \middle| \hat{\Omega} \right\rangle, \tag{II.B.1}$$

where $\hat{\alpha}$ are the defect operators. Let $\hat{J}_i$ be a generator of the defect symmetry, then one finds that each contribution in this conformal block expansion is an eigenfunction of the Casimir operator of the symmetry:

$$\hat{J}_{1i}\hat{J}_1^i \langle \mathcal{O}_1 \mathcal{O}_2 \rangle \supset \left\langle \hat{\Omega} \middle| [\hat{\mathcal{J}}_i, [\hat{\mathcal{J}}^i, \mathcal{O}_1]] \middle| \hat{\alpha} \right\rangle \left\langle \hat{\alpha} \middle| \mathcal{O}_2 \middle| \hat{\Omega} \right\rangle = C_{\hat{\alpha}} \left\langle \hat{\Omega} \middle| \mathcal{O}_1 \middle| \hat{\alpha} \right\rangle \left\langle \hat{\alpha} \middle| \mathcal{O}_2 \middle| \hat{\Omega} \right\rangle, \tag{II.B.2}$$

where $\hat{J}_{1i}$ is the symmetry generator acting on the first insertion point, $\hat{\mathcal{J}}_i$ is the operator corresponding to this generator, and $C_{\hat{\alpha}}$ is the value of the quadratic Casimir characterizing the representation in which $|\hat{\alpha}\rangle$ resides, given that $|\hat{\Omega}\rangle$ is invariant under this symmetry, i.e. $\hat{J}_i|\hat{\Omega}\rangle = 0$.

This means that the defect conformal block $\mathfrak{f}_{\hat{\Delta}}(\chi)\mathfrak{f}^R_{[\frac{n}{2},\frac{n}{2}]}(\chi_R)\mathfrak{h}_j(\psi)$ must be an eigenfunction of the quadratic Casimir of the residual bosonic symmetry. The quadratic Casimirs of each of $SO(2,2)$, $SO(4)_R$, and $SO(2)_t$ are

$$\hat{L}^2 \equiv \frac{1}{2}J_{1AB}J_1^{AB}, \quad \hat{L}_R^2 \equiv \frac{1}{2}R_{1AB}R_1^{AB}, \quad \hat{S}^2 \equiv (J_{112}+R_{112})^2 \tag{II.B.3}$$

respectively, where J_{iMN} are the generators of the $SO(1,5)$ Lorentz symmetry in the embedded six-dimensional space

$$J_{iMN} = P_{iM}\frac{\partial}{\partial P_i^N} - P_{iN}\frac{\partial}{\partial P_i^M} \tag{II.B.4}$$

acting on the i-th insertion point, and R_{iMN} are the generators of the $SO(6)_R$ R-symmetry

$$R_{iMN} = Y_{iM}\frac{\partial}{\partial Y_i^N} - Y_{iN}\frac{\partial}{\partial Y_i^M} \tag{II.B.5}$$

again acting on the i-th point. Each differential operator has a nontrivial dependence on only one of the cross-ratios. So, the Casimir equations can be written separately for each bosonic subgroup

$$(\hat{L}^2 + \hat{\Delta}(\hat{\Delta}-2))\mathfrak{f}_{\hat{\Delta}}(\chi) = 0, \tag{II.B.6}$$
$$(\hat{L}_R^2 + n(n+2))\mathfrak{f}^R_{[\frac{n}{2},\frac{n}{2}]}(\chi_R) = 0, \tag{II.B.7}$$
$$(\hat{S}^2 + j^2)\mathfrak{h}_j(\psi) = 0. \tag{II.B.8}$$

Refer to Sec. II.C.4 for the discussion on the dependence of the values of the Casimirs on the quantum numbers. Note that all the Casimir operators act on only one of the two

inserted points, let us say X_1, as in (II.B.2).

The action of the Casimir of $SO(2,2)$ can be rewritten in the same manner in terms of the cross-ratios as derived in [34]:

$$\left[(4-\chi^2)\frac{\partial}{\partial\chi^2}-3\chi\frac{\partial}{\partial\chi}+\hat{\Delta}(\hat{\Delta}-2)\right]\mathfrak{f}_{\hat{\Delta}}(\chi)=0. \tag{II.B.9}$$

Solving this equation, the eigenfunction for the conformal symmetry part is found to be

$$\mathfrak{f}_{\hat{\Delta}}(\chi)=\chi^{-\hat{\Delta}}{}_2F_1\left(\frac{\hat{\Delta}+1}{2},\frac{\hat{\Delta}}{2};\hat{\Delta};\frac{4}{\chi^2}\right). \tag{II.B.10}$$

The conformal block for the $SO(4)_R$ part can be obtained by replacing χ with χ_R and $\hat{\Delta}$ with $-n$. In this case, it is a polynomial for nonnegative integer n as expected:

$$\hat{f}^R_{[\frac{n}{2},\frac{n}{2}]}(\chi_R)=\chi_R^n{}_2F_1\left(\frac{-n+1}{2},-\frac{n}{2};n;\frac{4}{\chi_R^2}\right)=\sum_{m=0}^{\lfloor n/2\rfloor}(-1)^m\binom{\lfloor n/2\rfloor}{m}\frac{(n/2(+1/2))_m}{(n)_m}4^{2m}\chi_R^{n-2m}. \tag{II.B.11}$$

For the mixed $SO(2)_t$ part, the Casimir equation reduces to

$$\left[(1-\cos^2\psi)\frac{\partial^2}{\partial\cos\phi_+^2}-\cos\psi\frac{\partial}{\partial\cos\psi}+\hat{j}^2\right]=\mathfrak{h}_j(\psi)=0\implies\left[\frac{\partial^2}{\partial\psi^2}+\hat{j}^2\right]\mathfrak{h}_j(\psi)=0 \tag{II.B.12}$$

The solution is[8]

$$\mathfrak{h}_j(\psi)=e^{ij\psi} \tag{II.B.13}$$

We can perform a similar calculation to determine a general form of the η dependent part, even though the full decomposition cannot be determined due to the lack of sym-

[8] $e^{-ij\psi}$ is also a valid solution of this equation, but since the representations with j and $-j$ should always appear symmetrically, we choose to absorb this into the block with $\mathfrak{h}_{-j}(\psi)$.

metry. This η dependence is due to the fact that the defect vacuum may have a nonzero charge under the broken part of the $SO(2) \times SO(2)_R$ rotations. The Casimir of this broken $SO(2)$ acting on the i-th insertion point is

$$\hat{S'}_i^2 = (J_{i12} - R_{i12})^2 \tag{II.B.14}$$

From the two-dimensional theory point of view after dimensional reduction in the defect directions, this corresponds to the boundary condition characterized by $\pi_1((\mathbb{R}^2 \setminus \{0\}) \times (\mathbb{R}^2 \setminus \{0\}))/\pi_1(\mathbb{R}^2 \setminus \{0\}) \simeq \mathbb{Z}$ around the origin where the defect is inserted. Let us write the defect state in the general form $|\hat{\Omega}\rangle = \sum_\ell c_\ell |\hat{\Omega}_\ell\rangle$. Action of the Casimir operator on the two-point function evaluated with this vacuum state gives

$$\begin{aligned}
\hat{S'}_i^2 \langle \mathcal{O}_1 \mathcal{O}_2 \rangle &= \sum_{\ell,\ell'} \sum_{\hat{\alpha}} c_\ell c_{\ell'} \left\langle \hat{\Omega}_\ell \middle| [\hat{S'}, [\hat{S'}, \mathcal{O}_1]] \middle| \hat{\alpha} \right\rangle \left\langle \hat{\alpha} \middle| \mathcal{O}_2 \middle| \hat{\Omega}_{\ell'} \right\rangle \\
&= \sum_{\ell,\ell'} \sum_{\hat{\alpha}} c_\ell c_{\ell'} (\ell - \hat{j}')^2 \left\langle \hat{\Omega}_\ell \middle| \mathcal{O}_1 \middle| \hat{\alpha} \right\rangle \left\langle \hat{\alpha} \middle| \mathcal{O}_2 \middle| \hat{\Omega}_{\ell'} \right\rangle
\end{aligned} \tag{II.B.15}$$

given that $\hat{S'}|\hat{\Omega}\rangle = \ell|\hat{\Omega}\rangle$. $\hat{j}'$ is the charge of $|\hat{\alpha}\rangle$ under this broken $SO(2)$. The action of $\hat{S'}_2^2$ is in the similar manner. $\hat{S'}_i^2$ can be translated to the second derivative $4\partial^2/\partial\eta_i^2$. This leads to that each contribution in the decomposition is $\propto C_{\ell,+} e^{i(\ell - \hat{j}')\eta_i/2} + C_{\ell,-} e^{-i(\ell-\hat{j}')\eta_i/2}$. Overall, one can obtain the general form for the part depending on η_1, η_2 for a specific exchanged operator charged with $\hat{j}'$ under the broken $SO(2)$

$$\begin{aligned}
\mathcal{B}_{1,\hat{\rho}}(\eta_1)\mathcal{B}_{2,\hat{\rho}}(\eta_2) C^{\hat{\rho}}_{\hat{\Delta},n}(\eta) = \sum_{\ell,\ell'} &(c^{\hat{\rho}}_{\hat{\Delta},n,\ell} e^{i(\ell-\hat{j}')\eta_1/2} + \tilde{c}^{\hat{\rho}}_{\hat{\Delta},n,\ell} e^{-i(\ell-\hat{j}')\eta_1/2}) \\
&\times (c^{\hat{\rho}}_{\hat{\Delta},n,\ell'} e^{i(\ell'-\hat{j}')\eta_2/2} + \tilde{c}^{\hat{\rho}}_{\hat{\Delta},n,\ell'} e^{-i(\ell'-\hat{j}')\eta_2/2})
\end{aligned} \tag{II.B.16}$$

II.C Representations of $PSU(1,1|2)^2 \ltimes SO(2)_t$

Here, we study the classification of the representations of the residual symmetry $PSU(1,1|2)^2 \ltimes SO(2)_t$. We start by reviewing the classification of long and short multiplets of the complexified $\mathfrak{sl}(2|2)$ following [165]. The unitary representations of $\mathfrak{sl}(2|2)$ have finite dimensions. Its extension to the unitary representations of $\mathfrak{sl}(1,1|2)$, which are infinite dimensional, appearing in our discussion is fairly straightforward. A defect symmetry representation is constructed by combining a pair of $\mathfrak{psl}(1,1|2)$ multiplets with the same central charge under $\mathfrak{so}(2)_t$. We study how it decomposes into representations of the bosonic subalgebra $\mathfrak{so}(2,2) \oplus \mathfrak{so}(4)_R \oplus \mathfrak{so}(2)_t$ of the defect symmetry to find the combinations of the quantum numbers appearing in the superconformal block decomposition.

II.C.1 Finite-dimensional long representations of $\mathfrak{sl}(2|2)$

Let us first review the finite-dimensional long (non-BPS) representations of $\mathfrak{sl}(2|2)$. In this case, the behavior is the same for the massless and massive cases. The raising fermionic generators $\mathfrak{Q}^{\alpha}{}_{a}$ are in the representation $[\frac{1}{2},\frac{1}{2}]$[9] of the bosonic subalgebra $\mathfrak{g}_0$, so are the lowering generators $\mathfrak{S}^{\dot{a}}{}_{\dot{\alpha}}$. We label the long supermultiplet as $\{j_1,j_2\}$ whose top component has the $\mathfrak{g}_0 = \mathfrak{sl}(2) \oplus \mathfrak{sl}(2)$ representation $[j_1,j_2]$. The commutation relation

$$[(\mathfrak{L}_i)^{\alpha}{}_{\dot{\alpha}}, (\mathfrak{Q}_i)^{\beta}{}_{b}\} = 2\delta^{\beta}_{\dot{\alpha}}(\mathfrak{Q}_i)^{\alpha}{}_{b} - \delta^{\alpha}_{\dot{\alpha}}(\mathfrak{Q}_i)^{\beta}{}_{b}, \quad [(\mathfrak{R}_i)^{\dot{a}}{}_{a}, (\mathfrak{Q}_i)^{\beta}{}_{b}\} = -2\delta_{b\dot{a}}(\mathfrak{Q}_i)^{\beta}{}_{a} + \delta^{a}_{\dot{a}}(\mathfrak{Q}_i)^{\beta}{}_{b} \tag{II.C.1}$$

means that the $(\mathfrak{Q}_i)^{\alpha}{}_{a}$ operators maps the state $|s_1,s_2\rangle$ labeled with the eigenvalues of the Cartan generators in $[j_1,j_2]$ to a linear combination of the states in other representations labeled with $\left|s_1+\frac{(-1)^{\alpha-1}}{2}, s_2+\frac{(-1)^{a}}{2}\right\rangle$. This suggests that four independent odd opera-

[9] We denote the Dynkin labels of $\mathfrak{g}_0 = \mathfrak{sl}(2)\oplus\mathfrak{sl}(2)$ with square brackets $[\cdot,\cdot]$, the long representations of the whole superalgebra $(\mathfrak{p})\mathfrak{sl}(2|2)$ with curly brackets $\{\cdot,\cdot\}$, and the short representations with angular brackets $\langle\cdot,\cdot\rangle$. We take the convention in which the labels j_1,j_2 of $[j_1,j_2]$ can take values as either integer or half-integer values, or spins. They are half of the Dynkin labels of $\mathfrak{g}_0$.

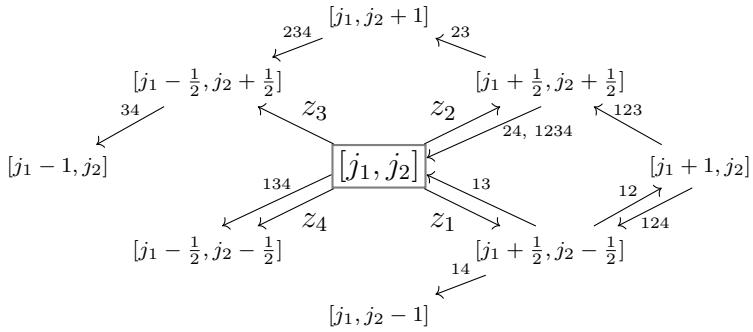

Figure II.2: The decomposition structure of the long representation $\{m, n\}$ of $\mathfrak{sl}(2|2)$ to the representations of the bosonic subalgebra $\mathfrak{g}_0 = \mathfrak{sl}(2) \oplus \mathfrak{sl}(2)$. The boxed component is the top component. The sequence of the numbers labeling the arrows denote which odd operators are turned on, e.g. 234 means the action with $z_4 z_3 z_2$.

tors z_i, $i = 1, 2, 3, 4$ that map a $\mathfrak{g}_0$ multiplet $[j_1, j_2]$ to another multiplet $[j_1 \pm \frac{1}{2}, j_2 \pm \frac{1}{2}]$, respectively, can be constructed linearly from $(\mathfrak{Q}_i)^{\alpha}{}_{a}$ together with bosonic operators. The nilpotency of the supercharges tells us that all $\mathfrak{g}_0$ multiplets are exhausted by acting $z_4^{n_4} z_3^{n_3} z_2^{n_2} z_1^{n_1}$ $(n_i = 0, 1)$ on the top component of the supermultiplet $\{m, n\}$. The long representation is thus composed of the finite web of the $\mathfrak{g}_0$ representations as fig. II.2.

II.C.2 Finite-dimensional short representations of $\mathfrak{sl}(2|2)$

The shortening conditions of the supermultiplet with the top component $[j_1, j_2]$ are [165]

$$C = \begin{cases} \pm 2\,(j_1 - j_2) & \textbf{(Type I)} \\ \pm 2\,(j_1 + j_2 + 1) & \textbf{(Type II)} \end{cases}. \tag{II.C.2}$$

If the first Type I condition $C = 2\,(j_1 - j_2)$ condition is satisfied with massive $C \neq 0$, then the action of z_2 annihilates (see fig. II.3a). We call this short multiplet $\langle j_1, j_2 \rangle_{\mathrm{I}+}$. There are some special cases with small values of j_1 or j_2. For example, in $\langle 0, j_2 \rangle_{\mathrm{I}+}$, only the nonnegative Dynkin label representations remain, plus the action of $z_3 z_1$ annihilates the top component. Hence, the branching rule consists of three bosonic components as in fig. II.4a. Similarly, $\langle j_1, 0 \rangle_{\mathrm{I}+}$ is as in fig. II.4b. The representations with $j_1 = \frac{1}{2}$ or $j_2 = \frac{1}{2}$ can be obtained by simply removing the $[j_1 - 1, j_2]$ or $[j_1, j_2 - 1]$ multiplet, respectively.

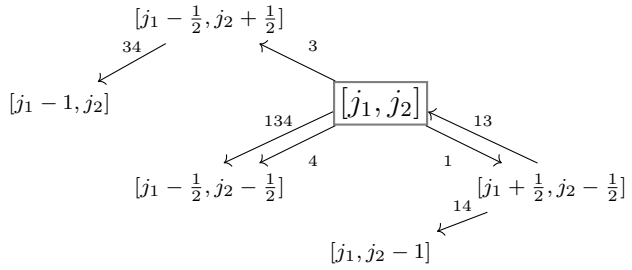

(a)

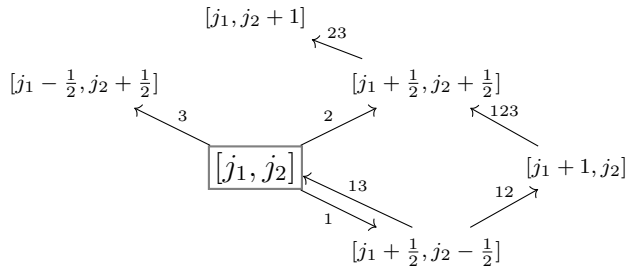

(b)

Figure II.3: The decomposition structure of the massive short representations $\langle j_1, j_2 \rangle_{\mathrm{I}\pm}$ with (a) $C = 2(j_1 - j_2)$ and (b) $C = -2(j_1 - j_2)$.

The massive Type I representation with $C = -2(j_1 - j_2)$ has the multiplets annihilated by z_4 (fig. II.3b). We call it $\langle j_1, j_2 \rangle_{\mathrm{I}-}$. In contrast to the $\langle 0, j_2 \rangle_{\mathrm{I}+}$ and $\langle j_1, 0 \rangle_{\mathrm{I}+}$ multiplets, nothing special happens for the cases of $j_1 = 0$ or $j_2 = 0$ rather than missing the multiplets with possibly negative labels.

For a massless $C = 0$ representation, both of the Type I conditions are satisfied if $j = j_1 = j_2$. We call this $\langle j, j \rangle_{\mathrm{I}\pm}$. It suggests that both z_2 and z_4 annihilate the components, and it is indeed the case (fig. II.5). This class of short representations includes the one-dimensional trivial representation $\langle 0, 0 \rangle_{\mathrm{I}\pm}$.

The right-hand side of the Type II shortening conditions $C = \pm 2(j_1 + j_2 + 1)$ is strictly nonzero for nonnegative j_1 and j_2, so it may be applicable only for massive $C \neq 0$ representations for finite representations. If the first condition $C = 2(j_1 + j_2 + 1)$ is satisfied, the top component is annihilated by z_1 (fig. II.6a). We call this multiplet

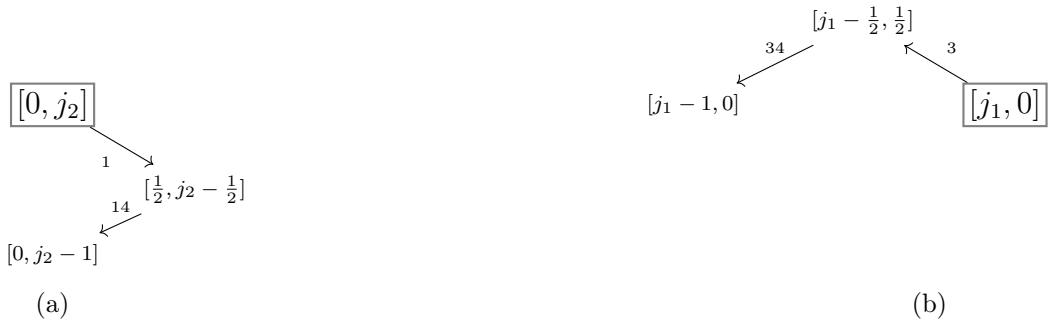

Figure II.4: Special cases of (a) $\langle j_1, 0\rangle_{\mathrm{I}+}$ or (b) $\langle 0, j_2\rangle_{\mathrm{I}+}$ for the representations satisfying the shortening condition $C = 2\,(j_1 - j_2)$.

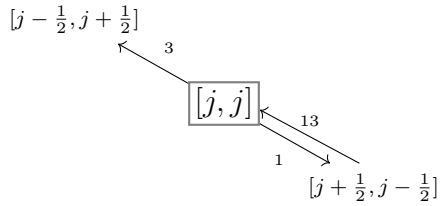

Figure II.5: The multiplet structure of a massless representation $\langle j, j\rangle_{\mathrm{I}\pm}$ with $j = j_1 = j_2$ satisfying both of the Type I conditions.

$\langle j_1, j_2\rangle_{\mathrm{II}+}$. For the small values of $j_1 = 0, \frac{1}{2}$ or $j_2 = 0, \frac{1}{2}$, the bosonic components with possibly negative labels would disappear. Besides, for $\langle 0, j_2\rangle_{\mathrm{II}+}$, the action of $z_4 z_2$ annihilates the top component. The story for the representations satisfying the condition $C = -2\,(j_1 + j_2 + 1)$ is very similar. The components are annihilated by the action of z_3 (fig. II.6b), and we call this multiplet $\langle j_1, j_2\rangle_{\mathrm{II}-}$. The special behavior occurs as $j_2 = 0$, where the top component is also annihilated by $z_4 z_2$ besides the ones generating the negative label components.

II.C.3 Infinite-dimensional representations of $\mathfrak{sl}(1,1|2)$

The supermultiplets appearing in our discussion of the bulk-defect OPE decomposition are all infinite-dimensional given the well-known fact that the unitary representations of the conformal symmetry appearing in the radial quantization of the 2d CFT are all infinite-dimensional. In other words, the spacetime $\mathfrak{sl}(1,1)$ part of the bosonic subalgebra

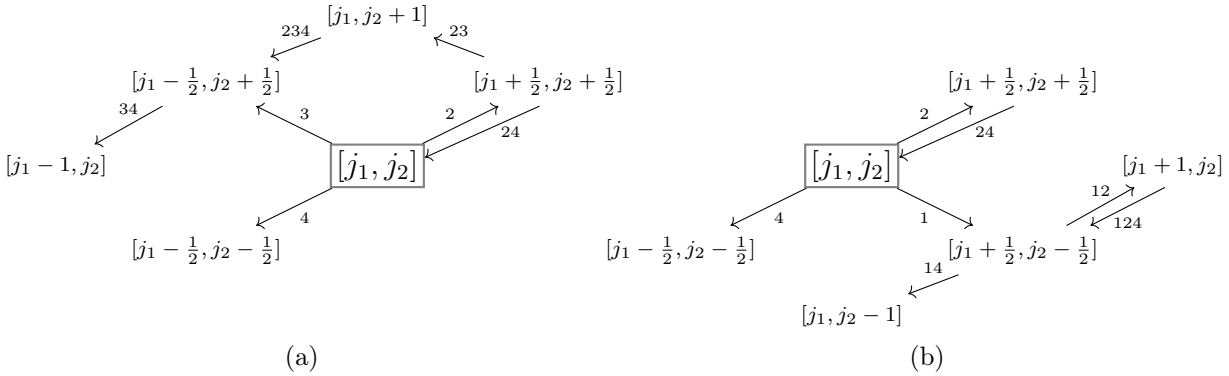

Figure II.6: The decomposition structure of the massive short representations $\langle j_1, j_2\rangle_{\mathrm{II}\pm}$ with (a) $C = 2\,(j_1 + j_2 + 1)$ and (b) $C = -2\,(j_1 + j_2 + 1)$.

$\mathfrak{g}_0 = \mathfrak{sl}(1,1) \oplus \mathfrak{sl}(2)$ of $\mathfrak{psl}(1,1|2)$ always has infinite-dimensional unitary representations, whereas the R-symmetry $\mathfrak{sl}(2)$ part has finite-dimensional representations. The infinite-dimensional $\mathfrak{sl}(1,1)$ representations we consider here are either highest-weight or lowest-weight representations with integer or half-integer conformal weights. We call them $\mathcal{V}(h)$ with $h \neq 0$, which is a lowest-weight representation with the lowest weight h if $h > 0$ or a highest-weight representation with the highest weight h if $h < 0$. We label the whole $\mathfrak{g}_0$ representation as $[\mathcal{V}(h), j_2]$. Recall that the labels j_1, j_2 of the finite representations of $\mathfrak{sl}(1,1)$ correspond to their highest weights. This suggests that the shortening conditions and the classification of the supermultiplets containing the infinite-dimensional highest-weight representation $\mathcal{V}(-h)$ ($h \in \mathbb{Z}_+/2$) are simply obtained by replacing the label $j_1 \in \mathbb{Z}_+/2$ for the finite-dimensional cases with the negative integer $-h$. The behaviors of the infinite-dimensional representations are symmetric between $\mathcal{V}(h)$ and $\mathcal{V}(-h)$. Hence, the classification of the multiplets containing the lowest weight representations $\mathcal{V}(h)$ is equivalent to that of $\mathcal{V}(-h)$.

We comment on some special situations appearing only for the infinite-dimensional multiplets. The Type II conditions can be now satisfied even for the massless $C = 0$ multiplets. The top component is either $[\mathcal{V}(1), 0]$ or $[\mathcal{V}(-1), 0]$. Both of the Type II conditions are satisfied for this case. This means that the top component is annihilated

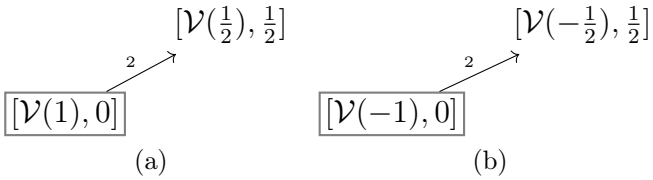

Figure II.7: The decomposition structure of the massless infinite-dimensional short multiplets satisfying both of the Type II shortening conditions.

by both z_1 and z_3, and also $z_4 z_2$ annihilates it since $j_2 = 0$ (fig. II.7).

II.C.4 Bosonic algebra and Casimir invariants

The conformal symmetry algebra is isomorphic to the direct sum of the two copies of $\mathfrak{sl}(1,1)$ generated by $(\mathfrak{L}_i)^{\alpha}{}_{\dot{\alpha}}$, namely

$$\{\mathfrak{h}_1, \mathfrak{e}_1, \mathfrak{f}_1\} = \left\{\frac{1}{2}(D + iM_{34}), P_{1\dot{1}}, K_{2\dot{2}}\right\}, \quad \{\mathfrak{h}_2, \mathfrak{e}_2, \mathfrak{f}_2\} = \left\{\frac{1}{2}(D - iM_{34}), P_{2\dot{2}}, K_{1\dot{1}}\right\} \tag{II.C.3}$$

in terms of the bulk $\mathfrak{psl}(2,2|4)$ generators. They follow the commutation relations of

$$[\mathfrak{h}_i, \mathfrak{e}_i] = \mathfrak{e}_i, \quad [\mathfrak{h}_i, \mathfrak{f}_i] = -\mathfrak{f}_i, \quad [\mathfrak{e}_i, \mathfrak{f}_i] = -2\mathfrak{h}_i. \tag{II.C.4}$$

Let us think of a lowest-weight representation. The lowest-weight state $|h\rangle$ is the $\mathfrak{h}_i$ eigenstate with the eigenvalue h and is annihilated by $\mathfrak{f} = K$. $\mathfrak{e} = P$ raises the weight by one. This means that the tensor product of the lowest states in the holomorphic and antiholomorphic parts $\left|h, \bar{h}\right\rangle \equiv |h\rangle \otimes \left|\bar{h}\right\rangle$ corresponds to the primary state[10] given that it is annihilated by all the special conformal transformation generators. The conformal weights of this state are $(h, \bar{h})$, giving the dimension and the spin of the state to be $\Delta = h + \bar{h} = D$ and $s = h - \bar{h} = iM_{34}$. The quadratic Casimir of the representation which $|h\rangle$ belongs to can be found by acting the Casimir operator on the lowest-weight

[10]To be more precise, we should call it the quasi-primary state since we are arguing the global symmetry of the 2d CFT.

state. On the holomorphic side, the action is found to be

$$\mathfrak{L}_i^2 \left|h\right\rangle = \left(2\mathfrak{h}_i^2 - \mathfrak{e}_i\mathfrak{f}_i - \mathfrak{f}_i\mathfrak{e}_i\right)\left|h\right\rangle = \left(2\mathfrak{h}_i^2 - 2\mathfrak{h}_i\right)\left|h\right\rangle = 2h(h-1)\left|h\right\rangle . \tag{II.C.5}$$

Adding it together with the andiholomorphic side, the Casimir for the whole conformal symmetry is

$$(\mathfrak{L}_1^2 + \mathfrak{L}_2^2)\left|h,\bar{h}\right\rangle = \left(2h(h-1) + 2\bar{h}(\bar{h}-1)\right)\left|h,\bar{h}\right\rangle = (\Delta(\Delta-2) + s^2)\left|h,\bar{h}\right\rangle . \tag{II.C.6}$$

In the Euclidean signature, $P_\mu^\dagger = K_\mu$, in other words $P_{1\dot{1}}^\dagger = K_{2\dot{2}}$ and $P_{2\dot{2}}^\dagger = K_{1\dot{1}}$. This restricts the value of h to be positive for the unitarity:

$$0 < |\left|h+1\right\rangle|^2 = \left\langle h|\mathfrak{f}_i\mathfrak{e}_i|h\right\rangle = \left\langle h|2\mathfrak{h}_i|h\right\rangle = 2h. \tag{II.C.7}$$

This means that the representations of the conformal symmetry are all infinite-dimensional composed of $\mathcal{V}(h)\otimes\mathcal{V}(\bar{h})$.

The story for the R-symmetry $SO(4)_R \simeq SU(2)\times SU(2)$ representation is similar, except that now $\mathfrak{e}_i^\dagger = -\mathfrak{f}_i$ for the above commutation relations, and the lowest-weight m is constrained to be negative. This means that the unitary representations are finite.

Chapter III: Spin Chains from large-N QCD at strong coupling

III.1 Introduction

The recent advances of quantum computing technology open a new avenue to perform numerical simulations of quantum field theories (QFTs). These allow us to simulate, at least in principle, the lattice theory in the Hamiltonian formalism and hence to circumvent the sign problem in the conventional Monte-Carlo methods with Lorentzian actions for simulating real-time dynamics.

In principle, if one could find the finite-dimensional Hilbert space containing the low-energy modes of the field theory and write the effective Hamiltonian as an operator (i.e. a spin operator for a digital quantum computer with qubits) in this finite Hilbert space, then it should be expected that the observables in interest can be simulated on a digital quantum computer [41]. Still, one has to rigorously check whether the original theory and the effective Hamiltonian are in the same universality class. For gauge theories, the Kogut-Susskind formulation of lattice gauge theory Hamiltonian [106] is a good starting point. Even though the gauge field Hilbert space is infinite-dimensional in their formalism as an ordinary bosonic field Hilbert space, several approaches have been proposed for deforming it to finite-dimensional. Roughly speaking, one has two choices to regularize the Hilbert space: (i) by introducing a cutoff to the electric flux by hand while effectively

preserving the Lie algebra structure of the gauge symmetry, based for example on the quantum link model [45, 36, 17, 36, 37, 38, 30] or the loop-string-hadron framework [145, 97], or (ii) by replacing the gauge symmetry with another that naturally leads to finite-dimensional representations and has the original gauge group as some limit, such as the discrete subgroup [166, 113] or the q-deformation [164, 85]. In either case, a full simulation of a theory like QCD requires computational resources far beyond of what is available on current devices, especially in dimensions higher than $1+1$-D [98, 16, 152].

Soon after the discovery of asymptotic freedom of QCD [78, 142, 81, 79], Wilson beautifully demonstrated that gauge theory in the strong coupling regime can be formulated on lattice spacetime, and the Wilson loop expectation value follows the area law, which indicates quark confinement [158]. One can interpret the flux tube in the strong coupling regime as a string-like object with confined quarks at its endpoints, since its energy is exactly proportional to its length as $g_{\rm YM} \to \infty$. This can be understood in the lattice formulation provided that the flux tube is the gluon excitation on a path connecting the quarks [106]. The confining string description becomes even clearer in the large N limit [1], where the nonplanar interactions of the confining strings are suppressed, corresponding to the genus expansion of string theory. Of course, the Lagrangian description of this confining string needs a modification from the pure Nambu-Goto worldsheet action due to its conformal anomaly since it propagates in spacetime with noncritical ($4 \neq 26$) dimensions. There have been several proposals for modifications of the confining string action such as [141, 63].

Based on this confining string approach for QCD, we propose a potential alternative approach to use quantum computers for lattice gauge theory by working in the Hamiltonian formalism of the strong coupling expansion. The framework restricts the lattice $SU(N)$ Yang-Mills theory in the large N limit to the sector with a Wilson line or a confining string, where the relevant part of the Kogut-Susskind Hamiltonian action ends up being reduced to a $1+1$-D spin chain Hamiltonian action for the coinfining

string. Note that the limit taken there is not the 't Hooft limit but a double scaling limit $\lambda, N \to \infty$ with $\lambda \gg N$ so that the strong coupling expansion makes sense. In this limit, the magnetic terms of the plaquette action are turned off at zeroth order. Instead, one diagonalizes the electric (kinetic) terms first and proceeds from there by utilizing the magnetic terms as a small perturbation.

In this limit, the Hilbert space near the vacuum is described as a non-interacting gas of strings, and the leading order corrections to the one string states close in the one string sector. The string states can be described as *words* of *letters* instructing the directions of the link excitations as one moves along the string. This is similar in spirit to the spin chains arising from $\mathcal{N} = 4$ SYM [32], but here the words actually indicate displacements on the lattice directions by the operator matrices. The plaquette actions on these states become manipulations of the letters making a word. Translating the letters to spin states, it provides a systematic construction of spin chains corresponding to the perturbation corrections from strong-coupling to the confining string states, generalizing the idea of formulating the perturbation analysis as a free fermion theory in [105]. The spin chains in certain subsectors were found to be integrable, while those in more general settings–including higher-order corrections, higher spacetime dimensions, or more general sectors–are expected to lose integrability. Part of the intention of this chapter is to address instances on where integrability is lost. In our previous work we showed that integrability would arise to leading order perturbation theory in all dimensions, so long as the zig-zag symmetry constraints were ignored. In that sense, these spin chains are closed to being integrable. Here, we explicitly write the effects of the zig-zag constraints. These require additional projectors in the spin chain to forbid states that are not allowed by the constraints. These projectors change the leading order nearest neighbor interaction to an interaction that includes four neighboring sites instead. We show that these can destroy the integrability of the spin chain, but many subsectors are still integrable.

Notice that because we obtain spin chains where the Hamiltonian is local on the spin

chain, they are suitable for quantum simulation with current devices. Remarkably, in the $2+1$-D spacetime, the spin chain Hamiltonian is found to be integrable within a larger set of subsectors than what one would have initially thought. Because of that some exact calculations are accessible at leading order in the perturbation of a large class of interesting states.

The philosophy of this idea is somewhat similar to the recent effort on quantum simulation of quantum gravity using matrix models [148]. The matrix models are well-defined quantum mechanical models, so they can be simulated on quantum computers in a straightforward way, even though the full simulation of quantum gravity itself is not feasible with our current understanding of quantum gravity.

We must accept some tradeoffs for the lower computational cost we are achieving. For a simulation of individual confining strings, it would not allow us to access QCD in the regime where it would be closest to nature: a strong coupling relativistic theory (the continuum limit of the lattice system). In particular, the deconfined phase would be beyond reach. The situation is similar for the case of matrix models. For example the BFSS model is conjectured to be dual to M-theory in asymptotically flat backgrounds [14]–it is not expected to grasp the whole eleven-dimensional quantum gravity theory especially in the strong-coupling regime where the nonperturbative effects involving saddle-point contributions from other possible eleven-dimensional geometries are non-negligible.

It is worth to note some recent advancements in quantum algorithms for lattice gauge theory taking advantage of the large N expansion. Ciavarella and Bauer [49] constructed a Hilbert space of gauge invariant states by acting with single plaquette operators on a vacuum state. The leading contributions in large N in the contractible loop sector comes only from states with isolated single plaquette excitations, and hence the state on each plaquette can be described with the discrete amount of color flux around it. With a truncation of the color flux, each plaquette can be mapped to a qubit. In [50], they demonstrated that the efficient quantum algorithm can also be constructed to subleading

order in their formulation. Their work [49] complements our approach in the sense that their framework can efficiently describe the states with contractable closed loops, while ours is more suitable for the Hilbert space of open strings with fixed quark caps and that of Polyakov loops. The open string Hilbert space is separated from the contractable loop Hilbert space as long as quarks have large enough mass, and the Polyakov loop space is separated more strictly due to distinct topological numbers. See also [133] for other attempts to exploit large N for lattice, in that case with fermions.

In this chapter, we propose a framework that translates the dynamics of open confining strings to simple manipulations of a "word" of "letters" and justify the framework. We explore generalizations with the eventual goal of studying generic confining strings in $3+1$-D (large N) QCD. The integrability structure of the spin chains describing the first-order perturbation in certain subsectors allows us to analytically calculate the physical quantities of the string, some of which we can use to check if this framework gives a path towards the correct extrapolation to the continuum limit.

This chapter is based on the results reported in [28, 29] and is organized as follows. In section III.2, we review the setting for our framework as the strong-coupling expansion of the Kogut-Susskind Hamiltonian. Regarding the magnetic or plaquette terms of the Hamiltonian as perturbation, our framework reduces to a diagrammatic expansion, and its further reduction to the representation as words is justified. Section III.3 derive the integrable spin chains for first-order corrections and discusses the integrability of some simple subsectors and the non-integrability of the more general four letter sector. In section III.4, we show the evidence of the validity of this framework by extrapolating the roughening transition point from our perturbation theory calculation, including some subleading corrections. We calculate them in two different string sectors that are expected to coincide in the continuum and demonstrate that they do indeed. Section III.5 briefly discusses the extension to higher dimensions. An example of an integrable spin chain for strings in the $3+1$-D spacetime is shown. We also propose another representation of the

string words in section III.6, which does not need an explicit projection for the zigzag constraints and hence may be more suitable for some quantum computing applications. We conclude this chapter in section III.7 with a discussion of our results and future directions.

III.2 Setup

The Hamiltonian formalism of the lattice pure gauge theory with the $SU(N)$ gauge group and coupling g can be realized with the Kogut-Susskind Hamiltonian [106]

$$H_{\rm KS} = H_E + H_B = \frac{\lambda}{2N}\sum_{\ell} E_\ell^2 - \frac{N}{2\lambda}\sum_P \mathrm{Tr}\Big[U_P + U_P^\dagger\Big]. \tag{III.2.1}$$

We omitted the overall dimensionful factor $1/a$. The first (kinetic) term H_E is a sum over all the lattice links (we call them the electric fields), and the second (potential) term H_B is the sum over all the single plaquettes in the spatial lattice (the magnetic terms). Each E_ℓ^a $(a = 1, 2, ..., \deg(SU(N)) = N^2 - 1)$ generates the $SU(N)$ group defined on each link ℓ and is in the fundamental representation, and $E_\ell^2 \equiv \sum_a E_\ell^a E_\ell^a$ denotes the quadratic Casimir of $SU(N)$. The couplings are written so that $\lambda = g^2 N$ is the 't Hooft coupling. The factor N/λ of the magnetic term has the standard N dependence associated to large N. The kinetic term arises from a Legendre transform of the Kogut-Susskind Lagrangian, which inverts both λ and N. The notion of the electric field is given by $E \simeq U^{-1}\dot{U}$ which acts as a canonical conjugate of U and is actually Lie algebra valued. There are actually two possibilities for E defined by the left action of the Lie algebra or the right action. These are related to each other by conjugation by U. We choose the left action, so that U is in a fundamental of the left action and $U^\dagger$ is in the antifundamental. The right handed $\tilde{E} = UEU^{-1}$ is written simply and is useful. Under $\tilde{E}$, U is in the antifundamental. We get the same answer as if we are reversing the notion of $U, U^\dagger = U^{-1}$. In order to pick one such choice, we need to add an orientation to each link, which determines in which

direction U acts as a matrix.

The quantity U_P is the product of the link operators U_ℓ taken along the single plaquette P, with U_ℓ in the fundamental, so that the orientations are anticyclically ordered. The complex conjugate $U_P^\dagger$ multiplies in the opposite orientation. The upper-case trace (Tr for the second term) is over the fundamental indices to denote that the plaquettes are closed loops, and hence the products have cyclic properties.

The operators defining the Hamiltonian satisfy the following commutation relations :

$$[E_\ell^a, E_{\ell'}^b] = if^{abc}E_\ell^c\delta_{\ell\ell'},\ [E_\ell^a, U_{\ell'}] = T^aU_\ell\delta_{\ell\ell'},\ [E_\ell^a, U_{\ell'}^\dagger] = -U_\ell^\dagger T^a\delta_{\ell\ell'}, \tag{III.2.2}$$

with the structure constants f^{abc} of $SU(N)$ and the $SU(N)$ generators T^a in the fundamental normalized as $\mathrm{Tr}\big(T^aT^b\big) = \delta^{ab}$. Also, all U matrix elements commute with each other at each link and between all links.

The coupling constant $\lambda = g^2N$ is the 't Hooft coupling. In the strong-coupling limit $\lambda \gg 1$, the first term dominates and the second term can be regarded as a perturbation with the perturbation parameter $-N/2\lambda$. The parameter $-N/2\lambda$ is kept small even after we take the large N limit. It is contrary to the 't Hooft limit where one takes large N while keeping λ constant, so the second term dominates. The non-perturbed eigenbasis, i.e. the eigenbasis of the first term has the following property. Since the electric fields commute between different links, each E_ℓ^2 commutes with the Hamiltonian and all the individual terms in the sum over the links can be diagonalized simultaneously. To each link we associate a representation of the gauge group G and the kinetic term is just the quadratic Cassirmir of said representation. The Hilbert space is generated as a vector space by polynomials of the components of U and U^{-1}, with the 1 function on G acting as the ground state, which has a vanishing Casimir. This ground state $|\Omega\rangle$ at each link has no energy. If the representation R is of dimension $\dim R$, the degeneracy of such a basis is actually $\dim R^2$, as the Peter-Weil theorem states that $L^2(G) \simeq \oplus_R R\otimes\bar{R}$. This is

a naive basis where we have not imposed gauge invariance. Since the local Hilbert space is generated by the U, gauge invariance is implemented at each corner by contracting U consecutively by matrix multiplication (being mindful of the orientations of the links).

In that sense, gluon excitations are generated by acting with link operators U on it.

Each U_ℓ associated with the link ℓ adds a segment starting on one vertex of the link and ending on the other that is dictated by the gauge quantum numbers (and our chosen orientation). For example, $U_\ell^\dagger$ adds a link excitation on ℓ with the flux in the opposite direction of U_ℓ, and the unitarity $U_\ell U_{\ell'}^\dagger = \delta_{\ell\ell'}$ indicates that these links cancel each other when we multiply them like a matrix. These links must form closed directed paths for gauge invariance. After all the gauge transformations act on each corner by being embedded diagonally on the left group actions of G at each link (provided all the orientations are outgoing). We also consider heavy quarks that allow open strings with fixed endpoints at the location of the quarks. Our analysis is in the bulk of the string, but these endpoints are convenient artifacts, so as not to have to deal with the cyclic property of the trace and zero modes. It also allows certain subsectors to be easily identified.

A string is therefore a directed path from one heavy quark to an anti-quark. A path can cross itself. The large N limit guarantees that these possible interconnections do not generate additional energetic contributions, except at subleading orders in $1/N$, which we ignore. The reason for this is that the quadratic Casimir of a representation of G with k boxes at leading order is proportional to kN. This also applies if we consider situations with a few boxes and a few antiboxes [80].

The non-perturbed energy eigenvalue of such a string state excited along the directed path Γ, $|\Gamma\rangle \equiv \mathcal{P}\prod_{\ell\in\Gamma} U_\ell\,|\Omega\rangle$ ($\mathcal{P}$ indicates the path-ordered product), can be calculated as

$$K\,|\Gamma\rangle = \frac{\lambda}{2N}\sum_{\ell\in\Gamma}\sum_a T^a T^a \prod_{\ell\in\Gamma} U_\ell\,|\Omega\rangle = \frac{N^2-1}{2N^2}\lambda L\,|\Gamma\rangle\,, \tag{III.2.3}$$

where L is the length of the path Γ in the lattice scale unit, and we used the requirement $E^a_\ell |\Omega\rangle = 0 \; \forall \ell$ to have the zero ground state energy. The value of the Casimir $\sum_a T^a T^a = C_F I = \frac{N^2-1}{N} I$ is determined so that it gives the proper normalization $\mathrm{Tr}\left(T^a T^b\right) = \delta^{ab}$ in the fundamental representation. Since we are interested in the large N limit, the string energy can be further found to be $\lambda L/2$ where L is the total length of the path. It is proportional to its length L, and the string tension is identified as $\sigma = \lambda/2$. Hence, the theory admits confinement with the string tension $\sigma = \lambda/2$ in the strong-coupling limit. Since there are many paths between the beginning and the endpoint that can have the same length, the problem of perturbation theory is a degenerate problem. For each fixed length, we need to compute the matrix elements of the perturbation in the basis of paths.

To compute the matrix elements of the perturbation on this basis, one needs to consider the actions of the single plaquette operators on these string states and compute their overlaps with other string states. There are three types of actions as discussed in [106] (also see fig. III.1):

- type A: the plaquette does not share any link with the string.
- type B: it shares some link(s), which have the same flux direction as the string flux.
- type C: the shared link(s) have opposite directions.

The details of how to compute overlaps of these deformed string states are described in the next section (section III.2.1). Most of the type A deformations do not overlap with the open string states and hence do not lead to nontrivial perturbative correction; they are identical to the corrections to the vacuum state. There is a special case of the type A action which nontrivially contributes to corrections higher than the first order. It is when the plaquette and the string excitation share one or more vertices. Then the state after the plaquette action has an overlap with a single string state with extra energy for an attached loop at the corner (fig. III.2). We call this type of deformation type A$'$. The overlap is in the order of $\mathcal{O}(1/N^c)$, where c is the number of connected corners.

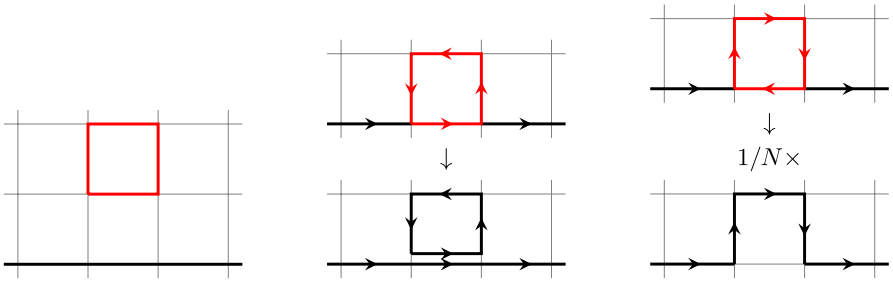

(a) Type A (b) Type B (c) Type C

Figure III.1: Possible actions of a single plaquette operator on a string state. The cost to attach a plaquette to a string that is already there is $1/N$ ($1/N$ is proportional to the string coupling constant in the 't Hooft counting), but the plaquette is accompanied by N/λ so the factors of N cancel.

The type B deformed state has an overlap in order of $\mathcal{O}(1/N^s)$ with a nontrivial string state (namely, a string with s self-intersections on the shared links) that has higher energy than the original string and hence it starts contributing once the second- or higher-order perturbations are considered.

Therefore, we can focus solely on the type C case for the first-order perturbations.

For the type C case, the integral over a single link with opposite flux $\int dU\ U^i{}_j U^{\dagger k}{}_\ell \propto \frac{1}{N}\delta^i_\ell \delta^k_j$ indicates that the excitation on the shared link(s) cancels, and hence the plaquette deforms the string with the extra factor $1/N$. The integral arises from an overlap calculation between the states at the individual link. After all, this is how we write the inner product in $L^2(G)$ of the corresponding link in the position basis. The cancellation allows the deformed string to possibly have the same energy as the original string, so it may contribute to the first-order degenerate perturbations. This extra $1/N$ factor cancels the usual N factor in H_B. Therefore, it results in a finite contribution to the energy. The large-N limit also ensures the locality of the effective theory on the string, similar to how it works in the $\mathcal{N} = 4$ SYM spin chain [32] (that is, we ignore self-intersections of the string with itself when discussing corrections: these would be non-local on the string, and they are suppressed by extra factors of $1/N$).

We label a string state by the path it takes. The string is a word with instructions on

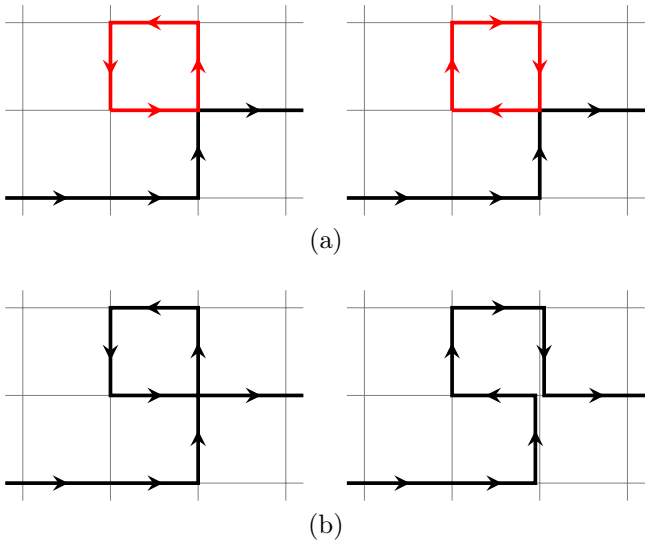

Figure III.2: Examples of the type A' deformations where a string shares a corner with the plaquette (figure (a)) and gives a nontrivial overlap with another single string state such as states in (b). These contributions are subleading in $1/N$ due to the change of topology.

what the next step is: up (u), down (d), left (l), right (r), etc. Each of these is treated as a letter of the alphabet of paths. An action of the plaquette changes the shape of the path. The $UU^\dagger = 1$ constraint is implemented by stating that a path cannot double back on itself immediately. That is, combinations such as $\ldots ud \ldots$, or $\ldots lr \ldots$ are forbidden. This is also called zigzag symmetry and is related to the reparametrization invariance on the worldsheet [143]. A way to think about this is that in this case (the string in $2+1$ dimensions), if at some point a letter is u, then after it there are only three possibilities u, l, r, so the number of states at length L is $4 \times 3^{L-1}$, as the first letter leaving the quark is unconstrained. If we insist on using the 4 letters, the Hilbert space is the set of words with ud, du, lr and rl combinations forbidden: we can write a projection operator π that projects onto the allowed space of letters at each link. It acts by $\pi(lr) = 0$, etc, on the forbidden combinations but $\pi(dl) = dl$ and similar for the allowed configurations. Since these are orthogonal to each other π is self-adjoint.

III.2.1 Norms and overlaps of the string states

The calculations of the overlaps between states with stringy excitations are achieved by path-integrating the link variables over the gauge group manifold in the general form of $\int (\prod_\ell dU_\ell)\ f(\{U_\ell\})$. Such integrals over the paths can be packaged into diagrammatical computations in our Hamiltonian formalism with some rules. Here, we list the diagrammatical rules for computing overlaps between stringy states and use them to demonstrate that the first-order corrections to single strings are indeed closed in large N, and hence their representations as words are valid.

The rules we must apply include the requirement of specifying the directions of the graph edges, the proper normalization of the nonperturbed vacuum states, contractions due to the zigzag (or unitarity) constraints, and the normalization of the trace over the fundamental indices.

1. **Directed edges:** whether a link excitation corresponds to the operator U or $U^\dagger$ is specified with a directed edge, with the endpoints specified with its fundamental indices. On the same link, U and $U^\dagger$ have opposite directions.

2. **Vacuum normalization:** the nonperturbed vacuum state is properly normalized: $\langle\Omega|\Omega\rangle = 1$. This is also automatically true on any link without lines going through it.

3. **Contractions:** for the edges on the same link, from the group integral computation, the following contraction occurs due to the unitarity of the link operators:

$$U_{ij}U^\dagger_{kl} = \begin{matrix} i \\ l \end{matrix} \longrightarrow\!\!\!\!\!\!\longleftarrow \begin{matrix} j \\ k \end{matrix} = \frac{1}{N} \times \left(\begin{matrix} i \\ l \end{matrix} \quad \begin{matrix} j \\ k \end{matrix} \right) = \frac{1}{N}\delta_{il}\delta_{jk}. \tag{III.2.4}$$

   By contracting the j and k indices, we obtain the unitarity constraint:

$$U_{ij}U^\dagger_{jk} = \begin{matrix} i \\ k \end{matrix} \quad \begin{matrix} \longrightarrow \\ \longleftarrow \end{matrix} \quad j = \begin{matrix} i \\ k \end{matrix} \quad \circlearrowright = \delta_{ik}. \tag{III.2.5}$$

Contractions involving higher power of the $U, U^\dagger$ operators can also be computed using the group integrals. Our discussion will only involve the second-power:

$$U_{ij}U^\dagger_{kl}U_{mn}U^\dagger_{pq} = \begin{matrix} i \\ l \\ m \\ q \end{matrix} \begin{matrix} \longrightarrow \\ \longleftarrow \\ \longrightarrow \\ \longleftarrow \end{matrix} \begin{matrix} j \\ k \\ n \\ p \end{matrix} = \frac{1}{N^2-1}\left(\begin{matrix} i \\ l \\ m \\ q \end{matrix} \circlearrowright \quad \circlearrowright \begin{matrix} j \\ k \\ n \\ p \end{matrix} + \begin{matrix} i \\ l \\ m \\ q \end{matrix} \circlearrowright \circlearrowright \quad \circlearrowright \begin{matrix} j \\ k \\ n \\ p \end{matrix} + \mathcal{O}\left(\frac{1}{N}\right)\right)$$
$$\sim \frac{1}{N^2}(\delta_{il}\delta_{jk}\delta_{mq}\delta_{np} + \delta_{iq}\delta_{jp}\delta_{lm}\delta_{kn}), \tag{III.2.6}$$

where $\sim$ means the contribution in the large N limit.

4. **Fundamental trace:** a zero-length closed loop, corresponding to $\mathrm{Tr}(I)$, contributes by a factor of N.

First, notice that these requirements guarantee that all of the nonperturbed eigenstates are normalized properly. For example, let us compute the norm of a single open string state diagrammatically. The ket and bra states correspond to a path going forward and backward, respectively, and they connect with each other at one of the endpoints once we take the inner product. The folded string fully contracts and ends up with an identity operator:

$$\langle\Gamma|\Gamma\rangle = \langle\Omega| \begin{matrix} \overset{\Gamma}{\longrightarrow} \bullet \\ \underset{\Gamma^{-1}}{\longleftarrow} \end{matrix} |\Omega\rangle = \langle\Omega| \begin{matrix} \longrightarrow \\ \longleftarrow \end{matrix} \bullet |\Omega\rangle = \cdots = \langle\Omega| \, \rotatebox{90}{$\circlearrowright$} \, |\Omega\rangle = \langle\Omega|\Omega\rangle = 1 \tag{III.2.7}$$

For the other open string states, we can apply a similar backtracking argument. The other nontrivial cases are the states containing closed-loop excitations. Let us confirm that these states also are normalized as well by considering a single loop as an example:

$$\langle C|C\rangle = \langle\Omega|$$ 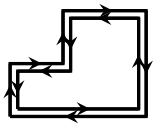 $$|\Omega\rangle = \frac{1}{N^6} \times \langle\Omega|$$ 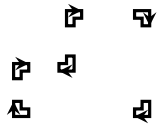 $$|\Omega\rangle = 1 \qquad \text{(III.2.8)}$$

Notice that closed loops have the same number of vertices and edges, so the $1/N$ factors from the edge contractions are canceled exactly with the zero-length closed loops remaining at the vertices following rule 4.

We can easily show the orthogonality of the states with excitations on different edges. In general, the nonperturbed vacuum expectation values of gluon link excitations on a path not contractable by rule 3 to zero length are required to be zero. This can be easily proven by picking one of the remaining gluon operators U_ℓ after all possible contractions and inserting the $E^a E^a$ operator acting on the link ℓ, which automatically gives zero acting on the vacuum state:

$$0 = \langle\Omega|\cdots U_\ell \cdots E^a_\ell E^a_\ell|\Omega\rangle = \langle\Omega|T^a T^a \cdots U_\ell \cdots|\Omega\rangle = \frac{N^2-1}{N}\langle\Omega|\cdots U_\ell \cdots|\Omega\rangle \quad \text{(III.2.9)}$$

for the single U_ℓ case (i.e. other U operators are acting on different links). A similar but more involved arguments apply to prove this statement for the states involving higher powers of U_ℓ.

The remaining nontrivial overlaps are the ones between two string states with the gluon excitations on the exactly same links but with different connectivity. These overlaps are all subleading in $1/N$, since the processes of changing the connectivity from one to another are nonplanar. Specifically, each crossing or overlapping graph can be exchanged to the other with a factor of $1/N$:

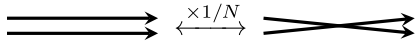

(III.2.10)

and hence the inner products scale as $\sim 1/N^s$ where $s \in \mathbb{Z}_{\geq 0}$ is the number of different

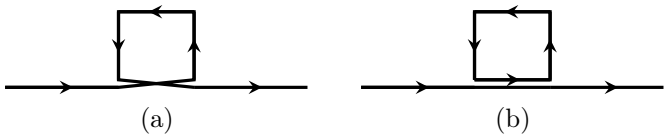

Figure III.3: An example of string configurations with excitations on the same links but with different connectivity.

crossings/overlaps as eq. (III.2.10). Let us diagrammatically calculate an example overlap between an open string with an attached twist (fig. III.3a), which can be represented as a single word, and a string with a separate loop (fig. III.3b), which cannot be represented as only one word. They have the same excited links, but different connectivity only around the twist or the loop. The overlap of these two states is at the next leading order of $1/N$:

$\langle$  $|$  $\rangle = \langle\Omega|$ 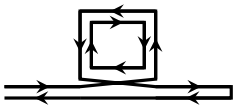 $|\Omega\rangle$

$$= \frac{1}{N^2-1}\,\langle\Omega|$$ 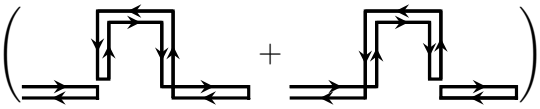 $|\Omega\rangle$

$$\sim \frac{2}{N}, \tag{III.2.11}$$

where the second equation is obtained by the contraction of $UU^\dagger UU^\dagger$ (eq. (III.2.6)). The combinatorial factor of two appears due to the two ways of contraction contributing by an equal amount. For the first-order corrections in the large N limit, we can ignore these overlaps between states with different topologies, which means that the first-order corrections are closed in the sector of single string states with equal length. Therefore, it is justified to represent the single strings as words of letters specifying the directions and to reduce the plaquette actions as manipulations of the letters. On the other hand, since we take the double scaling limit $\lambda \gg N \gg 1$, these nonplanar contributions may contribute at higher-orders in perturbation theory. Note that the discussion in this section is fully spacetime dimension independent, even though we carried out the above

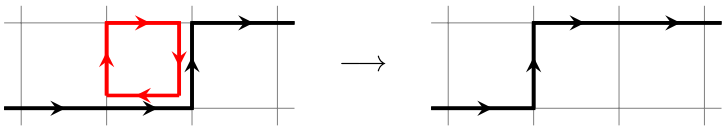

Figure III.4: One example of the type C deformations by a single plaquette action (red in the left figure) generating another degenerate state. Notice that the deformed string has exactly the same string length as the original state. This plaquette action exchanges the u and r letters next to each other.

example calculations in $2+1$-D. For the general case, we just have more letters (two for each spacetime direction and a similar restriction on consecutive letters).

III.3 First-order corrections

Here, we propose the framework for describing the confining string dynamics for various closed sectors with quantum spin chains and discuss their integrability. We also introduce the concept of "knottiness", which is a conserved quantity in a string sector in $2+1$ dimensions due to the zigzag constraint. As discussed in Sec. III.2, only type C deformations in fig. III.1c give contributions to the first-order corrections, and they can be described as manipulations of letters as one describes the single string states as words of letters. The letters can be considered as quantum spin states, and the letter manipulations as the actions of spin operators. The general string states in $2+1$-D are described with words containing four letters: u, d, l, r. The type C deformations act as the exchange of nearby $u, d \leftrightarrow l, r$ and similar. That is, there needs to be a hook at the location of the plaquette, so that two links are destroyed and two other links are created (fig. III.4). These must be going in perpendicular directions.

The extra factor $1/N$ due to the deformation cancels N in the numerator of the coupling factor of H_B, namely $-N/2\lambda$. The first-order corrections are closed under such degenerate type C deformations within the sectors of the fixed number of each letter. That is, the effective spin operator preserves the number of u, d, l, r independently of each other.

The first-order corrections are obtained by diagonalizing the matrix with the elements of $\langle\Gamma_i|\Pi\tilde{H}_B\Pi|\Gamma_j\rangle$, where $|\Gamma_i\rangle$ are the single string states, and Π is the projection operator prohibiting u and d or r and l to be next to each other. This needs only be applied to the final state if the initial state is already allowed by the projector. $\tilde{H}_B$ is the sum of the letter manipulations on a word as

$$\begin{aligned}\tilde{H}_B &= \sum_\ell \tilde{h}_\ell \\ &= -\frac{1}{2\lambda}\sum_\ell (u \text{ or } d \text{ at } \ell \leftrightarrow r \text{ or } l \text{ at } (\ell+1)) + (r \text{ or } l \text{ at } \ell \leftrightarrow u \text{ or } d \text{ at } (\ell+1)),\end{aligned} \tag{III.3.1}$$

where ℓ runs through every letter position of the word specifying the string configuration.

A similar way to write this is

$$\tilde{H}_B = \sum_\ell |ur\rangle\langle ru| + |dr\rangle\langle rd| + |ul\rangle\langle lu| + |dl\rangle\langle ld| + c.c. \tag{III.3.2}$$

And now we need to introduce the projector onto allowed states where $\Pi = \prod_\ell \pi_\ell$. The full first-order perturbation operator is $\Pi\tilde{H}_B\Pi$, which has a local description

$$\Pi\tilde{H}_B\Pi = \sum_\ell (\pi_{\ell-1}\otimes\pi_{\ell+1})\tilde{h}_\ell(\pi_{\ell-1}\otimes\pi_{\ell+1}), \tag{III.3.3}$$

and if the initial states are eigenstates of $\Pi|\Gamma\rangle = |\Gamma\rangle$, then the rightmost Π can be ignored.

Basically, here the π_ℓ operator projects out the state if its local configuration at $(\ell-1,\ell)$ or $(\ell+1,\ell+2)$ has suddenly become forbidden u and d or r and l next to each other. This means that the projected operator $\Pi\tilde{H}_B\Pi$ consists of local operators acting on four neighboring sites, rather than two, but the basic operator $\tilde{H}_B$ is only a nearest neighbor process. Indeed, if we ignore the Π altogether, which means we ignore the zigzag constraints, the nearest neighbor Hamiltonian described exactly by $\tilde{H}_B$ is

integrable. What this means is that the most important part of the analysis to test integrability or lack thereof needs to take the constraints imposed by Π, or equivalently the different π seriously.

We start our discussion with some simple sectors: the sectors of the configurations containing only two letters, namely u and r, and the sectors with only three letters, say u, d, r. We shall demonstrate that these two kinds of closed subsectors are integrable by translating this operator into spin chains only with nearest-neighbor interactions, whereas the general four-letter configuration sectors cannot. Specifying the two-letter or three-letter sector with the number of each letter corresponds to specifying the fixed end points or heavy nondynamical quarks. As the theory goes to continuum by having the lattice spacing $a \to 0$, the rotational symmetry must be recovered, and hence the low energy spectra of these two configurations must coincide. Once we promote the Yang-Mills action to QCD by turning on the fermion dynamics, the end points would be no longer fixed and these sectors would start mixing. We will leave this to future work. Even just pure glue with heavy quark endpoints is interesting on its own.

Let us comment on the projection by Π. The projection prohibits changing the orderings of u, d with each other and l, r with each other. We call these protected orderings the "knottiness". In a word with $4 \times 3^{L-1}$ states these would give 2^L superselection sectors that cannot mix with each other. A similar result would occur in higher dimensions. For the $2+1$-D string there are additional conservation laws, which we will call "secondary knottiness" and we will explain it when we consider the full problem with four letters.

Additionally, the $U(N)$ orientations leads to a protection of the orientation of the string: it distinguishes strings going from quark one to quark two from the opposite direction. The orientation can be evaluated as follows (see also fig. III.5 for an example). We choose some substring of the word containing all four kinds of letters but with the minimum length. This minimal substring contains a pair of two perpendicular letters on the left and right ends, and the bulk is filled with the arbitrary length of the other two

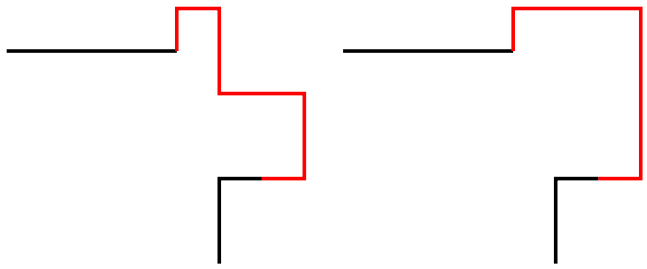

Figure III.5: An example of evaluating the local orientation of the string. (a) Let us focus on the substring $rrrrurddrrddlldd$ (depicted in red). It is bounded by u and l. (b) Exchanging the positions of the bulk letters r and d, the substring is now $urrrddddl$. The orientation is determined to be clockwise from this procedure.

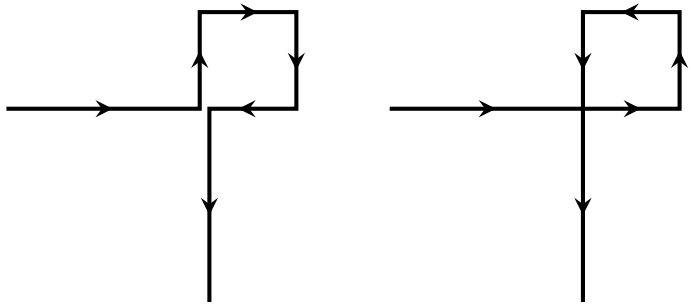

Figure III.6: An example of two string states excited on the same edges but with different local orientations. The zigzag constraint prohibits any Type C deformations to deform one to the other, and their overlaps are $1/N$-suppressed due to the different connectivity. These differ by what we termed secondary knottiness.

letters. One can act with Type C deformations to exchange the positions of the bulk letters, so that the same kind of letters are localized together. Now, the four kinds of the letters are ordered either (i) clockwise, i.e. "$urdl$" or its cyclic permutations, or (ii) counter-clockwise, i.e. "$uldr$" or its cyclic permutations. These two orientations cannot be reached from one to the other for any subset of the word containing four kinds of letters by any degenerate action of plaquette operators. It would require an exchange of either $u \leftrightarrow d$ or $r \leftrightarrow l$. Moreover, although it is possible to consider string excitations on the same edges with different local orientations, their overlaps are suppressed by at least $1/N$ (fig. III.6)

The way to describe what configurations are related to each other is that we need to keep track of zigs and zags (horizontal and vertical changes of directions). Call these h, v. A combination urd would count as an h as there is a vertical orientation shift, but uru would not. Similarly rul would count as v, but not rur. The pattern of hv is also assembled into an ordered string as we move along the flux tube. This pattern of hv words cannot be modified either by the plaquette actions. Basically, it would need to change $urdl$ to the opposite order of hv, $ruld$, but such a move is not allowed. What this means is that although three letter superselection sectors are relatively easy to analyze (there are only v swicthbacks let's say), the four letter ones require this extra superselection label and become more complicated.

III.3.1 Two-letter strings

As we mentioned above, the action of $\tilde{H}_B$ is closed within the subsectors of strings with a fixed combination of the letter numbers. The simplest nontrivial subsector we can consider contains only the strings with two letters. Strings with one letter are trivial: the Hamiltonian does not act on them keeping the length fixed, so there is nothing to calculate in the first order.

This subsector of two letters is the simplest in the sense that we do not need the projection Π as all possible combinations are allowed. Let us choose the subsector containing n of u and $L-n$ of r. One possible excitation is along the path as in the left figure of fig. III.7 with length L. The endpoint quarks are placed diagonally from the lattice axes in general. The single plaquette operator sharing exactly two links with the original configuration Γ as the red plaquette in fig. III.7 acts a type C deformation and generates another string excitation generated with the same string length and the same positions of the quark-antiquark endpoints. Hence, the states degenerate with the excitation along Γ are generated by a series of this kind of plaquette moves. The Hilbert space, which we call $\mathcal{H}_\Gamma$, spanned with these degenerate states has a dimension of $\binom{L}{n}$.

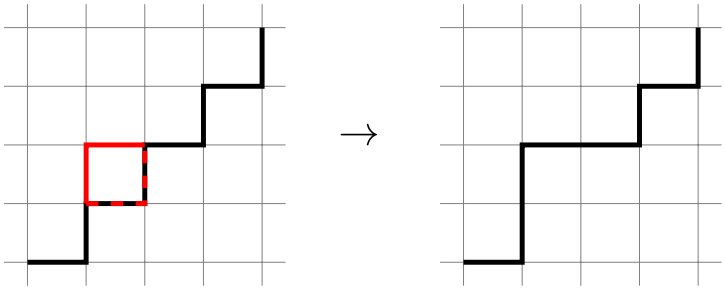

Figure III.7: The diagonal string Γ with m vertical links and $L-m$ vertical links (thick black path). If one acts the single plaquette operator (red) sharing two links (red dotted lines) on the diagonal string state, it changes the state to another with the same string length and the endpoints.

The first-order corrections to the strong-coupling limit eigenstates can be found by diagonalizing the $\binom{L}{n} \times \binom{L}{n}$ matrix

$$W_{ij} \equiv \langle \Gamma_i | \tilde{H}_B | \Gamma_j \rangle \tag{III.3.4}$$

where $|\Gamma_i\rangle \in \mathcal{H}_\Gamma$. The action of a single plaquette operator sharing two of its edges with the string can be seen as flipping a neighborhood vertical link u and a horizontal link r. We translate them to the spin-1/2 states, $u \leftrightarrow \uparrow$ and $r \leftrightarrow \downarrow$. In this language, the plaquette operator flips the spins of two neighborhood spin-1/2 sites with opposite spins, i.e.

$$\mathrm{Tr}\left[U_P + U_P^\dagger\right] \leftrightarrow \frac{1}{N}(\sigma_j^+ \sigma_{j+1}^- + \sigma_j^- \sigma_{j+1}^+) \tag{III.3.5}$$

where the spin operators act on each spin-1/2 state as $\sigma^+ |\downarrow\rangle = |\uparrow\rangle$, $\sigma^- |\uparrow\rangle = |\downarrow\rangle$, and $\sigma^+ |\uparrow\rangle = \sigma^- |\downarrow\rangle = 0$. The whole matrix W_{ij} coincide with the matrix representation of this spin operator summed over all the spin sites. Hence, the action of the plaquette perturbation V ends up being exactly the XX model Hamiltonian

$$H = -\frac{1}{2\lambda} \sum_{j=1}^{L} (\sigma_j^+ \sigma_{j+1}^- + \sigma_j^- \sigma_{j+1}^+). \tag{III.3.6}$$

This Hamiltonian conserves the magnetization, and one can decompose the Hilbert space into the sectors with different magnetization values as follows $H_{\mathrm{XX}} = \bigoplus_{m=0}^{L} \mathcal{H}_m$ where $\mathcal{H}_m$ is the sector having m down spins, whose dimension is $\binom{L}{m}$. The different subsectors exactly correspond to the different combinations $(n, L-n)$ for the numbers of u and r. The first-order perturbation matrix W_{ij} is the block of the XX model Hamiltonian in $\mathcal{H}_n$. The XX model is trivially integrable given that it is equivalent to two copies of a free massless fermion theory. It is also a critical theory. We take this to mean that the effective sigma model on the string world sheet is that of a $c = 1$ theory. It is two free massless fermions, but it can be bosonized to a $c = 1$ free boson, which is interpreted as the goldstone boson of translations that are spontaneously broken by the string. These bosons should be thought of as fluctuations about the diagonal.

Kogut et al. found this free fermion description for the diagonal string setup in [105] and studied just the ground state of the string in order to find how rotational symmetry is restored when the coupling becomes finite. Nearest-neighbor spin chains such as these are easily implementable in quantum computers, so it could be interesting to study states that are dynamical and not only the ground state.

The fact that this subsector is integrable should be no surprise: spin chains with only nearest-neighbor interactions preserving the spin σ_z and parity conserving (treat $\uparrow\downarrow$ equivalently) are all members of the XXZ family.

III.3.2 Three-letter strings

We now turn to the second case where string excitations consist of three letters. Let us choose u, d, r, that is we allow the link excitations to be up, down, or right. General three-letter configurations look like fig. III.8. To characterize these string configurations, we express them with three letters u, d, and r respectively, being careful to disallow ud and du words because we are implementing the zigzag symmetry. These words are identical to the configurations with a shorter string length and do not reside in the degenerate

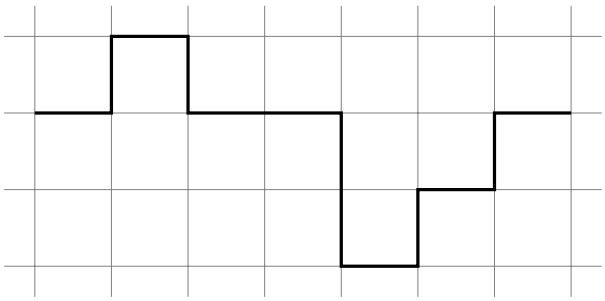

Figure III.8: An example of three-letter configuration. It corresponds to the word $rurdrrddrurur$.

sector. The energy-conserving action of a plaquette on ur and dr pieces of the string looks the same as that for the diagonal string case, which allows swapping the letters as $u(d) \leftrightarrow r$. The new wrinkle is that swapping the order urd, for example, can land one in the forbidden configuration ud. In that sense, those possibilities must be projected out. Such projections effectively turn the problem into one where the swap of letters is allowed depending on extra letters, a three- or four-letter problem. The upshot is that at this order in perturbation theory, ud letters can not swap their position. This property is similar to that of the eclectic and hyper-eclectic spin chain where some letters (states) act sometimes as walls [88, 5].

It is convenient to pass to a new basis, where we treat ud as walls, and use an occupation number basis for r in between each pair of walls. This is identical to the treatment employed to describe the XXX spin-chain with variable length in [27] (see also [26]). In this basis, the Hamiltonian for the perturbation becomes

$$H = -\frac{1}{2\lambda}\sum (c_i^\dagger c_{i+1} + c_i c_{i+1}^\dagger) \tag{III.3.7}$$

where c_i are the Cuntz oscillators satisfying $c_i c_i^\dagger = 1$, and they commute between different sites $i \neq j$. Their action is $c^\dagger |n\rangle = |n+1\rangle$ and $c|0\rangle = 0$ for each Fock space. We restrict the Hilbert space by requiring that the occupation number between any walls that change direction ud or du is greater than or equal to one. This means that we do not allow the ud to be neighbors without any restrictions. It turns out that this restriction leaves

the Cuntz algebra unchanged on the relevant states as if the occupation one state had occupation number zero: the algebra does not change if we do a shift by one plus a projection. In that sense, we can relabel the states with a modified Cuntz oscillator at these sites that ignores that constraint: it becomes an implicit padding of the words whenever it is required. That is, we take advantage of the basis change:

$$\begin{aligned} |1\rangle &\to |0\rangle : dru \to du, \\ |2\rangle &\to |1\rangle : drru \to dru, \\ &\vdots \end{aligned} \tag{III.3.8}$$

This padding now allows us to describe the whole problem as a nearest neighbor spin chain without extra projections.

The result is a simple Hamiltonian where one only swaps $d \leftrightarrow r$ and $u \leftrightarrow r$ and their reverse swaps are allowed. All other terms in the Hamiltonian vanish. We can map these to a spin-one system as $r \to |0\rangle$, $u \to |+\rangle$, $d \to |-\rangle$. The Hamiltonian is equivalent to the following spin-chain Hamiltonian acting on this Hilbert space $\mathcal{H} = (\mathbb{C}^3)^{\otimes L}$:

$$H = -\frac{1}{2\lambda} \sum_{j=1}^{L} \left(e_j^1 f_{j+1}^1 + f_j^1 e_{j+1}^1 + e_j^2 f_{j+1}^2 + f_j^2 e_{j+1}^2 \right) \tag{III.3.9}$$

with the generators of $\mathfrak{sl}(3, \mathbb{C})$:

$$\begin{aligned} h^1 &= \begin{pmatrix} 1 & 0 & 0 \\ 0 & -1 & 0 \\ 0 & 0 & 0 \end{pmatrix}, \; h^3 = \begin{pmatrix} 0 & 0 & 0 \\ 0 & 1 & 0 \\ 0 & 0 & -1 \end{pmatrix} \\ e^1 &= \begin{pmatrix} 0 & 1 & 0 \\ 0 & 0 & 0 \\ 0 & 0 & 0 \end{pmatrix}, \; e^2 = \begin{pmatrix} 0 & 0 & 0 \\ 0 & 0 & 0 \\ 1 & 0 & 0 \end{pmatrix}, \; e^3 = \begin{pmatrix} 0 & 0 & 0 \\ 0 & 0 & 1 \\ 0 & 0 & 0 \end{pmatrix} \\ f^1 &= \begin{pmatrix} 0 & 0 & 0 \\ 1 & 0 & 0 \\ 0 & 0 & 0 \end{pmatrix}, \; f^2 = \begin{pmatrix} 0 & 0 & 1 \\ 0 & 0 & 0 \\ 0 & 0 & 0 \end{pmatrix}, \; f^3 = \begin{pmatrix} 0 & 0 & 0 \\ 0 & 0 & 0 \\ 0 & 1 & 0 \end{pmatrix} \end{aligned} \tag{III.3.10}$$

L is the length of the words. The subscript j specifies that the operator is acting on the j-th spin site. Each term exchanges the neighbor $|0\rangle$ and either $|+\rangle$ or $|-\rangle$. $|+\rangle$ and $|-\rangle$ cannot pass through each other, as the exchange $u \leftrightarrow d$ is forbidden. A similar model was found independently by [6] and [76] with the only difference being the additional chemical potential term $\propto i$ [1], where $i = \sum_{j=1}^{L} i_j^3$ with

$$i^3 = \begin{pmatrix} 0 & 0 & 0 \\ 0 & 1 & 0 \\ 0 & 0 & 1 \end{pmatrix}. \tag{III.3.11}$$

This model has an $SU(2) \times U(1)_i$ symmetry generated by $h = \sum_{j=1}^{L} h_j^3$, $e = \sum_{j=1}^{L} e_j^3$, and $f = \sum_{j=1}^{L} f_j^3$ for the $SU(2)$, and i for $U(1)_i$. One can interpret the $SU(2)$ part as the invariance of the system under the exchange of $|+\rangle \leftrightarrow |-\rangle$. For each spin site, the $|0\rangle$ state forms a singlet under this $SU(2)$, and $|\pm\rangle$ forms a doublet. That is, each spin site is in the representation of $\mathbf{1} \oplus \mathbf{2} = \mathbf{1} \oplus \square$ of this $SU(2)$ symmetry. The Hilbert space of the whole spin chain can be decomposed as

$$\mathcal{H} = (\mathbf{1} \oplus \square)^{\otimes L} = \mathbf{1} \oplus \square^{L} \oplus \square\!\square^{\binom{L}{2}} \oplus \begin{array}{l}\square\\[-4pt]\square\end{array}^{\binom{L}{2}} \oplus \cdots \tag{III.3.12}$$

The number of the Young boxes corresponds to the $U(1)_i$ charge of the state in the representation, i.e. the total number of $|+\rangle$ and $|-\rangle$. The state in the first singlet is $|\Omega\rangle = |00...0\rangle$, which we choose as the Bethe reference state for solving this model in Appendix III.C. The theory has only elastic scatterings due to the conservation of the two $U(1)$ charges, corresponding to the $U(1)$ sub-symmetries generated each by i and h operators defined above. The conservation ensures that the $|\pm\rangle$ states behave as solitons. They do not create or annihilate with each other or deform from one to the other. This elasticity suggests that the model is integrable[2]. Indeed, the Hamiltonian can be constructed (up to the coupling $-1/2\lambda$ factor) from the R-matrix

[1] The authors would like to thank Hosho Katsura for pointing this out.

[2] The integrability can be predicted also from the symmetry of the (bulk) Hamiltonian not being limited to the finite-dimensional $SU(2) \times U(1)_i$ algebra but extended to the infinite-dimensional Yangian algebra $Y(SL(2))$.

$$R(\mu)$$
$$= -i \begin{pmatrix} \mathrm{sh}(\mu+\eta) & 0 & 0 & 0 & 0 & 0 & 0 & 0 & 0 \\ 0 & \mathrm{sh}(\mu) & 0 & \mathrm{sh}(\eta) & 0 & 0 & 0 & 0 & 0 \\ 0 & 0 & \mathrm{sh}(\mu) & 0 & 0 & 0 & \mathrm{sh}(\eta) & 0 & 0 \\ 0 & \mathrm{sh}(\eta) & 0 & \mathrm{sh}(\mu) & 0 & 0 & 0 & 0 & 0 \\ 0 & 0 & 0 & 0 & \mathrm{sh}(\mu+\eta) & 0 & 0 & 0 & 0 \\ 0 & 0 & 0 & 0 & 0 & 0 & 0 & \mathrm{sh}(\mu+\eta) & 0 \\ 0 & 0 & \mathrm{sh}(\eta) & 0 & 0 & 0 & \mathrm{sh}(\mu) & 0 & 0 \\ 0 & 0 & 0 & 0 & 0 & \mathrm{sh}(\mu+\eta) & 0 & 0 & 0 \\ 0 & 0 & 0 & 0 & 0 & 0 & 0 & 0 & \mathrm{sh}(\mu+\eta) \end{pmatrix}, \tag{III.3.13}$$

where sh is a shorthand for sinh, with the spectral parameter μ and the "anisotropy" $\eta = i\pi/2$. We focus on this specific value of η for our interest. The overall factor $-i$ is taken so that the R-matrix with the zero spectral parameter coincides with the permutation matrix. This R-matrix satisfies the Yang-Baxter (YB) equation

$$R_{12}(\lambda-\mu)R_{13}(\lambda)R_{23}(\mu) = R_{23}(\mu)R_{13}(\lambda)R_{12}(\lambda-\mu), \tag{III.3.14}$$

and hence the spin chain is integrable. The Hamiltonian is obtained by expanding the transfer matrix associated to R around $\mu = 0$ as the spectral parameter (see for example [147]). We compute the dispersion relation and the effective central charge of this massless model using the algebraic Bethe ansatz in Appendix III.C.

One can also see the integrability proving that this model is equivalent to free fermions [99]. The Hilbert space can be factorized as

$$\mathcal{H} = \left(\bigotimes_{j=1}^{L} \mathcal{H}_F \right) \otimes \mathcal{H}_{u,d}. \tag{III.3.15}$$

Here, $\mathcal{H}_F$ is a fermionic Fock space at each letter site where the $|0\rangle$ state corresponds to the r letter and $|1\rangle$ corresponds to either u or d. $\mathcal{H}_{u,d}$ are spanned by the states describing the order of u and d appearing in the words. Since the letters u and d cannot pass through each other, the Hamiltonian acts nontrivially only on the fermionic Fock spaces as free-

fermion hoppings and treats what we termed the knottiness as a label for the different superselection sectors. This model (with a deformation by a chemical potential term) has appeared before in [6, 7, 76, 126][3] where it was also shown to be integrable. Our important result is that the three-state spin chain with constraints can be converted to a nearest-neighbor spin chain without constraints, which happens to be a known integrable model. We may call this the three-state representation of the XX spin chain as it has the massless free fermion description with the same effective dispersion relation as shown in Appendix III.C. This is a good indication that this framework can reproduce the correct continuum behavior, given that the two-letter and three-letter strings would be no longer distinguishable from each other in the continuum.

III.3.3 Four-letter strings

We have showed the integrability structures of the first-order perturbation in the two-letter and three-letter sectors in the previous sections. Here, we list some phenomena in the most general sectors in $2+1$-D, the four-letter sectors, and show the evidence of non-integrability.

We can find a non-integrable scattering process only adding a few fourth (l) letters in the three-letter configuration. Consider the configuration with a loop at a corner of a long string stretching horizontally on one side and vertically on the other side due to one l configuration as fig. III.9. The scatterings far from the loop are the same as the three-letter case, which means they are elastic, but once they enter the region close enough to the loop, they become nontrivial. First, it should be noticed that the loop itself is a rigid structure on top of the horizontal plus vertical line. The constraints forbid any of the letters present to change location as such a process would violate one of the knottiness constraints. Such rigidity only appears because of the projectors and what we called secondary knottiness. Without the projectors, one can find a decay path of the

[3]The authors thank Hosho Katsura for pointing out these references.

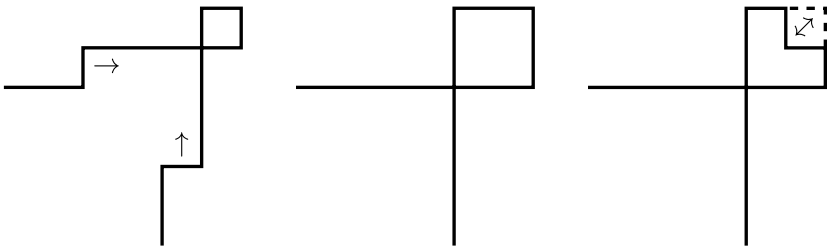

Figure III.9: A four-letter string configuration with a loop at a corner (non-trivial secondary knottiness). The defect scattering coming into the loop ((a)) may transform to a fluctuation inside of the loop ((b) and (c)). This is obviously a non-integrable scattering process, as the additional state only appears when two excitations from different sides of the loop collide simultaneously with the loop.

loop so that the loop can decay into moving excitations.

Now consider two additional defect excitations approaching the rigid loop as fig. III.9a. If they collide with the loop at the same time, the size of the loop becomes larger (fig. III.9b), allowing fluctuation inside of the loop (fig. III.9c). This kind of scattering processes is inelastic, suggesting the non-integrability of the four-letter sectors. The reason for this inelasticity is that the two defects must reach the rigid loop simultaneously in order to find the extra excitation of the loop. Each of the defects on its own would be reflected back with some phase shift. This counts effectively as a three body interaction that does not factorize.

We may consider another inelastic scattering process which can be translated to boundary conditions violating the boundary Yang-Baxter equation [4]. Think of a folded string as fig. III.10a. The position of the fold is rigid because of the knottiness constraints. In this case, we can say that the position of the fold is fixed by where we require the padding to be located. In that sense, as a system with three letters it corresponds to a configuration with all fermion sites occupied in the free fermion picture. Since the fermion sector is the only sector involving dynamics in the first order, this state is rigid.

Now add two kinks in opposite vertical directions (u and d) propagating on it towards

[4]This is a similar technique to the one used in [25] to show generic non-integrability for deformations of $\mathcal{N} = 4$ SYM.

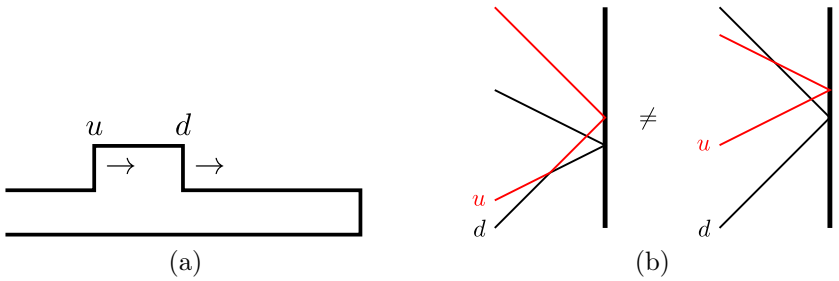

Figure III.10: (a) The two kinks (u and d) propagating on a folded string. d can pass through the folding point (the d edge between the r letters on the top and the l letters on the bottom), while u cannot pass through it but has to bounce back. (b) The two different scattering processes on this folded string depending on whether the two kinks can interact on the top side (right) or not (left) before d passes the folding.

the right, and the kink that is behind (let us say u) has a larger initial momentum than the other kink (d). The scattering processes qualitatively differs depending whether the two kinks interact on the top side (consisting of the r background letters) of the folding or not. If the u kink catches up with d on the top side of the folding, then the two kinks reflect carrying each other's momentum. On the other hand, if the d kink reaches the fold first, it can get past the fold easily as our map to the three-letter padded XX model would indicate. If that happens, the kinks do not interact with each other at all since the u kink cannot pass the folding: it must be reflected back always.

Regarding the folding point as the boundary and gluing the top and bottom sides together (just as the folding trick for an interface being mapped to a boundary [161]), the two scattering processes can be depicted as fig. III.10. In this picture, both processes where a d kink passes through the d folding point and a u kink bouncing back at the folding point are elastic reflections at the boundary. In such a reflection diagram they can interact in two possible ways, either a reflection (when they are on the same side of the folding) or an identity (they are on opposite sides). This obviously violates the boundary Yang-Baxter equation given that the final states are physically distinct. This is therefore a violation of integrability in the Yang-Baxter sense.

Another potential fact hinting at the non-integrability is that the boost operator,

which is naively defined as

$$B = \Pi\tilde{B}\Pi = \sum_{\ell} \ell\pi_\ell \tilde{h}_\ell \pi_\ell, \tag{III.3.16}$$

does not coincide with the boost operator of the integrable Hamiltonian for the three-letter configurations eq. (III.3.9): it does not generate the infinite set of conserved charges that one expected from the integrability of the three-letter problem. The basis change that pads the words correctly eq. (III.3.8) does not work for the general four-letter sectors, causing it to violate the possible integrability of the spin chain. Again, this is a violation in that the system does not seem to be solvable by Bethe Ansatz methods. Remember also that all of this structure arises exactly because of the projectors, as without the projectors the nearest neighbor spin chain is integrable.

III.4 Rotational symmetry restoration

One way to validate our scheme is to see if it reproduces the phenomena expected in the continuum limit. In the continuum, an infinitely long flux tube as we consider here is expected to be delocalized [124] (and references therein) due to by the quantum fluctuation of the Goldstone bosons caused by the breaking of the Poincaré symmetry. This does not hold for the lattice theory since the Poincaré symmetry is already broken to be discrete, and there indeed exist a stable flux tube sector in the strong coupling limit. As we weaken the coupling, there exists a so-called roughening transition point where the long flux tube delocalizes. Below this point, we expect our effective string description well reflects the behavior of the flux tube in continuum, including the restoration of the continuous Poincaré symmetry in the bulk YM theory.

We confirm this symmetry restoration by estimating the roughening transition in the two-letter and three-letter sectors using the degenerate corrections argued in Sec. III.3.1 and III.3.2. Fortunately, we found that both Hamiltonians are integrable, and hence the

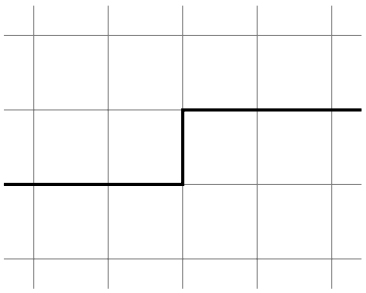

Figure III.11: A single kink on a straight string.

exact calculations are feasible.

One of the possible approaches is to identify the roughening transition point as the point where a single kink looking like fig. III.11 becomes massless. In the strong coupling limit, such a string state with a kink costs extra energy exactly by the amount of the string tension from the energy of the fully straight string given that the energy is proportional to the length of the string. As the coupling becomes weaker and the single kink becomes massless, there is no longer a cost for the string to go to the vertical direction. This leads to roughening of the string. This transition can be understood from the spin chain point of view by considering the unperturbed and perturbation parts of the Hamiltonian all together. The state under consideration consists of a number of r's except there is one u. In the two-letter sector with the XX spin chain description (Sec. III.3.1), this corresponds to the correction of the energy of a state with only one upspin, or a $-(L-2)$ magnetization state. In the basis of the first-order Hamiltonian in the three-letter sector (Sec. III.3.2), the unperturbed part can be added to the first-order Hamiltonian as a chemical potential term $\frac{\lambda}{2}\sum_{j=1}^{L} i_j^3$, i.e. the energy cost of the vertical kinks. In the strong-coupling limit, this unperturbed part dominates and hence the theory is massive, whereas the perturbation term eq. (III.3.9) dominates in the weak-coupling limit, which is massless. So, we expect the phase diagram of this model to have two regions, the massive phase and the massless phase, which are connected by a Berezinskii–Kosterlitz–Thouless (BKT)-like phase transition. This BKT-like transition point is identified as the roughening transition point. The transition in this class has

been observed by studying the Wilson/Polyakov line for example in the discrete $\mathbb{Z}_2$ lattice gauge theory in [96, 95]. Other setups for the electric flux roughening transition in $2+1$ D have been done in [58].

Actually, it is possible to directly observe the restoration of the spatial rotational symmetry for the two-letter string case as discussed in [105]. The angular dependence of the potential, which can be translated as the ground state energy in each magnetization sector of the XX model, should disappear once the symmetry is restored.

We estimate the values of the coupling λ restoring the rotational symmetry for these two cases by extrapolating from the strong-coupling expansions.

III.4.1 Roughening point from the two-letter strings

First-order correction to the kink mass

As we discussed earlier, the massive/massless transition of the kink mass corresponds to the roughening transition of the string if it occurs. In the strong coupling limit, the mass of the kink is exactly the energy of the single link excitation or the string tension, which is $\sigma = \lambda/2$. So, in the strong coupling region, the kink mass is nonzero, and this nonzero mass prohibits the string from extending in the vertical direction. On the other hand, if such a transition happens, and the kink mass becomes zero, the extension to the vertical direction no longer costs energy; this is what is called the roughening of the string. We calculate the value of the kink mass with the first-order correction to extrapolate the value of λ giving the massless kink. A state with a single kink can be interpreted as a state with one upspin in the XX spin chain description. It is diagonalized as a free fermion theory as

$$H_{\mathrm{XX}} = -\frac{1}{\lambda}\sum_{k=-L/2+1}^{L/2} \Lambda_k \hat{a}_k^\dagger \hat{a}_k, \quad \Lambda_k = \cos\left(\frac{2\pi k}{L}\right) \tag{III.4.1}$$

in the thermodynamic limit (details in Appendix III.B), and the operator counting the number of upspins is exactly the fermion number operator. Hence, the state of our interest has exactly one fermionic excitation with energy of $-\frac{1}{\lambda}\Lambda_k$. What we need to consider is the state consisting of a stationary kink, which is given by setting $k = 0$ corresponding to zero momentum. The corrected kink mass is

$$M_{\text{kink}} = \frac{\lambda}{2} - \frac{1}{\lambda} + \mathcal{O}\left(\frac{1}{\lambda^2}\right). \tag{III.4.2}$$

This becomes zero when $\lambda = \sqrt{2}$ which we identify as the roughening transition point up to the first order in the strong coupling expansion.

Direct first-order estimation of the symmetry restoration

As mentioned above, we can directly observe the symmetry restoration in the two-letter string sector, following [105]. The angular dependence is the choice of the combination $(n, L-n)$ for the numbers of the two letters for the first-order corrections, which is exactly equivalent to choosing a certain magnetization sector of the XX model as we saw in Sec. III.3.1. Let us say the lowest n fermi levels are filled, which means the state is in the corresponding magnetization $M = n$ sector in the spin description, or having n vertical and $L-n$ horizontal edges. The string state in the lowest energy in the n sector has the energy

$$E = \frac{\lambda}{2}L - \frac{1}{\lambda}\sum_{k=0}^{n-1}\cos\left(\frac{\pi k}{L}\right) = \frac{\lambda}{2}L - \frac{1}{2\lambda}\left(1 + \csc\left(\frac{\pi}{2L}\right)\sin\left(\frac{\pi(2n-1)}{2L}\right)\right). \tag{III.4.3}$$

In the continuum, we can write the parameters in the polar coordinates; defining ρ as the physical distance of the endpoints of the string and θ as their angle from the horizontal axis, the number of the horizontal edges is $\ell = \rho\cos\theta$, and the string length is $L = \rho\cos\theta + \rho\sin\theta$. Now, the ground state energy is expressed as

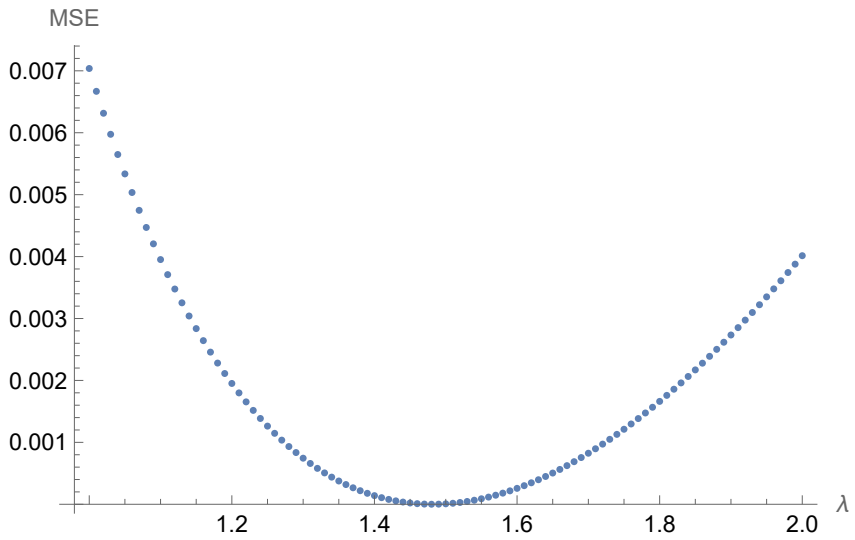

Figure III.12: The mean squared errors of E for different values of λ. It is minimized to be almost zero around $\lambda \approx 1.5$.

$$E = \rho(\cos\theta + \sin\theta)\left(\frac{\lambda}{2} - \frac{1}{\pi\lambda}\sin\left(\frac{\pi}{1+\tan\theta}\right)\right) + \mathcal{O}(\rho^0). \tag{III.4.4}$$

Its derivative by θ at $\theta = 0$, corresponding to a string consisting almost all r's, becomes 0 at $\lambda = \sqrt{2}$ in the leading order of ρ, which is exactly what we estimated by considering the first-order correction to the kink mass in the last section. Indeed, E is almost constant around $\lambda \approx 1.5$, as we can see by numerically calculating where E becomes the closest to a constant as a function of θ (fig. III.12).

III.4.2 Roughening point from the three-letter strings

Let us estimate the roughening transition point in the three-letter sector as well. Since the two-letter strings and the three-letter strings would be no longer distinguishable from each other once we reach continuum, the transition point should coincide if expansions in all orders were available. Indeed, we will demonstrate that the extrapolated value of λ in the first-order calculation already matches with the result from the two-letter sector calculation. We also carry out the second-order calculation to confirm two things. First

is to estimate the point when the string tension becomes negative, which we estimate to happen after the roughening phase transition. Second is that the extrapolated transition point does not deviate too far from the first-order result and hence our perturbative expansions are providing meaningful estimates.

First-order corrections

Let us compute the first-order correction to the kink mass, using the Hamiltonian eq. (III.3.9). The single kink state lives in the sector of $U(1)_i$ charge of $i = 1$. This corresponds to acting a single ($n = 1$) B matrix on the Bethe reference state $|\Omega\rangle$ (details in Appendix III.C). The energy and momentum spectra we found in eq. (III.C.20) lead to the dispersion relation for $n = 1$ to be

$$E^{(1)}_{1,\ell} = -\frac{1}{\lambda}\cos\Big(p^{(1)}_\ell\Big) \tag{III.4.5}$$

with $p^{(1)}_\ell = 2\pi\ell/L$ and $\ell = 0, 1, ..., L-1$. Here, we recovered the coupling factor $-1/2\lambda$. This is the first-order correction to the single kink mass which is overall $M_{\text{kink}} = \frac{\lambda}{2} - \frac{1}{\lambda}\cos\big(\frac{2\pi\ell}{L}\big) + \mathcal{O}(1/\lambda^2)$. Since we want to consider the stationary kink with $p^{(1)}_\ell = 0$, we have

$$M_{\text{kink}} = \frac{\lambda}{2} - \frac{1}{\lambda} + \mathcal{O}\left(\frac{1}{\lambda^2}\right) \tag{III.4.6}$$

This is exactly the expression we obtained in the two-letter sector (eq. (III.4.2)). Again, the roughening point is estimated as $\lambda = \sqrt{2}$.

Second-order corrections

We now want to consider second order corrections. Let us start with the corrections to the string tension for the horizontal state (in letters $rrrrrrr\ldots$). This state is rigid and can be considered a ground state with energy $E_0 = \sigma L$. Notice that there is no other

state with the same quantum numbers that is degenerate with it and that the expectation value of the perturbation plaquette vanishes on this state. When we add perturbations to second order perturbation theory, we need to compute

$$\Delta E = \sum_j \frac{V_{ij}^2}{E_0 - E_j} \tag{III.4.7}$$

where V_{ij} are the off-diagonal matrix elements. Since $E_0 < E_j$, the correction will be negative.

There are two types of moves allowed by inserting a plaquette. These are of type C, and another one of type B that joins a closed rigid loop at any location by intertwining the lines. We will call this operation B'.

The type C moves take a letter $r \to urd$ or $r \to dru$ and adds a kink-antikink pair. The matrix element is 1, times $(N/2\lambda)\frac{1}{N}$ for each of them. The difference in energy is 2σ as the length changes by 2. The contribution to the energy is therefore

$$\Delta E_{\rm C} = \sum_{\ell=1}^{L} \frac{2}{-2\sigma} \frac{1}{2^2\lambda^2} = -\frac{1}{2\lambda^3} L, \tag{III.4.8}$$

and we notice that this is proportional to the length, so the correction to the tension is

$$\Delta\sigma_{\rm C} = -\frac{1}{2\lambda^3}. \tag{III.4.9}$$

The second contribution requires adding (for example) a loop $uldr$ at some position, which is a loop on top of the string. We can also add the loop $ruld$, one step to the left. Both of these cause the same transition and therefore the combinatorial factor associated to this term is actually a factor of 2. This is exactly the combinatorial factor that appeared in eq. (III.2.11). The same $1/2\lambda$ is attached to plaquette, and the denominator is -4σ rather than -2σ. We get this way that (when we sum over up and down)

$$\Delta\sigma_{\rm B'} = \frac{-2}{4\sigma}\left[\frac{2}{2\lambda}\right]^2 = -\frac{1}{\lambda^3} \tag{III.4.10}$$

Summing the two terms, we get that

$$\Delta\sigma_{\mathrm{C+B'}} = -\frac{3}{2\lambda^3} \tag{III.4.11}$$

Notice that σ wants to become negative (tensionless) when $\lambda = 3^{1/4} \sim 1.31$, which is below the value where the mass of the kink becomes zero for the first time. That means that at least at this order, the massless kink that corresponds to the roughening transition comes first.

Let us further consider the second-order corrections to the single kink energy. The on-diagonal contribution to the single kink state $|x\rangle$ is

$$E_\ell^{(2)} = \sum_{k \notin D_{\text{1-kink}}} \frac{|\left\langle k^{(0)} \middle| V \middle| x \right\rangle|^2}{E^{(0)}_{D_{\text{1-kink}}} - E^{(0)}_k}, \tag{III.4.12}$$

where $D_{\text{1-kink}}$ is the degenerate sector spanned by all of the one-kink states. x denotes the position of the kink on the straight string. The nonzero contributions come from the states with a deformation made by a single plaquette from a one-kink state. In order to combine with the first-order correction, to be more precise, we actually have to take the state under consideration to be the eigenstate of the first-order correction matrix corresponding to a stationary kink, which would be a linear combination of $|x\rangle$. However, since the second-order corrections to single kink states are all equal with each other (at least in the region away from the string endpoints), we ignore this subtlety and simply consider a kink at a fixed position.

Most of the contributions are the same as the second-order corrections to the straight string without any kink, except for the corrections due to plaquette actions around the kink, which we will consider below. There are three things we need to take care of.

First, one needs to consider the type B′ deformations on the kink (fig. III.13). If we look at a word that goes rur and need to insert a loop, there are two choices for replacing $u \to u(rdlu)$, with a loop that twists to the right, which would add a word to the right of u, or we could add the word $(urdl)u$ to the left. Moreover, this interferes with adding

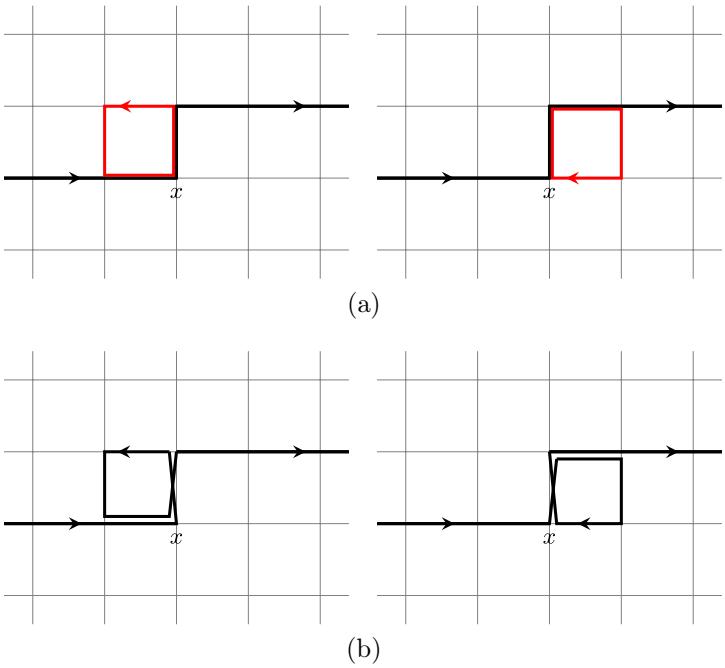

Figure III.13: (a) The type B deformations to a string state with a single kink at position x which have a nonzero overlap with another states depicted in (b), in the leading-order. The contributions from these overlaps do not appear in the corrections to the no-kink state.

$ur(dlur)$ with the next letter. The combinatorial factor for the off-diagonal element is therefore 3, compared to 2 when we have just a string of letters of type r. We get a similar contribution from a loop that loops to the left (eg, $u \to uldru$). We get

$$\Delta E_{\mathrm{B}'} = 2 \times \frac{9}{-4\sigma} \frac{1}{(2\lambda)^2} \tag{III.4.13}$$

However, we are double counting the contribution to the tension of the string from type B' moves (if we consider them independent) acting on the r edge overlapping with the loop, so we need to subtract the correction to the string tension correctly from the kink contribution. We arrive at

$$\Delta E_{\mathrm{B}'}(kink) = 2 \times \frac{9}{-4\sigma} \frac{1}{(2\lambda)^2} - 2 \times \frac{4}{-4\sigma} \frac{1}{(2\lambda)^2} = -\frac{5}{8\lambda^3}. \tag{III.4.14}$$

We also need to remove the C moves that are absent from the string tension but already taken care of in the first-order corrections for the kink (fig. III.15). Moreover,

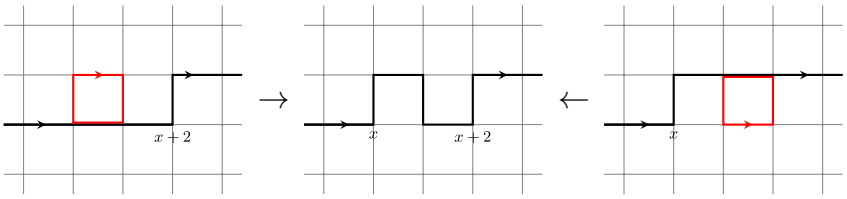

Figure III.14: Type C deformations can act on different kink states (left (urr) and right (rru) and result in the same intermediate state ($urdru$). This lead to off-diagonal contribution in the second order.

there is one more type C contribution that is not obvious. This also arise from C type moves, but it is off-diagonal. The idea is that the configurations of type $urdru$ can be accessed in two ways. Starting from $rru \to (urd)ru$ and $urr \to ur(dru)$ where we have put in parenthesis the replacement of the letter r by the C type move (one upwards and the other one downwards). This has energy denominator -2σ and produces an effective off-diagonal substitution $rru \leftrightarrow urr$ which corresponds to a next to nearest neighbor hop (fig. III.14, see also [105]). Since the on-diagonal corrections to these two states are identical, this off-diagonal contribution simply produces an extra term to the energy eigenvalue as

$$\Delta E_{\text{O.D.}} = \sum_j \frac{V_{ij}V_{jk}}{-2\sigma} = \frac{1}{-2\sigma}\frac{1}{(2\lambda)^2}(2\cos(2p_\ell)). \tag{III.4.15}$$

This modifies the momentum dependence of the dispersion relation. We need to evaluate it at $p_\ell = 0$, so.

$$\Delta E_{\text{O.D.}} = -\frac{1}{2\lambda^3} \tag{III.4.16}$$

Lastly, we need to include the nontrivial corrections due to overlaps with the type A′ deformations at either one of the two corners of the kink. This deformation corresponds to inserting either a single clockwise or counter-clockwise loop before or after the kink u. For example the two moves $u \to uuldr$, or $u \to ulurd$ generate corner terms with additional loops wit two possible orientations. The matrix elements of the perturbation V_{ij} for

these overlaps are again $(N/2\lambda)\frac{1}{N}$, where the extra $1/N$ factor comes from the topology change at the shared corner. The energy denominator is -4σ due to the additional single plaquette loop, and the correction is

$$\Delta E_{\mathrm{A}'}(kink) = 2 \times 2 \times \frac{1}{-4\sigma}\frac{1}{(2\lambda)^2} = -\frac{1}{2\lambda^3}. \tag{III.4.17}$$

These contributions give the energy correction in total as

$$\begin{aligned}
&\Delta E(kink) \\
&= \Delta E_{\mathrm{B}'}(kink) - \Delta\sigma_{\mathrm{C}} + \Delta E_{\mathrm{O.D.}} + \Delta E_{\mathrm{A}'}(kink) \\
&= -\frac{5}{8\lambda^3} + \frac{1}{2\lambda^3} - \frac{1}{2\lambda^3} - \frac{1}{2\lambda^3} \\
&= -\frac{9}{8\lambda^3}.
\end{aligned} \tag{III.4.18}$$

Hence, the kink mass with the corrections up to the second order dispersion is

$$M_{\mathrm{kink}} = \frac{\lambda}{2} - \frac{1}{\lambda} - \frac{9}{8\lambda^3} + \mathcal{O}\left(\frac{1}{L} + \frac{1}{\lambda^4}\right). \tag{III.4.19}$$

This becomes zero when $\lambda = (1 + \sqrt{13}/2)^{1/2} \approx 1.67$.

III.5 Higher dimensions

As noted in section III.2, our word representation of confining strings is valid regardless of the spacetime dimensions. This indicates that it is straight-forward to extend it to higher dimensions; it adds additional letters to the set of letters we already have and with the additional zigzag constraints and the notion of the knottiness (that for each pair of back and forth letters the order cannot change). Let us comment on some subsectors in $3+1$-dimensions.

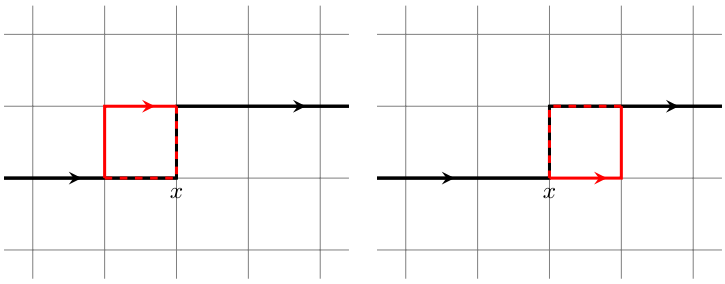

(a)

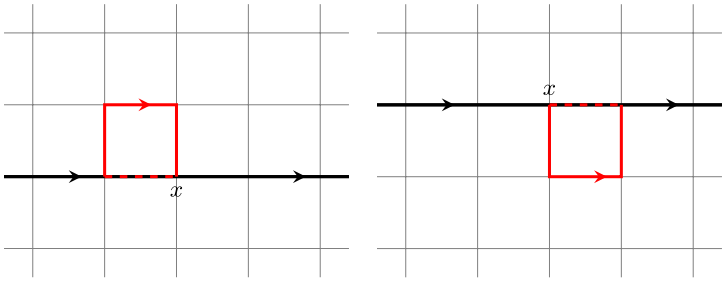

(b)

Figure III.15: (a) The type C deformations to a string state with a single kink at position x which do not contribute to the second-order corrections since they are already taken into account in the first-order corrections. (b) The corresponding type C deformations to the no-kink state which do contribute to the second-order corrections.

III.5.1 Three-letter sector in $3+1-D$

Consider $3+1$-dimensions, and string configurations with three letters that describe the edge excitations heading towards positive x, y, z directions. It is an analogue of the two-letter sector in $2+1$-D, given that the sector of these configurations do not require any projection, and the spin chain Hamiltonian describing the first-order corrections is an operator in $(\mathbb{C}^3)^{\otimes L}$:

$$H = -\frac{1}{2\lambda}\sum_{j=1}^{L}(e_j^1 f_{j+1}^1 + f_j^1 e_{j+1}^1 + e_j^2 f_{j+1}^2 + f_j^2 e_{j+1}^2 + e_j^3 f_{j+1}^3 + f_j^3 e_{j+1}^3) \tag{III.5.1}$$

where the operators e_i^a and f_i^a are the $\mathfrak{sl}(3)$ generators (III.3.10). This is exactly the bilinear-biquadratic spin-1 chain with

$$H \propto \sum_{j=1}^{L} \left(\cos\theta(\vec{S}_j \cdot \vec{S}_{j+1}) + \sin\theta(\vec{S}_j \cdot \vec{S}_{j+1})^2 \right) \tag{III.5.2}$$

at $\theta = \pi/4$, i.e. the Uimin-Lai-Sutherland point, up to the chemical potential term. This point is integrable (see e.g. [8] for the exact form of the R-matrix), and more importantly, it can be effectively described as the $SU(3)_1$ Wess-Zumino-Witten model [90], which has a central charge of $c = 2$.

III.5.2 Four and more letter sectors in $3+1$-D

The next simplest case is the four-letter sector, which consists of string configurations with edges heading the positive or negative x-directions or the positive y- or z-directions. Although this is analogous to the three-letter sector in $2+1$-D, requiring only one type of projection that prohibits neighboring $\pm x$ edges, the situation is drastically more complicated. The basis change like eq. III.3.8 would not work for this case, since now the $\pm x$ edges can have either an $+y$ edge or an $+z$ edge in between. The system also admits dynamics involving $+y$ and $+z$ edges, so we cannot simply discard one between the $\pm x$ edges. Actually, we should not even expect integrability for this sector, as one can see by regarding the $\pm x$ and $+y$ kinks as pseudo-particles on the vacuum of $+z$ edges or a long string in the $+z$-direction. Although the S-matrix for two-body scatterings between the $+x$ or $-x$ kink and the $+y$ kink is merely a permutation, three-body scatterings involving all three kinks cannot be decomposed into two-body scatterings as explained diagrammatically in fig. III.16. The zigzag constraint prohibits a three-body scattering like fig. III.16a to be decomposed to the product of two-body scatterings as in fig. III.16b since the $\pm x$ kinks are not allowed to be next to each other (their scatterings in the three-letter sector in $2+1$-D were special since they were allowed to be next to each other after the basis change eq. (III.3.8)).

The nonintegrability of sectors with more letters is clearer, since the strings contain

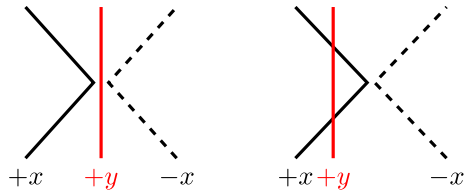

Figure III.16: An example of the three-body scattering on four-letter strings in $3+1$-D. The scattering process in (a) where the $\pm x$ kinks and the $+y$ kink collide at the same time could be decomposed to two-body scatterings as in (b) if there were no constraints. The zigzag constraints prohibit the direct interaction between $\pm x$ kinks so the reflection between them (the second two-body interaction in the decomposition (b)) is not in the S-matrix data of the model, and hence the decomposition is not allowed.

at least two sets of edges heading parallel but in opposite directions similarly as the four-letter sector in $2+1$-D. The same argument as section III.3.3 applies to these cases.

III.6 Another Language

So far we have investigated various subsectors of confining strings and their strong-coupling corrections. Even though there exist some subsectors where the projection due to the zigzag constraints is unnecessary, it might be more convenient to describe the string configurations with a different convention to avoid the description with projections altogether. If we think of the projections as a gauge constraint, this would be equivalent to finding the solutions to the constraint first, so that the dynamics becomes unconstrained in such a basis.

This is possible by expressing the words by the relative directions of the edges from each vertex relative to the incoming string segment. For example, for the strings in $2+1$-dimensions, the possible configuration for each edge is either straight (s), right (r), or left (l) relative to the incoming edge. Then, the zigzag symmetry constraint is implemented without any need of projections since the configurations going back and forth on the same edge are manifestly not included. In this language, one can also write the first-order corrections as the eigenvalues of a spin chain Hamiltonian, where each

spin belongs to a spin-1 chain, corresponding to the three possible relative directions. Instead of the projection, now the Hamiltonian includes next-to-nearest-neighbor interactions, since the letter after the two letters corresponding to the edges exchanged by the Type C deformation is also affected. The Hamiltonian density with three-site interaction exchange letters as one of the following four pairs:

$$\mathsf{srs} \leftrightarrow \mathsf{rlr}, \quad \mathsf{srl} \leftrightarrow \mathsf{rls}, \quad \mathsf{sls} \leftrightarrow \mathsf{lrl}, \quad \mathsf{slr} \leftrightarrow \mathsf{lrs}. \tag{III.6.1}$$

This language can be translated back to the former u, d, r, l language by assigning $\mathbb{Z}_4$ values $0, 1, 3$ respectively to s, r, l and summing these numbers from one end.

The interesting fact is that in this form, the equation (III.6.1) also looks like a relatively simple set of rules. The absence of projectors makes it in principle easier to implement. This is favorable from the viewpoint of computational resources for (quantum) simulation. The former language naively requires a $4^4 = 256$ dimensional operator for each plaquette action taking the projection π_ℓ into account, while this language requires an operator with only $3^3 = 27$ dimensions. The 4^4 requires 8 qubits to implement, where the 27 can be easily fit with 6 qubits (each set of 3 letters can be built from 2 qubits and leaving out one unwanted state).

From this dimension counting, one can see that another lattice geometry, namely a hexagonal lattice, would be even more efficient using this language. The string excitation on a hexagonal lattice can be described by using two letters specifying the relative directions, left (l) or right (r), i.e. it can be described as a spin-1/2 chain. The Type C deformation relevant for the first-order correction for a hexagonal lattice switches the excitations on three consecutive edges of a hexagon plaquette to the other three (fig. III.17). This corresponds to an action on four spin sites, for example lrrl becomes rllr and indeed, this is the only action of the plaquette that results in an allowed configuration. Counting the number of the dimensions for the plaquette operators, it can be represented as the

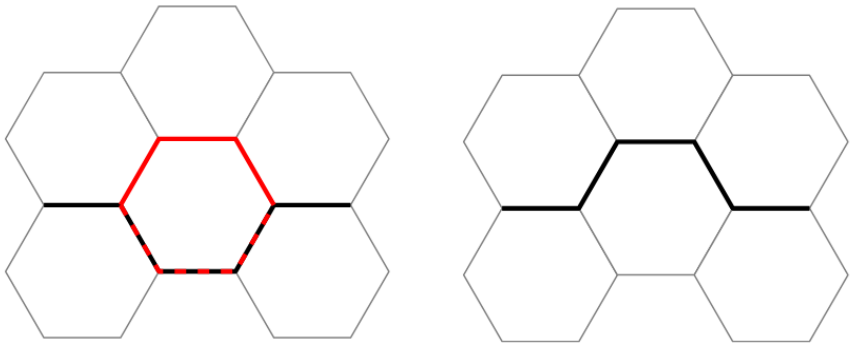

(a) (b)

Figure III.17: (a) The plaquette action (red) on a string excitation (black) in a hexagonal lattice contributing to the first-order corrections. The hexagon plaquette shares half of its six edges with the string. (b) The resulting deformed string state.

$2^4 = 16$-dimensional operator or 4 qubits for a hexagonal lattice while it needs a 27 dimensional Hilbert space or 6 qubits for a square lattice. This observation is interesting since in the original language, the string words in a hexagonal lattice need one more auxiliary letter from the equivalent configurations in a square lattice, as the hexagonal lattice can be obtained from the square lattice by "point-splitting" and adding an additional lattice direction between them just as the spin network setups [149]. The best thing one can do is projecting out the space involving the dynamics of the auxiliary letter, so the computational resource for the original language is bounded below by the minimum resource required for the square lattice. Studying the haxagonal lattice strings in detail is beyond the scope of the present work. We are also studying those lattices in future work.

III.7 Discussion and future directions

In this chapter, we showed that the first-order perturbation theory corrections to single string states at strong coupling for the large N lattice Yang-Mills theory are closed within the subsectors of fixed length, and these string states can be specified by the combination of the letters (directions in the lattice graph) that describes the path the string takes.

The actions of the plaquette operators are merely manipulations of the letters.

The Hamiltonian gives a nearest neighbor Hamiltonian, with additional projectors that enforce the zigzag symmetry. The goal of this chapter has been to understand the features of this spin chain Hamiltonian in more detail, especially by studying subsectors with fewer letters than the generic type of path.

The two- and three-letter sectors in $2+1$-D are integrable, being equivalent to free fermions. At leading order the differences in dynamics between the two-letter strings and three-letter strings in $2+1$-D are merely lattice artifacts.

We also argued here that the most general four letter sectors contain inelastic scattering events, as well as violations of the (boundary) Yang-Baxter equations, indicating that they are likely not-integrable. To leading order they have a rich spectrum of superselection sectors classified by a series of quantum numbers that we called knotiness and secondary knotiness. These describe the zigs and zags of the paths (the structure of the changes of directions) and how these are intertwined.

It is expected that at higher orders the dynamics will exhibit the same continuum physics (universality class) as one extrapolates from these sectors towards the continuum, and that should make the lattice system restore the rotational symmetry.

Higher order computations are necessary so that we can start seeing that the string motion is fully relativistic and quantizes a Nambu-Goto string worldsheet.

We also did not discuss the closed string states, which can also be called glueballs. These are interesting in their own right.

We discussed the extension of the open string setup to $3+1$-D, where we saw that an integrable structure appears also in a particular three-letter subsector. This sector does not require projections due to the zigzag constraints, but more generic sectors are not integrable. At this point, we can make a general statement that *the introduction of the zigzag constraints violates the spin chain integrability*, except in the special case of the three-letter sectors in $2+1$-D where a basis change is available to discard such

projections. A mathematically rigorous statement of non-integrability is still missing, which we leave for future work.

The present work also includes a reformulation of the spin chain in another language (changes of directions instead of a fixed set of directions for links) to describe the string configurations. It has an advantage over the more naive formulation because it already encodes the constraints, so it needs no explicit projection in the Hamiltonian to achieve the zigzag constraints. In that sense, the Hamiltonian density covers fewer sites.

This is important because if one where to try to simulate such a spin chain on a quantum computer, it requires fewer computational resources to simulate, at least to leading order. At the same time, the physical interpretation of the Hamiltonian action on the words is less obvious and needs to be read carefully from the moves induced by the plaquettes. We briefly explored the possibility of using a different lattice geometry for $2+1$ dimensions, namely, a hexagonal grid. The hexagonal grid in full seems to require fewer computational quantum resources to time evolve the system in $2+1$ dimensions relative to the square grid. Of course, one has to carefully evaluate which description and lattice geometry achieves in practice the minimal computational resources for a given hardware configuration, and for each Trotter step. We leave the development of such efficient quantum algorithms and the estimation of their computational complexity for future work.

It is really important to understand the continuum physics carefully. This requires understanding the approach to the roughening transition from strong coupling in detail. These computations require finding a way to systematically compute the higher-order corrections and also finding an efficient description of the glueball states.

Since we provided a systematic translation from a string configuration to a word consisting of finite species of letters, constructing spin chains for the planar higher-order corrections should be straightforward, except for the following subtlety: given that the higher-order contributions are due to states with different nonperturbative energies, i.e.

string lengths, then the perturbation takes us outside of the Hilbert space. One needs to integrate out the changes of length to go to an effective description with next to nearest neighbor corrections (plus projectors), etc. At least in principle, one should be able to parametrize such effects with improved lattice Hamiltonians on the spin chain (or the bulk). The next step in the program we are outlining would be to calculate the corrected spin chain in full generality with not only *nearest neighbor* terms, but also next to nearest neighbor terms, even if restricted just to the simplest 2 letter system n $2 = 1$ dimensions and $3+1$ dimensions, or the three letter setup, where we expect to start seeing violations of secondary knotiness induced by the perturbations in the $2 + 1$ problem. This three letter problem is also required to better understand the roughening transition and the restoration of rotational invariance better.

Another way to do possibly do things is to take into account variations of spin chain setups that allow clever ways to vary the length, as in [27]. One must also be careful with the possible non-planar contributions from the lower-order corrections spoiling a naive analysis. Such non-planar contributions can involve scattering with glueballs (closed paths). As stated before, the glueballs are also independently interesting objects to be studied.

Notice that the open strings we considered in the present work have fixed quark endpoints and hence the center of mass (COM) degrees of freedom have no dynamics. This is not the case for the closed string glueball states. Translations of glueballs are independent states, so a passage to spin chains must be more involved as it requires an extra Hilbert space to keep track of the center of mass degrees of freedom. Moreover, that Hilbert space of translates must also interact nontrivially with the Hilbert space for the local edge configurations. This is required so that different glueball states have a different dispersion relation (mass in the sense of the center of mass motion).

III.A Energy change by the plaquette action type B

Here, we calculate the nonperturbed energy of the state generated by a single plaquette action on a string state sharing one link as depicted in fig. III.1b. The original string state excited along the open path Γ with length L is generated by the product of the gluon link operators acting on the vacuum state $|\Omega\rangle$:

$$|\Gamma\rangle = \prod_{\ell\in\Gamma} U_\ell \,|\Omega\rangle \tag{III.A.1}$$

Let us call the plaquette we are acting P and the shared link m. Every link operator excited in the resulting state $|\Gamma'\rangle = U_P \prod_{\ell\in\Gamma} U_\ell \,|\Omega\rangle$, except those acting on the link m, contributes in the same manner to the nonperturbed energy as eq. (III.2.3), i.e. each contributes $\frac{\lambda}{2}$, and hence overall the energy of $\frac{\lambda}{2}(L+2)$ come from these non-shared operators. The only nontrivial contribution comes from $U_m U_m$ in the product. Denoting U_m as U to simplify the notations and writing the fundamental indices explicitly from now on, the nonzero contributions to the nonperturbed energy are

$$KU_{ij}U_{kl}\,|\Omega\rangle = \frac{\lambda}{2N}E^aE^aU_{ij}U_{kl}\,|\Omega\rangle = \left(\lambda\frac{N^2-2}{N^2}U_{ij}U_{kl} + \frac{\lambda}{2N}U_{il}U_{jk}\right)|\Omega\rangle \tag{III.A.2}$$

Even though we have the second term which generates another string state than the state $|\Gamma'\rangle$, namely the state excited along a single string with a "twist" at m, it is suppressed for large N. This means that only the first term survives in the large N limit, and the generated state $|\Gamma'\rangle$ by the single plaquette action stays as an eigenstate of the nonperturbed Hamiltonian. The plaquette acted state lives in the energy level of four units higher than the original string state. The same mechanism occurs in the cases of the single plaquettes sharing more than one link with the original state. It always raises the nonperturbed energy by four units in the leading order, and hence they do not contribute to the first-order corrections. We need to take them into account in the

second or higher-order corrections. The leading $\sim \mathcal{O}(1/N^0)$ order term gives the same correction as the vacuum correction, so the first nontrivial deviation comes from the subleading-order term in eq. III.A.2.

III.B Solving the two-letter Hamiltonian

One can straightforwardly check that the XX model (III.3.6) is equivalent to the free fermion theory using the Jordan-Wigner transformation as

$$H_{\mathrm{XX}} = -\frac{1}{\lambda} \sum_{k=-L/2+1}^{L/2} \Lambda_k \hat{a}_k^\dagger \hat{a}_k \tag{III.B.1}$$

Λ_k are eigenvalues of the matrix $\frac{1}{2}(\delta_{i,j+1}+\delta_{i,j-1})$ with $i,j = 1,...,L$. In the thermodynamic limit $L \to \infty$, the eigenvalues are $-\Lambda_k/\lambda = -\cos(2\pi k/L)/\lambda$, which is the energy of each of the fermion modes. One can regard $p = 2\pi k/L \in (-\pi, \pi]$ as the momentum of the mode in this limit. $\hat{a}_k$ and $\hat{a}_k^\dagger$ are the fermionic annihilation and creation operators, respectively:

$$\{\hat{a}_k, \hat{a}_\ell^\dagger\} = \delta_{k\ell}, \quad \{\hat{a}_k, \hat{a}_\ell\} = \{\hat{a}_k^\dagger, \hat{a}_\ell^\dagger\} = 0 \tag{III.B.2}$$

The magnetization operator of the spin chain is translated on this fermionic basis as the fermion number operator:

$$\hat{N} = \sum_k \hat{a}_k^\dagger \hat{a}_k \tag{III.B.3}$$

The ground state of the model has exactly $L/2$ of the fermions filling all the negative fermion modes up to the fermi surface $\Lambda_{k_F} = 0$ (corresponding to $p_F = \pm\pi/2$), and all the modes above the fermi surface are unoccupied.

The one-particle excited state in this sector has one of the fermions "popped" from the fermi sea to right outside of the surface. The lowest possible excited state has a fermion right below the fermi surface popped out to right above the surface, and such excitation is gapless in the thermodynamic limit. Let the fermion pop from $p \in [-\pi/2, \pi/2]$, then the energy gap of the state from the ground state energy is $\cos(p)/\lambda$. This means these one-fermion excitations have a linear dispersion around the fermi surface, $\epsilon(p) \sim |p - p_F|/\lambda$. Indeed, the XX model corresponds that is the complex massless free fermion theory which is a $c = 1$ CFT.

III.C Solving the three-letter Hamiltonian

III.C.1 Algebraic Bethe ansatz

We saw the integrability of the three-letter Hamiltonian, so one can find its energy spectrum using the Bethe ansatz method. Here, we use the algebraic Bethe ansatz to compute the spectrum. The monodromy matrix can be written component-wise in the auxiliary space as

$$T_0(\mu) = \begin{pmatrix} A(\mu) & B_1(\mu) & B_2(\mu) \\ C_1(\mu) & D_{11}(\mu) & D_{12}(\mu) \\ C_2(\mu) & D_{21}(\mu) & D_{22}(\mu) \end{pmatrix}. \tag{III.C.1}$$

In this expression, the transfer matrix is written as $t(\mu) = A(\mu) + \sum_a D_{aa}(\mu)$. The action of the A and D matrices on the reference state (the string state consisting only $rrrrr...$) can be found by looking at the upper-left components of the 3×3 blocks of the R-matrix:

$$A(\mu) |\Omega\rangle = (i \cosh(\mu))^L |\Omega\rangle , \tag{III.C.2}$$

$$D_{aa}(\mu) |\Omega\rangle = \sinh^L(\mu) |\Omega\rangle . \tag{III.C.3}$$

The algebraic Bethe ansatz constructs the series of the highest-weight states by acting B

matrices on the reference state $|\Omega\rangle$. Each B moves the state to be in the representation with one additional box in eq. (III.3.12). This corresponds to adding either one u (or $|+\rangle$) or d (or $|-\rangle$) to the string. To calculate the spectrum of the state acted by the B matrices, one needs to find the algebraic structure of the A, B, and D matrices. The first step is to think of the Yang-Baxter equation of the R-matrices supported on one (let us label it n) of the physical spin sites and two additional auxiliary Hilbert spaces 0 and $0'$:

$$R_{00'}(\lambda-\mu)R_{0n}(\lambda)R_{0'n}(\mu) = R_{0'n}(\mu)R_{0n}(\lambda)R_{00'}(\lambda-\mu). \tag{III.C.4}$$

By iteratively applying this relation to all of the physical spaces $n = 1, 2, ..., L$, then one finds the so-called TTR equation:

$$R_{00'}(\lambda-\mu)T_0(\lambda)T_{0'}(\mu) = T_{0'}(\mu)T_0(\lambda)R_{00'}(\lambda-\mu). \tag{III.C.5}$$

Looking at relevant matrix components of this equation, we can read off the commutation relations of the A, B, and D matrices as

$$A(\lambda)B_a(\mu) = -i\coth(\lambda-\mu)B_a(\mu)A(\lambda) + i\,\mathrm{csch}(\lambda-\mu)B_a(\lambda)A(\mu), \tag{III.C.6}$$
$$B_a(\lambda)B_b(\mu) = B_a(\mu)B_b(\lambda), \tag{III.C.7}$$
$$D_{ab}(\lambda)B_c(\mu) = i\coth(\lambda-\mu)P^{de}_{bc}B_e(\mu)D_{ad}(\lambda) - i\,\mathrm{csch}(\lambda-\mu)P^{de}_{bc}B_e(\mu)B_e(\lambda)D_{ad}(\mu), \tag{III.C.8}$$

where $P^{ab}_{cd} = \delta^a_d\delta^b_c$ is a permutation operator in $\mathbb{C}^2\otimes\mathbb{C}^2$. B_1 adds one $|+\rangle$ and B_2 adds one $|-\rangle$, so now we can think of the newly generated states by acting the series of the B matrices as

$$|\{\mu_k\};\Psi\rangle = B_{a_1}(\mu_1)\cdots B_{a_n}(\mu_n)\,|\Omega\rangle\,\Psi^{a_1\ldots a_n} \tag{III.C.9}$$

with a nonzero number of $|\pm\rangle$, or the states in representations with one or more Young boxes in eq. (III.3.12). n is the total number of $|+\rangle$ and $|-\rangle$, or the number of Young

boxes of the representation in which the state lives. The actions of the on-diagonal elements A and D on this state are

$$\begin{aligned} A(\mu)\,|\{\mu_k\};\Psi\rangle &= \prod_{k=1}^{n}(-i\coth(\mu-\mu_k))B_{a_1}(\mu_1)\cdots B_{a_n}(\mu_n)A(\mu)\,|\Omega\rangle\,\Psi^{a_1\cdots a_n} + (\text{others}) \\ &= (i\cosh(\mu))^L\prod_{k=1}^{n}(-i\coth(\mu-\mu_k))\,|\{\mu_k\};\Psi\rangle + (\text{others}) \end{aligned} \tag{III.C.10}$$

and

$$\begin{aligned} &D_{bb}(\mu)\,|\{\mu_k\};\Psi\rangle \\ &= i\coth(\mu-\mu_1)P^{c_1d_1}_{ba_1}B_{d_1}(\mu_1)D_{bc_1}(\mu)B_{a_2}(\mu_2)\cdots B_{a_n}(\mu_n)\,|\Omega\rangle\,\Psi^{a_1\cdots a_n} + (\text{others}) \\ &= \prod_{k=1}^{n}(\tilde{T}_n)^{\{d_k\}}_{\{a_k\}}(i\coth(\mu-\mu_k))B_{d_1}(\mu_1)B_{d_2}(\mu_2)\cdots B_{d_n}(\mu_n)D_{bc_n}(\mu)\,|\Omega\rangle\,\Psi^{a_1\cdots a_n} + (\text{others}), \end{aligned} \tag{III.C.11}$$

where $\tilde{T}_n$ is the shift operator

$$(\tilde{T}_n)^{\{d_k\}}_{\{a_k\}} = P^{c_1d_1}_{ba_1}P^{c_2d_2}_{c_1a_2}\cdots P^{c_{n-1}d_{n-1}}_{c_{n-2}a_{n-1}}P^{c_nd_n}_{c_{n-1}a_n}. \tag{III.C.12}$$

Note that we are interested in the action of the transfer matrix (i.e. $A+D_{11}+D_{22}$) after all, so we take the contraction over the index $b=1,2$ for the D matrix implicitly. The +(others) terms are off-diagonal parts wanted to be vanishing. The vanishing requirements lead to the constraints on μ, the so-called Bethe ansatz equations, which we will find soon later. Given that you take the sum over b and the only nonzero D_{ab} are for $a=b$ when acted on $|\Omega\rangle$, we can contract b and c_n in $\tilde{T}$. Hence, what we have is the product of the permutation matrices $P:\mathbb{C}^2\otimes\mathbb{C}^2\to\mathbb{C}^2\otimes\mathbb{C}^2$ with $w\otimes v\mapsto v\otimes w$[5]:

[5] $\tilde{t}$ is indeed the transfer matrix of the $SU(2)$ Heisenberg chain with zero spectral parameter. One may encounter more general cases where diagonalization of the $SU(2)$ transfer matrix with nonzero spectral parameter is required. It is why this method is called the nested Bethe ansatz; one needs to keep applying the Bethe ansatz method for the series of models with the smaller subgroup symmetries until it reaches to $SU(2)$.

$$\tilde{t}_n = P_{12}P_{23}\cdots P_{n-1n}. \tag{III.C.13}$$

So, if we take $\Psi^{a_1\cdots a_n}$ to be an eigenvector of $T^{\{d_k\}}_{\{a_k\}}$, $|\{\mu_k\};\Psi\rangle$ is an eigenvector of D_{bb} besides taking λ to be the solution of the Bethe ansatz equation to make the +(others) terms vanish. Since $\tilde{t}$ acts as a cyclic shift operator to the right (for example $|011\rangle \mapsto |101\rangle$ for $L = 3$), it is a root of the identity operator $\tilde{t}^n = I$. This fact implies that the eigenvalues $\tilde{\Lambda}$ of $\tilde{t}$ to be the roots of unity:

$$\tilde{\Lambda}_n^n = 1 \implies \tilde{\Lambda}_n = e^{i2\pi m/n} \text{ with } m = 0, 1, ..., n-1. \tag{III.C.14}$$

Plugging these eigenvalues back in eq. (III.C.11), we have the action of D to be

$$D_{bb}(\mu)\,|\{\mu_k\};\Psi\rangle = \prod_{k=1}^{n} \tilde{\Lambda}_n(i\coth(\mu-\mu_k))(\sinh(\mu))^L\,|\{\mu_k\};\Psi\rangle + (\text{others}). \tag{III.C.15}$$

We have the action of the transfer matrix on this state by summing the actions of the A and D matrices:

$$t(\mu)\,|\{\mu_k\},\Psi\rangle = \Lambda(\mu)\,|\{\mu_k\},\Psi\rangle + (\text{others}), \tag{III.C.16}$$

where

$$\Lambda(\mu) = \prod_{k=1}^{n}(i\coth(\mu-\mu_k))\left[(-1)^n(i\cosh(\mu))^L + \tilde{\Lambda}_n(\sinh(\mu))^L\right] \tag{III.C.17}$$

We need to require the +(others) terms to vanish so that $\Lambda(\mu)$ is the eigenvalue of the transfer matrix. This requirement is exactly the requirement of (III.C.16) to be analytic due to the analyticity of the transfer matrix. As mentioned, these constraints on the values of $\{\mu_k\}$ are the Bethe ansatz equations. The possible singularities of $\Lambda(\mu)$ are at $\mu = \mu_j$ for one of $j = 1, 2, ..., n$. Hence, the Bethe ansatz equations are

$$0 = \prod_{k\neq j}(i\coth(\mu_j - \mu_k))\left((-1)^n(i\cosh(\mu_j))^L + \tilde{\Lambda}_n(\sinh(\mu_j))^L\right). \tag{III.C.18}$$

The solutions of these equations are

$$\mu_j = i\,\mathrm{arccot}\left(e^{i\pi(2\ell_j+n-1-2m/n)/L}\right) \tag{III.C.19}$$

with some integer $\ell_j \in \{0, 1, ..., L-1\}$. The first $\prod_{k\neq j}(i\coth(\mu_j - \mu_k))$ factor diverges exponentially at $\mu_j = \mu_k$, so it prohibits multiple rapidities to coincide. The states $|\{\mu_k\}, \Psi\rangle$ become the eigenstates of the transfer matrix when $\{\mu_k\}$ are these solutions of the Bethe ansatz equations. In that case, the energy spectrum is

$$\begin{aligned} E_n &= i\frac{d}{d\mu}\log\left(\frac{\Lambda(\mu)}{(i\cosh\mu)^L}\right)\Bigg|_{\mu=0} \\ &= i\sum_{k=1}^{n}\mathrm{csch}(\mu_k)\,\mathrm{sech}(\mu_k) \\ &= \sum_{k=1}^{n} 2\cos\left(\frac{\pi(2\ell_k+n-1-2m/n)}{L}\right). \end{aligned} \tag{III.C.20}$$

And, the spectrum of the total momentum is

$$\begin{aligned} p_n &= i\log\left(\frac{\Lambda(\mu)}{(i\cosh\mu)^L}\right)\Bigg|_{\mu=0} \\ &= i\sum_{k=1}^{n}\log(i\coth(\mu_k)) \\ &= -\sum_{k=1}^{n}\frac{\pi(2\ell_k+n-1-2m/n)}{L}. \end{aligned} \tag{III.C.21}$$

The physical interpretation of the spectra is simple. The state generated by acting n of the B matrices contain n fermionic quasi-particle excitations with momentum of $p = -\frac{\pi(2\ell_j+n-1-2m/n)}{L}$ and energy of $E = 2\cos p$. The particles may not have degenerate values of momenta as required by the Bethe ansatz equations.

III.C.2 Ground state, dispersion relations, and finite size effect

From eq. (III.C.20), the ground state has exactly half of L, $n = L/2$ fermionic excitations filling up to the fermi surface with zero energy. Each fermion has the mode energy of $\epsilon_k = -2\sin\left(\frac{\pi(2\ell_k - 1 + 4m/L)}{L}\right)$. With $n = L/2$, the fermions fill in the region between $\ell_F \approx 0$ and $\approx L/2$. To be more precise, the ground-state energy is minimized with $m = 0$ and the fermions fill from $\ell_1 = 1$ to $\ell_n = L/2$. One can take the sum of these mode energies explicitly as

$$E_0 = \sum_{k=1}^{L/2} -2\sin\left(\frac{\pi(2k-1)}{L}\right) = -2\csc\left(\frac{\pi}{L}\right). \tag{III.C.22}$$

The first excited state has one hole in the fermi sea right below the surface and/or one fermion right above the surface. This is massless in the thermodynamic limit given that one can make them arbitrarily close to the surface. The existence of the massless states suggests that the model has the CFT as its low-energy description. The central charge of the theory can be found by calculating the finite-size effect of the ground state. The CFT calculation expects that the ground-state energy has size dependence as

$$E_0 = \epsilon_0 L - \frac{\pi v_F c}{6L} + \mathcal{O}(1/L^2). \tag{III.C.23}$$

Here, v_F is the fermi speed of the excitations. The energy gap above the ground state is $2\sin\left(\frac{2\pi\ell_k}{L}\right)$, so the excitation around the fermi surface indeed has, as expected from the masslessness, the linear dispersion relation $\sim 2|p - p_F|$, with which the fermi speed is determined to be $v_F = 2$. The expansion of eq. (III.C.22) about $1/L$ up to the second-leading order gives the finite size effect to be of

$$E_0 = -\frac{2}{\pi}L - \frac{\pi}{3L} + \mathcal{O}\left(1/L^2\right). \tag{III.C.24}$$

One can read from this finite-size ground state energy that the central charge of the corresponding CFT is $c = 1$.

Once we recover the overall coupling factor $-1/2\lambda$, the fermi speed is determined to be $v_F = 1/\lambda$. This matches exactly with the dispersion relation of the first-order spin chain for the two-letter string case as calculated in Sec. III.B.

Chapter IV: Conclusion

In this thesis, we have demonstrated the integrability structures that emerge in large-N gauge theories. It is remarkable that the aspects of higher-dimensional theories can be studied from the insights of integrable dynamics of two-dimensional systems. We can interpret the integrability as arising from the string-theoretic structure of gauge theory, which becomes apparent in the large-N limit. The simplifications from maximal supersymmetry or lattice regularization further allowed rigorous derivation of these structures. The integrable spin chains emerging from the weak-coupling expansion of $\mathcal{N} = 4$ SYM can be utilized to classify integrable defects as boundary states. Superconformal symmetry allows us to study various physical quantities involving the defects. It includes correlation functions in a defect background using superconformal block expansion and Ward identities, as we demonstrated. These computational tools are expected to be usable for relating various aspects of the defects with their (non-)integrability. Since the defects in general correspond to D-brane bound states, the analysis of defects using computational tools for integrable systems may give predictions in string theory, and vice versa. We also discussed the translation of the dynamics of confining strings in lattice gauge theory into spin chains. These spin chains happen to be integrable when the unitarity constraint is negligible. The violation of integrability due to the unitarity constraint matches with expectation since the constraint is one of the major distinctions of the confining string theory from the ordinary Nambu-Goto theory.

As an optimistic outlook, the integrability test of D-brane configurations can even-

tually lead to hint the string theory dual of the pure Yang-Mills theory or, moreover, real-world QCD. The AdS/QCD program [112] particularly addresses this problem by exploring various D-brane configurations that provide geometrical explanations for phenomena in QCD, such as chiral symmetry breaking [150]. If one can identify the specific D-brane configurations that exhibit breaking of integrability in a similar manner as the unitarity constraint, then it could be an indication of the precise string theory dual of pure Yang-Mills.

Even without the realization of such a precise duality, exploring the correspondence between gauge theory and string theory is expected to ultimately provide a geometrical understanding of confinement in gauge theory, just as it did for the thermal $\mathcal{N} = 4$ SYM case for which Witten [159] showed that the confinement/deconfinement transition corresponds to the Hawking-Page transition. Integrability would play a crucial role for refining it by providing tools for exact computations. Furthermore, the characteristics of its breaking would indicate possible modifications from the Nambu-Goto or Green-Schwarz strings.

Bibliography

[1] Gerard 't Hooft. "A Planar Diagram Theory for Strong Interactions". In: *Nucl. Phys. B* 72 (1974). Ed. by J. C. Taylor, p. 461. DOI: 10.1016/0550-3213(74)90154-0.

[2] Georges Aad et al. "Observation of a new particle in the search for the Standard Model Higgs boson with the ATLAS detector at the LHC". In: *Phys. Lett. B* 716 (2012), pp. 1–29. DOI: 10.1016/j.physletb.2012.08.020. arXiv: 1207.7214 [hep-ex].

[3] Ofer Aharony, Donald Marolf, and Mukund Rangamani. "Conformal field theories in anti-de Sitter space". In: *JHEP* 02 (2011), p. 041. DOI: 10.1007/JHEP02(2011)041. arXiv: 1011.6144 [hep-th].

[4] Ofer Aharony et al. "N=6 superconformal Chern-Simons-matter theories, M2-branes and their gravity duals". In: *JHEP* 10 (2008), p. 091. DOI: 10.1088/1126-6708/2008/10/091. arXiv: 0806.1218 [hep-th].

[5] Changrim Ahn and Matthias Staudacher. "The Integrable (Hyper)eclectic Spin Chain". In: *JHEP* 02 (2021), p. 019. DOI: 10.1007/JHEP02(2021)019. arXiv: 2010.14515 [hep-th].

[6] Francisco C. Alcaraz, Roland Koberle, and A. Lima-Santos. "All exactly solvable quantum spin 1 chains from Hecke algebra". In: *Int. J. Mod. Phys. A* 7 (1992), pp. 7615–7628. DOI: 10.1142/S0217751X92003458.

[7] Francisco C. Alcaraz et al. “Reaction - diffusion processes, critical dynamics and quantum chains”. In: *Annals Phys.* 230 (1994), pp. 250–302. DOI: 10.1006/aphy.1994.1026. arXiv: hep-th/9302112.

[8] Jan Ambjorn et al. “Fermionization of the spin S Uimin-Lai-Sutherland model: Generalization of supersymmetric t - J model to spin S”. In: *Nucl. Phys. B* 599 (2001), pp. 547–560. DOI: 10.1016/S0550-3213(00)00757-4. arXiv: cond-mat/9909432.

[9] Aaron J. Amsel and Donald Marolf. “Supersymmetric Multi-trace Boundary Conditions in AdS”. In: *Class. Quant. Grav.* 26 (2009), p. 025010. DOI: 10.1088/0264-9381/26/2/025010. arXiv: 0808.2184 [hep-th].

[10] V. I. Arnold. *Mathematical Methods of Classical Mechanics*. Graduate Texts in Mathematics. New York: Springer-Verlag, 1978. ISBN: 978-1-4757-1693-1. DOI: 10.1007/978-1-4757-1693-1. URL: https://www.springer.com/gp/book/9781475716931.

[11] Jonah Baerman, Adam Chalabi, and Charlotte Kristjansen. “Superconformal two-point functions of the Nahm pole defect in N=4 super-Yang-Mills theory”. In: *Phys. Lett. B* 853 (2024), p. 138642. DOI: 10.1016/j.physletb.2024.138642. arXiv: 2401.13749 [hep-th].

[12] Marco Baggio, Jan de Boer, and Kyriakos Papadodimas. “A non-renormalization theorem for chiral primary 3-point functions”. In: *JHEP* 07 (2012), p. 137. DOI: 10.1007/JHEP07(2012)137. arXiv: 1203.1036 [hep-th].

[13] Dongsu Bak and Soo-Jong Rey. “Integrable Spin Chain in Superconformal Chern-Simons Theory”. In: *JHEP* 10 (2008), p. 053. DOI: 10.1088/1126-6708/2008/10/053. arXiv: 0807.2063 [hep-th].

[14] Tom Banks et al. "M theory as a matrix model: A conjecture". In: *Phys. Rev. D* 55 (1997), pp. 5112–5128. DOI: 10.1201/9781482268737-37. arXiv: hep-th/9610043.

[15] Benjamin Basso, Shota Komatsu, and Pedro Vieira. "Structure Constants and Integrable Bootstrap in Planar N=4 SYM Theory". In: (May 2015). arXiv: 1505.06745 [hep-th].

[16] Christian W. Bauer et al. "Quantum Simulation for High-Energy Physics". In: *PRX Quantum* 4.2 (2023), p. 027001. DOI: 10.1103/PRXQuantum.4.027001. arXiv: 2204.03381 [quant-ph].

[17] B. B. Beard et al. "D-theory: Field theory via dimensional reduction of discrete variables". In: *Nucl. Phys. B Proc. Suppl.* 63 (1998). Ed. by C. T. H. Davies et al., pp. 775–789. DOI: 10.1016/S0920-5632(97)00900-6. arXiv: hep-lat/9709120.

[18] Christopher Beem et al. "Infinite Chiral Symmetry in Four Dimensions". In: *Commun. Math. Phys.* 336.3 (2015), pp. 1359–1433. DOI: 10.1007/s00220-014-2272-x. arXiv: 1312.5344 [hep-th].

[19] Niklas Beisert et al. "Review of AdS/CFT Integrability: An Overview". In: *Lett. Math. Phys.* 99 (2012), pp. 3–32. DOI: 10.1007/s11005-011-0529-2. arXiv: 1012.3982 [hep-th].

[20] Niklas Beisert. "The Analytic Bethe Ansatz for a Chain with Centrally Extended su(2|2) Symmetry". In: *J. Stat. Mech.* 0701 (2007), P01017. DOI: 10.1088/1742-5468/2007/01/P01017. arXiv: nlin/0610017.

[21] Niklas Beisert. "The complete one loop dilatation operator of N=4 superYang-Mills theory". In: *Nucl. Phys. B* 676 (2004), pp. 3–42. DOI: 10.1016/j.nuclphysb.2003.10.019. arXiv: hep-th/0307015.

[22] Niklas Beisert and Matthias Staudacher. "Long-range psu(2,2|4) Bethe Ansatze for gauge theory and strings". In: *Nucl. Phys. B* 727 (2005), pp. 1–62. DOI: 10.1016/j.nuclphysb.2005.06.038. arXiv: hep-th/0504190.

[23] Iosif Bena, Joseph Polchinski, and Radu Roiban. "Hidden Symmetries of the $AdS_5 \times S^5$ Superstring". In: *Phys. Rev. D* 69 (2004), p. 046002. DOI: 10.1103/PhysRevD.69.046002. arXiv: hep-th/0305116.

[24] David Berenstein. "On the central charge extension of the $\mathcal{N} = 4$ SYM spin chain". In: *JHEP* 05 (2015), p. 129. DOI: 10.1007/JHEP05(2015)129. arXiv: 1411.5921 [hep-th].

[25] David Berenstein and Sergey A. Cherkis. "Deformations of N=4 SYM and integrable spin chain models". In: *Nucl. Phys. B* 702 (2004), pp. 49–85. DOI: 10.1016/j.nuclphysb.2004.09.005. arXiv: hep-th/0405215.

[26] David Berenstein, Diego H. Correa, and Samuel E. Vazquez. "A Study of open strings ending on giant gravitons, spin chains and integrability". In: *JHEP* 09 (2006), p. 065. DOI: 10.1088/1126-6708/2006/09/065. arXiv: hep-th/0604123.

[27] David Berenstein, Diego H. Correa, and Samuel E. Vazquez. "Quantizing open spin chains with variable length: An Example from giant gravitons". In: *Phys. Rev. Lett.* 95 (2005), p. 191601. DOI: 10.1103/PhysRevLett.95.191601. arXiv: hep-th/0502172.

[28] David Berenstein and Hiroki Kawai. "Integrable Spin Chains from large-N QCD at strong coupling". In: (Aug. 2023). arXiv: 2308.11716 [hep-th].

[29] David Berenstein and Hiroki Kawai. "Spin Chains from large-N QCD at strong coupling". In: (Mar. 2026). arXiv: 2603.04506 [hep-th].

[30] David Berenstein, Hiroki Kawai, and Richard Brower. "U(1) fields from qubits: An approach via D-theory algebra". In: *Phys. Rev. D* 110.1 (2024), p. 014506. DOI: 10.1103/PhysRevD.110.014506. arXiv: 2201.02412 [hep-th].

[31] David Berenstein and Samuel E. Vazquez. "Integrable open spin chains from giant gravitons". In: *JHEP* 06 (2005), p. 059. DOI: 10.1088/1126-6708/2005/06/059. arXiv: hep-th/0501078.

[32] David Eliecer Berenstein, Juan Martin Maldacena, and Horatiu Stefan Nastase. "Strings in flat space and pp waves from N=4 superYang-Mills". In: *JHEP* 04 (2002), p. 013. DOI: 10.1088/1126-6708/2002/04/013. arXiv: hep-th/0202021.

[33] Lorenzo Bianchi and Madalena Lemos. "Superconformal surfaces in four dimensions". In: *JHEP* 06 (2020), p. 056. DOI: 10.1007/JHEP06(2020)056. arXiv: 1911.05082 [hep-th].

[34] Marco Billò et al. "Defects in conformal field theory". In: *JHEP* 04 (2016), p. 091. DOI: 10.1007/JHEP04(2016)091. arXiv: 1601.02883 [hep-th].

[35] Lars Brink, Olof Lindgren, and Bengt E. W. Nilsson. "The Ultraviolet Finiteness of the N=4 Yang-Mills Theory". In: *Phys. Lett. B* 123 (1983), pp. 323–328. DOI: 10.1016/0370-2693(83)91210-8.

[36] R. Brower, S. Chandrasekharan, and U. J. Wiese. "QCD as a quantum link model". In: *Phys. Rev. D* 60 (1999), p. 094502. DOI: 10.1103/PhysRevD.60.094502. arXiv: hep-th/9704106.

[37] R. Brower et al. "D theory: Field quantization by dimensional reduction of discrete variables". In: *Nucl. Phys. B* 693 (2004), pp. 149–175. DOI: 10.1016/j.nuclphysb.2004.06.007. arXiv: hep-lat/0309182.

[38] Richard C. Brower, David Berenstein, and Hiroki Kawai. "Lattice Gauge Theory for a Quantum Computer". In: *PoS* LATTICE2019 (2020), p. 112. DOI: 10.22323/1.363.0112. arXiv: 2002.10028 [hep-lat].

[39] Isak Buhl-Mortensen et al. "A Quantum Check of AdS/dCFT". In: *JHEP* 01 (2017), p. 098. DOI: 10.1007/JHEP01(2017)098. arXiv: 1611.04603 [hep-th].

[40] Isak Buhl-Mortensen et al. "One-point Functions in AdS/dCFT from Matrix Product States". In: *JHEP* 02 (2016), p. 052. DOI: 10.1007/JHEP02(2016)052. arXiv: 1512.02532 [hep-th].

[41] Tim Byrnes and Yoshihisa Yamamoto. "Simulating lattice gauge theories on a quantum computer". In: *Phys. Rev. A* 73 (2006), p. 022328. DOI: 10.1103/PhysRevA.73.022328. arXiv: quant-ph/0510027.

[42] Joao Caetano and Shota Komatsu. "Crosscap States in Integrable Field Theories and Spin Chains". In: *J. Statist. Phys.* 187.3 (2022), p. 30. DOI: 10.1007/s10955-022-02914-6. arXiv: 2111.09901 [hep-th].

[43] Pawel Caputa, Charlotte Kristjansen, and Konstantinos Zoubos. "On the spectral problem of N=4 SYM with orthogonal or symplectic gauge group". In: *JHEP* 10 (2010), p. 082. DOI: 10.1007/JHEP10(2010)082. arXiv: 1005.2611 [hep-th].

[44] Adam Chalabi, Charlotte Kristjansen, and Chenliang Su. "Integrable corners in the space of Gukov-Witten surface defects". In: *Phys. Lett. B* 866 (2025), p. 139512. DOI: 10.1016/j.physletb.2025.139512. arXiv: 2503.22598 [hep-th].

[45] S. Chandrasekharan and U. J. Wiese. "Quantum link models: A Discrete approach to gauge theories". In: *Nucl. Phys. B* 492 (1997), pp. 455–474. DOI: 10.1016/S0550-3213(97)00006-0. arXiv: hep-lat/9609042.

[46] Serguei Chatrchyan et al. "Observation of a New Boson at a Mass of 125 GeV with the CMS Experiment at the LHC". In: *Phys. Lett. B* 716 (2012), pp. 30–61. DOI: 10.1016/j.physletb.2012.08.021. arXiv: 1207.7235 [hep-ex].

[47] Bin Chen, Xiao-Jun Wang, and Yong-Shi Wu. "Integrable open spin chain in superYang-Mills and the plane wave / SYM duality". In: *JHEP* 02 (2004), p. 029. DOI: 10.1088/1126-6708/2004/02/029. arXiv: hep-th/0401016.

[48] Changha Choi, Jaume Gomis, and Raquel Izquierdo García. "Surface Operators and Exact Holography". In: (June 2024). arXiv: 2406.08541 [hep-th].

[49] Anthony N. Ciavarella and Christian W. Bauer. "Quantum Simulation of SU(3) Lattice Yang-Mills Theory at Leading Order in Large-Nc Expansion". In: *Phys. Rev. Lett.* 133.11 (2024), p. 111901. DOI: 10.1103/PhysRevLett.133.111901. arXiv: 2402.10265 [hep-ph].

[50] Anthony N. Ciavarella, Ivan M. Burbano, and Christian W. Bauer. "Efficient truncations of SU(Nc) lattice gauge theory for quantum simulation". In: *Phys. Rev. D* 112.5 (2025), p. 054514. DOI: 10.1103/ylqb-phv5. arXiv: 2503.11888 [hep-lat].

[51] Steve Corley, Antal Jevicki, and Sanjaye Ramgoolam. "Exact correlators of giant gravitons from dual N=4 SYM theory". In: *Adv. Theor. Math. Phys.* 5 (2002), pp. 809–839. DOI: 10.4310/ATMP.2001.v5.n4.a6. arXiv: hep-th/0111222.

[52] D. H. Correa and C. A. S. Young. "Reflecting magnons from D7 and D5 branes". In: *J. Phys. A* 41 (2008), p. 455401. DOI: 10.1088/1751-8113/41/45/455401. arXiv: 0808.0452 [hep-th].

[53] Diego H. Correa, Vidas Regelskis, and Charles A. S. Young. "Integrable achiral D5-brane reflections and asymptotic Bethe equations". In: *J. Phys. A* 44 (2011), p. 325403. DOI: 10.1088/1751-8113/44/32/325403. arXiv: 1105.3707 [hep-th].

[54] Marius De Leeuw, Charlotte Kristjansen, and Georgios Linardopoulos. "Scalar one-point functions and matrix product states of AdS/dCFT". In: *Phys. Lett. B* 781 (2018), pp. 238–243. DOI: 10.1016/j.physletb.2018.03.083. arXiv: 1802.01598 [hep-th].

[55] Marius De Leeuw et al. "Spin Chain Overlaps and the Twisted Yangian". In: *JHEP* 01 (2020), p. 176. DOI: 10.1007/JHEP01(2020)176. arXiv: 1912.09338 [hep-th].

[56] Amit Dekel and Yaron Oz. "Integrability of Green-Schwarz Sigma Models with Boundaries". In: *JHEP* 08 (2011), p. 004. DOI: 10.1007/JHEP08(2011)004. arXiv: 1106.3446 [hep-th].

[57] Oliver DeWolfe and Nelia Mann. "Integrable open spin chains in defect conformal field theory". In: *JHEP* 04 (2004), p. 035. DOI: 10.1088/1126-6708/2004/04/035. arXiv: hep-th/0401041.

[58] Francesco Di Marcantonio et al. "Roughening and dynamics of an electric flux string in a (2+1)D lattice gauge theory". In: (May 2025). arXiv: 2505.23853 [hep-lat].

[59] Francis A. Dolan, Laurent Gallot, and Emery Sokatchev. "On four-point functions of 1/2-BPS operators in general dimensions". In: *JHEP* 09 (2004), p. 056. DOI: 10.1088/1126-6708/2004/09/056. arXiv: hep-th/0405180.

[60] Reza Doobary and Paul Heslop. "Superconformal partial waves in Grassmannian field theories". In: *JHEP* 12 (2015), p. 159. DOI: 10.1007/JHEP12(2015)159. arXiv: 1508.03611 [hep-th].

[61] Nadav Drukker, Jaume Gomis, and Shunji Matsuura. "Probing N=4 SYM With Surface Operators". In: *JHEP* 10 (2008), p. 048. DOI: 10.1088/1126-6708/2008/10/048. arXiv: 0805.4199 [hep-th].

[62] Sergei Dubovsky. "The QCD β-function On The String Worldsheet". In: *Phys. Rev. D* 98.11 (2018), p. 114025. DOI: 10.1103/PhysRevD.98.114025. arXiv: 1807.00254 [hep-th].

[63] Sergei Dubovsky and Victor Gorbenko. "Towards a Theory of the QCD String". In: *JHEP* 02 (2016), p. 022. DOI: 10.1007/JHEP02(2016)022. arXiv: 1511.01908 [hep-th].

[64] Guido Festuccia and Nathan Seiberg. "Rigid Supersymmetric Theories in Curved Superspace". In: *JHEP* 06 (2011), p. 114. DOI: 10.1007/JHEP06(2011)114. arXiv: 1105.0689 [hep-th].

[65] Abhijit Gadde and Sergei Gukov. "2d Index and Surface operators". In: *JHEP* 03 (2014), p. 080. DOI: 10.1007/JHEP03(2014)080. arXiv: 1305.0266 [hep-th].

[66] Davide Gaiotto, Sergei Gukov, and Nathan Seiberg. "Surface Defects and Resolvents". In: *JHEP* 09 (2013), p. 070. DOI: 10.1007/JHEP09(2013)070. arXiv: 1307.2578 [hep-th].

[67] Murray Gell-Mann. "A Schematic Model of Baryons and Mesons". In: *Phys. Lett.* 8 (1964), pp. 214–215. DOI: 10.1016/S0031-9163(64)92001-3.

[68] Subir Ghoshal and Alexander B. Zamolodchikov. "Boundary S matrix and boundary state in two-dimensional integrable quantum field theory". In: *Int. J. Mod. Phys. A* 9 (1994). [Erratum: Int.J.Mod.Phys.A 9, 4353 (1994)], pp. 3841–3886. DOI: 10.1142/S0217751X94001552. arXiv: hep-th/9306002.

[69] Aleix Gimenez Grau et al. "A Quantum Check of Non-Supersymmetric AdS/dCFT". In: *JHEP* 01 (2019), p. 007. DOI: 10.1007/JHEP01(2019)007. arXiv: 1810.11463 [hep-th].

[70] Aleix Gimenez-Grau et al. "A quantum framework for AdS/dCFT through fuzzy spherical harmonics on S^4". In: *JHEP* 04 (2020), p. 132. DOI: 10.1007/JHEP04(2020)132. arXiv: 1912.02468 [hep-th].

[71] Simone Giombi and Shota Komatsu. "More Exact Results in the Wilson Loop Defect CFT: Bulk-Defect OPE, Nonplanar Corrections and Quantum Spectral Curve". In: *J. Phys. A* 52.12 (2019), p. 125401. DOI: 10.1088/1751-8121/ab046c. arXiv: 1811.02369 [hep-th].

[72] S. L. Glashow. "Partial Symmetries of Weak Interactions". In: *Nucl. Phys.* 22 (1961), pp. 579–588. DOI: 10.1016/0029-5582(61)90469-2.

[73] F. Gliozzi, Joel Scherk, and David I. Olive. "Supersymmetry, Supergravity Theories and the Dual Spinor Model". In: *Nucl. Phys. B* 122 (1977), pp. 253–290. DOI: 10.1016/0550-3213(77)90206-1.

[74] Tamas Gombor. "Exact overlaps for "all" integrable matrix product states of rational spin chains". In: (Oct. 2024). arXiv: 2410.23282 [hep-th].

[75] Tamás Gombor and Balázs Pozsgay. "On factorized overlaps: Algebraic Bethe Ansatz, twists, and Separation of Variables". In: *Nucl. Phys. B* 967 (2021), p. 115390. DOI: 10.1016/j.nuclphysb.2021.115390. arXiv: 2101.10354 [cond-mat.stat-mech].

[76] Cesar Gomez and German Sierra. "New integrable deformations of higher spin Heisenberg-Ising chains". In: *Phys. Lett. B* 285 (1992), pp. 126–132. DOI: 10.1016/0370-2693(92)91310-6. arXiv: hep-th/9203035.

[77] Jaume Gomis and Shunji Matsuura. "Bubbling surface operators and S-duality". In: *JHEP* 06 (2007), p. 025. DOI: 10.1088/1126-6708/2007/06/025. arXiv: 0704.1657 [hep-th].

[78] D. J. Gross and Frank Wilczek. "Asymptotically Free Gauge Theories - I". In: *Phys. Rev. D* 8 (1973), pp. 3633–3652. DOI: 10.1103/PhysRevD.8.3633.

[79] D. J. Gross and Frank Wilczek. "ASYMPTOTICALLY FREE GAUGE THEORIES. 2." In: *Phys. Rev. D* 9 (1974), pp. 980–993. DOI: 10.1103/PhysRevD.9.980.

[80] David J. Gross and Washington Taylor. "Two-dimensional QCD is a string theory". In: *Nucl. Phys. B* 400 (1993), pp. 181–208. DOI: 10.1016/0550-3213(93)90403-C. arXiv: hep-th/9301068.

[81] David J. Gross and Frank Wilczek. "Ultraviolet Behavior of Nonabelian Gauge Theories". In: *Phys. Rev. Lett.* 30 (1973). Ed. by J. C. Taylor, pp. 1343–1346. DOI: 10.1103/PhysRevLett.30.1343.

[82] Sergei Gukov and Edward Witten. "Gauge Theory, Ramification, And The Geometric Langlands Program". In: (Dec. 2006). arXiv: hep-th/0612073.

[83] Sergei Gukov and Edward Witten. "Rigid Surface Operators". In: *Adv. Theor. Math. Phys.* 14.1 (2010), pp. 87–178. DOI: 10.4310/ATMP.2010.v14.n1.a3. arXiv: 0804.1561 [hep-th].

[84] Anna Hasenfratz, Etelka Hasenfratz, and Peter Hasenfratz. "Generalized Roughening Transition and Its Effect on the String Tension". In: *Nucl. Phys. B* 180 (1981), pp. 353–367. DOI: 10.1016/0550-3213(81)90426-0.

[85] Tomoya Hayata and Yoshimasa Hidaka. "q deformed formulation of Hamiltonian SU(3) Yang-Mills theory". In: *JHEP* 09 (2023), p. 123. DOI: 10.1007/JHEP09(2023)123. arXiv: 2306.12324 [hep-lat].

[86] Diego M. Hofman and Juan Martin Maldacena. "Reflecting magnons". In: *JHEP* 11 (2007), p. 063. DOI: 10.1088/1126-6708/2007/11/063. arXiv: 0708.2272 [hep-th].

[87] Adolfo Holguin and Hiroki Kawai. "Integrability and conformal blocks for surface defects in $\mathcal{N} = 4$ SYM". In: *JHEP* 11 (2025), p. 043. DOI: 10.1007/JHEP11(2025)043. arXiv: 2503.09944 [hep-th].

[88] Asger C. Ipsen, Matthias Staudacher, and Leonard Zippelius. "The one-loop spectral problem of strongly twisted $\mathcal{N} = 4$ Super Yang-Mills theory". In: *JHEP* 04 (2019), p. 044. DOI: 10.1007/JHEP04(2019)044. arXiv: 1812.08794 [hep-th].

[89] Nabil Iqbal and Hong Liu. "Real-time response in AdS/CFT with application to spinors". In: *Fortsch. Phys.* 57 (2009). Ed. by Dieter Lust and Vladimir Dobrev, pp. 367–384. DOI: 10.1002/prop.200900057. arXiv: 0903.2596 [hep-th].

[90] Chigak Itoi and Masa-Hide Kato. "Extended massless phase and the Haldane phase in a spin-1 isotropic antiferromagnetic chain". In: *Phys. Rev. B* 55 (13 Apr. 1997), pp. 8295–8303. DOI: 10.1103/PhysRevB.55.8295. URL: https://link.aps.org/doi/10.1103/PhysRevB.55.8295.

[91] C. Itzykson, Michael E. Peskin, and Jean-Bernard Zuber. "Roughening of Wilson's Surface". In: *Phys. Lett. B* 95 (1980), pp. 259–264. DOI: 10.1016/0370-2693(80)90483-9.

[92] Vyacheslav Ivanovskiy et al. "Vacuum Condensates on the Coulomb Branch". In: (May 2024). arXiv: 2405.19043 [hep-th].

[93] Yunfeng Jiang, Shota Komatsu, and Edoardo Vescovi. "Structure constants in $\mathcal{N}$ = 4 SYM at finite coupling as worldsheet g-function". In: *JHEP* 07.07 (2020), p. 037. DOI: 10.1007/JHEP07(2020)037. arXiv: 1906.07733 [hep-th].

[94] Yunfeng Jiang, Jun-Bao Wu, and Peihe Yang. "Wilson-loop one-point functions in ABJM theory". In: *JHEP* 09 (2023), p. 047. DOI: 10.1007/JHEP09(2023)047. arXiv: 2306.05773 [hep-th].

[95] K. Jimmy Juge, Julius Kuti, and Colin Morningstar. "From Surface Roughening to QCD String Theory". In: *24th Johns Hopkins Workshop on Nonperturbative QFT Methods and Their Applications*. Mar. 2001, pp. 143–165. DOI: 10.1142/9789812799968_0006. arXiv: hep-lat/0103008.

[96] K. Jimmy Juge, Julius Kuti, and Colin J. Morningstar. "The QCD String Spectrum and Conformal Field Theory". In: *Nucl. Phys. B Proc. Suppl.* 106 (2002). Ed. by M. Muller-Preussker et al., pp. 691–693. DOI: 10.1016/S0920-5632(01)01818-7. arXiv: hep-lat/0110157.

[97] Saurabh V. Kadam, Indrakshi Raychowdhury, and Jesse R. Stryker. "Loop-string-hadron formulation of an SU(3) gauge theory with dynamical quarks". In: *Phys. Rev. D* 107.9 (2023), p. 094513. DOI: 10.1103/PhysRevD.107.094513. arXiv: 2212.04490 [hep-lat].

[98] Angus Kan and Yunseong Nam. "Lattice Quantum Chromodynamics and Electrodynamics on a Universal Quantum Computer". In: (July 2021). arXiv: 2107.12769 [quant-ph].

[99] Hosho Katsura. *Private communication*. 2023.

[100] H. Kawai et al. "VAE/WGAN-Based Image Representation Learning For Pose-Preserving Seamless Identity Replacement In Facial Images". In: (2019), pp. 1–6.

[101] Hiroki Kawai and Yuya O. Nakagawa. "Predicting excited states from ground state wavefunction by supervised quantum machine learning". In: *Machine Learning: Science and Technology* (2020). URL: http://iopscience.iop.org/10.1088/2632-2153/aba183.

[102] Teruhiko Kawano and Kazumi Okuyama. "Spinor exchange in AdS(d+1)". In: *Nucl. Phys. B* 565 (2000), pp. 427–444. DOI: 10.1016/S0550-3213(99)00639-2. arXiv: hep-th/9905130.

[103] A. Klümper. "Free energy and correlation lengths of quantum chains related to restricted solid-on-solid lattice models". In: *Annalen der Physik* 504.7 (Jan. 1992), pp. 540–553. DOI: 10.1002/andp.19925040707.

[104] Andreas Klümper. "Thermodynamics of the anisotropic spin-1/2 Heisenberg chain and related quantum chains". In: *Zeitschrift fur Physik B Condensed Matter* 91.4 (Dec. 1993), pp. 507–519. DOI: 10.1007/BF01316831. arXiv: cond-mat/9306019 [cond-mat].

[105] J. B. Kogut et al. "Fluctuating string of lattice gauge theory: The heavy-quark potential, the restoration of rotational symmetry, and roughening". In: *Phys. Rev. D* 23 (12 June 1981), pp. 2945–2961. DOI: 10.1103/PhysRevD.23.2945. URL: https://link.aps.org/doi/10.1103/PhysRevD.23.2945.

[106] John B. Kogut and Leonard Susskind. "Hamiltonian Formulation of Wilson's Lattice Gauge Theories". In: *Phys. Rev. D* 11 (1975), pp. 395–408. DOI: 10.1103/PhysRevD.11.395.

[107] Charlotte Kristjansen, Dennis Müller, and Konstantin Zarembo. "Integrable boundary states in D3-D5 dCFT: beyond scalars". In: *JHEP* 08 (2020), p. 103. DOI: 10.1007/JHEP08(2020)103. arXiv: 2005.01392 [hep-th].

[108] Charlotte Kristjansen, Dinh-Long Vu, and Konstantin Zarembo. "Integrable domain walls in ABJM theory". In: *JHEP* 02 (2022), p. 070. DOI: 10.1007/JHEP02(2022)070. arXiv: 2112.10438 [hep-th].

[109] Charlotte Kristjansen and Konstantin Zarembo. "'t Hooft loops and integrability". In: *JHEP* 08 (2023), p. 184. DOI: 10.1007/JHEP08(2023)184. arXiv: 2305.03649 [hep-th].

[110] Charlotte Kristjansen and Konstantin Zarembo. "'t Hooft loops in N=4 super-Yang-Mills". In: *JHEP* 02 (2025), p. 179. DOI: 10.1007/JHEP02(2025)179. arXiv: 2412.01972 [hep-th].

[111] Charlotte Kristjansen and Konstantin Zarembo. "Integrable Holographic Defect CFTs". In: Jan. 2024. arXiv: 2401.17144 [hep-th].

[112] Martin Kruczenski et al. "Towards a holographic dual of large N(c) QCD". In: *JHEP* 05 (2004), p. 041. DOI: 10.1088/1126-6708/2004/05/041. arXiv: hep-th/0311270.

[113] Henry Lamm, Scott Lawrence, and Yukari Yamauchi. "General Methods for Digital Quantum Simulation of Gauge Theories". In: *Phys. Rev. D* 100.3 (2019), p. 034518. DOI: 10.1103/PhysRevD.100.034518. arXiv: 1903.08807 [hep-lat].

[114] Marius de Leeuw and Adolfo Holguin. "Integrable Conformal Defects in N=4 SYM". In: (June 2024). arXiv: 2406.13741 [hep-th].

[115] Marius de Leeuw, Charlotte Kristjansen, and Georgios Linardopoulos. "One-point functions of non-protected operators in the SO(5) symmetric D3–D7 dCFT". In: *J. Phys. A* 50.25 (2017), p. 254001. DOI: 10.1088/1751-8121/aa714b. arXiv: 1612.06236 [hep-th].

[116] Marius de Leeuw, Charlotte Kristjansen, and Konstantin Zarembo. "One-point Functions in Defect CFT and Integrability". In: *JHEP* 08 (2015), p. 098. DOI: 10.1007/JHEP08(2015)098. arXiv: 1506.06958 [hep-th].

[117] Marius de Leeuw et al. "Two-point functions in AdS/dCFT and the boundary conformal bootstrap equations". In: *JHEP* 08 (2017), p. 020. DOI: 10.1007/JHEP08(2017)020. arXiv: 1705.03898 [hep-th].

[118] Pedro Liendo, Yannick Linke, and Volker Schomerus. "A Lorentzian inversion formula for defect CFT". In: *JHEP* 08 (2020), p. 163. DOI: 10.1007/JHEP08(2020)163. arXiv: 1903.05222 [hep-th].

[119] Pedro Liendo and Carlo Meneghelli. "Bootstrap equations for $\mathcal{N} = 4$ SYM with defects". In: *JHEP* 01 (2017), p. 122. DOI: 10.1007/JHEP01(2017)122. arXiv: 1608.05126 [hep-th].

[120] Pedro Liendo, Carlo Meneghelli, and Vladimir Mitev. "On Correlation Functions of BPS Operators in 3d $\mathcal{N} = 6$ Superconformal Theories". In: *Commun. Math. Phys.* 350.1 (2017), pp. 387–419. DOI: 10.1007/s00220-016-2715-7. arXiv: 1512.06072 [hep-th].

[121] Hai Lin, Oleg Lunin, and Juan Martin Maldacena. "Bubbling AdS space and 1/2 BPS geometries". In: *JHEP* 10 (2004), p. 025. DOI: 10.1088/1126-6708/2004/10/025. arXiv: hep-th/0409174.

[122] Georgios Linardopoulos. "String theory methods for defect CFTs". In: (Jan. 2025). arXiv: 2501.11985 [hep-th].

[123] Georgios Linardopoulos and Konstantin Zarembo. "String integrability of defect CFT and dynamical reflection matrices". In: *JHEP* 05 (2021), p. 203. DOI: 10.1007/JHEP05(2021)203. arXiv: 2102.12381 [hep-th].

[124] M. Luscher. "Symmetry Breaking Aspects of the Roughening Transition in Gauge Theories". In: *Nucl. Phys. B* 180 (1981), pp. 317–329. DOI: 10.1016/0550-3213(81)90423-5.

[125] M. Luscher, G. Munster, and P. Weisz. "How Thick Are Chromoelectric Flux Tubes?" In: *Nucl. Phys. B* 180 (1981), pp. 1–12. DOI: 10.1016/0550-3213(81)90151-6.

[126] Z. Maassarani and P. Mathieu. "The su(N) XX model". In: *Nucl. Phys. B* 517 (1998), pp. 395–408. DOI: 10.1016/S0550-3213(98)80004-7. arXiv: cond-mat/9709163.

[127] Juan Martin Maldacena. "The Large N limit of superconformal field theories and supergravity". In: *Adv. Theor. Math. Phys.* 2 (1998), pp. 231–252. DOI: 10.4310/ATMP.1998.v2.n2.a1. arXiv: hep-th/9711200.

[128] Stanley Mandelstam. "Light Cone Superspace and the Ultraviolet Finiteness of the N=4 Model". In: *Nucl. Phys. B* 213 (1983), pp. 149–168. DOI: 10.1016/0550-3213(83)90179-7.

[129] Nelia Mann and Samuel E. Vazquez. "Classical Open String Integrability". In: *JHEP* 04 (2007), p. 065. DOI: 10.1088/1126-6708/2007/04/065. arXiv: hep-th/0612038.

[130] R. R. Metsaev and Arkady A. Tseytlin. "Type IIB superstring action in AdS(5) x S**5 background". In: *Nucl. Phys. B* 533 (1998), pp. 109–126. DOI: 10.1016/S0550-3213(98)00570-7. arXiv: hep-th/9805028.

[131] J. A. Minahan and K. Zarembo. "The Bethe ansatz for N=4 superYang-Mills". In: *JHEP* 03 (2003), p. 013. DOI: 10.1088/1126-6708/2003/03/013. arXiv: hep-th/0212208.

[132] J. A. Minahan and K. Zarembo. "The Bethe ansatz for superconformal Chern-Simons". In: *JHEP* 09 (2008), p. 040. DOI: 10.1088/1126-6708/2008/09/040. arXiv: 0806.3951 [hep-th].

[133] Neel S. Modi et al. "Large Nc Truncations for SU(Nc) Lattice Yang-Mills Theory with Fermions". In: (Feb. 2026). arXiv: 2602.02344 [hep-lat].

[134] Alexander Monin et al. "Semiclassics, Goldstone Bosons and CFT data". In: *JHEP* 06 (2017), p. 011. DOI: 10.1007/JHEP06(2017)011. arXiv: 1611.02912 [hep-th].

[135] Gernot Munster and Peter Weisz. "On the Roughening Transition in Nonabelian Lattice Gauge Theories". In: *Nucl. Phys. B* 180 (1981), pp. 330–340. DOI: 10.1016/0550-3213(81)90424-7.

[136] Y Nambu. "QUARK MODEL AND THE FACTORIZATION OF THE VENEZIANO AMPLITUDE." In: *pp 269-78 of Symmetries and Quark Models. /Chand, Ramesh (ed.). New York Gordon and Breach, Science Publishers, Inc. (1970).* (Jan. 1970). URL: https://www.osti.gov/biblio/4118139.

[137] Holger Bech Nielsen. "An Almost Physical Interpretation of the Integrand of the n-Point Veneziano Model". NORDITA preprint, Niels Bohr Institute. 1969.

[138] Jack E. Paton and Hong-Mo Chan. "Generalized veneziano model with isospin". In: *Nucl. Phys. B* 10 (1969), pp. 516–520. DOI: 10.1016/0550-3213(69)90038-8.

[139] Lorenzo Piroli, Balázs Pozsgay, and Eric Vernier. "What is an integrable quench?" In: *Nucl. Phys. B* 925 (2017), pp. 362–402. DOI: 10.1016/j.nuclphysb.2017.10.012. arXiv: 1709.04796 [cond-mat.stat-mech].

[140] Joseph Polchinski. "Dirichlet Branes and Ramond-Ramond charges". In: *Phys. Rev. Lett.* 75 (1995), pp. 4724–4727. DOI: 10.1103/PhysRevLett.75.4724. arXiv: hep-th/9510017.

[141] Joseph Polchinski and Andrew Strominger. "Effective string theory". In: *Phys. Rev. Lett.* 67 (1991), pp. 1681–1684. DOI: 10.1103/PhysRevLett.67.1681.

[142] H. David Politzer. "Reliable Perturbative Results for Strong Interactions?" In: *Phys. Rev. Lett.* 30 (1973). Ed. by J. C. Taylor, pp. 1346–1349. DOI: 10.1103/PhysRevLett.30.1346.

[143] Alexander M. Polyakov. "String theory and quark confinement". In: *Nucl. Phys. B Proc. Suppl.* 68 (1998), pp. 1–8. DOI: 10.1016/S0920-5632(98)00135-2.

[144] Balázs Pozsgay, Lorenzo Piroli, and Eric Vernier. "Integrable Matrix Product States from boundary integrability". In: *SciPost Physics* 6.5 (May 2019). ISSN: 2542-4653. DOI: 10.21468/scipostphys.6.5.062. URL: http://dx.doi.org/10.21468/SciPostPhys.6.5.062.

[145] Indrakshi Raychowdhury and Jesse R. Stryker. "Loop, string, and hadron dynamics in SU(2) Hamiltonian lattice gauge theories". In: *Phys. Rev. D* 101.11 (2020), p. 114502. DOI: 10.1103/PhysRevD.101.114502. arXiv: 1912.06133 [hep-lat].

[146] N. Yu. Reshetikhin. "A method of functional equations in the theory of exactly solvable quantum systems". In: *Letters in Mathematical Physics* 7.3 (May 1983), pp. 205–213. ISSN: 1573-0530. DOI: 10.1007/BF00400435. URL: https://doi.org/10.1007/BF00400435.

[147] Ana L. Retore. "Introduction to classical and quantum integrability". In: *J. Phys. A* 55.17 (2022), p. 173001. DOI: 10.1088/1751-8121/ac5a8e. arXiv: 2109.14280 [hep-th].

[148] Enrico Rinaldi et al. "Matrix-Model Simulations Using Quantum Computing, Deep Learning, and Lattice Monte Carlo". In: *PRX Quantum* 3.1 (2022), p. 010324. DOI: 10.1103/PRXQuantum.3.010324. arXiv: 2108.02942 [quant-ph].

[149] D. Robson and D. M. Webber. "Gauge Covariance in Lattice Field Theories". In: *Z. Phys. C* 15 (1982), p. 199. DOI: 10.1007/BF01475006.

[150] Tadakatsu Sakai and Shigeki Sugimoto. "Low energy hadron physics in holographic QCD". In: *Prog. Theor. Phys.* 113 (2005), pp. 843–882. DOI: 10.1143/PTP.113.843. arXiv: hep-th/0412141.

[151] Abdus Salam and John Clive Ward. "Weak and electromagnetic interactions". In: *Nuovo Cim.* 11 (1959), pp. 568–577. DOI: 10.1007/BF02726525.

[152] Gopal Chandra Santra et al. "Quantum Resources in Non-Abelian Lattice Gauge Theories: Nonstabilizerness, Multipartite Entanglement, and Fermionic Non-Gaussianity". In: (Oct. 2025). arXiv: 2510.07385 [quant-ph].

[153] John H. Schwarz. "The Early History of String Theory and Supersymmetry". In: (Jan. 2012). arXiv: 1201.0981 [physics.hist-ph].

[154] Leonard Susskind. "Dual symmetric theory of hadrons. 1." In: *Nuovo Cim. A* 69 (1970), pp. 457–496. DOI: 10.1007/BF02726485.

[155] G. Veneziano. "Construction of a crossing - symmetric, Regge behaved amplitude for linearly rising trajectories". In: *Nuovo Cim. A* 57 (1968), pp. 190–197. DOI: 10.1007/BF02824451.

[156] Yifan Wang. "Taming defects in $\mathcal{N} = 4$ super-Yang-Mills". In: *JHEP* 08.08 (2020), p. 021. DOI: 10.1007/JHEP08(2020)021. arXiv: 2003.11016 [hep-th].

[157] Steven Weinberg. "A Model of Leptons". In: *Phys. Rev. Lett.* 19 (1967), pp. 1264–1266. DOI: 10.1103/PhysRevLett.19.1264.

[158] Kenneth G. Wilson. "Confinement of Quarks". In: *Phys. Rev. D* 10 (1974). Ed. by J. C. Taylor, pp. 2445–2459. DOI: 10.1103/PhysRevD.10.2445.

[159] Edward Witten. "Anti-de Sitter space, thermal phase transition, and confinement in gauge theories". In: *Adv. Theor. Math. Phys.* 2 (1998). Ed. by L. Bergstrom and U. Lindstrom, pp. 505–532. DOI: 10.4310/ATMP.1998.v2.n3.a3. arXiv: hep-th/9803131.

[160] Edward Witten. "Baryons and branes in anti-de Sitter space". In: *JHEP* 07 (1998), p. 006. DOI: 10.1088/1126-6708/1998/07/006. arXiv: hep-th/9805112.

[161] E. Wong and I. Affleck. "Tunneling in quantum wires: A Boundary conformal field theory approach". In: *Nucl. Phys. B* 417 (1994), pp. 403–438. DOI: 10.1016/0550-3213(94)90479-0. arXiv: cond-mat/9311040.

[162] Chen-Ning Yang and Robert L. Mills. "Conservation of Isotopic Spin and Isotopic Gauge Invariance". In: *Phys. Rev.* 96 (1954). Ed. by Jong-Ping Hsu and D. Fine, pp. 191–195. DOI: 10.1103/PhysRev.96.191.

[163] Peihe Yang et al. "Three-point functions in ABJM and Bethe Ansatz". In: *JHEP* 01 (2022), p. 002. DOI: 10.1007/JHEP01(2022)002. arXiv: 2103.15840 [hep-th].

[164] Torsten V. Zache, Daniel González-Cuadra, and Peter Zoller. "Quantum and Classical Spin-Network Algorithms for q-Deformed Kogut-Susskind Gauge Theories". In: *Phys. Rev. Lett.* 131.17 (2023), p. 171902. DOI: 10.1103/PhysRevLett.131.171902. arXiv: 2304.02527 [quant-ph].

[165] Yao-Zhong Zhang and Mark D. Gould. "A Unified and complete construction of all finite dimensional irreducible representations of gl(2|2)". In: *J. Math. Phys.* 46 (2005), p. 013505. DOI: 10.1063/1.1812829. arXiv: math/0405043.

[166] Erez Zohar et al. "Digital lattice gauge theories". In: *Phys. Rev. A* 95.2 (2017), p. 023604. DOI: 10.1103/PhysRevA.95.023604. arXiv: 1607.08121 [quant-ph].

[167] G. Zweig. "An SU(3) model for strong interaction symmetry and its breaking. Version 1". In: (Jan. 1964). DOI: 10.17181/CERN-TH-401.